Analysis of nonlinear subdivision and multi-scale transforms

by

Stanislav Harizanov

A thesis submitted in partial fulfilment
of the requirements for the degree of

Doctor of Philosophy
in Mathematics

Approved, Thesis Committee

Prof. Dr. Peter Oswald

Chair, Jacobs University Bremen

Prof. Dr. Lars Linsen

Jacobs University Bremen

Prof. Dr. Johannes Wallner

Technische Universität Graz

Prof. Dr. Nira Dyn

Tel-Aviv University

Date of Defense: September 20, 2011

School of Engineering and Science

Abstract

Analysis of nonlinear subdivision and multi-scale transforms

by

Stanislav Harizanov
Doctoral Candidate of Philosophy in Mathematics

Jacobs University Bremen

Professor Peter Oswald, Chair

Subdivision is a process of recursively refining discrete data using a set of subdivision rules to generate limits (curves, surfaces, height fields, etc.) with desirable properties such as continuity, smoothness, reproduction of shape features, and many more. The wide range of applications as well as the necessity of improving the performance of the existing algorithms lead to the invention of a great variety of subdivision schemes. In many cases, such as preserving the data shape, using normal meshes for better compression rates, removing heavily-tailed noise, working with manifold-valued data, etc., linear multi-scale transforms give unsatisfactory results or cannot be applied at all, and nonlinear alternatives are necessary. There are still very few results about Lipschitz stability and Hölder regularity of nonlinear subdivision schemes and the associated multi-scale transforms, which is a very active research field with many open problems, that is driven by both theory and applications.

In this thesis we develop a general stability analysis of both univariate schemes and their associated multi-scale transforms in the nonlinear functional setting. We show that, unlike the linear setting, convergence and stability analysis are no longer equivalent, and we derive numerical criteria for the verification of each of them. We extend the univariate convergence and stability results to the multivariate regular setting via local approximation techniques.

We establish a general theory for normal multi-scale transforms for curves, based on approximating prediction operators. We propose a globally-convergent normal multi-scale transform, and build an adaptive algorithm based on it that defines a well-posed transform with smooth limits and high detail decay rates. We investigate several extensions of the classical setup for normal multi-scale transforms, namely we use another subdivision operator to generate the normal directions, the combined action of two different subdivision operators for the prediction step, and nonlinear geometry-based predictors, respectively, and show that the properties of the normal multi-scale transforms improve when such extensions are considered.

Acknowledgments

There are many people who deserve my gratitude: First, and foremost, I want to express my sincere thanks to my advisor, Peter Oswald, for providing me with this fruitful topic, and for his constant support, guidance, and patience.

I also wish to thank Peter Binev, Nira Dyn, Philipp Grohs, Olof Runborg, Johannes Wallner, Andreas Weinmann, for the thoughtful and helpful mathematical discussions.

Many thanks to my colleagues at Jacobs University Bremen for the easygoing and friendly working atmosphere, and their encouragement during the preparation of the thesis.

During my work I have received financial support from Jacobs University Bremen, and the German Research Foundation (DFG) under the grant OS-122/3-1.

CONTENTS

1. INTRODUCTION

1.1 Subdivision schemes and multiresolution

Subdivision is a process of recursively refining discrete data using a set of subdivision rules to generate limits (curves, surfaces, height fields, etc.) with desirable properties such as continuity, smoothness, reproduction of shape features, and many more. It has numerous applications, such as image reconstruction, design of curves and surfaces, shape preservation in data and geometric objects, approximation of arbitrary functions, etc. On the other hand, subdivision lies in the core of multiresolution analysis (MRA) and wavelet transforms, and thus plays a central role in data compression, noise removal, and so on. The wide range of applications as well as the necessity of improving the performance of the existing algorithms lead to the invention of a great variety of subdivision schemes. Important mathematical issues to be investigated for a subdivision scheme are convergence as the number of subdivision steps goes to infinity, the smoothness of the limit objects, and the stability of the subdivision process and the associated multi-scale representations. In the linear case, due to standard techniques [15, 31], there is a complete theory about convergence of both subdivision schemes and multi-scale transforms, as well as about determining the smoothness of the first. Moreover, uniform convergence of the subdivision scheme also implies stability of the scheme, which in turn guarantees stability of the associated multi-scale transform.

However, there are many cases in which linear multi-scale transforms give unsatisfactory results, and nonlinear alternatives are necessary. Tentatively, we can group the so-far proposed nonlinear subdivision schemes and multi-scale transforms into four: schemes that are shape preserving or capture singularities, normal multi-scale transforms, statistical and morphological pyramids, and manifold subdivision. The first group consists of schemes that deal with Gibbs-type phenomena that are typical for linear schemes near jump singularities in the data [64, 79, 95], or address shape preservation (monotonicity, convexity, etc.) without loss of smoothness in the limit [73, 71]. Normal meshes and multi-scale transforms [55] deal with the efficient encoding of curves and surfaces, and nonlinearity in these schemes appears in the way details are computed, because they are of different type than the initial data. Examples from the third group have been proposed in connection with removing heavily-tailed (Cauchy) noise, nonlinearity here results mainly from the use of nonlinear robust estimators, such as the median [30]. The nonlinearity in the last group comes from the restriction of the control points to a nonlinearly constrained set in the ambient space such as a manifold, a surface, or a Lie group [89, 102]. Although most of the above references provide analysis only in the univariate case, many of the schemes have natural multivariate analogues and have been introduced with view towards multivariate applications.

In the nonlinear case, there are still very few results about stability and smoothness. This is due to the fact that many theorems from the linear setup can not be directly extended to the nonlinear

one, and that convergence and stability analysis are no longer equivalent. For example, there are nonlinear subdivision schemes such as the essentially non-oscillatory (ENO) scheme [21] which are uniformly convergent but not stable. Moreover, certain stable schemes, e.g., the dyadic median-interpolating scheme [85], do not possess a stable associated multi-scale transform. In summary, analyzing subdivision schemes and the associated multi-scale transforms is a very active research field with many open problems, that is driven by both theory and applications.

Let us briefly introduce some notions and fix notation. The presented definitions are with respect to the so called *functional setting* we build most of our analysis on. In every subdivision scheme, a family of "nested" grids $\Gamma^j, j \geq 0$, is given (i.e., $\Gamma^j \subset \Gamma^{j+1}, \forall j$), the initial data v^0 is a uniformly bounded sequence on the coarsest grid ($v^0 \in \ell_\infty(\Gamma^0)$), and the subdivision operators $S_{[j]} : \ell_\infty(\Gamma^{j-1}) \to \ell_\infty(\Gamma^j)$ map sequences corresponding to two consecutive grids into each other. The grids may be finite or infinite, and data can be arbitrary. We will denote by v^j the data sequence on Γ^j, generated by v^0 after j subdivision steps. The subdivision process is *local* if the operators $S_{[j]}$ are built from local rules, *regular* if the grids $\{\Gamma^j\}_{j=0}^\infty$ are uniform, *univariate* if all the grids are topologically equivalent to $\mathbb{Z}$, and *linear* if all the operators $S_{[j]}$ are linear. Multiresolution, as defined by Harten in [63], is a multi-scale transform that, starting from fine-scale data, constructs data on coarser scales by restriction and so called "details" (analysis step), and conversely reconstructs the original data from their coarse-scale part and the details (synthesis step). More precisely, for a given $J \in \mathbb{N}$ in addition to the set of nested grid $\{\Gamma^j\}_0^J$ and the family of subdivision operators $\{S_{[j]}\}_1^J$ we define a set of restriction operators $R_{[j]} : \ell_\infty(\Gamma^j) \to \ell_\infty(\Gamma^{j-1}), j = 1, \ldots, J$, such that $R_{[j+1]}S_{[j+1]} = I_j,\ j = 0, \ldots, J-1$, where I_j is the identity operator on $\ell_\infty(\Gamma^j)$. From a given data sequence $v^J \in \ell_\infty(\Gamma^J)$ we construct sequences on all coarser grids $\Gamma^j, j = 1, \ldots, J$, via $v^{j-1} := R_{[j]}v^j$. We also compute *detail* sequences $d^j \in \ell_\infty(\Gamma^j)$ that encode in a lossless way the difference between the fine-scale data v^j and the data $S_{[j]}v^{j-1}$, generated from the coarse-scale data v^{j-1} by the given subdivision scheme. Thus, using $\{R_{[j]}\}_1^J$ and $\{S_{[j]}\}_1^J$, one can uniquely decompose every sequence v^J into its coarse-scale part v^0 and a sequence of details $\{d^j\}_1^J$, such that there is a one-to-one correspondence

$$v^J \qquad \longleftrightarrow \qquad \{v^0, d^1, \ldots, d^J\}.$$

Our work is mainly focused on univariate processes (i.e., multi-scale processing of data sampled from univariate functions or from curves) and there are several reasons for that. First of all, there are still many unsolved problems in the univariate theory, and new types of nonlinearity that have not been completely understood. Second of all, the univariate case is a simplified, but yet rich enough setting, where principles usually become clearer. Finally, the univariate analysis often provides sufficient guidance for the multivariate one, where many results are derived as proper extensions of the corresponding 1D argument [57, 31, 22, 4, 87]. For the univariate case, we consider regular, local, shift-invariant subdivision schemes, and thus restrict the grids Γ^j to be $r^{-j}\mathbb{Z}$, where $r \in \mathbb{N}$, $r \geq 2$. More precisely, we work mostly with dyadic transforms, where $\Gamma^j = 2^{-j}\mathbb{Z}$. Due to the shift-invariance, we perform our analysis on $\ell_\infty(\mathbb{Z})$, and we additionally unify the subdivision operators $S_{[j]}$ to a single one $S : \ell_\infty(\mathbb{Z}) \to \ell_\infty(\mathbb{Z})$. Hence from now on we drop the index $[j]$ and talk about the *subdivision scheme* S. Since S is local, changing the initial data at one place will have a local effect on the limit function, i.e., the new limit will differ from the original one only in a neighborhood of the initial point. As a welcome benefit, the locality reduces the analysis of the scheme to a finite-dimensional subspace of $\ell_\infty(\mathbb{Z})$.

Our investigation on multi-scale transforms is related to the asymptotical behavior of the process, and we assume the number of scales J to be large enough. Moreover, we consider smooth geometric objects and we do not allow discontinuities in the generated limit curve as $J \to \infty$. Again, we unify the restriction operators $R_{[j]}$, drop the index, and write $R : \ell_\infty(\mathbb{Z}) \to \ell_\infty(\mathbb{Z})$. In most of the applications the detail sequences $\{d^j\}$, $j \leq J$, and the multi-scale data $\{v^j\}$ are linked via the coarse-to-fine formula $v^j = Sv^{j-1} + d^j$. Sometimes, however [24, 89], like in the normal multi-scale framework, the detail sequence cannot be simply added to the predicted data Sv^{j-1} and the more general formulas $v^j = Sv^{j-1} + Fd^j$ or even $v^j = F(v^{j-1}, d^j)$ are introduced, where F is another (possibly nonlinear) operator. For the purposes of the thesis, we concentrate only on a "coarse-to-fine" analysis, for which the role of the restriction operator R is hidden in the action of F. Therefore, we will not mention it further, and we will refer to the process as *the multi-scale transform associated to* S. We denote its corresponding operator via M, and it is defined by the formula $v^j = Mv^{j-1} := Sv^{j-1} + d^j$, provided the details are additive. Note that, although M depends on two sequences v^{j-1} and d^j, we have chosen not to indicate the argument d^j to keep the exposition as easy to follow as possible. M is *linear* if S is linear.

All the norms that we use are *infinity-norms* and hence we will simply denote them by $\|\cdot\|$. Whether the norm is on an operator, on a sequence, or on a function will be clear from the context. Denote by $\triangle^n : \ell_\infty(\mathbb{Z}) \to \ell_\infty(\mathbb{Z})$ the *n-th order forward finite difference operator*, i.e. $(\Delta v)_i = v_{i+1} - v_i$, and $\Delta^n = \Delta \circ \Delta^{n-1}$. We say that a subdivision scheme S is *uniformly convergent*, if for any $v^0 \in \ell_\infty(\mathbb{Z})$, the piece-wise linear interpolants f^j of the data $v^j = S^j v^0$ with respect to the grid $\Gamma^j = r^{-j}\mathbb{Z}$ uniformly converge to a continuous, nontrivial limit f. (Nontrivial means, that if v^0 is not the zero sample, f cannot be identically zero.) We define Lipschitz stability of S, and its corresponding multi-scale transform M as follows: There exists a constant C such that

$$\|S^J v^0 - S^J \tilde{v}^0\| \leq C\|v^0 - \tilde{v}^0\|, \tag{1.1.1}$$

$$\|M^J v^0 - M^J \tilde{v}^0\| \leq C\Big(\|v^0 - \tilde{v}^0\| + \sum_{j=1}^{J} \|d^j - \tilde{d}^j\|\Big), \tag{1.1.2}$$

for all $J \in \mathbb{N}$ and all sequences involved.

The following example helps to better understand the above definitions. Consider the 4-point subdivision scheme S_c based on central Lagrange cubic interpolation. More precisely, let $\Gamma^j = 2^{-j}\mathbb{Z}$ and define $S_c v^j$ as follows: The values at the "old" grid points $2^{-j}\mathbb{Z}$ are inherited from the corresponding entries of v^j (i.e., S_c is *interpolatory*) while the value at "new" grid points is given by $p_k(2^{-(j+1)}(2k+1))$, where p_k is a cubic polynomial that interpolates v^j at the four points $2^{-j}l, l = k-1, \ldots, k+2$ neighboring it (Fig. 1.1a). The above procedure defines an operator $S_c : \ell_\infty(\mathbb{Z}) \to \ell_\infty(\mathbb{Z})$. Direct computations lead to the following explicit formula

$$\begin{aligned} v_{2k}^{j+1} &= (S_c v^j)_{2k} = v_k^j \\ v_{2k+1}^{j+1} &= (S_c v^j)_{2k+1} = -\frac{1}{16}v_{k-1}^j + \frac{9}{16}v_k^j + \frac{9}{16}v_{k+1}^j - \frac{1}{16}v_{k+2}^j. \end{aligned} \tag{1.1.3}$$

Recall that v_k^j is the value of f^j at $2^{-j}k$ for every j, k. S_c is linear and local, since the entries of v^{j+1} are finite linear combinations of those of v^j; univariate and regular, because the grids $\{\Gamma^j\}$ are equidistant subsets of $\mathbb{R}$; stationary and shift-invariant, as the coefficients in (1.1.3) do not depend

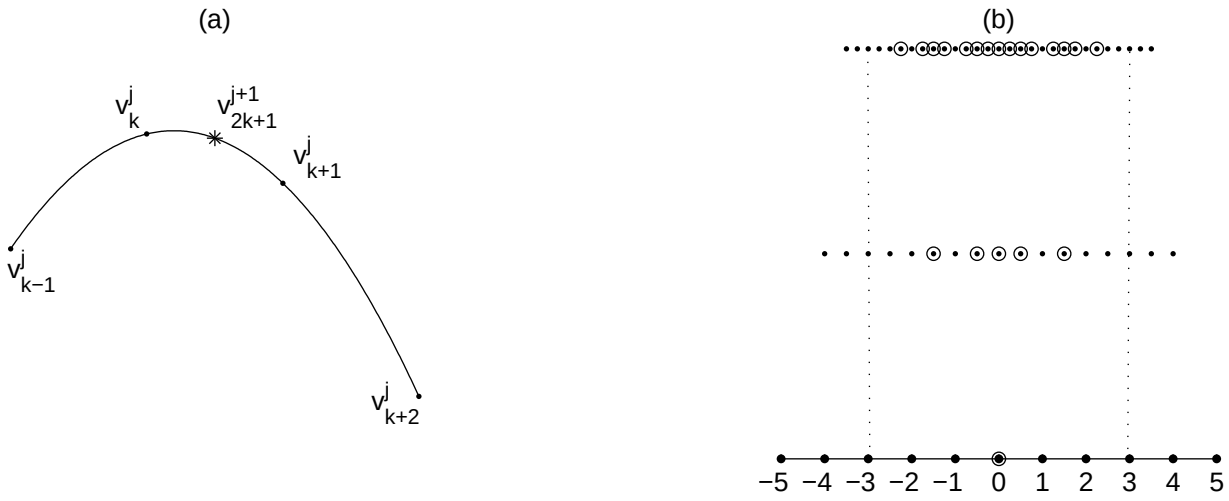

Fig. 1.1: (a) The action of S_c, (b) The range of the dependence of v_0^0 after two subdivision steps.

on the subdivision level j and the position k; and dyadic, because of the dilation factor two. Due to the locality and the shift-invariance of S_c, the action of the subdivision operator can be described by a single finitely supported sequence a, called *mask*, such that

$$(S_c v)_K = \sum_k a_{K-2k} v_k, \qquad K \in \mathbb{Z}. \tag{1.1.4}$$

The only nonzero entries of a are $a_{-3} = a_3 = -\frac{1}{16}$; $a_{-1} = a_1 = \frac{9}{16}$; $a_0 = 1$. Fig. 1.1b shows that changing the data entry v_0^0 affects the limit function only in the interval $[-3, 3]$. On the other hand, in order to globally characterize the limit f, generated via S_c from a $v^0 \in \ell_\infty(\mathbb{Z})$, it suffices to analyze the behavior of f only in the interval $[0, 1]$. But $f|_{[0,1]}$ depends solely on the initial data v^0 at positions $I_0 = \{-2, -1, 0, 1, 2, 3\}$, meaning that one can build the whole analysis of S_c over the set of finite initial sequences $v^0|_{I_0}$.

Examples of nonlinear subdivision schemes and multi-scale transforms, and a discussion on both the difficulties and the progress of their analysis are included in the next section, together with the historical references of the papers, where those processes, resp. results, were first introduced.

1.2 Survey of the existing literature

In the context of image (curve, surface) representation as well as in the context of numerically computing weak solutions of nonlinear conservation laws, piecewise smooth data with jump discontinuities appear. Due to the Gibbs phenomena, a linear multi-scale transform cannot simultaneously localize these discontinuities and provide smooth approximation to the initial function away from the singularities. Another problem is that convexity preserving interpolatory linear subdivision schemes are at most C^1 smooth. These drawbacks motivate the investigation of non-linear subdivision schemes and their usage in nonlinear multi-scale transforms.

Several schemes have been introduced and analyzed so far. Harten *et al.* [64] proposed the essentially non-oscillatory (ENO) subdivision scheme, which uses not only central cubic interpolation like

S_c but also its left and right shifts (i.e., the interpolating nodes are shifted by one once to the left, and once to the right, respectively). If we denote by p_k^l, p_k^c, and p_k^r the corresponding interpolating polynomials, then for v_{2k+1}^{j+1} we use the value at $2^{-(j+1)}(2k+1)$ of the least oscillatory one among them (Fig. 1.2a). This process is uniformly convergent [21], behaves like S_c away from singularities, and prevents the Gibbs phenomena around them. Unfortunately, small perturbations of the data may change the choice of the interpolating polynomial, and thus ENO is unstable. Therefore, the weighted ENO (WENO) subdivision scheme has been suggested [79], where instead of taking only one of the interpolating polynomials for the imputation step, the authors use a convex combination

$$p_k = \alpha_1 p_k^l + \alpha_2 p_k^c + \alpha_3 p_k^r, \qquad \alpha_1 + \alpha_2 + \alpha_3 = 1; \;\; \alpha_1, \alpha_2, \alpha_3 \geq 0,$$

of all the three polynomials with data-dependent weights $\{\alpha_i\}_1^3$. Extensions of these schemes by tensor-product techniques to 2D edge-adaptive image representations have been considered and numerically investigated in [2, 3, 19, 20]. Both ENO and WENO are built on linear subdivision rules, but the data-dependence of these rules is what makes the whole process nonlinear. In [21] Cohen *et al.* analyze the convergence, smoothness, and stability of a larger class of so called quasi-linear data-dependent subdivision schemes, defined by an operator-valued map Φ, such that

$$Sv = \Phi(v)v, \qquad \forall v \in \ell_\infty(\mathbb{Z}), \tag{1.2.1}$$

and $\Phi(v) : \ell_\infty(\mathbb{Z}) \to \ell_\infty(\mathbb{Z})$ is linear for every v. Using the theory they developed, the authors prove stability of the WENO scheme. However, due to the form of the weights $\{\alpha_k\}_1^3$, the constant C from (1.1.1) heavily depends on a fixed parameter ϵ and is not uniformly bounded when $\epsilon \to 0$. A more general smoothness analysis has been performed in [82], while a more general stability analysis has been developed in [61, 41]. Based on the setup from [7, 21] and the framework of our paper [61], another theoretical paper [44] has recently appeared. It is devoted to Lipschitz-linear, instead of quasi-linear subdivision schemes S, and the stability results are extended to ℓ_p norms, as well. The scope of their ℓ_∞ analysis is broader than the one in [21], and narrower than the one in [61]. However, their stability criteria is numerically simpler than the one in [61] and may be verified in a more efficient way.

The accent in the papers [64, 79] is on the smooth linear subdivision operator S_c, and how this operator to be (nonlinearly) adapted in the presence of discontinuities, so that the Gibbs phenomenon does not appear. A different approach is to build the desired nonlinear scheme on the simplest linear subdivision rule - the midpoint-interpolating operator S_1, defined by $(S_1 v)_{2k} = v_k$, $(S_1 v)_{2k+1} = (v_k + v_{k+1})/2$, and to perturb it away from singularities so that the smoothness of the limit increases. Two classes of subdivision schemes, based on that idea, which in addition are monotonicity [73] and convexity [71] preserving have been introduced. The most exploited member of the second class is the piecewise polynomial harmonic (PPH) scheme, introduced also in [42]. The PPH scheme is interpolatory and dyadic with

$$(S_{PPH} v)_{2k+1} = \frac{v_k + v_{k+1}}{2} - \frac{1}{8} H(\Delta^2 v_{k-1}, \Delta^2 v_k), \tag{1.2.2}$$

where $H : \mathbb{R}^2 \to \mathbb{R}$ is the harmonic mean defined by

$$H(x,y) = \begin{cases} \frac{2xy}{x+y}, & xy > 0 \\ 0, & otherwise \end{cases}. \tag{1.2.3}$$

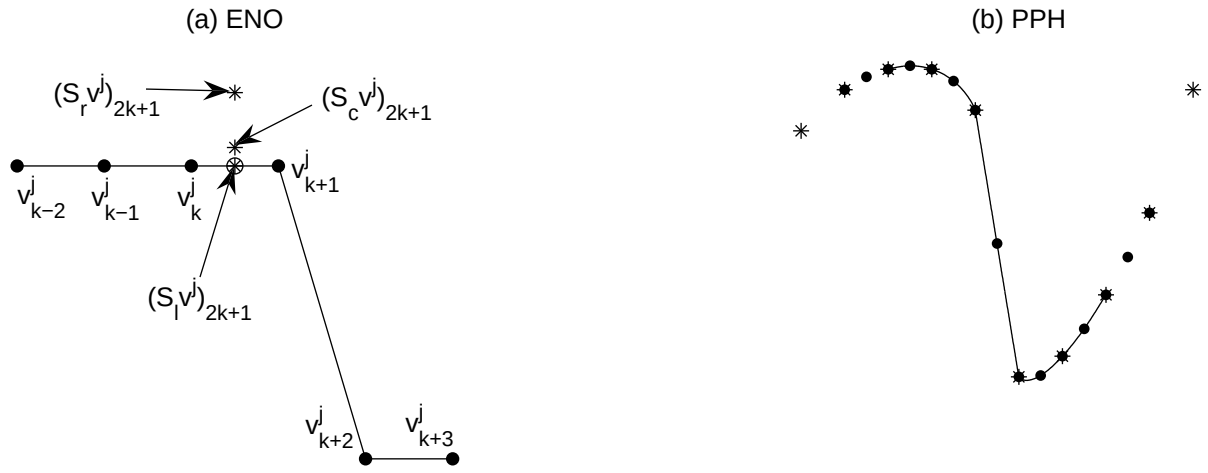

Fig. 1.2: (a) ENO algorithm: the three candidates for imputation, and the less oscillatory choice; (b) one step of PPH and the limit function.

PPH is a second order perturbation of S_1, i.e., $S_{PPH}v = S_1 v + F(\Delta^2 v)$, where F is a nonlinear operator. On the other hand, PPH can be viewed as a perturbation of S_c, as well, since

$$(S_c)_{2k+1} = \frac{v_k + v_{k+1}}{2} - \frac{1}{8}A(\Delta^2 v_{k-1}, \Delta^2 v_k),$$

with $A(x, y) = (x + y)/2$ being the arithmetic mean. The latter formula relates the "S_1 approach" to the S_c one, indicating that both the ideas lead to the construction of similar subdivision schemes at the end. In [8] stability of PPH and the corresponding multi-scale transform is proven. Proof for stability of a large subclass of the schemes proposed in [71], including PPH, can be found in [74]. In [7] a bivariate scheme, based on PPH and constructed via tensor product techniques is introduced and analyzed in terms of convergence and stability. More recent results in this direction can be found in [22, 4, 6, 5].

Experimentations with the ENO method have indicated several practical drawbacks, therefore a new class of reconstruction procedures, the Power ENO methods, has been introduced in [95]. These schemes are based on replacing $H(\cdot, \cdot)$ in (1.2.3) by an extended class of limiters

$$\text{power}_p(x, y) = \frac{(x + y)}{2}\Big(1 - \Big|\frac{x - y}{x + y}\Big|^p\Big),$$

reduce smearing near discontinuities, provide good resolution of corners and local extrema, and contain both WENO and PPH (take $p = 2$ in the power$_p$ mean) as members. Moreover, a new weighted ENO method (Weighted Power-ENO5) is proposed in [95], which has the highest possible order of polynomial reproduction - six. The convergence of these methods and their extensions to 2D are subject of [22].

Normal meshes and multi-scale transforms (MTs) for curves and surfaces is a recent concept in efficient geometry representation based on local data-dependent coordinate systems that are

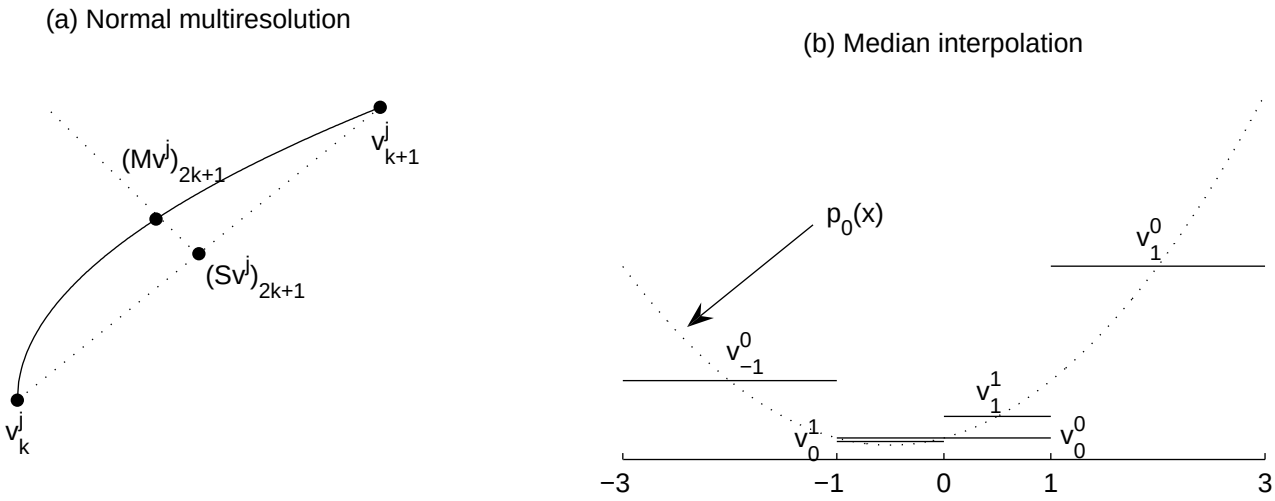

Fig. 1.3: (a) Normal multi-scale transform using the midpoint-interpolating subdivision scheme. (b) One step of the dyadic median-interpolating subdivision scheme

adapted to tangential and normal directions. In the curve setting, as illustrated on Fig. 1.3a for the normal MT based on mid-point interpolation, the predictor S is usually a linear univariate operator, applied componentwise to the 2D data v^j. However, the detail coefficient d^{j+1}_{2k+1} is the signed distance between the predicted point Sv^j_{2k+1} and the newly inserted point Mv^j_{2k+1}, obtained via intersecting the *normal line* through Sv^j_{2k+1} and orthogonal to Δv^j_k with the initial curve. The different nature of data (vector-valued) and details (scalar-valued), and the detail (nonlinear) dependance on the coarse-scale data make the process nonlinear. Hence, instead of having $Mv = Sv + d$ we have $Mv = Sv + Fd$, where F is nonlinear. More precisely, for the considered example we compute

$$(Mv^j)_{2k+1} = (Sv^j)_{2k+1} + (\sigma_j d^{j+1}\mathbf{n}_j)_k, \qquad (Mv^j)_{2k} = v^j_k, \qquad v^j = (x^j, y^j) \in \ell_\infty(\mathbb{Z}) \times \ell_\infty(\mathbb{Z}),$$

where $\mathbf{n}_j = \frac{\Delta v^{j,\perp}}{|\Delta v^j|} := \frac{(-\Delta y^j, \Delta x^j)}{|\Delta v^j|}$ is the unit normal vector. This idea has been originally introduced by Guskov *et al.* in [55], and for the curve setting, it will be elaborated in detail in Chapter 4. A more substantial review of the existing literature on the topic is also presented there.

In signal processing, linear multiresolution is a promising approach for successfully removing Gaussian noise. However, linear transforms perform poorly in the presence of strongly non-Gaussian noise, typically witnessed in analogue telephony, radar signal processing, and laser radar imaging. Indeed, classical statistical models show that maximum likelihood estimators are often linear in the Gaussian case, but highly nonlinear when Cauchy noise appears. The remedy is to use robust estimators. In [30] a class of nonlinear, triadic subdivision schemes based on median interpolation has been introduced. One of its members, the quadratic median-interpolating scheme $S_{med,3}$, allows for a closed-form representation and is the main object of investigation in [30]. Its dyadic version $S_{med,2}$ [85] is computationally easier to deal with, and although it does not have the same denoising properties as the original triadic scheme, it can be used for the mathematical analysis.

Let f be a real-valued continuous function on a bounded interval I with positive Lebesgue measure ($m(I) > 0$). Then the *median* of f on I is defined by

$$med(f; I) := \sup\Big\{\alpha : m(\{x : f(x) < \alpha\}) \le \frac{1}{2} m(I)\Big\}. \tag{1.2.4}$$

$S_{med,2}$ uses the coarse-level information on three consecutive intervals to construct the quadratic polynomial p that has the same medians in this intervals as the given data. Then the grid is refined and the central interval is split into two. Finally, $S_{med,2}$ uses the medians of p on those intervals to impute the data on the next level (Fig. 1.3b). $S_{med,3}$ does absolutely the same with the only exception that every coarse-scale interval is subdivided into three fine-scale intervals, instead of two. In [30] uniform convergence and Hölder-α regularity for $S_{med,3}$ is proved with $\alpha > 0.0997$. The smoothness result has been improved to $\alpha > 0.8510$ in [85], before the optimal $\alpha > 1 - \epsilon$ was established in [109], which is exactly the critical Hölder exponent for $S_{med,3}$, as conjectured in [30]. The median-interpolating multi-scale transform, associated to $S_{med,3}$ has been developed and analyzed in [30]. There are several distinguishable features in their construction. Firstly, unlike the so far mentioned transforms, the process is cell-centered and it is better to associate a piece-wise constant function to the sequence $v^j \in \ell_\infty(\mathbb{Z})$ rather than the linearly interpolating one (Fig. 1.3b), i.e.,

$$g_j(\cdot) = \sum_{k\in\mathbb{Z}} v_k^j 1_{I_{j,k}}(\cdot), \qquad I_{j,k} = [k2^{-j}, (k+1)2^{-j}).$$

Secondly, $S_{med,3}$ is triadic and non-interpolatory, thus its transform is expensive. Finally, the restriction operator (taking the discrete median of the values at the three fine-level intervals) is nonlinear. Despite all these "oddities", the median-interpolating pyramid transform satisfies the typical properties of a wavelet transform, such as coefficient localization, coefficient decay, and Gaussian-noise removal. In the same time, it removes Cauchy noise with the same efficiency as Gaussian one.

In [45, 46] a general theory for constructing linear as well as nonlinear pyramid and wavelet decomposition schemes for signal analysis and synthesis has been presented. The main assumptions correspond to the Harten approach and are: "perfect reconstruction", which states that subdivision followed by restriction returns the original signal, and nestedness of the scale grids. The proposed theory unites different tools for constructing multi-scale signal decomposition transforms, such as pyramids, wavelets, morphological skeletons and granulometries, and gives a complete characterization of both the restriction and the subdivision operators between two adjacent levels.

The necessity of considering manifold-valued data arises from real-life examples like: headings, orientations, rigid motions, deformation tensors, distance matrices, projections, subspaces, etc. If the control points of a subdivision process are restricted to a certain manifold, surface, or a Lie group, then, due to these restrictions, even when the original scheme is linear, its modification becomes nonlinear. The questions about how to modify the linear subdivision scheme and which of its properties can be inherited by the associated manifold-valued scheme are discussed in the works of Wallner *et al.* [102, 101, 105, 103, 52, 104], Grohs [47, 48, 50, 51, 49], and Yu *et al.* [110, 111, 112, 113]. The analysis of manifold-valued subdivision is based on its *proximity* to the linear scheme it is derived from. This general principle has been used before, e.g. in the analysis of non-stationary linear [36], and stationary nonlinear [24, 109, 110] schemes, respectively.

In [89] a generalized wavelet analysis on manifold-valued data is introduced. It is analogous to the wavelet analysis in $\mathbb{R}$, but like in normal multi-scale transforms, there is an important structural distinction between the coarse-scale information, which belongs to the manifold $\mathcal{M}$ and the fine scale information (i.e., the details) which consists of tangent vectors to $\mathcal{M}$. The main idea of the authors' approach is to project the manifold-valued data onto a tangent space $T_{p_0}(\mathcal{M})$ via

the *Exp* map, where $p_0 \in \mathcal{M}$ is suitably chosen, then to apply the corresponding real-valued linear subdivision scheme, and finally to go back on $\mathcal{M}$ via the *Log* map. This procedure works only locally, i.e., when the data $p(k)$ (this is the part of p which is necessary for obtaining p_{2k+1}), and the imputed point p_{2k+1} can be mapped onto a single tangent plane. Due to different applications, both "point-concentrated" (based on the 4-point scheme S_c) and "interval-concentrated" (based on "average interpolation") pyramids are considered. This approach is shown to work well on various test and real-life examples, but no mathematical proofs are given in [89].

In [102] proximity conditions are defined, and general theorems for convergence and C^1 smoothness of a nonlinear scheme T that satisfy proximity condition with an affine-invariant, interpolatory, linear, univariate subdivision scheme S are proved. Then, since S can be expressed in terms of repeated affine averages

$$\mathrm{av}_\alpha(x, y) := (1 - \alpha)x + \alpha y, \quad \alpha \in \mathbb{R},$$

the authors suggest in order to restrict the data to a manifold either to substitute the affine averages by geodesic ones or to project them onto the manifold. Finally, it is proved that (under some local restrictions) for a given S all the analogous geodesic schemes (both for a surface and for a matrix group of constant velocity), and all the analogous projecting schemes fulfil proximity conditions, and hence inherit the C^0 and C^1 smoothness of S. The paper [101] is a continuation of [102], where the proximity analysis is extended and applied for studying C^k smoothness, $k \in \mathbb{N}$. Again, only the univariate case is considered, and the geodesic and projective constructions from the previous article are shown to inherit C^2 smoothness, as well. The general framework from [101] leads to convergence and smoothness (up to C^2) results for the log-exponential and projection analogues of linear subdivision schemes on particular manifolds [103, 52, 112, 110, 48, 104]. Finally, [47] extends the theory from [102] to the multivariate case. It is proved that the proximity conditions are satisfied for a large class of nonlinear multivariate schemes, namely the bivariate geodesic-average and projection-average analogues (defined in [102]), the "closest point projection" as well as the Log-Exp analogue (defined in [52]). Thus, (under some local restrictions on the initial data) the above proximity schemes, defined on an arbitrary abstract Riemannian manifold or an arbitrary abstract Lie group have the same smoothness (up to C^1) as the underlaying linear subdivision scheme S. Apart from smoothness analysis, general stability theory for manifold-valued subdivision schemes has been established [51], and used for verifying approximation order properties of the schemes [49, 113].

The subdivision schemes, considered so far have been defined in the functional setting, i.e., the data has always been assigned to an underlying grid and interpreted as a function on it. However, shape-preservation, normal multi-scale transforms, and manifold-valued subdivision are related to the geometric properties of the data, as well. There are also examples of geometry-based subdivision schemes and multi-scale transforms in the literature. In contrast to the functional setting, even univariate geometric schemes operate on vector data (vertex points, edge, and normal vectors of polygonal lines), and in a way that prevents us from analyzing them componentwise, i.e.,

$$S \begin{pmatrix} x \\ y \end{pmatrix} \neq \begin{pmatrix} Sx \\ Sy \end{pmatrix}.$$

A simple example are the circle-interpolating subdivision operators [41], where the newly generated points are taken from circular arcs through the corresponding old points.

Up to our knowledge, all the investigated geometric subdivision schemes can be interpreted as versions of the interpolatory 4-point scheme with tension parameter [38]

$$(Sv)_{2k+1} = -w(v_{k-1} + v_{k+2}) + (\frac{1}{2} + w)(v_k + v_{k+1}) \qquad \forall v \in \ell_\infty(\mathbb{Z}),\, \forall k \in \mathbb{Z},\; w \in (0, \frac{1}{8}). \quad (1.2.5)$$

In [40], a geometry-based subdivision operator that extends the "dual" Chaikin rule for lines has been investigated. This scheme can be regarded as refining the support lines of the corresponding control polygon rather than refining the underlined set of control points, and generates C^1 convex limit curves from a strictly convex, closed initial polygon. A convexity-preserving bivariate interpolatory 2-point Hermite-type scheme that generates C^1 piecewise quadratic Bézier limit curves has been presented in [100]. In [81], the tension parameter w from (1.2.5) is adapted to the geometry of the four control points taking part in the definition of an inserted point, guaranteeing that the newly inserted point does not coincide with any of its "parents". The newly proposed geometric schemes remain local and in the same time eliminate artifacts and are convexity-preserving. In [32], the insertion rule is based on mid-point cubic interpolation like the rule for the linear scheme S_c (note that S_c is in the class of four-point schemes and corresponds to $w = 1/16$). However, the interpolating polynomial is not built with respect to the uniform parameterization, but with respect to the centripetal and the chordal ones, that depend on the geometry of the control polygon. In [9] another nonlinear 4-point scheme based on local spherical coordinates has been constructed. A circle-preserving version of the 4-point scheme has been presented in [93]. The latter interpolating scheme, together with a certain relaxed approximating variant of it and four other (functional) variations of S_c have been considered in [10]. All the investigated six subdivision processes improve on the quality of the limit curves, compared to those generated by S_c, with the relaxed circle-preserving scheme providing the best visual performance. A subdivision scheme based on circular arc interpolation has been proposed in [41] and used as a prediction operator in a normal multi-scale transform. A new family of subdivision schemes for curve interpolation can be found in [115]. Their insertion rule consists of three steps: firstly, it adaptively places points on the edges of the coarse-scale polygon, then for each new point it computes a displacement vector, based on the unit normals of the endpoints of the edge, and finally, moves the point with respect to it. Unlike the normal MT setting, the normal vectors proposed in [115] are vertex-centered and the size of the displacements depend solely on the old control polygon. The normal approach has been further developed in [116], where the displacement vectors are computed as weighted averages of the curvature normal vectors of the corresponding vertices. This additional rescaling of the normal component leads to reproduction of conic curves, a property that has already been studied in [11]. Edge-centered unit normal vectors are used in [83] for generating nice-looking curvature-continuous curves of round shapes. The proposed scheme can be viewed as the reconstruction step of the mid-point normal MT (Fig. 1.3a) with details depending in a geometric way on the coarse-scale data. Another class of refinement schemes for curve interpolation, where the new-point positions are determined by solving an optimization problem has been established in [70]. Since the authors there try to always find the smoothest possible refined polygons, the subdivision process is neither local nor stationary.

So far geometry-based subdivision schemes and geometric multi-scale transforms have been investigated in case studies only, and tools for their systematic analysis have yet to be developed.

1.3 Main results and review of the content of the thesis

The main contributions of our thesis can be tentatively divided into three groups.

- ***Developing a general framework for Lipschitz stability analysis of both univariate subdivision schemes S and their associated multi-scale transforms in the non-linear functional setting.*** For univariate linear subdivision, uniform convergence of the scheme S implies Lipschitz stability of S, which implies Lipschitz stability of the associated multi-scale transform M. Hence the stability analysis there comes for free, once uniform convergence of the process is established. When nonlinearity is introduced, however, both of the above implications are no longer true in general, and the stability analysis becomes an independent topic. Our main contribution is Theorem 2.2.8. Our approach differs from those used before, since we investigate the joint spectral radius based on the Jacobian of the derived scheme, rather than the derived scheme itself. In addition, we extend the stability analysis to subdivision schemes, defined via piecewise differentiable Lipschitz functions, and thus, significantly enlarge the application range. For instance, we are able to analyze median interpolating multi-scale transforms, as well as power-p subdivision schemes, which both do not fit within the previously known framework, described in [21]. These results led to the publications [61, 59]. Finally, we propose a specific extension of the univariate analysis to multivariate subdivision using local approximation techniques. Even though the theory is equivalent to the direct use of divided difference operators [15, 31], it enriches the set of analytic tools, and thus may lead to improvements in terms of speed and memory storage for the numerical verification of the convergence and stability criteria. In addition, some of the results remain valid in the semi-regular case, as well, implying that the local approximation approach is suitable for further theoretical generalizations.

- ***Investigating a general theory for normal multi-scale transforms for curves, and introducing a globally convergent approximating normal multi-scale transform.*** Normal multi-scale transforms for curves, based on interpolating subdivision rules have been analyzed in [24] and the authors there left as an open question the study of B-spline normal MTs. Using it as a starting point, we manage to formulate and prove Theorem 4.2.3, that covers both the interpolating and approximating settings. It can be viewed as an extension of the results from [24], when replacing order of polynomial reproduction with order of exact polynomial reproduction in the statement. The two notions coincide for interpolating processes, but differ for approximating ones. Moreover, we consider a wider class of admissible normal vectors, i.e., normal with respect to a point from the corresponding local piece of the initial curve $\mathcal{C}$, instead of normal only with respect to the corresponding coarse-scale edge. This research led to the paper [62]. Another important contribution is Theorem 4.3.1. It is known that for the normal MT there is a tradeoff between global well-definedness, and fast detail decay rate and high smoothness of the normal re-parameterization. In Theorem 4.3.1 we show that the normal multi-scale transform based on the Chaikin operator S_2 is globally well-posed and convergent, where by well-posedness we mean that for any given point set on a continuous, rectifiable curve, and for any newly predicted point, the normal line through it intersects the curve, and the obtained refined point set inherits the connectivity of the initial one. Moreover, in contrast to the globally convergent normal MT based on linear subdivision

S_1 [91], the S_2 normal MT offers an additional advantage of "smoothing" the initial point set. Thus, after finitely many refinement steps the S_2 normal MT generates a point set $\mathbf{v}^j$ that can be used as an initial point set for normal MT with other S, guaranteeing that the process remains well-defined on all refinement levels. This is a practical recipe of constructing admissible initial point sets for a normal MT based on an arbitrary subdivision rule.

- ***Improving the properties of standard normal MTs via new 2 point and 4 point subdivision schemes.*** In order to come up with a normal MT that is globally well-posed, yet possesses high order of detail decay and smoothness of the normal re-parameterization, we propose and investigate three generalizations of the prediction step. The first one is based on locally adapted choice of the subdivision operators, the second one is built on the combined action of several operators, and the third one uses non-linear, geometric operators. The adaptive algorithm we present exploits the advantages of the S_2 normal MT, already mentioned at the end of the previous item. However, instead of having several refinement steps of pure S_2 normal MT, followed by pure S normal MT, the algorithm checks a local criteria to chose between the two prediction rules for the computation of every prediction point. This extra freedom improves the efficiency of the algorithm in terms of memory storage and compression rates, which is illustrated in several simulations. Our research in this direction led to the paper [60]. Another original idea is the introduction of combined normal MTs. Working in local frames, we see that the detail decay rate of the normal MT depends on the normal component of the prediction, while the well-posedness and the smoothness of the re-parameterization depend on the tangential one. Moreover, early experimental data indicated significant improvement in the theoretically assured smoothness order of the normal re-parameterization, provided the normal vectors are chosen in a clever way. In particular, the normal re-parameterization of low order B-spline normal MTs reaches the smoothness order of the linear subdivision scheme itself, while, without additional assumptions on the normals, the theory can assure only C^2 limits. Therefore, we slightly generalize the normal MT paradigm and introduce another subdivision rule that we use for generating the normal vectors as a convex combination of the standard normal vectors, i.e., the ones with respect to the coarse-scale edges. Our main contribution is Theorem 5.2.2 which provides optimal detail decay rate of order 4 and optimal $C^{2,1}$ smoothness of the normal re-parameterization for the normal MT based on cubic B-spline prediction in the tangential direction, and classical 4-point prediction in the normal direction. The normal vectors are generated by the linear scheme S_1. Such a combined scheme outperforms each of the two corresponding "pure" MTs it is built of. Finally, we consider normal MT based on circle-preserving subdivision, and prove optimal detail decay rate of order 4 for a particular member of this family that is an analog of the Neville's algorithm. The prediction rule is interpolatory and a geometrical generalization of the 4-point scheme. Up to the knowledge of the author, Theorem 5.3.1 is the first result on normal MTs involving nonlinear prediction operators.

The outline of the remaining chapters of the thesis is as follows:

In **Chapter 2** a general theory on Lipschitz stability of univariate subdivision schemes and their associated multi-scale transforms is established. The classical linear univariate theory [31, 15, 37] is covered briefly in Section 2.1, and then extended to the nonlinear case in Section 2.2, which coincides with the theoretical part of [61]. Subsection 2.2.1 sets up the notation and builds the

bridge between the linear theory and its future nonlinear generalization. Namely, the derived scheme $S^{[k]}$ for a general k-offset invariant scheme S is introduced and the commutation property $\Delta^k \circ S = S^{[k]} \circ \Delta^k$ is derived. With these tools at hand, an abstract theorem for Lipschitz stability of both the subdivision scheme S and its associated multi-scale transform M is formulated and proved in Section 2.2.2. Section 2.2.3 is devoted to creating efficient numerical criteria for the practical verification of the conditions in Theorem 2.2.3. More precisely, the abstract contractivity condition (2.2.5) is reformulated in terms of joint spectral radii associated with the first derivative $DS^{[k]}$, $k \geq 1$, of the corresponding derived schemes. This "differential" approach differs from the one, considered in [21], where the authors work directly with $S^{[k]}$, rather than with their Jacobians $DS^{[k]}$. In its present form (Theorem 2.2.4), the developed stability analysis is built on the differentiability of the functions f_s, used to define the action of the operator S. In manifold-valued subdivision, most of the applications (e.g., the log-exp analogues of linear subdivision schemes in Riemannian manifolds) are based on even analytic subdivision operators, so the C^1 assumption seems to be a negligible restriction there. Moreover, after the necessary adjustments to the specifics of the manifold-valued setting, the "differential" approach, together with analysis by proximity, give rise to a general theory on Lipschitz stability of manifold-valued subdivision schemes and multi-scale transforms [51]. However, for subdivision processes, where the nonlinearity is introduced as a tool for generating limits that preserve certain analytic properties of the initial data (shape-preserving schemes) or for making the processes more robust (statistical and morphological pyramids), the differentiability assumption in Theorem 2.2.4 is often violated. Therefore, we spend the rest of Section 2.2.3 on relaxing it, and, in the end, we derive our main theoretical result in the chapter (Theorem 2.2.8). The analyzed family of subdivision schemes in Theorem 2.2.8, defined via only piecewise differentiable Lipschitz functions f_s is rich enough and covers most of the applications we are familiar with. This is illustrated in Section 2.3. There, we perform our stability analysis for two classes of shape-preserving subdivision schemes (convexity-preserving [71] and monotonicity-preserving [73]), median interpolating multi-scale transform [30], and the family of power-p schemes [95], respectively. Both the median interpolating multi-scale transform and the power-p schemes do not satisfy the assumptions in [21] and their Lipschitz stability has not been analyzed before.

In **Chapter 3**, we use local polynomial approximation techniques for the analysis of multivariate subdivision schemes. In higher dimensions the divided difference operator Δ^k maps the vector space $\ell_\infty(\mathbb{Z}^s)$ to a tensor product of several copies N_k of it, where the number N_k increases exponentially with respect to both k and s. Our motivation for choosing the alternative analysis via local maps is to improve the efficiency of the numerical verifications of both the convergence and stability criteria. In the regular case, Δ^k can be related to a particular local approximation map, so the presented approach is simply an abstraction of the classical theory, and is in line with the idea of "relative contractivity" in [15, 31], as well as with the use of a more general linear operator δ rather than Δ^k in [4, 22]. On the other hand, the local approximation technique can be interpreted as restricting the action of the subdivision operator S to some finite dimensional subspace $V \subset \ell_\infty(\mathbb{Z}^s)$ (namely quotient spaces of $\ell_\infty(\lambda_0)$ with respect to low-degree polynomial data, where $\lambda_0 \subset \mathbb{Z}^s$ is bounded). Thus our work can be viewed as a nonlinear generalization in the ℓ_∞ scalar-valued case of the JSR theory, developed in [67] and further investigated in [57, 56]. (For a better insight into the choices of V considered there, see the survey [13].) Extending upon the univariate results from Section 2.2.2, a convergence and stability analysis of regular nonlinear multivariate subdivision schemes is established in Section 3.1, and Section 3.2, respectively. As already observed for the

linear case in [18, 17], the local map approach and the divided difference approach give rise to the same theoretical results. However, based on local approximations we propose new and versatile analytic tools for the estimations of the corresponding spectral radii, that may lead to less expensive numerical computations. This is illustrated in Section 3.3, where two different families of bivariate subdivision schemes, based on the univariate family $\mathcal{S}_p$ of power-p operators, are considered and proved to converge. The first one follows [22], while the second one is three-directional, or parallel. Section 3.4 is devoted to semi-regular triangulated meshes and to the limited extension for them of the already developed regular theory.

In **Chapter 4**, we provide the theoretical analysis of normal MTs for curves with general linear predictor S, and a more flexible choice of normal directions. Our theory extends upon previous work [24, 91] on normal MTs with interpolating S. Furthermore, we present a globally convergent normal MT that improves the regularity of the refined data. Finally, we propose an adaptive algorithm for obtaining normal MTs with high detail decay rate and smoothness of the normal re-parameterization from an arbitrary initial sample, provided the initial curve $\mathcal{C}$ is smooth. Section 4.1 contains basic introduction to normal MT for curves and reviews some of the existing literature on the subject. The general analysis on normal MTs is developed in Section 4.2. Normal MT can be viewed as a particular instance of manifold-valued subdivision, where the generated surface is the manifold itself, and thus the first question is whether the process is well-defined. If the answer is positive, the convergence and the smoothness of the transform are the next to be analyzed. But since the generated limit is given a priori (it is the initial curve $\mathcal{C}$) and is smooth as a geometric object (i.e., with respect to its arc-length parameterization), the analytic properties of the normal re-parameterization $\mathbf{v}(t)$ are the ones to be considered. Here $\mathbf{v}(t)$ is the limit, if exists, of the linear interpolants $\mathbf{v}^j(t)$ for the j-th level data vector $\mathbf{v}^j$ at the grid $2^{-j}\mathbb{Z}$ as $j \to \infty$. The computation of the detail decay rate completes the analysis of the decomposition (analytic) step of the normal MT. The stability analysis is related to the reconstruction (synthesis) step of the normal MT, and is not performed in the section, as it seems to be very technical (see the last remark in Section 4.3). In Section 4.2.1 the notation is fixed and the necessary tools for our future analysis are established. More precisely, we justify the use of local frames for obtaining asymptotic results, define a regularity condition on the initial data set, that assures well-posedness of the normal MT, and describe the admissible class of normal directions. In Section 4.2.2 the main result is formulated and only a sketch of the proof is given. The full proof can be found in our paper [62]. In Section 4.3 we introduce the normal MT based on the Chaikin operator S_2, illustrate how the general theory from the previous section is applied, and show that the S_2 normal MT is globally convergent and improves the regularity of the refined data. The material in this section consists of [62, Section 4.1] and [60, Section 2]. The goal of Section 4.4 is the invention of an adaptive procedure that gives rise to a well-defined normal MT that possesses high detail decay rates and regularity of the normal re-parameterization. At the beginning of the section it is shown that there is no single subdivision operator S, such that the S normal MT satisfies all the above conditions, e.g., it is shown that global well-posedness implies detail decay of order at most 2 and at most $C^{1,1}$ normal re-parameterization. Then, Proposition 4.4.3 in Section 4.4.1 implies that no matter what the initial curve $\mathcal{C}$, the initial sample $\mathbf{v}^0 \subset \mathcal{C}$, and the considered prediction operator S are, finitely many refinements via the S_2 normal MT generate a point set $\mathbf{v}^j$, such that the S normal MT is well-defined for $\mathcal{C}$, when sampled at $\mathbf{v}^j$. Hence, adaptivity provides a solution to the problem, performing the S_2/S normal MT for a suitable choice of S. In Section 4.4.2 a more efficient version in terms of memory storage and data

compression of the above adaptive idea is presented. The proposed algorithm allows for mixing the two prediction rules within the same level of refinement, and choosing between S_2 and S for the computation of every prediction point. Although the results from such relaxation cannot be guaranteed by theoretical arguments, the simulations in Section 4.4.3 indicate that the algorithm performs well in practice. The material in Section 4.4.1, Section 4.4.2, and Section 4.4.3 coincide with the one in the corresponding subsections of [60, Sections 3 and 4].

In **Chapter 5**, we improve the analytic properties of particular normal MTs by relaxing various parameters from their classical framework. Section 5.1 deals with the smoothness of the normal re-parameterization, while Section 5.2 and Section 5.3 deal with the detail decay rates. The main observation in the first direction, is that additional smoothness for the normal re-parameterization can be sometimes assured when the inequality $P_e < s_\infty(S)$ holds for the prediction operator S. In this case, due to the relatively low order of exact polynomial reproduction, the size of the details is large, and different choices of normal directions affect the regularity properties of the refined data. Thus, if appropriate normals are considered, the data regularity may increase significantly. The benefits of the above idea are illustrated in Section 5.1.1 on normal MTs based on B-spline subdivision operators. Such schemes are chosen because the predictor is very smooth, and in the same time has order of exact polynomial reproduction only two, making the improvements very visible. The main observation in the second direction is that the two limitations on the detail decay rate $\mu < \min(s_\infty(S) + 1, P_e)$, imposed by the analysis in Theorem 4.2.3, can be treated separately. The first one is related to the regularity of the coarse-scale data, and thus to the smoothness properties of the normal re-parameterization, again. The second one is related to the approximation power of the prediction operator. Moreover, with respect to local frames, the first one is sensitive to tangential displacements, while the second one is sensitive to normal displacements of the multi-level data. The notion of combined normal MTs is introduced in Section 5.2, where one uses an "updated" (as in Section 5.1) approximating predictor S in the tangent direction, and an interpolating predictor T in the normal one. The process can be viewed as S normal MT with additional T-preprocessing in the normal direction, and on all levels the points generated by the combined procedure coincide with those, generated by the pure S normal MT. Hence, the analysis of well-posedness, convergence and smoothness is the same, and only the detail decay rates are different. In Section 5.2.1 we test the new setup to normal MTs based on the combined action of a B-spline S_p and a Deslauriers-Dubuc T_p prediction operators, and as in Section 5.1.1 we observe optimal detail decay rates for small values of p. A remarkable consequence is the introduction of the hybrid (S_3, S_1, T_3) subdivision operator, that incorporates the cubic B-spline S_3 and the 4-point operators. This new scheme can be seen as another generalization of the 4-point scheme. The associated normal MT possesses optimal smoothness and detail decay rates that are by a whole factor better than the detail decay rates of any of the both pure S_3 and pure T_3 normal MTs. Finally, in Section 5.3 we consider S_{NL} normal MTs, where S_{NL} is a non-linear geometric operator, related to interpolation via circle arcs. The setup can be viewed as a particular instance of a combined normal MT, associated with the linear operator S_1 and S_{NL}, thus related to the analysis in the previous section. We show that for any member S_{NL} of the "circle-arc family" the detail decay rate of the S_{NL} normal MT is 3. Furthermore, for the S_{NL} that is an analog of the Neville's scheme, the corresponding normal MT has detail decay order 4, which is the optimal rate that can be achieved by such transforms.

2. UNIVARIATE STABILITY ANALYSIS

2.1 Linear subdivision schemes and multi-scale transforms

In the shift-invariant, linear setup, there is a complete theory [15, 31] about convergence, smoothness, and stability of a subdivision scheme S and its associated multi-scale transform M. Here, the analysis of S and M significantly simplifies, due to the following implications

$$\text{Uniform Convergence of } S \Longrightarrow \text{Stability of } S \Longrightarrow \text{Stability of } M. \tag{2.1.1}$$

In this section, we closely follow [31].

For the purpose of the thesis, we consider only r-adic, local, and shift-invariant subdivision schemes. We start with the explicit definition of uniform convergence. The r-adic scheme S is *uniformly convergent* if for every sequence $v^0 \in \ell_\infty(\mathbb{Z})$, there exists a continuous function $f : \mathbb{R} \to \mathbb{R}$ such that

$$\lim_{j\to\infty} \|S^j v^0 - f(\frac{\cdot}{r^j})\| = 0, \tag{2.1.2}$$

where $f(\cdot r^{-j})$ denotes the sequence $\{f(i/r^j) : i \in \mathbb{Z}\}$. Furthermore, the map

$$S^\infty : \ell_\infty(\mathbb{Z}) \to C(\mathbb{R}), \qquad S^\infty v^0 = f,$$

should not be trivially zero. It is easy to check that (2.1.2) is equivalent to uniform convergence in $L_\infty(\mathbb{R})$ of the piece-wise linear interpolations f^j of the data $v^j = S^j v^0$. The limit is the same function f.

The linear MRA is based on the order of polynomial reproduction of the underlying subdivision scheme. It is defined as follows: S has *order of polynomial reproduction* $P \in \mathbb{N}$, if S reproduces constants (i.e., $S\mathbf{1} = \mathbf{1}$, where $\mathbf{1} \in \ell_\infty(\mathbb{Z})$ is the constant sequence 1), and P is the maximal number with the property: for every $n < P$, and every monic polynomial $p(x)$ of degree n, there exists a monic polynomial $q(x)$ of degree n such that

$$S(p|_{\mathbb{Z}}) = q|_{r^{-1}\mathbb{Z}}.$$

We also say that S *reproduces polynomials* of degree n, for every $n < P$. Now, if a shift-invariant linear subdivision scheme S reproduces constants, then there exists a linear subdivision scheme $S^{[1]}$, called *first derived scheme of* S such that

$$\Delta^1 \circ S = S^{[1]} \circ \Delta^1. \tag{2.1.3}$$

Having established the necessary notation, the convergence and stability analysis of both S and its associate multi-scale transform is given via the following

Theorem 2.1.1 (Theorem 3.2 from [31]). *A univariate, linear, shift-invariant subdivision scheme S is uniformly convergent, if and only if S reproduces constants and the* spectral radius *of its first derived scheme is less then one:*

$$\rho(S^{[1]}) = \liminf_{j\to\infty} \|(S^{[1]})^j\|^{1/j} = \rho < 1. \tag{2.1.4}$$

Note that, in order to compute the spectral radius of $S^{[1]}$, one may use an arbitrary norm on the space of linear operators over $\ell_\infty(\mathbb{Z})$, not necessarily the induced operator norm. There are two more equivalent formulations of the contracting property (2.1.4). The first one is: there exists a positive integer n, and $\rho \in (0,1)$, such that for all $v^0 \in \ell_\infty(\mathbb{Z})$

$$\|(S^{[1]})^n v^0\| \le \rho \|v^0\|, \tag{2.1.5}$$

and the second one just writes the above inequality in terms of S rather then of $S^{[1]}$:

$$\|\Delta^1 S^n v^0\| \le \rho \|\Delta^1 v^0\|. \tag{2.1.6}$$

Theorem 2.1.1 provides an explicit algorithm for checking convergence and stability of a univariate linear subdivision scheme, namely, we need to find the first $n \in \mathbb{N}$ such that $\|(S^{[1]})^n\| < 1$. From theoretical point of view the number of iterations n is not uniformly bounded (for every $n \in \mathbb{N}$ one can always find a uniformly convergent scheme S such that $\|(S^{[1]})^n\| \ge 1$), but from practical point of view, if $n > 10$ no convergence occurs in the actual performance of the scheme, where only a small number of steps are carried out.

The *Hölder regularity* (or *smoothness indicator*) $s_\infty(S)$ of S is defined by

$$s_\infty(S) := \sup\{s > 0 : \ f^\infty \in C^s(\mathbb{R}) \text{ for all } v^0 \in \ell_\infty(\mathbb{Z})\}, \tag{2.1.7}$$

where C^s is the space of functions of Hölder smoothness s. The quantity (2.1.7) describes the minimally guaranteed Hölder smoothness for the limits f^∞, generated by S. The smoothness indicator $s_\infty(S)$ is bounded from below by

$$s_\infty(S) \ge -\log_r(\rho(S^{[1]})) > 0,$$

and, under reasonable assumptions on the decay rate of the detail sequences d^j, carries over to the multi-scale transform M, as well. More precise statements on the exact Hölder exponent are available, and involve higher-order derived schemes (e.g., $S^{[2]}$ can be defined recursively as the derived scheme of $S^{[1]}$, and so on). We discuss them in Chapter 4.

2.2 Theoretical approach to the non-linear case.

This section extends the linear theory from Section 2.1 to the nonlinear setting, and repeats our paper [61, Section 2].

2.2.1 Notation and preliminary facts

Although some of the things have already been mentioned, we prefer to repeat the important ones here and back them up with explicit formulas, that appear to be useful in our proofs. We denote by S both the subdivision scheme and the operator (rule) on $\ell_\infty(\mathbb{Z})$ that generates it and it will be clear from the context which one we refer to at a given moment. The same holds for the multi-scale transform M. We assume that $S\mathbf{0} = \mathbf{0}$ (throughout the chapter, $\mathbf{0}$ and $\mathbf{1}$ denote constant sequences consisting of zeros and ones, respectively), and that S is local and *r-shift invariant*. I.e., there are an integer $L \geq 0$ and functions $f_s : \mathbb{R}^{2L+1} \to \mathbb{R}$, $s = 0, 1, \ldots, r-1$, such that the action of S is given by

$$(Sv)_{ri+s} = f_s(v_{i-L}, \ldots, v_{i+L}), \qquad i \in \mathbb{Z}, \quad s = 0, \ldots, r-1. \tag{2.2.1}$$

Under the locality assumption, it is clear that S is well-defined on all real-valued sequences, and not just on $\ell_\infty(\mathbb{Z})$. The integer L characterizes the *support size* of S. Equivalently, r-shift invariance means that $\theta^r \circ S = S \circ \theta$, where θ is the shift operator given by $(\theta v)_i = v_{i+1}$.

Following [109] we will call S *offset invariant* if $S(v+\alpha\mathbf{1}) = Sv+\alpha\mathbf{1}$ for all $v \in \ell_\infty(\mathbb{Z})$ and $\alpha \in \mathbb{R}$. Off-set invariance implies the reproduction of constant sequences, $S(\alpha\mathbf{1}) = \alpha\mathbf{1}$ (but not vice versa). Locality, r-shift invariance, and offset invariance are often satisfied for practically useful nonlinear subdivision schemes. Moreover, these natural restrictions on the subdivision operator allow us to talk about nonlinear derived schemes, which has a central role in our stability analysis.

Lemma 2.2.1. *If S is local, r-shift and offset invariant, then there exists a unique local (with the same support size) and r-shift invariant operator $S^{[1]}$ (the so-called first-order derived subdivision operator associated with S) such that $\Delta \circ S = S^{[1]} \circ \Delta$.*

Proof. We give the explicit construction. For any fixed $i \in \mathbb{Z}$, write

$$v_{i+l} = v_i + w_{i+l}, \qquad w_{i+l} = \begin{cases} \sum_{m=0}^{l-1} (\Delta v)_{i+m}, & l > 0, \\ 0, & l = 0, \\ -\sum_{m=l}^{-1} (\Delta v)_{i+m}, & l < 0. \end{cases}$$

Now apply offset invariance and (2.2.1):

$$(Sv)_{ri+s} = (S(w + v_i\mathbf{1}))_{ri+s} = v_i + f_s(w_{i-L}, \ldots, w_{i+L}), \quad s = 0, \ldots, r-1, \tag{2.2.2}$$

note that w depends on the arbitrarily fixed $i \in \mathbb{Z}$. From this, we see that

$$(\Delta Sv)_{ri+s} = f_{s+1}(w_{i-L}, \ldots, w_{i+L}) - f_s(w_{i-L}, \ldots, w_{i+L}) =: f_s^{[1]}((\Delta v)_{i-L}, \ldots, (\Delta v)_{i+L-1})$$

for $s = 0, \ldots, r-2$, and

$$\begin{aligned} (\Delta Sv)_{ri+r-1} &= (\Delta v)_i + f_0(-\sum_{m=L}^{-1} (\Delta v)_{i+1+m}, \ldots, \sum_{m=0}^{L-1} (\Delta v)_{i+1+m}) - f_{r-1}(w_{i-L}, \ldots, w_{i+L}) \\ &=: f_{r-1}^{[1]}((\Delta v)_{i-L}, \ldots, (\Delta v)_{i+L}). \end{aligned}$$

This shows the claim (uniqueness is obvious). □

The proof also shows that boundedness and differentiability properties of the functions f_s defining S via (2.2.1) automatically carry over to the functions $f_s^{[1]}$ defining $S^{[1]}$. The following statement is an immediate consequence of (2.2.2).

Lemma 2.2.2. *If S is local, r-shift and offset invariant, with the functions f_s in (2.2.1) globally Lipschitz continuous then for any two sequences $v, \tilde{v} \in \ell_\infty(\mathbb{Z})$ we have*

$$\|Sv - S\tilde{v}\| \leq \|v - \tilde{v}\| + C\|\Delta(v - \tilde{v})\|.$$

By induction, one can introduce higher-order derived schemes $S^{[k]}$. More precisely, assume that S is local and r-shift invariant, and that we have already defined the derived subdivision operators $S^{[1]}, \ldots, S^{[k-1]}$ for some $k \geq 2$. Then, if $S^{[k-1]}$ satisfies

$$S^{[k-1]}(w + \alpha\mathbf{1}) = S^{[k-1]}w + \frac{\alpha}{r^{k-1}}\mathbf{1} \qquad \forall w \in \ell_\infty(\mathbb{Z}),$$

using the same argument as in Lemma 2.2.1 we can construct a unique local and r-shift invariant operator $S^{[k]}$ such that $\Delta^k \circ S = S^{[k]} \circ \Delta^k$. We note without proof that the existence of $S^{[k]}$ is equivalent to requiring the following *offset invariance condition for polynomials of order k* for S:

$$(S(v + p))_i = (Sv)_i + p(i/r) + q(i), \qquad i \in \mathbb{Z}, \tag{2.2.3}$$

holds for all $v \in \ell_\infty(\mathbb{Z})$, all polynomial sequences p generated by a polynomial $p(\cdot)$ of degree $k-1$ (i.e., given by $p_i = p(i)$, $i \in \mathbb{Z}$), with some other polynomial $q(\cdot)$ of degree less than $k-1$ (whose coefficients may depend on v and p). A less stringent condition requiring (2.2.3) only for $v = \mathbf{0}$ is used in [21, 82] in connection with the study of quasi-linear subdivision schemes but does not imply the existence of the nonlinear derived subdivision operator $S^{[k]}$ as introduced above. Both definitions are natural extensions of the notion of polynomial reproduction of order k for linear subdivision schemes. Unfortunately, derived subdivision operators $S^{[k]}$ rarely exist for larger values of k. In many practical cases, although true for $k = 1$, (2.2.3) already fails for $k = 2$, e.g., the median interpolating pyramid transform, introduced in Section 1.2. For some convexity-preserving schemes such as power-p methods, also $S^{[2]}$ exists. Despite these observations, we formulate our results for general k.

Throughout the remainder of the chapter a subdivision operator $S : \ell_\infty(\mathbb{Z}) \to \ell_\infty(\mathbb{Z})$ will be called *k-continuous* (resp. *k-Lipschitz*, resp. *k-differentiable*) if S is local, r-shift invariant, offset invariant for polynomials of order $\leq k$, satisfies $S\mathbf{0} = \mathbf{0}$, and the functions f_s which define S via (2.2.1) (and thus all $f_s^{[m]}$ defining the derived subdivision operators $S^{[m]}$, $m = 1, \ldots, k$) are continuous (resp. globally Lipschitz, resp. continuously differentiable with bounded partial derivatives). Some comments are in order. First, k-differentiability implies the k-Lipschitz property, and the latter implies k-continuity. Also, since $S\mathbf{0} = \mathbf{0}$, a k-Lipschitz S is automatically bounded, in the sense that $\|S^{[m]}v\| \leq C\|v\|$ for all v and $m = 0, \ldots, k$. Secondly, many of the used subdivision schemes in practice are k-Lipschitz, but not k-differentiable. However, since the conditions of the stability theorem below require precise estimates for Lipschitz constants, additionally assuming the existence (in some meaningful sense) of continuous first-order derivatives for $f_s^{[k]}$ would simplify this task. The technicalities triggered by the fact that the functions $f_s^{[k]}$ possess only piecewise continuous partial derivatives will be discussed in Subsection 2.2.3 below. Finally, an extension to only locally k-Lipschitz S and to $\ell_p(\mathbb{Z})$ norms for $1 \leq p < \infty$ (though possible, see [21, 82]) is not included below, partly because the considered examples do not require this generalization but also to keep the exposition more readable. The interested reader can find the ℓ_p extension in [41].

2.2.2 Main stability theorem

In this section, we formulate an abstract condition for Lipschitz stability of S and M which formally does not require any additional conditions on the subdivision operator. This is the main result of our Master's Thesis [58], built on a thorough analysis of the stability theorem for subdivision schemes in [21], and the proof of stability for the PPH multi-scale transform in [8].

Theorem 2.2.3. *Let $S : \ell_\infty(\mathbb{Z}) \to \ell_\infty(\mathbb{Z})$ be a given subdivision operator. Assume that for some nonnegative constants $C_0, C_1 \in \mathbb{R}$, some $\rho \in (0,1)$, and finite $k, n \in \mathbb{N}$, the inequalities*

$$\|Sv - S\tilde{v}\| \le \|v - \tilde{v}\| + C_0\|\Delta^k(v - \tilde{v})\|, \tag{2.2.4}$$

$$\|\Delta^k(v^n - \tilde{v}^n)\| \le \rho\|\Delta^k(v^0 - \tilde{v}^0)\| + C_1 \sum_{j=1}^{n} \|d^j - \tilde{d}^j\|, \tag{2.2.5}$$

hold for arbitrary $v, \tilde{v} \in \ell_\infty(\mathbb{Z})$ respectively for two arbitrary sets of multi-scale data $\{v^0, d^1, \ldots, d^J, \ldots\}$, $\{\tilde{v}^0, \tilde{d}^1, \ldots, \tilde{d}^J, \ldots\}$, with their multi-scale transforms defined by $v^j = Sv^{j-1} + d^j$, $\tilde{v}^j = S\tilde{v}^{j-1} + \tilde{d}^j$, $j \ge 1$. Then M is stable, i.e.,

$$\|v^J - \tilde{v}^J\| \le C_2\|v^0 - \tilde{v}^0\| + C_3 \sum_{j=1}^{J} \|d^j - \tilde{d}^j\| \tag{2.2.6}$$

holds with constants C_2, C_3 which depend on k, n, ρ, C_0, and C_1, but not on $J \ge 1$.
To obtain the stability result for the associated subdivision scheme S, set $d^j = \tilde{d}^j = \mathbf{0}$ in the above formulations.

Proof. Fix $0 \le j \le J-1$. (2.2.4) gives rise to

$$\begin{aligned}\|v^{j+1} - \tilde{v}^{j+1}\| &= \|Sv^j + d^{j+1} - (S\tilde{v}^j + \tilde{d}^{j+1})\| \le \|Sv^j - S\tilde{v}^j\| + \|d^{j+1} - \tilde{d}^{j+1}\| \\ &\le \|v^j - \tilde{v}^j\| + C_0\|\Delta^k(v^j - \tilde{v}^j)\| + \|d^{j+1} - \tilde{d}^{j+1}\|.\end{aligned}$$

Applying this result iteratively J times we derive

$$\begin{aligned}\|v^J - \tilde{v}^J\| &\le \|v^{J-1} - \tilde{v}^{J-1}\| + C_0\|\Delta^k(v^{J-1} - \tilde{v}^{J-1})\| + \|d^J - \tilde{d}^J\| \\ &\le \|v^0 - \tilde{v}^0\| + \underbrace{C_0 \sum_{i=0}^{J-1} \|\Delta^k(v^i - \tilde{v}^i)\|}_{:=A} + \sum_{i=1}^{J} \|d^i - \tilde{d}^i\|.\end{aligned} \tag{2.2.7}$$

Now to prove our theorem, it suffices to show that A can be estimated by the expression in the right-hand side of (2.2.6). Let $s := \lfloor i/n \rfloor$, i.e., s is the largest integer not greater than i/n. Then (2.2.5) implies

$$\|\Delta^k(v^i - \tilde{v}^i)\| \le \rho^s\|\Delta^k(v^{i-sn} - \tilde{v}^{i-sn})\| + C_1 \sum_{r=0}^{s-1} \rho^r \sum_{t=rn}^{(r+1)n-1} \|d^{i-t} - \tilde{d}^{i-t}\|, \tag{2.2.8}$$

and after summation and using $\rho < 1$ we derive

$$A \le C(\rho)\Big(\sum_{j=0}^{n-1} \|\Delta^k(v^j - \tilde{v}^j)\| + \sum_{j=1}^{J} \|d^j - \tilde{d}^j\|\Big).$$

To estimate $\|\Delta^k(v^j - \tilde{v}^j)\|$ for $j = 1, \dots, n-1$, we use (2.2.4):

$$\|Sv^{j-1} - S\tilde{v}^{j-1}\| \le \|v^{j-1} - \tilde{v}^{j-1}\| + C_0\|\Delta^k(v^{j-1} - \tilde{v}^{j-1})\| \le (2^k C_0 + 1)\|v^{j-1} - \tilde{v}^{j-1}\|,$$

which, applied j times, gives rise to

$$\begin{aligned}\|\Delta^k(v^j - \tilde{v}^j)\| &\le 2^k\|Sv^{j-1} - S\tilde{v}^{j-1}\| + 2^k\|d^j - \tilde{d}^j\| \\ &\le 2^k(2^k C_0 + 1)\|v^{j-1} - \tilde{v}^{j-1}\| + 2^k\|d^j - \tilde{d}^j\| \\ &\le 2^k(2^k C_0 + 1)^j\|v^0 - \tilde{v}^0\| + 2^k\sum_{i=0}^{j-1}(2^k C_0 + 1)^i\|d^{j-i} - \tilde{d}^{j-i}\|.\end{aligned}$$

Thus,

$$\|\Delta^k(v^j - \tilde{v}^j)\| \le 2^k(2^k C_0 + 1)^{n-1}\|v^0 - \tilde{v}^0\| + 2^k(2^k C_0 + 1)^{n-2}\sum_{i=1}^{n-1}\|d^i - \tilde{d}^i\|. \tag{2.2.9}$$

Combining (2.2.7), (2.2.8), (2.2.9) and

$$\sum_{i=0}^{J-1}\rho^s \le \sum_{i=0}^{\infty}\rho^s = \sum_{i=0}^{\infty}\rho^{\lfloor i/n\rfloor} = n\sum_{i=0}^{\infty}\rho^i = \frac{n}{1-\rho},$$

we derive

$$\begin{aligned}\|v^J - \tilde{v}^J\| &\le \|v^0 - \tilde{v}^0\| + C_0\sum_{i=0}^{J-1}\rho^s\Big(2^k(2^k C_0 + 1)^{n-1}\|v^0 - \tilde{v}^0\| + 2^k(2^k C_0 + 1)^{n-2}\sum_{j=1}^{n-1}\|d^j - \tilde{d}^j\|\Big) \\ &+ C_1\sum_{i=1}^{J}\sum_{r=0}^{s-1}\rho^r\sum_{t=rn}^{(r+1)n-1}\|d^{i-t} - \tilde{d}^{i-t}\| + \sum_{i=1}^{J}\|d^i - \tilde{d}^i\| \\ &\le\Big(1 + \frac{2^k C_0(2^k C_0 + 1)^{n-1}n}{1-\rho}\Big)\|v^0 - \tilde{v}^0\| + C_3\sum_{j=1}^{J}\|d^j - \tilde{d}^j\|.\end{aligned}$$

The constant C_3 is finite, and does not depend on J because one can easily check that for any fixed $1 \le j \le J$ the coefficient in front of $\|d^j - \tilde{d}^j\|$ is of the same type as the coefficient in front of $\|v^0 - \tilde{v}^0\|$, i.e., a finite sum of geometric series with respect to ρ times some uniformly bounded constants. □

Let us comment on the assumptions in Theorem 2.2.3. First of all, the validity of the conditions of this statement automatically implies convergence of S and M. This can be seen if one sets $\tilde{v}_0 = \tilde{d}^1 = \tilde{d}^2 = \ldots = \mathbf{0}$, and compares with the statements in [21] or [84]. The constant $\rho < 1$ also

provides a lower bound for the Hölder smoothness of the limiting functions corresponding to S and M (to speak about convergence of the multi-scale transform M, a natural sufficient condition is to require that $\sum_{j=1}^{\infty} \|d^j\| < \infty$).

The condition (2.2.4) depends only on the subdivision operator S, and is usually easy to verify. Due to Lemma 2.2.1, this condition automatically holds with $k = 1$ for any 1-Lipschitz S. A similar statement can be obtained for $k = 2$ (assuming that S is 2-Lipschitz). However, it is easy to show that even in the linear case (2.2.4) cannot be fulfilled with $k \geq 3$, unless the mask of S is non-negative and S has order of polynomial reproduction at least k [58]. A reformulation of condition (2.2.4) so that it holds in a sensible way for all k might be possible but since in case studies we have so far always used Theorem 2.2.3 with either $k = 1$ or $k = 2$, we will not stress this issue further.

2.2.3 Nonlinear spectral radius conditions

The crucial second condition (2.2.5) in Theorem 2.2.3 is, as a rule, harder to verify than (2.2.4). If formulated for the case of subdivision stability ($d^j = \tilde{d}^j = \mathbf{0}$) it essentially represents a contraction property, similar to (2.1.4). More precisely, if S is k-Lipschitz, i.e., if $S^{[k]}$ exists and all the $f_s^{[k]}$, $s = 0, \ldots, r-1$ that define it are Lipschitz continuous, the condition (2.2.5) just states that some power $(S^{[k]})^n$ is globally strictly contracting, i.e., $(S^{[k]})^n$ possesses a Lipschitz constant strictly less than one for some finite n (compare with (2.1.5)). In this subsection we present a convenient reformulation of the contraction property (2.2.5), based on nonlinear spectral radii.

Let us first consider the case when the subdivision operator S is k-differentiable. Let two sets of multi-scale data as in Theorem 2.2.3 be given. Define absolutely continuous paths in $\ell_\infty(\mathbb{Z})$

$$\gamma^0(t) := \Delta^k(tv^0 + (1-t)\tilde{v}^0), \qquad \delta^j(t) := \Delta^k(td^j + (1-t)\tilde{d}^j), \quad j \geq 1, \quad t \in [0,1],$$

with their k-th order differences as endpoints. Obviously, the derivatives

$$\frac{\mathrm{d}\gamma^0}{\mathrm{d}t} = \Delta^k(v^0 - \tilde{v}^0), \qquad \frac{\mathrm{d}\delta^j}{\mathrm{d}t} = \Delta^k(d^j - \tilde{d}^j), \quad j \geq 1,$$

are constant (and thus uniformly bounded in $\ell_\infty(\mathbb{Z})$) on $[0,1]$. For each $t \in [0,1]$, consider the k-th-order derived analog $\{\gamma^0(t), \ldots, \gamma^j(t), \ldots\}$ of the multi-scale transform M:

$$\gamma^j(t) = M^{[k]}(\gamma^{j-1}(t), \delta^j(t)) := S^{[k]}\gamma^{j-1}(t) + \delta^j(t), \qquad j \geq 1.$$

The newly created paths $\gamma^j : [0,1] \to \ell_\infty(\mathbb{Z})$ remain absolutely continuous, with derivatives belonging to L_∞ and a.e. given by the formula

$$\begin{aligned} \frac{\mathrm{d}\gamma^j}{\mathrm{d}t} &= DS^{[k]}_{\gamma^{j-1}(t)} \frac{\mathrm{d}\gamma^{j-1}}{\mathrm{d}t} + \frac{\mathrm{d}\delta^j}{\mathrm{d}t} \\ &= DS^{[k]}_{\gamma^{j-1}(t)} \frac{\mathrm{d}\gamma^{j-1}}{\mathrm{d}t} + \Delta^k(d^j - \tilde{d}^j), \end{aligned}$$

where $DS^{[k]}_\gamma$ is a bounded linear operator on $\ell_\infty(\mathbb{Z})$ representing the Frechet derivative of $S^{[k]}$ at γ. Unless S is linear, $\gamma^j(t) \neq \Delta^k(tv^j + (1-t)\tilde{v}^j)$ for $j \geq 1, t \in (0,1)$. However, at the end points of the paths the equalities $\gamma^j(0) = \Delta^k\tilde{v}^j$ and $\gamma^j(1) = \Delta^k v^j$ always hold.

The above recursive formula leads to the introduction of a nonlinear spectral radius associated with M (more precisely with the associated k-th order derived transform $M^{[k]}$) which we define as follows

$$\rho_s(M,k) := \liminf_{j\to\infty} \sup_{(w^0,w^1,\ldots,w^{j-1})\in(\ell_\infty(\mathbb{Z}))^j} \|DS^{[k]}_{w^{j-1}} DS^{[k]}_{w^{j-2}} \ldots DS^{[k]}_{w^0}\|^{1/j}. \tag{2.2.10}$$

Note that in this definition the supremum is taken over all possible choices of w^l.

For S it is more appropriate to set

$$\rho_s(S,k) := \liminf_{j\to\infty} \sup_{w\in\ell_\infty(\mathbb{Z})} \|DS^{[k]}_{(S^{[k]})^{j-1}w} DS^{[k]}_{(S^{[k]})^{j-2}w} \ldots DS^{[k]}_{w}\|^{1/j}. \tag{2.2.11}$$

To see the difference with (2.2.10), set $w^0 = w$, $w^l = (S^{[k]})^l w$, $l \geq 1$, and note that the w^l are now not arbitrary but depend on a single $w \in \ell_\infty(\mathbb{Z})$ (and the supremum is only taken with respect to the latter). Thus, we generally have $\rho_s(S,k) \leq \rho_s(M,k)$ but in many cases the inequality is strict.

Similar spectral radii (based on $S^{[k]}$ rather than on $DS^{[k]}$) have been defined in [21, 82] and [84] for the investigation of convergence and smoothness of nonlinear univariate subdivision schemes S. In both papers, the assumption was that, for some $k \geq 1$ and all $l = 0, \ldots, k$, there exist families of data-dependent bounded linear subdivision operators $\{S^{[l]}_v\}_{v\in\ell_\infty(\mathbb{Z})}$ on $\ell_\infty(\mathbb{Z})$, such that

$$\Delta^l(Sv) = S^{[l]}_v \Delta^l v.$$

This is weaker than assuming the existence of nonlinear l-th order derived operators $S^{[l]}$ for all $l \leq k$ because despite the fact that by definition

$$\Delta^l(Sv) = S^{[l]}w = S^{[l]}_v w, \qquad w = \Delta^l v,$$

the allowed dependence of $S^{[l]}_v$ on v and not only on $w = \Delta^l v$ gives greater flexibility (but also adds ambiguity). In [21, 82], the nonlinear spectral radius

$$\rho_c(M,k) := \liminf_{j\to\infty} \sup_{v^0,\ldots,v^{j-1}\in\ell_\infty(\mathbb{Z})} \|S^{[k]}_{v^{j-1}} S^{[k]}_{v^{j-2}} \ldots S^{[k]}_{v^0}\|^{1/j},$$

was introduced while in [84]

$$\rho_c(S,k) := \liminf_{j\to\infty} \sup_{v\in\ell_\infty(\mathbb{Z})} \|S^{[k]}_{S^{j-1}v} S^{[k]}_{S^{j-2}v} \ldots S^{[k]}_{v}\|^{1/j} \tag{2.2.12}$$

was proposed. Assuming $\rho_c(M,k) < 1$ is a sufficient condition for convergence of the subdivision scheme S, and the value of $-\log_r(\rho_c(M,k))$ provides a lower bound for the Hölder smoothness of the limit function (certainly, the weaker assumption $\rho_c(S,k) < 1$ yields the same conclusions). Following the proof in [21], it is not hard to verify that $\rho_c(M,k) < 1$ also ensures the convergence of the multi-scale transform M for arbitrary data $\{v^0, d^1, d^2, \ldots\}$ if $\sum_{j=1}^\infty \|d^j\| < \infty$.

Having introduced the notions of joint spectral radii, we can prove a spectral radius version of Theorem 2.2.3.

Theorem 2.2.4. *Let S be k-differentiable, and assume that (2.2.4) is satisfied with this $k \geq 1$. Then*

(i) S is stable if $\rho_s(S,k) < 1$,

(ii) M is stable if $\rho_s(M,k) < 1$.

Proof. Using the notation above, for any two sets of multi-scale data $\{v^0, d^1, \ldots, d^J, \ldots\}$ and $\{\tilde{v}^0, \tilde{d}^1, \ldots, \tilde{d}^J, \ldots\}$, we can write

$$\begin{aligned}
\Delta^k(v^n - \tilde{v}^n) &= \gamma^n(1) - \gamma^n(0) = \int_0^1 \frac{\mathrm{d}\gamma^n}{\mathrm{d}t}\,\mathrm{d}t \\
&= \int_0^1 \left(DS^{[k]}_{\gamma^{n-1}(t)} \frac{\mathrm{d}\gamma^{n-1}}{\mathrm{d}t} + \Delta^k(d^n - \tilde{d}^n) \right) \mathrm{d}t \\
&= \int_0^1 \left(DS^{[k]}_{\gamma^{n-1}(t)} DS^{[k]}_{\gamma^{n-2}(t)} \frac{\mathrm{d}\gamma^{n-2}}{\mathrm{d}t} + DS^{[k]}_{\gamma^{n-1}(t)} \Delta^k(d^{n-1} - \tilde{d}^{n-1}) + \Delta^k(d^n - \tilde{d}^n) \right) \mathrm{d}t \\
&= \ldots = \int_0^1 \left(\Pi_0^{n-1}(t)\Delta^k(v^0 - \tilde{v}^0) + \sum_{j=1}^{n} \Pi_j^{n-1}(t)\Delta^k(d^j - \tilde{d}^j) \right) \mathrm{d}t,
\end{aligned}$$

where for short $\Pi_j^{n-1}(t) = DS^{[k]}_{\gamma^{n-1}(t)} DS^{[k]}_{\gamma^{n-2}(t)} \ldots DS^{[k]}_{\gamma^j(t)}$ for $j \le n-1$ (for $j = n$ it is just the identity operator). Thus, we have

$$\begin{aligned}
\|\Delta^k(v^n - \tilde{v}^n)\| \;\le\; & (\max_{t\in[0,1]} \|\Pi_0^{n-1}(t)\|)\|\Delta^k(v^0 - \tilde{v}^0)\| \\
& + 2^k \sum_{j=1}^{n} (\max_{t\in[0,1]} \|\Pi_j^{n-1}(t)\|)\|d^j - \tilde{d}^j\|.
\end{aligned}$$

Obviously, if $\rho_s(M,k) < 1$, then for any $\rho_s(M,k) < \tilde{\rho} < 1$, there is a constant $C = C_{\tilde{\rho}}$ such that

$$\|DS^{[k]}_{w^{j-1}} DS^{[k]}_{w^{j-2}} \ldots DS^{[k]}_{w^0}\| \le C\tilde{\rho}^j,$$

independently of the choices for w^l. In particular, $\max_{t\in[0,1]} \|\Pi_j^{n-1}(t)\| \le C\hat{\rho}^{n-j}$ for all $j = 0, \ldots, n$, and (2.2.5) follows by choosing n such that $\rho := C\tilde{\rho}^n < 1$.

The same consideration applies to the case $d^j = \tilde{d}^j = \mathbf{0}$ in (2.2.5), i.e., if only the stability of S is of concern.

Now the result follows from Theorem 2.2.3 □

Remark 2.2.5. *The spectral radius conditions of Theorem 2.2.4 are close to optimal, i.e., when S is k-differentiable, the opposite (strict) inequality $\rho_s(M,k) > 1$ implies the existence of counterexamples to the stability inequality of the multi-scale transform M while $\rho_s(S,k) > 1$ implies that stability for S should not be expected, i.e.,*

$$\sup_{v,\tilde{v}\in\ell_\infty(\mathbb{Z}), v\neq\tilde{v}} \frac{\|S^J v - S^J \tilde{v}\|}{\|v - \tilde{v}\|} \longrightarrow \infty, \qquad J \to \infty.$$

We sketch the argument for S. If $\rho_s(S,k) > 1$ then for each large enough J, there is a sequence $w \in \ell_\infty(\mathbb{Z})$ such that

$$\|DS^{[k]}_{w^{J-1}} \dots DS^{[k]}_{w^0}\| > \hat{\rho}^J,$$

where $w^j = (S^{[k]})^j w$, $j = 0, \dots, J-1$, and $\hat{\rho}$ is chosen such that $1 < \hat{\rho} < \rho_s(S,k)$. By the definition of the operator norm this means that there is a $u \in \ell_\infty(\mathbb{Z})$ with unit norm $\|u\| = 1$ such that

$$\|u^J\| > \hat{\rho}^J, \qquad u^J := DS^{[k]}_{w^{J-1}} \dots DS^{[k]}_{w^0} u.$$

More precisely, without loss of generality we can assume that there is an index $l_J \in \mathbb{Z}$ such that $(u^J)_{l_J} > \hat{\rho}^J$. Using the locality and r-shift-invariance of S (and thus of $S^{[k]}$ and $DS^{[k]})_w$ as well, and the continuity of all $Df_s^{[k]}$ it is clear that we have a similar inequality $(u^J)_{l_J} > \frac{1}{2}\hat{\rho}^J$ for all w in a small open neighborhood W of the initial w, and that this still holds true if we change the entries w_l and u_l of any of these sequences outside a fixed interval $l_0 - L_1 \le l \le l_0 + L_1$ of indices (without loss of generality, we can assume that $\max_{l_0-L_1 \le l \le l_0+L_1} |u_l| = 1$). By using a trivial continuation argument, this allows us to choose the sequences $v, z \in \ell_\infty(\mathbb{Z})$ such that $(\Delta^k v - w)_l = (\Delta^k z - u)_l = 0$ for all l in this specified interval, and $\|z\| \le A\|\Delta^k z\| \le A$ holds with some absolute constant A.

Set $\tilde{v} := v + \lambda z$, and consider $v(t) := v + t(\tilde{v} - v) = v + t\lambda z$. Fix $\lambda > 0$ small enough so that $w(t) := \Delta^k v(t) = w + t\lambda u$ is completely in W. Define $v^j(t) = S^j v(t)$, $v^j = v^j(0)$, $\tilde{v}^j = v^j(1)$, and $w^j(t) = \Delta^k v^j(t) = (S^{[k]})^j w(t)$, $j \ge 0$. Then

$$\begin{aligned}
\|v^J - \tilde{v}^J\| &\ge 2^{-k}\|\Delta^k v^J(1) - \Delta^k v^J(0)\| = 2^{-k}\left\|\int_0^1 \frac{\mathrm{d}w^J(t)}{\mathrm{d}t}\mathrm{d}t\right\| \\
&\ge \lambda 2^{-k}\left|\int_0^1 (\underbrace{(DS^{[k]})_{w^{J-1}(t)} \dots (DS^{[k]})_{w^0(t)} u}_{=u^J(t)})_{l_J}\,\mathrm{d}t\right| \\
&\ge \lambda 2^{-k-1}\hat{\rho}^J \ge \lambda A^{-1}2^{-k-1}\hat{\rho}^J\|z\| \ge c\hat{\rho}^J\|v^0 - \tilde{v}^0\|.
\end{aligned}$$

For $J \to \infty$, this shows that S cannot be stable.

The adjustment for the case of M is simple. For given w^j (which are now, in contrast to the previous case, not related to each other) such that

$$\|DS^{[k]}_{w^{J-1}} \dots DS^{[k]}_{w^0}\| > \hat{\rho}^J,$$

where $1 < \hat{\rho} < \rho_s(M,k)$, we choose $\delta^j := w^j - S^{[k]}w^{j-1}$ such that $w^j = M^{[k]}(w^{j-1}, \delta^j)$ for all $j \ge 1$. Then, using the same localization trick, we introduce the appropriate sequences z, $u = \Delta^k z$, v^j, and d^j such that $\Delta^k v^j = w^j$, $\Delta^k d^j = \delta^j$, $\|z\| \le A\|\Delta^k z\| \le A$. With this, considering the two sets of multi-scale data

$$\{v^0, d^1, \dots, d^J\}, \qquad \{v^0 + \lambda z, d^1, \dots, d^J\}, \quad \lambda > 0,$$

will establish the failure of Lipschitz stability for M.

Note that the counterexample for M is rather exotic, as the detail sequences d^j are determined from the w^j via the formulas $\Delta^k d^j = \delta^j = w^j - S^{[k]}w^{j-1}$. Thus, a property such as $\|d^j\| \to 0$ which is often part of the application scenario, does not necessarily hold for the above constructed

counterexample. It is a topic of future research to specify the notion of stability for multi-scale transforms in such a way that available a priori information on the details d^j is properly taken into account.

Remark 2.2.6. *For k-differentiable S, Theorem 2.2.4 implies the stability result for S in [21].*

We will concentrate on the case $k = 1$, i.e., we will assume that S is 1-differentiable, and sketch the verification of $\rho_s(S, 1) < 1$ from the assumptions of [21] (as was mentioned above, for $k = 1$ the first condition (2.2.4) is almost automatic). The stability theory in [21] assumes the following. Let the subdivision operator S preserve at least constant sequences, and write it in the form $Sv = S_v v$, where $\{S_v\}_{v\in\ell_\infty(\mathbb{Z})}$ is the above-mentioned family of bounded linear but data-dependent operators also preserving constants. Concerning the resulting family of first-order derived operators $\{(S_v)^{[1]}\}_{v\in\ell_\infty(\mathbb{Z})}$, two assumptions are made in [21]:

$$\|(S_v)^{[1]} - (S_{\tilde{v}})^{[1]}\| \le C\|v - \tilde{v}\|, \quad \forall\, v, \tilde{v} \in \ell_\infty(\mathbb{Z}), \tag{2.2.13}$$

and

$$\rho_c(M, 1) < 1. \tag{2.2.14}$$

Obviously, (2.2.14) implies $\|(S_{v^{j-1}})^{[1]} \dots (S_{v^0})^{[1]}\| \le C\tilde{\rho}^j$, with some $\tilde{\rho} < 1$, some constant C, and all $j \ge 1$. Since S is 1-differentiable, having that $DS_w^{[1]}$ is the derivative of $S^{[1]}$ at $w = \Delta v$, we can use $S^{[1]}w = S_v^{[1]}w$ and formally differentiate:

$$DS_w^{[1]} = D(S_v^{[1]})_w w + S_v^{[1]}.$$

It is not hard to see that due to the locality and r-shift invariance of S, the definition of $S_v^{[1]}$, and the differentiability assumptions on the $f_s^{[1]}$, condition (2.2.13) implies the boundedness of $D(S_v^{[1]})_w$ such that

$$\|D(S_v^{[1]})_w w\| \le C\|w\|$$

holds. Now apply this to estimating the operator products in the definition of $\rho_s(S, 1)$. Set $v^j = S^j v$, $w^j = \Delta v^j$. Then

$$\begin{aligned} \Pi_j &:= DS_{w^{j-1}}^{[1]} \dots DS_{w^0}^{[1]} = ((S_{v^{j-1}})^{[1]} + E_{j-1}) \dots ((S_{v^0})^{[1]} + E_0) \\ &= \sum_{l=0}^{j-1} (S_{v^{j-1}})^{[1]} \dots (S_{v^{l+1}})^{[1]} E_l \Pi_l + (S_{v^{j-1}})^{[1]} \dots (S_{v^0})^{[1]}, \end{aligned}$$

where $E_l = D(S_{v^l}^{[1]})_{w^l} w^l$ is a small perturbation since

$$\|E_l\| \le C\|w^l\| = C\|\Delta v^l\| \le C\tilde{\rho}^l$$

according to the convergence theory. Moreover,

$$\|(S_{v^{j-1}})^{[1]} \dots (S_{v^{l+1}})^{[1]}\| \le C\tilde{\rho}^{j-l-1},$$

and using the notation $A_l := \|\Pi_l\|$, $B_j = 1 + \sum_{l=0}^{j} A_l$, we obtain the recursions

$$A_j \le C\tilde{\rho}^j (1 + \sum_{l=0}^{j-1} A_l) = C\tilde{\rho}^j B_{j-1}, \qquad B_j \le (1 + C\tilde{\rho}^j) B_{j-1}, \qquad j \ge 0.$$

This gives $B_j \leq C$, and eventually $A_j \leq C\tilde{\rho}^j$, independently of the choice of $v = v^0$. Thus, $\rho_s(S,1) \leq \tilde{\rho} < 1$ as well. A closer look at the argument also shows that (2.2.14) can be replaced by the weaker condition $\rho_c(S,1) < 1$. The weakness of the stability theory in [21] is the additional condition (2.2.13) which is rarely satisfied for nonlinear subdivision schemes. In particular, it is not true for the power-p schemes as well as for the median interpolating pyramid transform. Details of the argument will be given for the power-p schemes in Section 2.3.3.

The main drawback of Theorem 2.2.4 is that it cannot be directly applied in practice. In most of the schemes, the functions f_s that define them are only piecewise continuously differentiable. In order to apply the developed machinery to k-Lipschitz schemes of this type, we need an extension of the chain rule for the superposition $\tilde{\gamma} := \phi \circ \gamma : [0,1] \to \mathbb{R}$ of a Lipschitz curve $\gamma : [0,1] \to \mathbb{R}^m$ and a piecewise C^1 Lipschitz function $\phi : \mathbb{R}^m \to \mathbb{R}$. Here m is some fixed integer which may vary from application to application. Obviously, $\tilde{\gamma}$ is again Lipschitz, and thus possesses a derivative $\tilde{\gamma}'$ a.e. on $[0,1]$. The question of concern is whether this derivative can be computed a.e. from derivatives of γ and ϕ in a meaningful way. Since the image of γ in $\mathbb{R}^m$ has measure zero this question does not have a simple answer if no additional conditions on ϕ are made.

We introduce a class C^1_{pw} of piecewise differentiable Lipschitz functions which is sufficiently broad to cover the applications of this manuscript (as a matter of fact, we do not know off-hand if there are interesting examples that require more than what is proved below). A continuous function $\phi : \mathbb{R}^m \to \mathbb{R}$ belongs to C^1_{pw} if there exists a locally finite polyhedral partition $\{\Omega_i\}$ of $\mathbb{R}^m$ such that the following conditions hold:

(a) Each Ω_i is a closed connected polyhedral domain in $\mathbb{R}^m$, with non-empty interior Ω_i^0. The polyhedra Ω_i may be unbounded and non-convex. The pairwise intersections $\Omega_{ij} := \Omega_i \cap \Omega_j$, $i \neq j$, are either empty or represent d-dimensional polyhedral faces, $d = 0, 1, \ldots, m-1$, with non-empty interior Ω_{ij}^0 as subsets of the associated d-dimensional hyperplane (if $d = 0$, i.e., if Ω_{ij} is a point, then we set $\Omega_{ij}^0 = \Omega_{ij}$). Consequently, if we set $\Omega_{ii} = \Omega_i$ then $\{\Omega_{ij}^0\}$ is a partition of $\mathbb{R}^m$ into pairwise disjoint sets.

(b) The restriction of ϕ to any of the non-empty open sets $\Omega_{ii}^0 = \Omega_i^0$ and Ω_{ij}^0, $i \neq j$, is C^1, and a uniform bound on all occurring derivatives exists.

For such ϕ, we call $D\phi : \mathbb{R}^m \to \mathbb{R}^m$ an admissible derivative if $D\phi|_{\Omega_{ij}^0}$ is continuous, and for any $x \in \Omega_{ij}^0$ the directional derivative of $\phi|_{\Omega_{ij}^0}$ in a direction along the face Ω_{ij} given by a unit vector u equals $D\phi(x)u$ (if Ω_{ij} is a point ($d = 0$) then there is no restriction on the value of $D\phi$).

Lemma 2.2.7. *Let $\phi \in C^1_{pw}$, and let $D\phi : \mathbb{R}^m \to \mathbb{R}^m$ be an admissible derivative of ϕ. Then for any Lipschitz curve $\gamma : [0,1] \to \mathbb{R}^m$ the superposition $\tilde{\gamma} := \phi \circ \gamma : [0,1] \to \mathbb{R}$ satisfies*

$$\tilde{\gamma}' = (D\phi \circ \gamma)\gamma' \tag{2.2.15}$$

a.e. on $[0,1]$.

Proof. Since $\tilde{\gamma}$ is Lipschitz on $[0,1]$, the set $E := \{t \in (0,1) : \tilde{\gamma}' \text{ exists}\}$ has full measure. Set $E_{ij} := \{t \in (0,1) : \gamma(t) \in \Omega_{ij}^0\} \cap E$. Then $\cup_{i,j} E_{ij} = E$. If E_{ij} has measure zero, set $F_{ij} = E_{ij}$. In all other cases, let F_{ij} be the set of isolated points in E_{ij}, a set of measure zero. Let $t_0 \in E_{ij} \backslash F_{ij}$, and

assume that Ω_{ij} is not a point ($d > 0$). Then there is a sequence $t_n \to t_0$ of points $t_n \in E_{ij} \subset \Omega_{ij}^0$, $t_n \neq t_0$, $n = 1, 2, \ldots$, for which

$$\phi(\gamma(t_n)) - \phi(\gamma(t_0)) = D\phi(\xi_n)(\gamma(t_n) - \gamma(t_0)) = D\phi(\xi_n)\gamma'(\tau_n)(t - t_0)$$

holds with certain $\xi_n \in \Omega_{ij}^0$, $\xi_n \to \gamma(t_0)$, and $\tau_n \in (0, 1)$, $\tau_n \to t_0$. This follows from the admissibility of $D\phi$, the assumed C^1 property of $\phi_{\Omega_{ij}^0}$, and the differentiability of γ at t_0. Thus,

$$\tilde{\gamma}'(t_0) = \lim_{n\to\infty} \frac{\phi(\gamma(t_n)) - \phi(\gamma(t_0))}{t_n - t_0} = \lim_{n\to\infty} D\phi(\xi_n)\gamma'(\tau_n) = D\phi(\gamma(t_0))\gamma'(t_0).$$

If Ω_{ij} is a point ($d = 0$), then evidently $\tilde{\gamma}'(t_0) = 0$ and $\gamma'(t_0) = 0$ for such a t_0, and the above equality holds for any choice of $D\phi(\gamma(t_0))$. This proves (2.2.15) for all $t_0 \in \cup_{i,j} E_{ij} \backslash F_{ij} = E \backslash \cup_{i,j} F_{ij}$. Since the measure of $\cup_{i,j} F_{ij}$ is zero, the Lemma is proved. □

We note that the proof also goes through if the underlying polyhedral partition is deformed by any non-degenerate C^1 diffeomorphism of $\mathbb{R}^m$. For the applications in our thesis, the much simpler case of a partition obtained by the intersection of finitely many straight lines in $\mathbb{R}^2$ suffices. Moreover, in these applications, definitions of $D\phi$ on the subsets Ω_{ij}^0, $i \neq j$, are obtained by continuous extension from $D\phi|_{\Omega_i^0}$ resp. $D\phi|_{\Omega_j^0}$ which eases the computation of numerical estimates for the spectral radii of interest.

Let Σ_k denote the class of k-Lipschitz subdivision schemes S, where each $f_s^{[k]}$, $s = 0, \ldots, r-1$, is the composition of finitely many functions from C_{pw}^1. Then the statement of Theorem 2.2.4 holds for any $S \in \Sigma_k$ if in the definition of the spectral radii we use operators $DS_v^{[k]}$ that are defined using admissable derivatives for the C_{pw}^1 functions the $f_s^{[k]}$, $s = 0, \ldots, r-1$, are composed of. Applying Lemma 2.2.7 at each subdivision level, the proof follows line by line the proof of Theorem 2.2.4.

Theorem 2.2.8. *Let $S \in \Sigma_k$, and assume that (2.2.4) is satisfied with this $k \geq 1$. Then*

(i) S is stable if $\rho_s(S, k) < 1$,

(ii) M is stable if $\rho_s(M, k) < 1$.

We conclude the section with some remarks, that are in order. Note that the statement about the sharpness of the spectral radius criterion for M in Remark 2.2.5 remains true if the required large value of $\|DS_{w^{J-1}}^{[k]} \ldots DS_{w^0}^{[k]}\|$ can be found by derivative calculations for the involved C_{pw}^1 functions that only use arguments belonging to the domains Ω_i^0, and not to the lower-dimensional Ω_{ij}^0. This is obvious from the proof given for Remark 2.2.5. In the examples in the next section, this additional assumption can easily be verified.

As it will become more evident from the examples in Section 2.3, due to the assumed locality and r-shift invariance of S (and consequently of $S^{[k]}$ and $(DS^{[k]})_v$), the estimation of the spectral radii in Theorem 2.2.8 reduces to the study of the dynamics of certain low-dimensional nonlinear iterated function systems (IFS). We use relatively crude estimates involving a few iterations of such nonlinear IFS, a thorough study of the dynamical systems aspect is left for future work.

In manifold-valued subdivision, most of the applications (e.g., the log-exp analogues of linear schemes in Riemannian manifolds) deal with even analytic subdivision operators, so the C^1 assumption in Theorem 2.2.4 is a negligible restriction there. Moreover, combining the "differential approach" with analysis by proximity, a general theory on Lipschitz stability of manifold-valued subdivision schemes and multi-scale transforms can be established [51]. However, our stability results and those from [51] are quite different, due to the specifics of the manifold-valued setting, where algebraic factorizations like Lemma 2.2.1 do not hold, and where the implications (2.1.1) are preserved by the assumed proximity conditions.

The framework developed in this subsection gives rise to an intimate connection between the stability of a nonlinear subdivision operator and the approximation order properties of the corresponding subdivision scheme (see [49] for details). Thus, the "differential approach" also allows for particularly short and natural proofs of the latter, once stability has been established.

2.3 Examples

In this section, we illustrate how the theory from Section 2.2 is applied in practice for analyzing the Lipschitz stability of particular subdivision schemes and multi-scale transforms. The first example is included because of the straightforwardness of its stability analysis, and because it avoids a large amount of technical computations in the proof, making the argument easy to follow. The other two considered examples emphasize a couple of points. Firstly, they show the failure of the implication (2.1.1) in the non-linear setting, and secondly, they demonstrate that our stability analysis is more generally applicable than the one in [21]. Indeed, the dyadic median-interpolating pyramid transform is stable, but its associate multi-scale transform is not, the power-p schemes $\mathcal{S}_p$, $p > 4$ are uniformly convergent, but not stable, and none of those subdivision schemes satisfy the condition (2.2.13), needed for the framework of [21].

2.3.1 Shape-preserving subdivision schemes

In this subsection, we consider two classes of shape-preserving subdivision processes, namely *convexity* [71] and *monotonicity* [73] preserving schemes. The results we present cover those from [72] (Theorem 7 and Theorem 9, respectively). In addition, we prove stability of the multi-scale transform, associated with convexity preserving schemes. The text is taken from our paper [59].

Following [71] we define the following family of convexity preserving subdivision schemes

$$(Sv)_{2i} = v_i, \qquad (Sv)_{2i+1} = \frac{v_i + v_{i+1}}{2} - \tilde{F}(\Delta^2 v_{i-1}, \Delta^2 v_i), \tag{2.3.1}$$

where

$$\tilde{F}(x,y) = \begin{cases} F(x,y), & \forall x,y > 0 \\ -F(-x,-y), & \forall x,y < 0 \\ 0, & \text{otherwise} \end{cases}, \qquad 0 \le F(x,y) \le \frac{1}{4}\min\{x,y\}. \tag{2.3.2}$$

Theorem 2.3.1. *Let $F : \mathbb{R}^+ \times \mathbb{R}^+ \to [0, \infty)$ be C^1_{pw} and homogeneous of degree 1, i.e.,*

$$F(\lambda a, \lambda b) = \lambda F(a, b), \qquad \forall \lambda,\ a,\ b \in \mathbb{R}^+.$$

Then the subdivision scheme S given by (2.3.1)-(2.3.2), and its associated multi-scale transform M are Lipschitz stable.

Proof. Since F is homogeneous of degree 1, we can apply the Euler identity

$$F(a, b) = a\frac{\partial F}{\partial x}(a, b) + b\frac{\partial F}{\partial y}(a, b).$$

This, together with (2.3.2) give rise to

$$\frac{\partial F}{\partial x}(a, b),\ \frac{\partial F}{\partial y}(a, b) \geq 0, \qquad \frac{\partial F}{\partial x}(a, b) + \frac{\partial F}{\partial y}(a, b) \leq \frac{1}{4}, \qquad \forall\ a, b \in \mathbb{R}^+. \tag{2.3.3}$$

Hence, if we define

$$\partial\tilde{F}/\partial x(a, b) = \partial\tilde{F}/\partial y(a, b) = 0, \quad \forall a, b :\ ab \leq 0,$$

we derive that $\tilde{F} \in C^1_{pw}$ with partial derivatives, satisfying (2.3.3) as well. This, (2.3.1), and the mean value theorem imply that for any $v, \tilde{v} \in \ell_\infty(\mathbb{Z})$

$$\|Sv - S\tilde{v}\| \leq \|v - \tilde{v}\| + \max_i |\tilde{F}(\Delta^2 v_{i-1}, \Delta^2 v_i) - \tilde{F}(\Delta^2\tilde{v}_{i-1}, \Delta^2\tilde{v}_i)| \leq \|v - \tilde{v}\| + \frac{1}{4}\|\Delta^2 v - \Delta^2\tilde{v}\|. \tag{2.3.4}$$

For the second derived scheme $S^{[2]}$ we have the explicit formulae

$$(S^{[2]}w)_{2i} = 2\tilde{F}(w_{i-1}, w_i), \qquad (S^{[2]}w)_{2i+1} = w_i/2 - \tilde{F}(w_{i-1}, w_i) - \tilde{F}(w_i, w_{i+1}). \tag{2.3.5}$$

Therefore, the non-zero entries of the Jacobian $DS^{[2]}_w$ satisfy

$$\begin{aligned}
&(DS^{[2]}_w)_{2i,i-1} = 2\frac{\partial\tilde{F}}{\partial x}(w_{i-1}, w_i) \geq 0, \qquad (DS^{[2]}_w)_{2i,i} = 2\frac{\partial\tilde{F}}{\partial y}(w_{i-1}, w_i) \geq 0,\\
&(DS^{[2]}_w)_{2i+1,i-1} = -\frac{\partial\tilde{F}}{\partial x}(w_{i-1}, w_i) \leq 0, \quad (DS^{[2]}_w)_{2i+1,i+1} = -\frac{\partial\tilde{F}}{\partial y}(w_i, w_{i+1}) \leq 0,\\
&(DS^{[2]}_w)_{2i+1,i} = \frac{1}{2} - \frac{\partial\tilde{F}}{\partial y}(w_{i-1}, w_i) - \frac{\partial\tilde{F}}{\partial x}(w_i, w_{i+1}) \geq 0.
\end{aligned} \tag{2.3.6}$$

Obviously, $S \in \Sigma_2$ and direct computations give that $\sum_j |(DS^{[2]}_w)_{2i,j}| \leq 1/2$, $\sum_j |(DS^{[2]}_w)_{2i+1,j}| \leq 1$. This, together with the sign pattern (2.3.6), implies that for any $u, w \in \ell_\infty(\mathbb{Z})$, and any $i \in \mathbb{Z}$

$$\begin{aligned}
\sum_{j\in\mathbb{Z}} \Big| \sum_{l\in\mathbb{Z}} (DS^{[2]}_u)_{4i+s,l}(DS^{[2]}_w)_{l,j} \Big| &\leq \sum_{l\in\mathbb{Z}} |(DS^{[2]}_u)_{4i+s,l}| \Big(\sum_{j\in\mathbb{Z}} |(DS^{[2]}_w)_{l,j}| \Big)\\
&\leq \begin{cases}
\sum_l |(DS^{[2]}_u)_{4i+s,l}| \leq 1/2, \quad s = 0, 2\\
-(DS^{[2]}_u)_{4i+1,2i-1} + 1/2(DS^{[2]}_u)_{4i+1,2i} - (DS^{[2]}_u)_{4i+1,2i+1} \leq 3/4\\
-1/2(DS^{[2]}_u)_{4i+3,2i} + (DS^{[2]}_u)_{4i+3,2i+1} - 1/2(DS^{[2]}_u)_{4i+3,2i+2} \leq 3/4
\end{cases}.
\end{aligned}$$

Hence, $\rho_s(M, 2) \leq \sup_{u,w\in\ell_\infty(\mathbb{Z})} \|DS^{[2]}_u DS^{[2]}_w\| \leq \sqrt{3/4} < 1$, and Theorem 2.2.8 completes the proof. □

Following [73] we define the following family of monotonicity preserving subdivision schemes

$$(Sv)_{2i} = v_i, \qquad (Sv)_{2i+1} = \frac{v_i + v_{i+1}}{2} + H(\Delta v_{i-1}, \Delta v_i, \Delta v_{i+1}), \tag{2.3.7}$$

where

$$H(x,y,z) = \begin{cases} \frac{y}{2} G(|x/y|, |z/y|), & y \neq 0, \\ 0, & y = 0, \end{cases} \qquad G(s,t) = \frac{s-t}{\ell_1 + (1+\ell_2)(s+t) + \ell_3 st}, \tag{2.3.8}$$

with nonnegative constants $\{\ell_i\}_{i=1}^3$, such that $\ell_1 + 2\ell_2 + \ell_3 = 6$. Obviously, $H \in C(\mathbb{R}^3)$ for any choice of the ℓ_i's.

Theorem 2.3.2. *For any admissible choice of the constants ℓ_i, the subdivision scheme S defined via* (2.3.7)-(2.3.8) *is Lipschitz stable.*

Proof. Using the explicit formulae

$$(S^{[1]}w)_{2i} = \frac{1}{2} w_i (1 + G(|w_{i-1}/w_i|, |w_{i+1}/w_i|)), \quad (S^{[1]}w)_{2i+1} = \frac{1}{2} w_i (1 - G(|w_{i-1}/w_i|, |w_{i+1}/w_i|)),$$

and (2.3.8), it is not hard to prove that $S \in \Sigma_1$. Moreover, Lemma 2.2.2 assures that (2.2.4) holds for S with $k = 1$. Let $w^0 \in \ell_\infty(\mathbb{Z})$ be an arbitrary sequence with nonzero entries. The case, when w^0 possess trivial entries is straightforward and is left to the reader. The formulae for $G(s,t)$ and for $S^{[1]}$ imply that for any $j \in \mathbb{Z}$ the entries of $w^j = (S^{[1]})^j w^0$ are nonzero, too. Theorem 17 from [73] states that

$$\max_i \left| \max\left\{ \left| \frac{w_{i-1}^j}{w_i^j} \right|, \left| \frac{w_{i+1}^j}{w_i^j} \right| \right\} - 1 \right| \leq C \left(\frac{\sqrt{3}}{2} \right)^j, \quad \forall\, j \in \mathbb{Z},$$

and, thus, $|w^j| \to c\mathbf{1}$ as $j \to \infty$, where c depends on w^0, and $\mathbf{1}$ is the constant 1 sequence. Since $G(1,1) = 0$, and $\partial G/\partial s(1,1) = -\partial G/\partial t(1,1) = 1/8$, we derive that the relevant entries in the matrix representation of the first derivative of $S^{[1]}$ at $c\mathbf{1}$ are

$$DS^{[1]}_{c\mathbf{1}}\Big|_{\{2i,2i+1\}\times\{i-1,i,i+1\}} = \begin{pmatrix} 1/16 & 1/2 & -1/16 \\ -1/16 & 1/2 & 1/16 \end{pmatrix}.$$

Since $\|DS^{[1]}_{c\mathbf{1}}\|_{\ell_\infty} = 5/8$, by continuity we conclude that $\rho_s(S,1) \leq 5/8 < 1$. □

2.3.2 Median interpolating pyramid transform

This subsection is taken from our paper [61, Section 3.1].

The quadratic triadic median-interpolating pyramid transform (MIPT) was introduced in [30], and a dyadic version of the scheme was considered in [85]. For a real-valued continuous function f on a bounded interval I, the median of f on I is defined by

$$med(f; I) := \sup\left\{ \alpha : m(\{x : f(x) < \alpha\}) \leq \frac{1}{2} m(I) \right\},$$

where m is the Lebesgue measure. For any $v^0 \in \ell_\infty(\mathbb{Z})$ and any $i \in \mathbb{Z}$ denote by $p_i(x)$ the unique quadratic polynomial that satisfies

$$med(p_i; [i-l, i-l+1]) = v^0_{i-l}, \quad l = -1, 0, 1.$$

Then the subdivision step is given via

$$v^1_{3i+l} = med\Big(p_i; \Big[\frac{3i+l}{3}, \frac{3i+l+1}{3}\Big]\Big), \quad l = 0, 1, 2,$$

or via

$$v^1_{2i+l} = med\Big(p_i; \Big[\frac{2i+l}{2}, \frac{2i+l+1}{2}\Big]\Big), \quad l = 0, 1,$$

in the triadic, respectively the dyadic cases. We denote by $S_{med,3}$ and $S_{med,2}$ the corresponding subdivision operators.

Following [85] we write the corresponding subdivision operators as functions of the centers c_i of p_i (when p_i is linear, we formally set $c_i = \pm\infty$):

$$\begin{aligned}
(S_{med,3}v)_{3i} &= \frac{2}{9}v_{i-1} + \frac{8}{9}v_i - \frac{1}{9}v_{i+1} - \alpha_0(c_i)\Delta^2 v_{i-1},\\
(S_{med,3}v)_{3i+1} &= v_i - \alpha_1(c_i)\Delta^2 v_{i-1},\\
(S_{med,3}v)v_{3i+2} &= -\frac{1}{9}v_{i-1} + \frac{8}{9}v_i + \frac{2}{9}v_{i+1} - \alpha_2(c_i)\Delta^2 v_{i-1},
\end{aligned} \tag{2.3.9}$$

and

$$\begin{aligned}
(S_{med,2}v)_{2i} &= \frac{5}{32}v_{i-1} + \frac{15}{16}v_i - \frac{3}{32}v_{i+1} - \tilde{\alpha}_0(c_i)\Delta^2 v_{i-1},\\
(S_{med,2}v)_{2i+1} &= -\frac{3}{32}v_{i-1} + \frac{15}{16}v_i + \frac{5}{32}v_{i+1} - \tilde{\alpha}_1(c_i)\Delta^2 v_{i-1},
\end{aligned} \tag{2.3.10}$$

where

$$\begin{aligned}
&\alpha_0 = \frac{8\epsilon_0 + 2\epsilon_{-2} - \epsilon_2 - \tilde{\epsilon}_{-2/3}}{9(32 - 2\epsilon_0 + \epsilon_{-2} + \epsilon_2)}, \quad \alpha_1 = \frac{9\epsilon_0 - \tilde{\epsilon}_0}{9(32 - 2\epsilon_0 + \epsilon_{-2} + \epsilon_2)}, \quad \alpha_2 = \frac{8\epsilon_0 - \epsilon_{-2} + 2\epsilon_2 - \tilde{\epsilon}_{2/3}}{9(32 - 2\epsilon_0 + \epsilon_{-2} + \epsilon_2)},\\
&\tilde{\alpha}_0 = \frac{30\epsilon_0 + 5\epsilon_{-2} - 3\epsilon_2 - 8\tilde{\epsilon}_{-1/2}}{32(32 - 2\epsilon_0 + \epsilon_{-2} + \epsilon_2)}, \quad \tilde{\alpha}_1 = \frac{30\epsilon_0 - 3\epsilon_{-2} + 5\epsilon_2 - 8\tilde{\epsilon}_{1/2}}{32(32 - 2\epsilon_0 + \epsilon_{-2} + \epsilon_2)},
\end{aligned} \tag{2.3.11}$$

with

$$\begin{aligned}
\epsilon_{-2} &= (1 - 4(c+2)^2)_+; & \epsilon_0 &= (1 - 4c^2)_+; & \epsilon_2 &= (1 - 4(c-2)^2)_+;\\
\tilde{\epsilon}_{-2/3} &= (1 - 4(2+3c)^2)_+; & \tilde{\epsilon}_0 &= (1 - 36c^2)_+; & \tilde{\epsilon}_{2/3} &= (1 - 4(2-3c)^2)_+;\\
\tilde{\epsilon}_{-1/2} &= (1 - 4(-1-2c)^2)_+; & \tilde{\epsilon}_{1/2} &= (1 - 4(1-2c)^2)_+.
\end{aligned}$$

For later use, we introduce some further notation. It is also not hard to prove that the quantity $\zeta_i := -(\Delta v_{i-1} + \Delta v_i)/\Delta^2 v_{i-1}$ is a continuous, piecewise differentiable, and strictly monotone function

of c_i. This function we denote by $\zeta = \zeta(c)$. Consequently, the center c_i is a continuous, piecewise differentiable function of ζ_i (and thus of the involved first-order differences as well), i.e., $c_i = c(\Delta v_{i-1}, \Delta v_i) := \zeta^{-1}(\zeta_i)$. We mention a few important symmetries that help our stability analysis:

$$\alpha_0(c) = \alpha_2(-c); \quad \alpha_1(c) = \alpha_1(-c); \quad \tilde{\alpha}_0(c) = \tilde{\alpha}_1(-c); \quad \zeta(c) = -\zeta(-c). \tag{2.3.12}$$

Both schemes are known to be convergent [30, 85], with limits enjoying a certain Lipschitz regularity. In [58] we showed that the dyadic MIPT is stable, but its associated multi-scale transform is not, unless some restrictions on the admissible class of details are given. In this section, we prove the following

Theorem 2.3.3. *The triadic, quadratic, median-interpolating pyramid transform $S_{med,3}$ and its associated multi-scale transform M are Lipschitz stable.*

Proof. First of all, it is not hard, yet technical to see that $S_{med,3} \in \Sigma_1$ (see [61, lemma 3.1] for the proof), so what remains is to estimate the nonlinear spectral radii $\rho_s(M, 1)$. Using (2.3.9) we derive

$$\begin{aligned}
(\Delta S_{med,3} v)_{3i} &= \frac{2\Delta v_{i-1} + \Delta v_i}{9} + (\alpha_0 - \alpha_1)(c_i)\Delta^2 v_{i-1}, \\
(\Delta S_{med,3} v)_{3i+1} &= \frac{\Delta v_{i-1} + 2\Delta v_i}{9} + (\alpha_1 - \alpha_2)(c_i)\Delta^2 v_{i-1}, \\
(\Delta S_{med,3} v)_{3i+2} &= \frac{-\Delta v_{i-1} + 5\Delta v_i - \Delta v_{i+1}}{9} + \alpha_2(c_i)\Delta^2 v_{i-1} - \alpha_0(c_{i+1})\Delta^2 v_i.
\end{aligned}$$

Therefore, setting $w := \Delta v$, using (2.3.12), and doing straightforward computations, we obtain the following formulae for the nonzero entries of $DS^{[1]}_{med,3}$:

$$\begin{aligned}
((DS^{[1]}_{med,3})_w)_{3i,i-1} &= \frac{2}{9} - (A - C)(c_i), & ((DS^{[1]}_{med,3})_w)_{3i,i} &= \frac{1}{9} + (B - D)(c_i), \\
((DS^{[1]}_{med,3})_w)_{3i+1,i-1} &= \frac{1}{9} + (B - D)(-c_i), & ((DS^{[1]}_{med,3})_w)_{3i+1,i} &= \frac{2}{9} - (A - C)(-c_i), \\
((DS^{[1]}_{med,3})_w)_{3i+2,i-1} &= -\frac{1}{9} - B(-c_i), & ((DS^{[1]}_{med,3})_w)_{3i+2,i+1} &= -\frac{1}{9} - B(c_{i+1}), \\
((DS^{[1]}_{med,3})_w)_{3i+2,i} &= \frac{5}{9} + A(-c_i) + A(c_{i+1}),
\end{aligned}$$

where

$$A := \alpha_0 + \frac{\alpha_0'}{\zeta'}(1 - \zeta), \quad B := \alpha_0 - \frac{\alpha_0'}{\zeta'}(1 + \zeta), \quad C := \alpha_1 + \frac{\alpha_1'}{\zeta'}(1 - \zeta), \quad D := \alpha_1 - \frac{\alpha_1'}{\zeta'}(1 + \zeta).$$

By definition these functions are piecewise continuous and bounded functions of the center c.

For further use, let us denote the entries of $(DS^{[1]}_{med,3})_w$ by $t_{i,j} := ((DS^{[1]}_{med,3})_w)_{i,j}$. Direct computations show that the elements $t_{3i,i-1}$, $t_{3i,i}$, $t_{3i+1,i-1}$, $t_{3i+1,i}$, $t_{3i+2,i}$ are positive, and that the elements $t_{3i+2,i-1}$, $t_{3i+2,i+1}$ are negative. By shift invariance, this gives complete knowledge about the sign pattern of the non-zero entries in $(DS^{[1]}_{med,3})_w$. More precisely, the ranges for each one of these entries

have been numerically computed as follows (since all functions involved are piecewise rational and explicitly available, this can be backed by tedious analytic estimates as well):

$$\begin{pmatrix} t_{3i,i-1} & t_{3i,i} & 0 \\ t_{3i+1,i-1} & t_{3i+1,i} & 0 \\ t_{3i+2,i-1} & t_{3i+2,i} & t_{3i+2,i+1} \end{pmatrix} = \begin{pmatrix} (0.1546, 0.3232) & (0.0771, 0.1616) & 0 \\ (0.0771, 0.1616) & (0.1546, 0.3232) & 0 \\ (-0.3016, -0.0476) & (0.3536, 0.9366) & (-0.3016, -0.0476) \end{pmatrix}.$$

We will use these bounds throughout the remainder of this subsection.

To prepare for norm estimates for the operators $(DS^{[1]}_{med,3})_w$ and their products, observe that

$$\begin{aligned} \sum_j |t_{3i,j}| &= t_{3i,i-1} + t_{3i,i} = \frac{1}{3} + (B - A + C - D)(c_i), \\ \sum_j |t_{3i+1,j}| &= t_{3i+1,i-1} + t_{3i+1,i} = \frac{1}{3} + (B - A + C - D)(-c_i), \\ \sum_j |t_{3i+2,j}| &= -t_{3i+2,i-1} + t_{3i+2,i} - t_{3i+2,i+1} \\ &= \frac{7}{9} + (A + B)(-c_i) + (A + B)(c_{i+1}), \end{aligned}$$

and thus

$$\sum_j |((DS^{[1]}_{med,3})_w)_{3i+l,j}| \le 0.4166, \qquad l = 0, 1, \qquad \sum_j |((DS^{[1]}_{med,3})_w)_{3i+2,j}| \le 1.0318.$$

This is not enough for establishing stability. To do so, we need the following lemma.

Lemma 2.3.4. *For any $u, w \in \ell_\infty(\mathbb{Z})$*

$$\|(DS^{[1]}_{med,3})_u (DS^{[1]}_{med,3})_w\| \le 0.9706.$$

Proof. Let us denote by $t_{i,j}$ as before the elements of both $(DS^{[1]}_{med,3})_w$ and $(DS^{[1]}_{med,3})_u$ (by the indices of an element it will be clear, exactly to which matrix it belongs), and by $t^2_{i,j}$ - the elements of the product $(DS^{[1]}_{med,3})_u (DS^{[1]}_{med,3})_w$. By standard techniques for $l = 0, 1, 3, 4, 6, 7$ we have:

$$\sum_j |t^2_{9i+l,j}| \le \sum_{j,s} |t_{9i+l,s} t_{s,j}| \le \sum_s |t_{9i+l,s}| (\sum_j |t_{s,j}|) \le 0.4166 \cdot 1.0318 = 0.4298.$$

Consider $l = 2$. Since $(DS^{[1]}_{med,3})_u$ and $(DS^{[1]}_{med,3})_w$ are local and shift-invariant, we can perform our analysis on a finite-dimensional subspace of $\ell_\infty(\mathbb{Z})$. Therefore, to determine the elements $\{t^2_{9i+2,j}\}$ we need to consider only the following product of a 1×3 vector and a 3×3 matrix

$$\begin{pmatrix} t_{9i+2,3i-1} & t_{9i+2,3i} & t_{9i+2,3i+1} \end{pmatrix} \begin{pmatrix} t_{3i-1,i-2} & t_{3i-1,i-1} & t_{3i-1,i} \\ 0 & t_{3i,i-1} & t_{3i,i} \\ 0 & t_{3i+1,i-1} & t_{3i+1,i} \end{pmatrix} = \begin{pmatrix} - & + & - \end{pmatrix} \begin{pmatrix} - & + & - \\ 0 & + & + \\ 0 & + & + \end{pmatrix}.$$

Using again the ranges of the entries $t_{i,j}$ given above, we obtain the following bounds for the absolute values of $t^2_{9i+2,\cdot}$:

$$|t^2_{9i+2,i-2}| \leq 0.0910; \quad |t^2_{9i+2,i-1}| \leq 0.2782; \quad |t^2_{9i+2,i}| \leq 0.2350,$$

and, thus

$$\sum_j |t^2_{9i+2,j}| \leq 0.6042.$$

Due to symmetries, the case $l = 5$ is absolutely analogous to the case $l = 2$.

It remains to look at the case $l = 8$, where we have the following situation:

$$\begin{pmatrix} t_{9i+8,3i+1} & t_{9i+8,3i+2} & t_{9i+8,3i+3} \end{pmatrix} \begin{pmatrix} t_{3i+1,i-1} & t_{3i+1,i} & 0 \\ t_{3i+2,i-1} & t_{3i+2,i} & t_{3i+2,i+1} \\ 0 & t_{3i+3,i} & t_{3i+3,i+1} \end{pmatrix} = \begin{pmatrix} - & + & - \end{pmatrix} \begin{pmatrix} + & + & 0 \\ - & + & - \\ 0 & + & + \end{pmatrix}.$$

According to the sign pattern of the $t_{i,j}$, both $t^2_{9i+8,i-1}$ and $t^2_{9i+8,i+1}$ are non-positive. If we assume that $t^2_{9i+8,i}$ is non-positive as well, and substitute the bounds for $t_{i,j}$ from the previous page, we derive that

$$\sum_j |t^2_{9i+8,j}| = -\sum_{j=i-1}^{i+1} t^2_{9i+8,j} \leq 0.6836.$$

Otherwise, if $t^2_{9i+8,i}$ is positive then we write

$$\begin{aligned} \sum_j |t^2_{9i+8,j}| = &-t_{9i+8,3i+1}(t_{3i+1,i-1} - t_{3i+1,i}) + t_{9i+8,3i+2}(-t_{3i+2,i-1} + t_{3i+2,i} - t_{3i+2,i+1}) \\ &- t_{9i+8,3i+3}(-t_{3i+3,i} + t_{3i+3,i+1}). \end{aligned}$$

While for the first and third term we can simply use the bounds for $t_{i,j}$, e.g.,

$$-t_{9i+8,3i+1}(t_{3i+1,i-1} - t_{3i+1,i}) \leq 0.3016(0.1616 - 0.1546) = 0.0021,$$

for the second term we use the previously established inequalities

$$t_{9i+8,3i+2} \leq 0.9366, \qquad -t_{3i+2,i-1} + t_{3i+2,i} - t_{3i+2,i+1} \leq 1.0318.$$

This leads to the desired estimate

$$\sum_j |t^2_{9i+8,j}| \leq 2 \cdot 0.0021 + 0.9366 \cdot 1.0318 = 0.9706.$$

This finishes the proof of the lemma. □

Lemma 2.3.4 assures that the spectral radius $\rho_s(M, 1)$ of the multi-scale transform M associated with $S_{med,3}$ is less than one. Applying Theorem 2.2.8 completes the proof of the theorem. □

2.3.3 Power-p Scheme

The univariate family of power-p schemes was introduced in [95]. These schemes are used for numerically solving hyperbolic PDEs, as well as for compression of piecewise smooth data. Given $p \in [1, \infty)$, the power-p subdivision operator $\mathcal{S}_p$ is defined by the formula

$$(\mathcal{S}_p v)_{2i} = v_i, \qquad (\mathcal{S}_p v)_{2i+1} = \frac{v_i + v_{i+1}}{2} - \frac{1}{8} H_p(\Delta^2 v_{i-1}, \Delta^2 v_i), \qquad i \in \mathbb{Z}, \tag{2.3.13}$$

where

$$H_p(x, y) = \begin{cases} \frac{x+y}{2}\left(1 - \left|\frac{x-y}{x+y}\right|^p\right), & xy > 0, \\ 0, & xy \le 0. \end{cases} \tag{2.3.14}$$

Each power-p subdivision scheme is convergent, with Hölder exponent 1 (see [95] for details). For $p \in [1, 2]$, $\mathcal{S}_p$ satisfies (2.3.1)-(2.3.2), meaning that those schemes are convexity preserving and their stability analysis has already been covered by Theorem 2.3.1. Furthermore, $\mathcal{S}_2$ coincides with the so-called PPH scheme [42, 71] whose stability in the sense of both S and M was settled also in [8].

Straightforward computations with $w := \Delta^2 v$ lead to

$$(\mathcal{S}_p^{[2]} w)_{2i} = \frac{1}{4} H_p(w_{i-1}, w_i), \qquad (\mathcal{S}_p^{[2]} w)_{2i+1} = \frac{w_i}{2} - \frac{1}{8}(H_p(w_{i-1}, w_i) + H_p(w_i, w_{i+1})). \tag{2.3.15}$$

Moreover, the formulae (see [61, Lemma 3.6])

$$\begin{aligned} \frac{\partial H_p}{\partial x}(x, y) = \phi(-t) &:= \begin{cases} 1/2(1 + (p-1)|t|^p - pt|t|^{p-2}), & |t| < 1 \\ 0, & |t| > 1 \end{cases} \in [0, p), \\ \frac{\partial H_p}{\partial y}(x, y) = \phi(t) &:= \begin{cases} 1/2(1 + (p-1)|t|^p + pt|t|^{p-2}), & |t| < 1 \\ 0, & |t| > 1 \end{cases} \in [0, p), \end{aligned} \tag{2.3.16}$$

where $t = (x - y)/(x + y)$, together with the convention $\partial H_p/\partial x(x, y) = \partial H_p/\partial y(x, y) = 0$, when $|t| = 1$ guarantee that for all $p \ge 1$ $\mathcal{S}_p \in \Sigma_2$ and

$$\|\mathcal{S}_p v - \mathcal{S}_p \tilde{v}\| \le \|v - \tilde{v}\| + \frac{p}{4}\|\Delta^2(v - \tilde{v})\|, \qquad \forall v, \tilde{v} \in \ell_\infty(\mathbb{Z}).$$

Thus, the stability analysis of $\mathcal{S}_p$ depends only on the value of the joint spectral radius $\rho_s(\mathcal{S}_p, 2)$. From (2.3.15) we derive the following expressions for the entries of $((D\mathcal{S}_p^{[2]})_w$:

$$\begin{aligned} ((D\mathcal{S}_p^{[2]})_w)_{2i,i-1} &= \frac{1}{4}\frac{\partial H_p}{\partial x}(w_{i-1}, w_i), & ((D\mathcal{S}_p^{[2]})_w)_{2i,i} &= \frac{1}{4}\frac{\partial H_p}{\partial y}(w_{i-1}, w_i), \\ ((D\mathcal{S}_p^{[2]})_w)_{2i+1,i-1} &= -\frac{1}{8}\frac{\partial H_p}{\partial x}(w_{i-1}, w_i), & ((D\mathcal{S}_p^{[2]})_w)_{2i+1,i+1} &= -\frac{1}{8}\frac{\partial H_p}{\partial y}(w_i, w_{i+1}), \\ ((D\mathcal{S}_p^{[2]})_w)_{2i+1,i} &= \frac{1}{2} - \frac{1}{8}\frac{\partial H_p}{\partial y}(w_{i-1}, w_i) - \frac{1}{8}\frac{\partial H_p}{\partial x}(w_i, w_{i+1}). \end{aligned}$$

Hence, in order to determine the submatrix $(D\mathcal{S}_p^{[2]})_w\Big|_{\{2i,2i+1,2i+2\}\times\{i-1,i,i+1\}}$, we just need to know $t := (w_{i-1} - w_i)/(w_{i-1} + w_i)$ and $\bar{t} := (w_i - w_{i+1})/(w_i + w_{i+1})$. Let us denote by

$$T := \frac{(\mathcal{S}_p^{[2]}w)_{2i} - (\mathcal{S}_p^{[2]}w)_{2i+1}}{(\mathcal{S}_p^{[2]}w)_{2i} + (\mathcal{S}_p^{[2]}w)_{2i+1}}, \qquad \bar{T} := \frac{(\mathcal{S}_p^{[2]}w)_{2i+1} - (\mathcal{S}_p^{[2]}w)_{2i+2}}{(\mathcal{S}_p^{[2]}w)_{2i+1} + (\mathcal{S}_p^{[2]}w)_{2i+2}}. \tag{2.3.17}$$

Our goal is to express both T and $\bar{T}$ in terms of t and $\bar{t}$. First, we use

$$H_p(w_{i-1}, w_i) = \begin{cases} w_i\frac{1-|t|^p}{1-t}, & |t| < 1, \\ 0, & |t| \geq 1, \end{cases} \qquad H_p(w_i, w_{i+1}) = \begin{cases} w_i\frac{1-|\bar{t}|^p}{1+\bar{t}}, & |\bar{t}| < 1, \\ 0, & |\bar{t}| \geq 1. \end{cases}$$

Note that, setting $t = -1$ and $\bar{t} = 1$ whenever $|t| \geq 1$, resp. $|\bar{t}| \geq 1$ allows us to use single expressions for both $H_p(w_{i-1}, w_i)$ and $H_p(w_i, w_{i+1})$. This trick and (2.3.15) lead to

$$T = \frac{(\mathcal{S}_p^{[2]}w)_{2i} - (\mathcal{S}_p^{[2]}w)_{2i+1}}{(\mathcal{S}_p^{[2]}w)_{2i} + (\mathcal{S}_p^{[2]}w)_{2i+1}} = \frac{-\frac{w_i}{2} + \frac{3w_i(1-|t|^p)}{8(1-t)} + \frac{w_i(1-|\bar{t}|^p)}{8(1+\bar{t})}}{\frac{w_i}{2} + \frac{w_i(1-|t|^p)}{8(1-t)} - \frac{w_i(1-|\bar{t}|^p)}{8(1+\bar{t})}},$$

and an analogous formula for $\bar{T}$, which, after cancelation of w_i and and the common denominators, give rise to

$$\begin{aligned} T &= \frac{-4(1-t)(1+\bar{t}) + 3(1-|t|^p)(1+\bar{t}) + (1-|\bar{t}|^p)(1-t)}{4(1-t)(1+\bar{t}) + (1-|t|^p)(1+\bar{t}) - (1-|\bar{t}|^p)(1-t)}, \\ \bar{T} &= \frac{4(1-t)(1+\bar{t}) - (1-|t|^p)(1+\bar{t}) - 3(1-|\bar{t}|^p)(1-t)}{4(1-t)(1+\bar{t}) - (1-|t|^p)(1+\bar{t}) + (1-|\bar{t}|^p)(1-t)}. \end{aligned} \tag{2.3.18}$$

Therefore, we can construct a map $\mathcal{T} : [-1,1) \times (-1,1] \to [-1,1) \times (-1,1]$, such that $\mathcal{T}(t,\bar{t}) = (T,\bar{T})$, that uses (2.3.18), whenever $|T|, |\bar{T}| < 1$ and sets $T = -1$, if $|T| \geq 1$, resp. $\bar{T} = 1$, if $|\bar{T}| \geq 1$.

A remark is necessary. Note that the objects T and $\bar{T}$ themselves are of no interest, and they will be used only as a tool to additionally simplify the analysis of $(D\mathcal{S}_p^{[2]})_w\Big|_{\{2i,2i+1,2i+2\}\times\{i-1,i,i+1\}}$, making it a function of two instead of three parameters! Therefore, even though we seem imprecise at some points (e.g., letting $t = -1$ and $\bar{t} = 1$, dividing by zero, when $w_i = 0$) and assign "artificial" values to T and $\bar{T}$ in cases when they are not defined with respect to (2.3.17), we do it in such a way that the entries of the submatrix remain the same (as can be easily verified by the reader)

$$(D\mathcal{S}_p^{[2]})_{\mathcal{S}_p^{[2]}w}\Big|_{\{4i+2,4i+3,4i+4\}\times\{2i,2i+1,2i+2\}} = \begin{pmatrix} \frac{1}{4}\phi(-T) & \frac{1}{4}\phi(T) & 0 \\ -\frac{1}{8}\phi(-T) & \frac{1}{2} - \frac{1}{8}\phi(T) - \frac{1}{8}\phi(-\bar{T}) & -\frac{1}{8}\phi(\bar{T}) \\ 0 & \frac{1}{4}\phi(-\bar{T}) & \frac{1}{4}\phi(\bar{T}) \end{pmatrix}.$$

From now on we work with $\mathcal{T}$. Let us first mention some of its properties. Due to symmetries $t \leftrightarrow -\bar{t}$ leads to $T \leftrightarrow -\bar{T}$. The points $(0,0)$ and $(-1,1)$ are fixed points of $\mathcal{T}$ (actually they are the only fixed points as shown in the Appendix). For $(t,\bar{t}) \in I := [-1,0] \times [0,1]$ we have that

$$|4(1-t)(1+\bar{t}) \pm (1-|t|^p)(1+\bar{t}) \mp (1-|\bar{t}|^p)(1-t)| \geq 3(1-t)(1+\bar{t}) \geq 3,$$

and, thus, $\mathcal{T}$ is continuous in I. Consider $w(\epsilon)|_{i-1,i,i+1} = \{\epsilon/(2-\epsilon), 1, \epsilon/(2-\epsilon)\}$, where $\epsilon \geq 0$, implying $t(\epsilon) = -1+\epsilon$, and $\bar{t}(\epsilon) = -t(\epsilon) = 1-\epsilon$. The spectral radius of the limit matrix

$$A = \lim_{\epsilon \to 0} (D\mathcal{S}_p^{[2]})_{w(\epsilon)}\big|_{\{2i,2i+1,2i+2\}\times\{i-1,i,i+1\}} = \begin{pmatrix} p/4 & 0 & 0 \\ -p/8 & 1/2 & -p/8 \\ 0 & 0 & p/4 \end{pmatrix} \tag{2.3.19}$$

equals $p/4$ and is greater than one, whenever $p > 4$.

Fix $t \in (-1, 0)$ and consider an initial sequence $\tilde{w}^0 := w^0|_{i-1,i,i+1}$ for which $t^0 = -\bar{t}^0 = t$ (for example $\tilde{w}^0 = \{(1+t)/(1-t), 1, (1+t)/(1-t)\}$). Then, according to (2.3.18) for any $j \in \mathbb{Z}$, $\tilde{w}^j = (S^{[2]})^j \tilde{w}^0$ has $t^j = -\bar{t}^j$, such that $t^j = T(t^{j-1})$, where

$$T(t) = \frac{t - |t|^p}{1-t}.$$

Obviously, $T : [-1, 0] \to [-1, 0]$ and monotonically increases, since $T'(t) = 2\phi(-t)/(1-t)^2$, and $\phi(t) \in [0, p]$. For $p > 4$, the function

$$F(t) := T(t) - t = \frac{t^2 - |t|^p}{1-t},$$

is continuous and nonnegative in $[-1, 0]$. Moreover, $F(t)$ is strictly positive in $(-1, 0)$.

Theorem 2.3.5. *For $p > 4$, $\mathcal{S}_p$ is not Lipschitz stable.*

Proof. To prove the theorem, we will show that $\rho_s(\mathcal{S}_p, 2) \geq p/4 > 1$, $\forall p > 4$. From the definition of joint spectral radius, it follows that in order $\rho_s(\mathcal{S}_p, 2)$ to be strictly less than $p/4$, for any ρ, such that $\rho_s(\mathcal{S}_p, 2) < \rho < p/4$, there should exist an integer $n = n(\rho)$, such that

$$\|DS^{[2]}_{w^{m-1}} DS^{[2]}_{w^{m-2}} \dots DS^{[2]}_{w^0}\| < \rho^m, \qquad \forall w^0 \in \ell_\infty(\mathbb{Z}),\ \forall m \geq n,$$

where $w^j = (\mathcal{S}_p^{[2]})^j w^0$. Therefore, it suffices to show that for any $1 < \rho < p/4$ and any $n \in \mathbb{N}$, there exists a sequence $w^0 = w^0(\rho, n) \in \ell_\infty(\mathbb{Z})$ with

$$\|DS^{[2]}_{w^{n-1}} DS^{[2]}_{w^{n-2}} \dots DS^{[2]}_{w^0}\| > \rho^n.$$

To do so, it is enough to work only with the restriction $\tilde{w}^0 = \{w^0_{-1}, w^0_0, w^0_1\}$ and to estimate $\|DS^{[2]}_{\tilde{w}^{n-1}} DS^{[2]}_{\tilde{w}^{n-2}} \dots DS^{[2]}_{\tilde{w}^0}\|$, which is a finite product of 3×3 matrices.

Fix $\rho \in (1, p/4)$. Since $\rho(A) = p/4$, for any $n \in \mathbb{N}$

$$\|A^n\| \geq (p/4)^n = (\rho + (p/4 - \rho))^n \geq \rho^n + n\rho^{n-1}(p/4 - \rho) \geq \rho^n + (p/4 - \rho).$$

Since for $t^0 \in (-1, 0)$, $F(t^0) > 0$ and $T(t^0) \in (-1, 0)$, we derive that for any initial $\tilde{u}$ defined via the pair $(t^0, \bar{t}^0 = -t^0)$ and any $j \in \mathbb{Z}$, the pair $(t^j, \bar{t}^j)$ that corresponds to $(S^{[2]})^j \tilde{u}$ satisfies $(t^{j-1}, 0) \ni t^j = -\bar{t}^j$, i.e., the sequence $\{t^j\}$ is monotonically increasing and bounded by zero.

Let us now redefine $\phi(t)$ in order to make it left-continuous, instead of right-continuous (e.g., $\phi(1) = p$, not $\phi(1) = 0$). Then $DS^{[2]}_{\tilde{u}} = A$, if $\tilde{u}$ is defined via the pair $(-1, 1)$. Note that

$f(x_1, x_2, \ldots, x_n) := \|x_1 x_2 \ldots x_n\|$ is a continuous function of its arguments. It is enough to sketch the proof for $n = 2$ and x_2. If $\|x_2 - \tilde{x}_2\| < \delta$, then

$$\delta\|x_1\| = \|x_1\|\|x_2 - \tilde{x}_2\| \geq \|x_1(x_2 - \tilde{x}_2)\| = \|x_1 x_2 - x_1\tilde{x}_2\| \geq \big|\|x_1 x_2\| - \|x_1\tilde{x}_2\|\big| = |f(x_1, x_2) - f(x_1, \tilde{x}_2)|.$$

Hence, considering the arguments to be 3×3 matrices, there exists $\epsilon > 0$, such that if $\|X_j - A\| < \epsilon$, $\forall j = 0, \ldots, n-1$, then $\|X_{n-1} X_{n-2} \ldots X_0\| > \rho^n + (p/4 - \rho)/2$.

On the other hand, the entries of $DS^{[2]}_{\tilde{w}}$ are continuous functions of $(t, \bar{t})$ in I, and so is the supremum norm. Therefore, there exists $\delta_1 > 0$, such that for any $\tilde{u}$ in $\mathcal{U} := (-1, -1 + \delta_1) \times (1 - \delta_1, 1)$, we have $\|DS^{[2]}_{\tilde{u}} - A\| < \epsilon$. Moreover, since $T^{n-1}(t) := T \circ T \underbrace{\circ \cdots \circ}_{n-2} T(t)$ is continuous and monotonically increasing for $t \in [-1, 0]$, and $T^{n-1}(-1) = -1$, there exists $\delta_2 > 0$, such that $t \in (-1, -1 + \delta_2)$ implies $T^{n-1}(t) \in (-1, -1 + \delta_1)$.

Now take $t^0 \in (-1, -1 + \delta_2)$. Then for the sequence $\tilde{w}^0$ that corresponds to the pair $(t^0, -t^0)$ we have that $\tilde{w}^j \in \mathcal{U}, \forall j = 0, \ldots, n-1$, and, thus,

$$\|DS^{[2]}_{\tilde{w}^{n-1}} DS^{[2]}_{\tilde{w}^{n-2}} \ldots DS^{[2]}_{\tilde{w}^0}\| > \rho^n + (p/4 - \rho)/2 > \rho^n. \tag{2.3.20}$$

Remark 2.2.5 completes the proof. The explicit computations can be found in the Appendix. □

In [61] it was proven that both $\mathcal{S}_p$ and its associated multi-scale transform are Lipschitz stable whenever $1 \leq p < 8/3$. For $p \in [8/3, 4]$, up to the knowledge of the author, the stability question remains open, and is a subject of future work. Some ideas and preliminary results can be found in the Appendix.

We finish the section with showing that the stability theorem from [21] is not applicable to the power-p subdivision. Following [61], suppose we were able to write

$$Sv = S_v v$$

with a Lipschitz continuous family of linear subdivision operators S_v, which are local 2-shift invariant and have order of polynomial reproduction 2. Then

$$S^{[2]}_w = (S_v)^{[2]} w \qquad w = \Delta^2 v,$$

where $(S_v)^{[2]}$ is another well-defined family of Lipschitz continuous, local, 2-shift invariant subdivision operators.

Then we must have

$$\left(S^{[2]}_w\right)_0 = \frac{1}{4} H_p(w_{-1}, w_0) = \sum_{|k| \leq L} a_k(v|_{[-L,L]}) w_{-k}$$

where the coefficient functions a_k represent the entries $\left((S_v)^{[2]}\right)_{0,-k}$ and are thus Lipschitz continuous.

Let us now specialize to sequences of the form

$$v_i = \begin{cases} y(i-1), & i \geq 1, \\ -xi, & i \leq 0. \end{cases}$$

Obviously $w_{-1} = x$, $w_0 = y$, $w_i = 0$ otherwise, and

$$H_p(x, y) = \tilde{a}_{-1}(x, y)x + \tilde{a}_0(x, y)y$$

with Lipschitz continuous $\tilde{a}_{-1}$ and $\tilde{a}_0$.
Now set $x = (1 + \alpha)y$ with fixed but arbitrary $\alpha > 0$, and let $y \to 0$:

$$\tilde{a}_{-1}(0, 0)(1 + \alpha) + \tilde{a}_0(0, 0) = \lim_{y\to 0} \frac{x + y}{2y}\Big(1 - \big(\frac{x - y}{x + y}\big)^p\Big) = \big(1 + \frac{\alpha}{2}\big)\Big(1 - \big(\frac{\alpha}{2 + \alpha}\big)^p\Big).$$

Such an identity can not hold for any $p \geq 1$. Indeed, for a non-integer $p > 1$ this is obvious, while for an integer $p \geq 2$ the right-hand side is a rational function of α with a non-trivial denominator, and thus can not coincide with the linear function from the left-hand side. For $p = 1$ we get

$$\tilde{a}_{-1}(0, 0)(1 + \alpha) + \tilde{a}_0(0, 0) = 1,$$

i.e., $\tilde{a}_{-1}(0, 0) = 0$, $\tilde{a}_0(0, 0) = 1$, which leads to a contradiction if we repeat the same exercise with $y = (1 + \alpha)x$.

3. ANALYSIS OF MULTIVARIATE SUBDIVISION SCHEMES VIA LOCAL MAPS

Extending upon the univariate Theorem 2.2.3, in Chapter 3 we analyze multivariate subdivision schemes and multi-scale transforms, using tools from local (polynomial) approximation theory. There are two major concepts [18] for analyzing a subdivision scheme, namely via its derived schemes [15, 37], or via a set of local subdivision maps [67]. Even though they seem intrinsically different, those two approaches characterize the subdivision process (convergence, smoothness, stability) in terms of the same quantity [18, 17]. The theory based on derived schemes has already been extended to higher dimensions on tensor-product grids, isomorphic to $\mathbb{Z}^s$ in both the linear [31, 15] and the non-linear [22, 50, 44] settings. Here we aim at exploring the "local subdivision maps" approach and its multivariate generalization. More precisely, we pick a bounded set $\lambda_0 \subset \mathbb{Z}^s$ and perform low-order-polynomial approximation on it. This, combined with the action of the subdivision operator S, induces a family of local maps, for which we compute the corresponding joint spectral radius to analyze convergence and stability of S, respectively. On $\mathbb{Z}^s$ the two approaches remain equivalent, and for linear schemes the one based on $S^{[k]}$ is numerically preferred, since it gives rise to a sequence of linear optimization problems [17, Section 4.6] each of which can be solved in finite (but in general also exponentially growing) time. However, linear programming is not applicable to nonlinear processes, plus, due to the specifics of the divided difference operator Δ^k, even for linear subdivision the computational time grows exponentially with the dimension s and the order k. Thus, considering the alternative approach for improving the numerical efficiency of the spectral radii estimations is justified. Moreover, as illustrated in [23, 53], the use of local maps is a step in the direction of developing tools for the analysis on semi-regular and even irregular subdivision schemes, where simple differencing can not be used.

Let us briefly recall some notions and fix the notation. Throughout the section we work only with scalar-valued data (the functional setting) and the initial sequence $v^0 : \Gamma^0 \to \mathbb{R}$ is uniformly bounded on the coarsest grid, i.e., $v^0 \in \ell_\infty(\Gamma^0)$. Everywhere but in Section 3.4 we consider all the grids Γ^j isomorphic to $\mathbb{Z}^s$, i.e., the regular tensor-product case, so we use this setting for the remaining definitions, as well. The subdivision operator $S : \ell_\infty(\mathbb{Z}^s) \to \ell_\infty(\mathbb{Z}^s)$ maps sequences corresponding to two consecutive grids into each other and is always assumed to be local and r-shift-invariant, i.e.,

$$S \circ T_i = T_{ri} \circ S, \qquad \forall i \in \mathbb{Z}^s,$$

where $(T_i v)_l = v_{i+l}$ is the translation operator, while the integer $r > 1$ coincides with the density of the grids, i.e., $\Gamma^j = r^{-j}\mathbb{Z}^s$. (In other words, S has a dilation matrix rI, where I is the $s \times s$ identity matrix). All the norms that we use are infinity-norms and hence we will simply denote them by $\|\cdot\|$. Whether the norm is on an operator, on a sequence, or on a function will be clear from the context. We use lowercase Greek letters $\alpha, \beta, \ldots$ to denote multi-indices in $\mathbb{Z}^s_+$ and all the

arithmetic operations on them are applied componentwise, e.g.,

$$\alpha = (\alpha_1, \dots, \alpha_s), \quad |\alpha| = \alpha_1 + \alpha_2 + \cdots + \alpha_s, \quad \alpha! = \alpha_1! \dots \alpha_s!, \quad x^\alpha = x_1^{\alpha_1} \dots x_s^{\alpha_s},$$

while lowercase Latin letters $i, l, \dots$ stay for multi-indices in $\mathbb{Z}^s$.

We use the multivariate analogues of (2.1.2), (1.1.1), (1.1.2) to define uniform convergence for S, stability of S, and stability of its associated multi-scale transform, respectively. For a given initial sequence $v^0 \in \ell_\infty(\mathbb{Z}^s)$ we will denote the limit function f from (2.1.2) (when it exists) by $S^\infty v^0$, and we will use f^j for the piecewise multi-linear interpolant of the data $S^j v^0$ with respect to $2^{-j}\mathbb{Z}^s$. We use $\{e_\ell\}_{\ell=1}^s$ for the orthonormal basis of $\mathbb{R}^s$ induced by $\mathbb{Z}^s$, i.e., $e_\ell = (0, \dots, 0, 1, 0, \dots 0) \in \mathbb{Z}^s$ with the only nonzero entry being the ℓ-th one. This allows us to extend the notion of finite differences to higher dimensions:

$$\Delta^1 : \ell_\infty(\mathbb{Z}^s) \to (\ell_\infty(\mathbb{Z}^s))^s, \qquad (\Delta^1 v)_i = \left\{ \Delta^1_{e_\ell} v_i := v_{i+e_\ell} - v_i : 1 \le \ell \le s \right\},$$

and, recursively, $\Delta^k = \Delta^{k-1} \circ \Delta^1$, $k > 1$. Defined that way $\Delta^k : \ell_\infty(\mathbb{Z}^s) \to (\ell_\infty(\mathbb{Z}^s))^{s^k}$. However, there are obvious redundancies, because of symmetries of the partial derivatives, e.g.,

$$\Delta^2_{e_1+e_2} := \Delta^1_{e_1} \circ \Delta^1_{e_2} = \Delta^1_{e_2} \circ \Delta^1_{e_1} = \Delta^2_{e_2+e_1},$$

that allow us to decrease the dimension of the vector-valued output and to work with the following operator, which we will again denote by Δ^k

$$\Delta^k = \{ \Delta^k_\alpha := \Delta^{\alpha_1}_{\alpha_1 e_1} \circ \cdots \circ \Delta^{\alpha_s}_{\alpha_s e_s} \mid |\alpha| = k \}.$$

For the above definition we used the coordinate representation $\alpha = \sum_{l=1}^s \alpha_l e_l$ as well as the convention $\Delta^n_{ne_l} = \Delta^1_{e_l} \circ \cdots \circ \Delta^1_{e_l}$. Thus, Δ^k acts on $(\ell_\infty(\mathbb{Z}^s))^{N_k}$, where $N_k = \binom{k+s-1}{s-1}$. We define the norm $\|\Delta^k v\|$ via

$$\|\Delta^k v\| = \sup_{i \in \mathbb{Z}^s} \|\Delta^k v_i\| = \sup_{i \in \mathbb{Z}^s} \max_{|\alpha|=k} |\Delta^k_\alpha v_i|. \tag{3.0.1}$$

In Chapter 2 we already saw that the standard analysis for univariate S is built upon the existence of derived scheme $S^{[1]}$ and the validity of the commutation formula (2.1.3). Indeed, S is uniformly convergent if $\rho_c(S, 1) = \rho(S^{[1]}) < 1$, and Lipschitz stable if $\rho_s(S, 1) = \rho(DS^{[1]}) < 1$, provided S is 1-differentiable. Moreover, due to regularity of $\Gamma^j = r^{-j}\mathbb{Z}$, the following equality

$$\frac{d}{dx} S^\infty v^0 = (rS^{[1]})^\infty \Delta^1 v^0; \quad \left(\frac{d}{dx}\right)^k S^\infty v^0 = (r^k S^{[k]})^\infty \Delta^k v^0; \qquad \forall v \in \ell_\infty(\mathbb{Z}),$$

holds whenever the k-th derived scheme $S^{[k]}$ is well-defined (see for example [31, Proposition 3.1] for the linear case), implying that the Hölder regularity of S is at least $s_\infty(S) \ge -\log_r \rho(S^{[k]})$. The standard analysis for multivariate S on $\Gamma^j = r^{-j}\mathbb{Z}^s$ follows the same recipe and, at least for convergence and smoothness of linear S, it has already been worked out [31, Sections 6 and 7]. However, the specifics of the operator Δ^k lead to significantly more computationally involved numerical verification of the convergence/smoothness criteria for $s > 1$. For instance, Δ^1 maps $\ell_\infty(\mathbb{Z})$ into itself, and for any finitely supported $w \in \ell_\infty(\mathbb{Z})$ there exists a $v \in \ell_\infty(\mathbb{Z})$ (actually a whole one-parameter family of v), such that $w = \Delta^1 v$, locally. On the other hand, Δ^1 maps $\ell_\infty(\mathbb{Z}^2)$

to the product space $(\ell_\infty(\mathbb{Z}^2))^2$, and furthermore, due to symmetry of partial derivatives, its image is a proper subspace of the latter (e.g., if $w = (w_1, w_2) \in (\ell_\infty(\mathbb{Z}^2))^2$ such that $\Delta v = w$ for some $v \in \ell_\infty(\mathbb{Z}^2)$, then $\Delta_y w_1 = \Delta_x w_2$). Thus, the definition (2.2.12) of $\rho_c(S, 1)$ needs to be restricted only to this image space, and in general $\rho(S^{[1]}|_\Delta) < \rho(S^{[1]})$, where by $\rho(S^{[1]}|_\Delta)$ we have denoted the above mentioned *restricted spectral radius* (RSR) (see [17] or [18] for complete theory on the subject). The strict inequality in the last equation, together with the bigger image space make the numerical algorithms, based on $S^{[k]}$ and used for the analysis of S, to blow up within the number of parameters. Below we try to "translate" the contractive properties of the derived schemes into the language of local maps, and to propose more condensed numerical schemes for the estimation of the corresponding spectral radii. As before, we concentrate on the convergence and the stability analysis of the subdivision scheme and leave the related smoothness analysis out.

3.1 Convergence

Proposition 3.1.1. *Let S be a stationary regular subdivision scheme, defined via an operator $S : \ell_\infty(\mathbb{Z}^s) \to \ell_\infty(\mathbb{Z}^s)$. If there exists a function $F : \ell_\infty(\mathbb{Z}^s) \to \mathbb{R}^+$, satisfying*

i) $\exists C_1 \in \mathbb{R}^+$, *such that*

$$\|f^1 - f^0\| \le C_1 F(v), \tag{3.1.1}$$

where f^1, f^0 are the piecewise linear interpolants of Sv, v on $2^{-1}\mathbb{Z}^s$, $\mathbb{Z}^s$, respectively;

ii) $\exists n \in \mathbb{N}$, $\rho \in (0, 1)$ *such that*

$$F(S^n v) \le \rho F(v); \tag{3.1.2}$$

iii) $\exists C_2 \in \mathbb{R}^+$, *such that*

$$F(v) \le C_2 \|v\|, \tag{3.1.3}$$

for any $v \in \ell_\infty(\mathbb{Z}^s)$, then S converges uniformly.

Proof. Fix a $v \in \ell_\infty(\mathbb{Z}^s)$. Since $C(\mathbb{R}^s)$ is a Banach space, we just need to show that $\{f^j\}_0^\infty$ is a Cauchy sequence. From (3.1.1) and (3.1.3) we obtain

$$\|Sv\| - \|v\| = \|f^1\| - \|f^0\| \le \|f^1 - f^0\| \le C_1 F(v) \le C_1 C_2 \|v\| \quad \Longrightarrow \quad \|Sv\| \le (1 + C_1 C_2)\|v\|.$$

Hence

$$\begin{aligned} \|f^{j+1} - f^j\| \le C_1 F(S^j v) &\le C_1 \rho^{[j/n]} F(S^{j-n[j/n]} v) \le C_1 \rho^{[j/n]} C_2 \|S^{j-n[j/n]} v\| \\ &\le \underbrace{C_1 C_2 (1 + C_1 C_2)^{n-1}}_{C<\infty} \|v\| \rho^{[j/n]} \le C \|v\| \rho^{[j/n]}. \end{aligned}$$

Since

$$\sum_{j=0}^{\infty} \rho^{[j/n]} = \frac{n}{1 - \rho},$$

for any $\epsilon > 0$ there exists a $N = N(\epsilon, v)$, such that

$$\sum_{j=N}^{\infty} \rho^{[j/n]} \leq \frac{\epsilon}{C\|v\|},$$

and thus, for any $l > m \geq N$ we have

$$\begin{aligned}\|f^l - f^m\| &\leq \|f^l - f^{l-1}\| + \|f^{l-1} - f^{l-2}\| + \cdots + \|f^{m+1} - f^m\| \\ &\leq C\|v\| \sum_{j=m}^{l-1} \rho^{[j/n]} \leq C\|v\| \sum_{j=N}^{\infty} \rho^{[j/n]} \leq C\|v\| \frac{\epsilon}{C\|v\|} = \epsilon.\end{aligned}$$

Hence, S uniformly converges. □

Introducing contractivity criteria with respect to a general function F is not a new idea. It has appeared in the literature, since the foundation of the subdivision theory, see for example [15, Chapter 3.1] or [31, Section 6]. There the authors use the terminology *S is contractive relative to F*, whenever (3.1.2) holds. In [4, 22], the authors also build their analysis on F-contractivity (in their notation F is replaced by δ), but our restrictions on F are more relaxed, and our analysis is more generally applicable in comparison to theirs. However, up to the knowledge of the author, even when the theory is based on the abstraction F mainly the standard choice $F(v) = \|\Delta^k v\|$ for some $k \in \mathbb{N}$, has been considered in the applications. The goal of this section is to replace measuring differences by measuring the order of local polynomial approximation, a method called *characterization by local oscillations* in the theory of function spaces.

Let $F,\ G : \ell_\infty(\mathbb{Z}^s) \to \mathbb{R}^+$. We say that F is *equivalent* to G ($F \cong G$) if there exist positive constants A and B, such that

$$A \cdot F(v) \leq G(v) \leq B \cdot F(v), \qquad \forall v \in \ell_\infty(\mathbb{Z}^s). \tag{3.1.4}$$

Obviously, $\cong$ is an equivalence relation, and if $G \cong F$, then G satisfies the conditions in Theorem 3.1.1 if and only if F does. Indeed,

$$\|f^1 - f^0\| \leq C_1 F(v) \leq \underbrace{C_1 B}_{C_1'} \cdot G(v), \quad G(Sv) \leq \frac{1}{A} F(Sv) \leq \underbrace{C_2/A}_{C_2'} \|v\|,$$

and

$$G(S^n v) \leq \frac{1}{A} F(S^n v) \leq \frac{\rho}{A} F(v) \leq \frac{B}{A} \rho G(v)$$

leads to

$$G(S^{ln} v) \leq \frac{B}{A} \rho^l G(v), \qquad \forall l \in \mathbb{N}.$$

Since $\rho < 1$, and A and B are fixed, there exists $l_0 \in \mathbb{N}$ such that $\mu := \rho^{l_0}(B/A) < 1$. Denote by $m := nl_0$. Then

$$G(S^m v) \leq \mu G(v).$$

Moreover, one can use different (but equivalent!) functions F_1, F_2, and F_3 in (3.1.1), (3.1.2), and (3.1.3) respectively.

The generic univariate example one should have in mind when trying to understand the usefulness of the definition above is the following: Let $\lambda_i := [i-l, i+l]$, $\forall i \in \mathbb{Z}$, where $l \in \mathbb{Z}_+$ is a fixed number, and let $\Lambda := \{\lambda_i : i \in \mathbb{Z}\}$. For any $v \in \ell_\infty(\mathbb{Z})$ consider

$$F(v) := \|\Delta^1 v\| \qquad \text{and} \qquad G(v) := \sup_{\lambda\in\Lambda} \Big\{ \inf_{a\in\mathbb{R}} \|(v - a\mathbf{1})\big|_\lambda\| \Big\}.$$

Then, direct computations show that

$$\frac{1}{2}F(v) \le G(v) \le lF(v),$$

and, thus, $F \cong G$.

Now let us generalize the example above. Let $\lambda_0 \subset \mathbb{Z}^s$ be a bounded neighborhood of 0 and let $\Lambda = \{\lambda_i := T_i\lambda_0 \ : \ i \in \mathbb{Z}^s\}$ consists of all integral shifts of λ_0. As before, if we denote by $\Pi_k(\mathbb{R}^s)$ the space of all polynomials on $\mathbb{R}^s$ of total degree less or equal to k, then for any $k \in \mathbb{N}$ and any $v \in \ell_\infty(\mathbb{Z}^s)$ we define

$$|\!|\!| v |\!|\!|_k := \sup_{\lambda\in\Lambda} \inf_{p\in\Pi_{k-1}(\mathbb{R}^s)} \|v\big|_\lambda - p\big|_\lambda\|. \tag{3.1.5}$$

Here $v|_\lambda = \{v_i : i \in \lambda\}$, and $p|_\lambda = \{p(i) : i \in \lambda\}$ stand for the projection of the data onto the finite set λ. Sometimes we will use the equivalent notation $\|v - p\|_\lambda$. It is an easy exercise to check that $|\!|\!| \cdot |\!|\!|_k$ is a seminorm. Note that it depends on λ_0, as well, but in order to keep the notation as simple as possible, this is not explicitly indicated. When λ_0 is too small, the above seminorm is trivially zero, and thus for our analysis we need to assure that λ_0 is sufficiently "rich". To do so, we introduce the simplex

$$\mathcal{T}_k := \{\beta \in \mathbb{N}^s \ : \ |\beta| \le k\}.$$

When $s = 1$, $\mathcal{T}_k$ is just the interval $[0, k]$. Note that for the analysis we develop in this chapter more general sets $\mathcal{T}_k$ can be used (e.g., affine transformations of the introduced simplex), but for the sake of simplicity we choose to formulate our results in terms of the $\mathcal{T}_k$ fixed above.

Lemma 3.1.2. *Fix $k \in \mathbb{N}$. Let λ_0 be any bounded set in $\mathbb{Z}^s$ that contains $\mathcal{T}_k$ (i.e., there exists an $N \in \mathbb{N}$ such that $\mathcal{T}_k \subseteq \lambda_0 \subseteq [-N, N]^s$). Let $\Lambda = \{\lambda_i = T_i\lambda_0 \ : \ i \in \mathbb{Z}^s\}$. Then*

$$\|\Delta^k \cdot\| \cong |\!|\!| \cdot |\!|\!|_k. \tag{3.1.6}$$

Proof. Let $v \in \ell_\infty(\mathbb{Z}^s)$ be arbitrary. Fix $i \in \mathbb{Z}^s$. Then, for any polynomial $p \in \Pi_{k-1}(\mathbb{R}^s)$ we have

$$\max_{|\alpha|=k} |\Delta^k_\alpha v_i| = \max_{|\alpha|=k} |\Delta^k_\alpha (v-p)_i| \le 2^k \|v - p\|_{T_i\mathcal{T}_k} \le 2^k \|v - p\|_{\lambda_i},$$

and, thus,

$$\|\Delta^k v\| \le 2^k \sup_{i\in\mathbb{Z}^s} \inf_{p\in\Pi_{k-1}(\mathbb{R}^s)} \|v - p\|_{\lambda_i} = 2^k |\!|\!| v |\!|\!|_k. \tag{3.1.7}$$

For the other direction, due to shift-invariance, it is enough to show that

$$\|(v - I_0^{k-1}v)\|_{\lambda_0} \le C\|\Delta^k v\|, \qquad \forall v \in \ell_\infty(\mathbb{Z}^s),$$

where $I_0^{k-1}v \in \Pi_{k-1}(\mathbb{R}^s)$ is the unique polynomial that interpolates v on $\mathcal{T}_{k-1}$, and C is a uniformly bounded constant, which depends on k and N, but not on v. Take $w\big|_{\lambda_0} := (v - I_0^{k-1}v)\big|_{\lambda_0}$.

In the univariate case the result follows by induction on the length of λ_0, since $w_0 = w_1 = \cdots = w_{k-1} = 0$, $w_k = \Delta^k w_0 = \Delta^k v_0$, and $w_{-1} = (-1)^k \Delta^k w_{-1} = (-1)^k \Delta^k v_{-1}$. Thus, the Abel transform gives rise to

$$w_j = \sum_{l=0}^{j-k} a_l^j \Delta^k v_l, \quad w_{-j+k-1} = \sum_{l=0}^{j-k} (-1)^k a_l^j \Delta^k v_{-1-l} \qquad \forall j \geq k,$$

with $C = \sum_{l=0}^{j-k} |a_l^j|$ depending only on j, and being uniformly bounded whenever $j \leq N$ is finite. Note that $j \geq k$ always holds, due to $\mathcal{T}_k = [0, k] \subseteq \lambda_0$. To find an explicit bound for C one may use the Newton's interpolating formula and derive

$$\begin{aligned} \|(v - I_0^{k-1} v)\|_{\lambda_0} = \|I_0^j v - I_0^{k-1} v\|_{\lambda_0} &\leq \sup_{x \in \lambda_0} \left(\left| \frac{\Delta^k v_0}{k!} \prod_{l=0}^{k-1} (x - l) \right| + \cdots + \left| \frac{\Delta^j v_0}{j!} \prod_{l=0}^{j-1} (x - l) \right| \right) \\ &\leq \frac{\|\Delta^k v\|}{k!} \prod_{l=0}^{k-1} (N + k - l) + \cdots + \frac{\|\Delta^j v\|}{j!} \prod_{l=0}^{j-1} (N + k - l) \qquad (3.1.8) \\ &\leq \sum_{l=k}^{j} \binom{N+k}{l} 2^{l-k} \|\Delta^k v\| \leq \frac{3^{N+k}}{2^k} \|\Delta^k v\|. \end{aligned}$$

For $s = 2$, since $w_{(i,0)} = 0,\ i = 0, \ldots, k-1$, the above univariate result gives rise to

$$|w_{(j,0)}| \leq A_0 \|\Delta^k_{(k,0)} v\| \leq A_0 \|\Delta^k v\|, \qquad \forall j \in [-N, N],$$

where A_0 depends on k and N, but not on v.

For the next row, we have $w_{(i,1)} = 0,\ i = 0, \ldots, k-2$ and $w_{(k-1,1)} = \Delta^k_{(k-1,1)} w_{(0,0)} = \Delta^k_{(k-1,1)} v_{(0,0)}$. Hence

$$w_{(k,1)} = \Delta^k_{(k,0)} w_{(0,1)} + k w_{(k-1,1)} = \Delta^k_{(k,0)} v_{(0,1)} + k \Delta^k_{(k-1,1)} v_{(0,0)},$$

and by induction every entry $w_{j,1}$, $j \in [-N, N]$ can be represented as a finite combination of k-order divided differences of v. Thus

$$|w_{(j,1)}| \leq A_1 \|\Delta^k v\|, \qquad \forall j \in [-N, N],$$

for some A_1 that depends on k and N but not on v. In the end, we derive that there exists uniform constants A_i such that

$$|w_{(j,i)}| \leq A_i \|\Delta^k v\|, \qquad \forall j \in [-N, N];\ \forall i = 0, 1, \ldots, k-1.$$

By symmetry, we have the same inequalities for $|w_{(i,j)}|$, too. Finally, we expand the argument to the whole square $[-N, N] \times [-N, N]$ and conclude that

$$\|(v - I_{0,0}^{k-1} v)\|_{\lambda_0} \leq \|(v - I_{0,0}^{k-1} v)\|_{[-N,N] \times [-N,N]} \leq C \|\Delta^k v\|, \qquad \forall v \in \ell_\infty(\mathbb{Z}^2),$$

with a constant C that depends on N and k, but not on v. Induction on s completes the proof. □

In practice, the element of best approximation is difficult to determine and there is no cheap algorithm for finding it. Therefore the following remark is important for applications.

Corollary 3.1.3. *Let P be a bounded and finite dimensional linear projector onto $\Pi_{k-1}(\mathbb{R}^s)$, i.e., there exists $N \in \mathbb{N}$, $B \in \mathbb{R}^+$, and a neighborhood $\mathcal{T}_k \subseteq \lambda_0 \subseteq [-N, N]^s$, such that for every $v \in \ell_\infty(\mathbb{Z}^s)$ $P : v\big|_{\lambda_0} \to \Pi_{k-1}(\mathbb{R}^s)\big|_{\lambda_0}$, for every $p \in \Pi_{k-1}(\mathbb{R}^s)$ $P(p\big|_{\lambda_0}) = p\big|_{\lambda_0}$, and $\|P\| \le B$. Then*

$$G(v, P) := \sup_{i \in \mathbb{Z}^s} \|v|_{T_i\lambda_0} - P(v|_{T_i\lambda_0})\| \cong \|\Delta^k v\|.$$

Indeed, in the proof of Lemma 3.1.2 we already showed that for any such neighborhood λ_0 we have $G(v, I_0^{k-1}) = \sup_{i\in\mathbb{Z}^s} \|v|_{T_i\lambda_0} - I_0^{k-1}(v|_{T_i\lambda_0})\| \le C\|\Delta^k v\|$. But

$$\|\!|v|\!\|_k \le G(v, P) = \sup_{i\in\mathbb{Z}^s} \|T_i v - I_0^{k-1}T_i v - P(T_i v - I_0^{k-1}T_i v))\|_{\lambda_0} \le (1 + \|P\|)G(v, I_0^{k-1}) \le C_1\|\Delta^k v\|,$$

and since $\|\!|\cdot|\!\|_k \cong \|\Delta^k \cdot\|$ the argument is completed. In the computations above we used the trivial identity $v|_{T_i\lambda_0} = (T_i v)|_{\lambda_0}$.

The following identity should be emphasized

$$G(v, I_0^{k-1}) \equiv \|\Delta^k v\|, \qquad \lambda_0 = \mathcal{T}_k, \tag{3.1.9}$$

meaning that the divided difference operator belongs to the class of projectors, considered in Corollary 3.1.3, and the corollary is an abstraction of the classical analysis via derived schemes.

In this form, Proposition 3.1.1 is often not applicable, because (3.1.1) is too restrictive. Indeed, being a difference between two consecutive refinements, the left-hand side is expected to be a function of the first divided difference $\|\Delta^1 v^0\|$, while if we want to use $F \cong \|\!|v^0|\!\|_k$ with $k > 1$, the right-hand-side is a function of $\|\Delta^k v^0\|$. Hence, in order for (3.1.1) to hold, if $v^0 = p|_{\mathbb{Z}^s}$ for some $p \in \Pi_{k-1}(\mathbb{R}^s)$ the right-hand side vanishes, and then the left-hand side should equal zero, as well. But the latter is not true, in general. For example, one can check that (3.1.1) with $F(v) = \|\Delta^2 v\|$ is not satisfied for the Chaikin scheme [16], while in [15, 31] it was shown that for this F (3.1.2) is still enough for convergence. Following arguments similar to those in Chapter 2, we will show that in many cases (3.1.1) is artificial and can be dropped. To achieve that, we work once again with the special class of k-offset-invariant schemes, defined in the multivariate setting via

$$S(v + p\big|_{\mathbb{Z}^s}) = Sv + q\big|_{r^{-1}\mathbb{Z}^s}, \tag{3.1.10}$$

where $p \in \Pi_{k-1}(\mathbb{R}^s)$ is arbitrary, and $q \in \Pi_{k-1}(\mathbb{R}^s)$ depends on p and has the property $p - q \in \Pi_{k-2}(\mathbb{R}^s)$.

Theorem 3.1.4. *Let $S : \ell_\infty(\mathbb{Z}^s) \to \ell_\infty(\mathbb{Z}^s)$ be local, r-shift and k-offset invariant, as well as bounded operator, i.e., there exists a constant $C \in \mathbb{R}$ such that for any $v \in \ell_\infty(\mathbb{Z}^s)$ $\|Sv\| \le C\|v\|$. Fix a bounded set $\lambda_0 \subset \mathbb{Z}^s$ that contains $\mathcal{T}_k$ and let $\Lambda = \{\lambda_i = T_i\lambda_0,\ i \in \mathbb{Z}^s\}$, where T_i is the translation operator on $\mathbb{Z}^s$. If there exists $n \in \mathbb{N}$ and $\rho \in (0, 1)$ such that*

$$\|\!|S^n v|\!\|_k \le \rho\|\!|v|\!\|_k, \qquad \forall v \in \ell_\infty(\mathbb{Z}^s), \tag{3.1.11}$$

then the associated subdivision scheme S is uniformly convergent.

Proof. To prove the theorem, we only need a replacement of (3.1.1) and then to apply Proposition 3.1.1 with $F = \|\!|\cdot|\!\|_k$, since (3.1.2) and (3.1.3) are covered by our assumptions.

Lemma 3.1.5. *If S is local, r-shift and k-offset invariant ($k \geq 1$), then*

$$\|\Delta^{k-1} Sv\| \leq \frac{1}{r^{k-1}} \|\Delta^{k-1} v\| + C_k \|\!| v |\!\|_k, \qquad \forall v \in \ell_\infty(\mathbb{Z}^s). \tag{3.1.12}$$

Proof. Fix an $i \in \mathbb{Z}^s$ and a big enough $\lambda \subset \mathbb{Z}^s$ that completely determines the sequence Sv on $\bar{\lambda} = T_i \mathcal{T}_{k-1}$. In other words, we can compute $(\Delta^{k-1} Sv)_i$, knowing only $v|_\lambda$. Obviously, since S is local and shift-invariant, λ is bounded and contains at least one translation of $\mathcal{T}_{k-1}$. Let this translation be $T_{i'}\mathcal{T}_{k-1}$ (for example for interpolatory schemes $i' = [i/r]$). For any $v \in \ell_\infty(\mathbb{Z}^s)$ let $p_i = I_{i'}^{k-1} v$ be the polynomial of total degree $k-1$ that interpolates v on $T_{i'}\mathcal{T}_{k-1}$. Then for every $\alpha \in \mathbb{Z}_+^s, |\alpha| = k-1$

$$|(\Delta_\alpha^{k-1} Sv)_i| = |(\Delta_\alpha^{k-1} S(v - p_i \mathbf{1} + p_i \mathbf{1}))_i| = |(\Delta_\alpha^{k-1} S(v - p_i \mathbf{1}))_i + \Delta_\alpha^{k-1} q_i|,$$

where $q_i \in \Pi_{k-1}(\mathbb{R}^s)$ has the same leading coefficients as p_i. But we know that for any s-variate polynomial $p = \sum_{|\beta| \leq k-1} a_\beta x^\beta$, $\Delta_\alpha^{k-1} p = (k-1)! r^{k-1} a_\alpha$. Thus, $\Delta_\alpha^{k-1} q_i = r^{-(k-1)} \Delta_\alpha^{k-1} p_i = r^{-(k-1)} \Delta_\alpha^{k-1} v_{i'}$. Therefore

$$|(\Delta_\alpha^{k-1} Sv)_i| \leq |(\Delta_\alpha^{k-1} S(v - p_i \mathbf{1}))_i| + r^{-(k-1)} |\Delta_\alpha^{k-1} v_{i'}| \leq 2^{k-1} C \|\!| v |\!\|_k + \frac{1}{r^{k-1}} |\Delta_\alpha^{k-1} v_{i'}|,$$

and thus

$$\|\Delta^{k-1} Sv\| \leq \frac{1}{r^{k-1}} \|\Delta^{k-1} v\| + 2^{k-1} C \|\!| v |\!\|_k.$$

The lemma is proved. □

We will show the proof of Theorem 3.1.4 only for $s = 1$. First, the existence of a global constant C such that $\|Sv\| \leq C\|v\|$ leads to the existence of a global constant $C_1 \geq 1$ (that depends on C and the length l of λ_0) such that $\|\!| Sv |\!\|_k \leq C_1 \|\!| v |\!\|_k$ for all $v \in \ell_\infty(\mathbb{Z})$. Indeed,

$$\|\!| Sv |\!\|_k = \sup_{i \in \mathbb{Z}} \inf_{p \in \Pi_{k-1}(\mathbb{R})} \|(Sv - p)\|_{\lambda_i}.$$

Let $\bar{\lambda}_0$ be the interval on $\mathbb{Z}$ that completely determines Sv on λ_0, i.e., $(Sv)|_{\lambda_0} = S(v|_{\bar{\lambda}_0})\big|_{\lambda_0}$. Such an interval exists and it is finite, due to the locality of the scheme. Moreover, since S is k-offset invariant, the support of S should be at least of length k, and so does the length of $\bar{\lambda}_0$. Let $\bar{\Lambda}$ be the collection of all integer shifts of $\bar{\lambda}_0$. Corollary 3.1.3 gives

$$\sup_{\bar{\lambda} \in \bar{\Lambda}} \inf_{p \in \Pi_{k-1}(\mathbb{R})} \|(v - p)\|_{\bar{\lambda}} \leq C' \sup_{\lambda \in \Lambda} \inf_{p \in \Pi_{k-1}(\mathbb{R})} \|(v - p)\|_\lambda, \qquad \forall v \in \ell_\infty(\mathbb{Z}), \tag{3.1.13}$$

where C' does not depend on v. Now take any $v \in \ell_\infty(\mathbb{Z})$ and let $\bar{p}$ be the element of best approximation of order k to v on $\bar{\lambda}_0$. Since S is k-offset invariant, there exists a $\bar{q} \in \Pi_{k-1}(\mathbb{R})$ such that

$$S(v - \bar{p})|_{\bar{\lambda}_0} = (Sv - \bar{q})|_{\lambda_0}.$$

Therefore

$$\begin{aligned} \inf_{p \in \Pi_{k-1}(\mathbb{R})} \|Sv - p\|_{\lambda_0} &\leq \|Sv - \bar{q}\|_{\lambda_0} = \|S(v - \bar{p})\|_{\bar{\lambda}_0} \\ &\leq C \|v - \bar{p}\|_{\bar{\lambda}_0} \leq C \sup_{\bar{\lambda} \in \bar{\Lambda}} \inf_{p \in \Pi_{k-1}(\mathbb{R})} \|v - p\|_{\bar{\lambda}} \\ &\leq C C' \sup_{\lambda \in \Lambda} \inf_{p \in \Pi_{k-1}(\mathbb{R})} \|v - p\|_\lambda = C_1 \|\!| v |\!\|_k. \end{aligned} \tag{3.1.14}$$

Since S is shift-invariant, the above result holds for every λ_i, and thus for the supremum over all i.

Let $m \in \mathbb{N}$ and let $m = m_1 n + m_2$, where $m_2 \in \{0, 1, \ldots, n-1\}$. Then for any $v \in \ell_\infty(\mathbb{Z})$

$$\|\!| S^m v |\!\|_k \le \rho^{m_1} \|\!| S^{m_2} v |\!\|_k \le C_1^{m_2} \rho^{m_1} \|\!| v |\!\|_k \le \underbrace{C_1^{n-1}/\rho}_{:=A} \underbrace{(\rho^{1/n})^m}_{:=\mu} \|\!| v |\!\|_k \le A\mu^m \|\!| v |\!\|_k, \tag{3.1.15}$$

where $\mu \in (0,1)$.

Now we are able to prove the theorem. When $k = 1$, the result follows from Proposition 3.1.1 and (3.1.13), since for a fixed $v \in \ell_\infty(\mathbb{Z})$

$$\begin{aligned} \|f^1 - f^0\| &= \sup_{i\in\mathbb{Z}} \max_{j\in\{0,\ldots,r-1\}} \left| (Sv)_{ri+j} - \frac{j}{r} v_{i+1} - \frac{r-j}{r} v_i \right| \\ &\le \sup_{i\in\mathbb{Z}} \|Sv - v_i \mathbf{1}\|_{\lambda_i'} \le \sup_{i\in\mathbb{Z}} C \|v - v_i \mathbf{1}\|_{\bar{\lambda}'_i} \le CG(v, I_0^1) \le C |\!\| v |\!\|_1, \end{aligned}$$

where $\lambda_i' = [r(i-1), r(i+1)]$, while $\bar{\lambda}'_i$ is the minimal interval on $\mathbb{Z}$ that completely determines Sv on λ_i'. S is local and r-shift-invariant, so $\bar{\lambda}'_i$ is of finite length and for any $j \in \mathbb{Z}$, $\bar{\lambda}'_j = T_{j-i} \bar{\lambda}'_i$.

For $k > 1$, combining Lemma 3.1.5 and (3.1.15), we derive

$$\|\Delta^{k-1} v^{j+1}\| \le \frac{1}{r^{k-1}} \|\Delta^{k-1} v^j\| + C_k |\!\| v^j |\!\|_k \le \frac{1}{r^{k-1}} \|\Delta^{k-1} v^j\| + C_k A \mu^j |\!\| v |\!\|_k, \qquad \forall j \in \mathbb{Z}.$$

Since j was arbitrary

$$\begin{aligned} \underbrace{\|\Delta^{k-1} v^j\|}_{d^j} &\le \frac{1}{r^{k-1}} d^{j-1} + C_k A \mu^{j-1} |\!\| v |\!\|_k \le \frac{1}{(r^{k-1})^2} d^{j-2} + \frac{C_k A \mu^{j-2}}{r^{k-1}} |\!\| v |\!\|_k + C_k A \mu^{j-1} |\!\| v |\!\|_k \le \ldots \\ &\le \frac{1}{(r^{k-1})^j} d^0 + C_k A |\!\| v |\!\|_k \left(\sum_{i=0}^{j-1} \frac{\mu^i}{(r^{k-1})^{j-1-i}} \right) \le \frac{|\!\| v |\!\|_{k-1}}{(r^{k-1})^j} \left(C + C_k B r \sum_{i=0}^{j-1} \left(\mu r^{k-1} \right)^i \right) \\ &\le C'' \tilde{\mu}^j |\!\| v |\!\|_{k-1}, \text{ where } \begin{cases} 1 > \tilde{\mu} > \mu & \text{if } \mu \ge 1/r^{k-1} \\ \tilde{\mu} = 1/r^{k-1} & \text{if } \mu < 1/r^{k-1} \end{cases}. \end{aligned} \tag{3.1.16}$$

Therefore

$$|\!\| v^j |\!\|_{k-1} \le C' \|\Delta^{k-1} v^j\| \le C' C'' \tilde{\mu}^j |\!\| v |\!\|_{k-1}$$

and, thus there exists $n' \in \mathbb{N}$ and $\tilde{\rho} \in (0,1)$ such that for any $v \in \ell_\infty(\mathbb{Z})$

$$|\!\| S^{n'} v |\!\|_{k-1} \le \tilde{\rho} |\!\| v |\!\|_{k-1}.$$

By induction, it follows that there exists $n'' \in \mathbb{N}$ and $\tilde{\tilde{\rho}} \in (0,1)$ such that for any $v \in \ell_\infty(\mathbb{Z})$

$$|\!\| S^{n''} v |\!\|_1 \le \tilde{\tilde{\rho}} |\!\| v |\!\|_1,$$

and we are again in the case $k = 1$.

In the multivariate setting ($s > 1$), the proof follows absolutely the same steps. There one just needs to replace lengths of intervals with sizes of bounded sets in $\mathbb{Z}^s$, and to argue that $\bar{\lambda}_0$ contains a shift of $\mathcal{T}_k$ instead of an interval of length k. The details are left to the reader. □

Remark 3.1.6. *The proof of Theorem 3.1.4 implies that whenever* (3.1.11) *holds for some triple* (n, k, ρ)*, it holds for a triple* $(n', 1, \rho')$*, too.*

Hence, for the sake of convergence, it suffices to work only with $\|\!|\cdot|\!\|_1$. However, if (3.1.11) holds for a triple (n, k, ρ), with $k > 1$, n may be much smaller than n', and thus, the numerical verification of (3.1.11) may be faster. Furthermore, using only $k = 1$ restricts the smoothness analysis of S to smoothness exponents < 1. Indeed, Lemma 2.2.1 can be extended to higher dimension, assuring that for any local, r-shift and k-offset invariant scheme S there exists the k-th derived scheme $S^{[k]}$, satisfying the commutation formula (2.1.3), and we already mentioned at the beginning of the chapter, that the Hölder regularity of S depends on the contractivity properties of $S^{[k]}$. Note that, the smoothness analysis does not depend on the representative of the equivalence class $\|\!|\cdot|\!\|_k$ used for verifying (3.1.11)! Usually, the higher the k, the smaller the ρ, and thus, the better the smoothness result.

If we restrict ourselves to the class of univariate, linear subdivision schemes, Theorem 3.1.4 is necessary and sufficient for uniform convergence (see [15, 31]).

The freedom of choosing different neighborhoods λ and an arbitrary linear projector P given by Theorem 3.1.4 may improve (in terms of speed and memory space) the efficiency of the numerical verification of (3.1.11). In particular, if λ_0 is the *invariant neighborhood* of S, i.e., the minimal neighborhood such that $S^\infty(v)\big|_{[0,1]^s}$ depends solely on $v^0|_{\lambda_0}$, (3.1.11) is equivalent to the problem of computing the joint spectral radius of an iterated function system (IFS) with r^s elements. To illustrate this, consider the power-p schemes (2.3.13). In the univariate case the invariant neighborhood is $\lambda_0 = [-2, 3]$, while for the bivariate generalizations we have $\lambda_0 = [-2, 3]^2$. For any linear projector P onto $\Pi_1(\mathbb{R}^2)$ we define four functions $F_i^P : \mathbb{R}^{33} \to \mathbb{R}^{33}$, $i = \{(0,0), (0,1), (1,0), (1,1)\}$ that map $v|_{\lambda_0} - P(v|_{\lambda_0})$ into $Sv|_{\lambda_i} - P(Sv|_{\lambda_i})$, respectively, where λ_i are the invariant neighborhoods of the four cells on $2^{-1}\mathbb{Z}^2$, contained in $[0, 1]^2$ (see Fig 3.1). We work on 33-dimensional vector space V, since the size of λ_0 is 36, while the range of P is of dimension $dim(\Pi_1(\mathbb{R}^2)) = 3$. Now (3.1.11) holds with $k = 2$ if and only if

$$\rho(F^P) := \limsup_{J\to\infty} \max_{i_1,\ldots,i_J\in\{1,2,3,4\}} \max_{\substack{w\in V\\ \|w\|=1}} \|F_{i_J}^P \circ F_{i_{J-1}}^P \circ \cdots \circ F_{i_1}^P w\|^{1/J} < 1. \tag{3.1.17}$$

Formula (3.1.17) links our results with the convergence analysis of linear subdivision schemes based on the estimation of the joint spectral radius (JSR) of a finite set of matrices derived from the mask of S [67, 56]. Indeed, the JSR is defined as (see [67] for more detail)

$$\rho(\mathcal{A}|_V) := \limsup_{J\to\infty} \max_{i_1,\ldots,i_J\in[0,1]^s} \left|\mathcal{A}_{i_1}|_V \cdot \ldots \cdot \mathcal{A}_{i_J}|_V\right|^{1/J}. \tag{3.1.18}$$

There $\{\mathcal{A}_i : i = 1, \ldots, 4\}$ is the collection of linear operators on $\ell_\infty(\lambda_0)$, s.t., $\mathcal{A}_0(v)$ is an algebraic adjoint operator of $(Sv)|_{\lambda_0}$ with respect to a certain bilinear form defined in [67], while the other three operators are the corresponding shifts of $\mathcal{A}_0(v)$ for the remaining subcells of $[0, 1]^2$. The space V is a finite-dimensional subspace of $\ell_\infty(\lambda_0)$, which is invariant under all $\mathcal{A}_i$, and $\{\mathcal{A}_i|_V\}$ is a collection of matrix representations of $\{\mathcal{A}_i\}$ with respect to a basis of V. The JSR analysis states that a linear scheme S is uniformly convergent if and only if $\rho(\mathcal{A}|_V) < 1$. Hence, our convergence analysis is a nonlinear extension of the JSR concept.

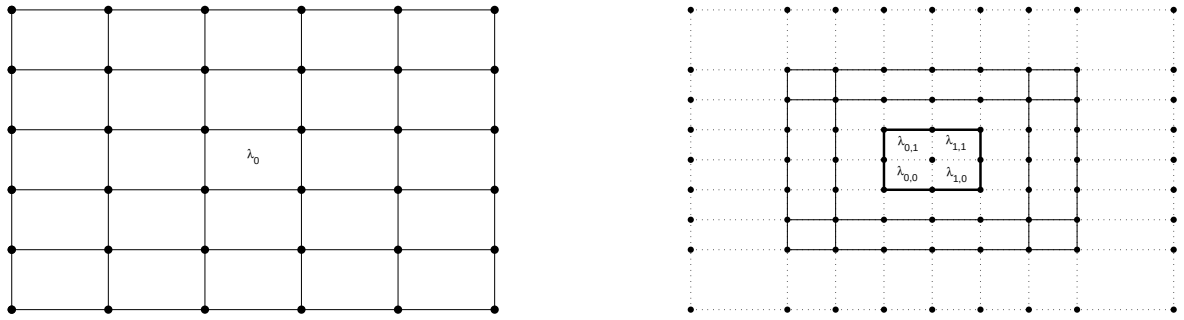

Fig. 3.1: The invariant neighborhood of $\lambda = [0,1]^2$ for the bivariate Power-p scheme, and the corresponding invariant neighborhoods of it successors after one step of subdivision.

Different choices for the projector P lead to different sets of functions F_i^P, and thus, to different joint spectral radius problems (regarding the fact that due to Theorem 3.1.4 all the answers will be the same). Smoothness analysis can be based on joint spectral radii, too [82]. The important thing to stress is that, unlike the operator $\Delta^k : \ell_\infty(\mathbb{Z}^s) \to (\ell_\infty(\mathbb{Z}^s))^{N_k}$, linear projectors P lead to local maps $\{F^P\}$ that remain endomorphisms, implying that the computation of the corresponding joint spectral radii is more efficient.

3.2 Stability

With the machinery developed in the previous section, we can obtain stability results, too. The only adjustment is that for stability one is not interested in the refinement of a single sequence $v \in \ell_\infty(\mathbb{Z}^s)$, but in the distance between two such refinements. The exposition in this section follows closely the previous one, and most of the proofs are skipped since they are analogous to the corresponding ones from the convergence analysis.

Proposition 3.2.1. *Let S be a stationary regular subdivision scheme, defined via an operator $S : \ell_\infty(\mathbb{Z}^s) \to \ell_\infty(\mathbb{Z}^s)$. If there exists a function $F : \ell_\infty(\mathbb{Z}^s) \to \mathbb{R}^+$, satisfying*

i) $\exists C_1 \in \mathbb{R}^+$, *such that*

$$\|Sv - S\tilde{v}\| \leq \|v - \tilde{v}\| + C_1 F(v - \tilde{v}); \tag{3.2.1}$$

ii) $\exists n \in \mathbb{N},\ \rho \in (0,1)$ *such that*

$$F(S^n v - S^n \tilde{v}) \leq \rho F(v - \tilde{v}); \tag{3.2.2}$$

iii) $\exists C_2 \in \mathbb{R}^+$ *independent of v, such that*

$$F(v) \leq C_2 \|v\|, \tag{3.2.3}$$

for all $v,\ \tilde{v} \in \ell_\infty(\mathbb{Z}^s)$, then S is (Lipschitz) stable.

Proof. Fix $J \in \mathbb{N}$, and two sequences $v,\ \tilde{v} \in \ell_\infty(\mathbb{Z}^s)$. (3.2.1) implies

$$\|S^J v - S^J \tilde{v}\| \le \|S^{J-1} v - S^{J-1}\tilde{v}\| + C_1 F(S^{J-1}v - S^{J-1}\tilde{v}) \le \cdots \le \|v - \tilde{v}\| + C_1 \sum_{j=0}^{J-1} F(S^j v - S^j \tilde{v}). \tag{3.2.4}$$

For any $j \in \mathbb{N}$, (3.2.2) gives rise to

$$F(S^j v - S^j \tilde{v}) \le \rho^{[j/n]} F(S^{j-n[j/n]} v - S^{j-n[j/n]} \tilde{v}), \tag{3.2.5}$$

and for every $i \in \{1, \dots, n-1\}$ we have

$$\begin{aligned} F(S^i v - S^i \tilde{v}) &\le C_2 \|S^i v - S^i \tilde{v}\| \le C_2\big(\|S^{i-1} v - S^{i-1}\tilde{v}\| + C_1 F(S^{i-1}v - S^{i-1}\tilde{v})\big) \\ &\le C_2(1 + C_1 C_2)\|S^{i-1} v - S^{i-1}\tilde{v}\| \le \cdots \le \underbrace{C_2(1 + C_1 C_2)^{n-1}}_{C<\infty} \|v - \tilde{v}\|. \end{aligned} \tag{3.2.6}$$

Finally, combining (3.2.4), (3.2.5), and (3.2.6) we derive

$$\begin{aligned} \|S^J v - S^J \tilde{v}\| &\le \|v - \tilde{v}\| + C_1 \sum_{j=0}^{J-1} F(S^j v - S^j \tilde{v}) \le \|v - \tilde{v}\| + C_1 C \|v - \tilde{v}\| \sum_{j=0}^{J-1} \rho^{[j/n]} \\ &\le \big(1 + C_1 C \sum_{j=0}^{\infty} \rho^{[j/n]}\big)\|v - \tilde{v}\| = \left(1 + \frac{n C_1 C}{1 - \rho}\right)\|v - \tilde{v}\|. \end{aligned} \tag{3.2.7}$$

The proof of Proposition 3.2.1 is completed. □

Theorem 3.2.2. *Let $S : \ell_\infty(\mathbb{Z}^s) \to \ell_\infty(\mathbb{Z}^s)$ be local, r-shift and k-offset invariant. Fix a bounded set $\lambda_0 \subset \mathbb{Z}^s$ that contains $\mathcal{T}_k$ and let $\Lambda = \{\lambda_i = T_i \lambda_0,\ i \in \mathbb{Z}^s\}$, where T_i is the translation operator on $\mathbb{Z}^s$. Assume that there exists a constant $C \in \mathbb{R}$ such that for any $v, \tilde{v} \in \ell_\infty(\mathbb{Z}^s)$ $\|Sv - S\tilde{v}\| \le C\|v - \tilde{v}\|$. Then, if there exists $n \in \mathbb{N}$ and $\rho \in (0,1)$ such that*

$$\|\!|S^n v - S^n \tilde{v}|\!\|_k \le \rho \|\!|v - \tilde{v}|\!\|_k, \qquad \forall v,\ \tilde{v} \in \ell_\infty(\mathbb{Z}^s), \tag{3.2.8}$$

S is Lipschitz stable.

Proof. We sketch the proof only for $s = 1$. Exactly as in the proof of Theorem 3.1.4 we show that the existence of a global constant C such that $\|Sv - S\tilde{v}\| \le C\|v - \tilde{v}\|$ leads to the existence of a global constant $C_1 \ge 1$ (that depends on C and the length l of λ) such that $\|\!|Sv - S\tilde{v}|\!\|_k \le C_1 \|\!|v - \tilde{v}|\!\|_k$ for all $v, \tilde{v} \in \ell_\infty(\mathbb{Z})$.

Then, letting $\mu = \rho^{1/n} \in (0,1)$, we derive that for any $v, \tilde{v} \in \ell_\infty(\mathbb{Z})$

$$\|\!|S^m v - S^m \tilde{v}|\!\|_k \le A \mu^m \|\!|v - \tilde{v}|\!\|_k, \qquad \forall m \in \mathbb{N}, \tag{3.2.9}$$

where A is a constant, that does not depend on v, $\tilde{v}$, or m.

The next observation is that (3.2.1) with $F = \|\!|\cdot|\!\|_1$ follows from the Lipschitz continuity of S. Indeed, fix $i \in \mathbb{Z}$ and let $\bar{\lambda}_i = [\bar{i}, \bar{i}+L]$ be the smallest interval that determines Sv_i (L is the support size of S). Then for any $v, \tilde{v} \in \ell_\infty(\mathbb{Z})$

$$\begin{aligned} |Sv_i - S\tilde{v}_i| &= |(Sv - v_{\bar{i}}\mathbf{1} + v_{\bar{i}}\mathbf{1} - S\tilde{v} + \tilde{v}_{\bar{i}}\mathbf{1} - \tilde{v}_{\bar{i}}\mathbf{1})_i| \\ &\le |v_{\bar{i}} - \tilde{v}_{\bar{i}}| + |\big(S(v - v_{\bar{i}}\mathbf{1}) - S(\tilde{v} - \tilde{v}_{\bar{i}}\mathbf{1})\big)_i| \\ &\le \|v - \tilde{v}\|_{\bar{\lambda}_i} + C\|v - \tilde{v} - (v - \tilde{v})_{\bar{i}}\mathbf{1}\|_{\bar{\lambda}_i} \\ &\le \|v - \tilde{v}\| + \tilde{C}\|\!|v - \tilde{v}|\!\|_1. \end{aligned} \tag{3.2.10}$$

For the last inequality we used Corollary 3.1.3. Since i was arbitrary

$$\|Sv - S\tilde{v}\| \le \|v - \tilde{v}\| + \tilde{C}\|\!|v - \tilde{v}|\!\|_1, \qquad \forall v, \tilde{v} \in \ell_\infty(\mathbb{Z}).$$

Now we are able to prove the theorem. When $k = 1$, using

$$\|\!|v|\!\|_1 \le \bar{C}\|\Delta^1 v\| \le 2\bar{C}\|v\|, \qquad \forall v \in \ell_\infty(\mathbb{Z})$$

the result follows from Proposition 3.2.1, where we have taken $F = \|\!|\cdot|\!\|_1$.

For $k > 1$ we use recursion and the following straightforward generalization of Lemma 3.1.5.

Lemma 3.2.3. *If $S : \ell_\infty(\mathbb{Z}^s) \to \ell_\infty(\mathbb{Z}^s)$ is local, r-shift and k-offset invariant ($k > 1$), then*

$$\|\Delta^{k-1}(Sv - S\tilde{v})\| \le \frac{1}{r^{k-1}}\|\Delta^{k-1}(v - \tilde{v})\| + C_k\|\!|v - \tilde{v}|\!\|_k, \qquad \forall v, \tilde{v} \in \ell_\infty(\mathbb{Z}). \tag{3.2.11}$$

Now, combining Lemma 3.2.3 and (3.2.9) we derive that for any $v, \tilde{v} \in \ell_\infty(\mathbb{Z})$

$$\|\Delta^{k-1}(S^j v - S^j \tilde{v})\| \le C''\tilde{\mu}^j\|\!|v - \tilde{v}|\!\|_{k-1}, \text{ where } \begin{cases} 1 > \tilde{\mu} > \mu & \text{if } \mu \ge 1/r^{k-1} \\ \tilde{\mu} = 1/r^{k-1} & \text{if } \mu < 1/r^{k-1} \end{cases}. \tag{3.2.12}$$

Therefore

$$\|\!|S^j v - S^j \tilde{v}|\!\|_{k-1} \le C'\|\Delta^{k-1}(S^j v - S^j \tilde{v})\| \le C'C''\tilde{\mu}^j\|\!|v - \tilde{v}|\!\|_{k-1}, \qquad \forall j \in \mathbb{N}$$

and, thus there exists $n' \in \mathbb{N}$ and $\tilde{\rho} \in (0, 1)$ such that for any $v, \tilde{v} \in \ell_\infty(\mathbb{Z})$

$$\|\!|S^{n'} v - S^{n'} \tilde{v}|\!\|_{k-1} \le \tilde{\rho}\|\!|v - \tilde{v}|\!\|_{k-1}.$$

By induction, it follows that there exists $n'' \in \mathbb{N}$ and $\tilde{\tilde{\rho}} \in (0, 1)$ such that for any $v, \tilde{v} \in \ell_\infty(\mathbb{Z})$

$$\|\!|S^{n''} v - S^{n''} \tilde{v}|\!\|_1 \le \tilde{\tilde{\rho}}\|\!|v - \tilde{v}|\!\|_1,$$

and we are again in the case $k = 1$. Like in Theorem 3.1.4, the case $s > 1$ is analogous. □

In the univariate case for $F = \|\Delta^k \cdot\|$, Theorem 3.2.2 is nothing else but Theorem 2.2.3, and Theorem 2.2.8 provides a recipe for the numerical verification of (3.2.8). As already explained in the previous chapter, it is based on estimating the joint spectral radius $\rho_s(S, k)$ of the first derivative of the k-th derived scheme. Up to the knowledge of the author, other functions have not been considered so far.

3.3 Example: Convergence of bivariate Power-p subdivision schemes

We demonstrate our local-map approach on a family of bivariate power-p subdivision schemes. First of all, in the univariate case (2.3.13) due to

$$|H_p(x,y)| \le \frac{|x+y|}{2}, \qquad \forall\, x,y \in \mathbb{R},$$

we conclude that for any sequence v and index i

$$\left|H_p(\Delta^2 v_{i-1}, \Delta^2 v_i)\right| \le \frac{|\Delta v_{i+1} - \Delta v_{i-1}|}{2} \le \max\{|\Delta v_{i-1}|, |\Delta v_{i+1}|\}.$$

Hence,

$$\|\Delta \mathcal{S}_p v\| \le \frac{5}{8}\|\Delta v\|, \qquad \forall v \in \ell_\infty(\mathbb{Z}),\ p \ge 1, \tag{3.3.1}$$

implying that every power-p scheme is convergent. Furthermore, one can show that the obtained limit functions are at least Lipschitz continuous, e.g., the smoothness of each of the schemes is 1.

The factor $5/8$ in (3.3.1) is sharp. However, if we limit the range of the parameter p, it can be improved. For example, precise computations involving the partial derivatives (2.3.16) of H_p give rise to $\|\Delta \mathcal{S}_p v\| \le \frac{1}{2}\|\Delta v\|$, whenever $p \le 4$, and that the contracting factor monotonically increases with $p \to \infty$. Therefore, the estimations below are not optimal, if p is fixed a priori.

In this section we consider two particular bivariate extensions of $\mathcal{S}_p$, which we prove to be uniformly convergent. The first one follows [22], where for any $\ell_\infty(\mathbb{Z}^2)$ and each pair $(i,j) \in \mathbb{Z}^2$ the authors define

$$\begin{aligned}
(\mathbb{S}_p v)_{2i,2j} &= v_{i,j};\\
(\mathbb{S}_p v)_{2i+1,2j} &= \frac{v_{i,j} + v_{i+1,j}}{2} - \frac{1}{8} H_p((\Delta_x^2 v_{\cdot,j})_{i-1}, (\Delta_x^2 v_{\cdot,j})_i);\\
(\mathbb{S}_p v)_{2i,2j+1} &= \frac{v_{i,j} + v_{i,j+1}}{2} - \frac{1}{8} H_p((\Delta_y^2 v_{i,\cdot})_{j-1}, (\Delta_y^2 v_{i,\cdot})_j);\\
(\mathbb{S}_p v)_{2i+1,2j+1} &= \frac{(\mathbb{S}_p v)_{2i,2j+1} + (\mathbb{S}_p v)_{2i+2,2j+1}}{2} - \frac{1}{8} H_p((\Delta_x^2 \mathbb{S}_p v_{2\cdot,2j+1})_{i-1}, (\Delta_x^2 \mathbb{S}_p v_{2\cdot,2j+1})_i).
\end{aligned} \tag{3.3.2}$$

In other words, we use the univariate $\mathcal{S}_p$ once horizontally for predicting the data on the horizontal midpoints of the old square grid, then vertically for predicting the data on the vertical midpoints of the old square grid, and finally horizontally again for predicting the data in the centers of the squares of the old grid by using the already predicted vertical midpoint data. In this setting one step of the first order divided difference operator is enough for proving convergence, meaning that we use Theorem 3.1.4, and Corollary 3.1.3 with (3.1.9). Indeed, from (3.3.1) we have

$$\max\left\{|(\Delta_x \mathbb{S}_p v_{\cdot,2j})_i|, |(\Delta_y \mathbb{S}_p v_{2i,\cdot})_j|\right\} \le \frac{5}{8}\|\Delta v\|, \qquad \forall i,j \in \mathbb{Z}. \tag{3.3.3}$$

Moreover, repeating one more time the above argument

$$\begin{aligned}
\left|(\mathbb{S}_p v)_{2i+1,2j+1} - (\mathbb{S}_p v)_{2i,2j+1}\right| &= \left|\frac{(\Delta_x \mathbb{S}_p v_{2\cdot,2j+1})_i}{2} - \frac{1}{8} H_p((\Delta_x^2 \mathbb{S}_p v_{2\cdot,2j+1})_{i-1}, (\Delta_x^2 \mathbb{S}_p v_{2\cdot,2j+1})_i)\right|\\
&\le \frac{5}{8}\|\Delta_x \mathbb{S}_p v_{2\cdot,2j+1}\|,
\end{aligned}$$

together with

$$|(\Delta_x \mathbb{S}_p v_{2\cdot,2j+1})_i| = |\Delta_x \mathbb{S}_p v_{2i+2,2j+1} - \Delta_x \mathbb{S}_p v_{2i,2j+1}| \le \Big|\frac{v_{i+1,j} - v_{i,j}}{2} + \frac{v_{i+1,j+1} - v_{i,j+1}}{2} - \frac{1}{8}\big(H_p((\Delta_y^2 v_{i+1,\cdot})_{j-1}, (\Delta_y^2 v_{i+1,\cdot})_j) - H_p((\Delta_y^2 v_{i,\cdot})_{j-1}, (\Delta_y^2 v_{i,\cdot})_j)\big)\Big| \le \frac{5}{4}\|\Delta v\|,$$

gives rise to

$$|(\Delta_x \mathbb{S}_p v_{\cdot,2j+1})_i| \le \frac{5}{8}\cdot\frac{5}{4}\|\Delta v\| \le \frac{25}{32}\|\Delta v\|. \tag{3.3.4}$$

Finally, we have

$$\begin{aligned}\big|(\mathbb{S}_p v)_{2i+1,2j+1} - (\mathbb{S}_p v)_{2i+1,2j}\big| =& \Big|\frac{(\mathbb{S}_p v)_{2i+2,2j+1} - v_{i+1,j}}{2} + \frac{(\mathbb{S}_p v)_{2i,2j+1} - v_{i,j}}{2} \\ &- \frac{1}{8}\big(H_p((\Delta_x^2 \mathbb{S}_p v_{2\cdot,2j+1})_{i-1}, (\Delta_x^2 \mathbb{S}_p v_{2\cdot,2j+1})_i) - H_p((\Delta_x^2 v_{\cdot,j})_{i-1}, (\Delta_x^2 v_{\cdot,j})_i)\big)\Big| \\ &\le \frac{\|\Delta_y \mathbb{S}_p v_{2(i+1),\cdot}\|}{2} + \frac{\|\Delta_y \mathbb{S}_p v_{2i,\cdot}\|}{2} + \frac{\|\Delta_x \mathbb{S}_p v_{2\cdot,2j+1}\|}{8} + \frac{\|\Delta_x v_{\cdot,j}\|}{8} \\ &\le \big(\frac{1}{2}\cdot\frac{5}{8} + \frac{1}{2}\cdot\frac{5}{8} + \frac{1}{8}\cdot\frac{5}{4} + \frac{1}{8}\big)\|\Delta v\| \le \frac{29}{32}\|\Delta v\|,\end{aligned}$$

which is equivalent to

$$|(\Delta_y \mathbb{S}_p v_{2i+1,\cdot})_j| \le \frac{29}{32}\|\Delta v\|. \tag{3.3.5}$$

Now, combining 3.3.3, 3.3.4, and 3.3.5 we conclude

$$\|\Delta \mathbb{S}_p v\| \le \frac{29}{32}\|\Delta v\|, \qquad \forall v \in \ell_\infty(\mathbb{Z}^2),\ p \ge 1. \tag{3.3.6}$$

This implies uniform convergence for the whole family $\mathbb{S}_p$, while [22, Theorem 4] assures smoothness for the limits of order at least $-\log_2(29/32) \approx 0.1420$. These results improve the one from [22] where convergence was proved only for $p \in [1, 4]$, and the minimal smoothness was ≈ 0.03. However, the smoothness factor is still far away from the conjectured Hölder regularity of order 1 for $\mathbb{S}_p$.

The second family of bivariate subdivision schemes $\{\mathbb{S}'_p\}$ we investigate is the "fully parallel" power-p one. The difference between $\mathbb{S}_p$ and $\mathbb{S}'_p$ is only in the choice of direction for predicting data in the centers of the squares of the coarse grid. For $\mathbb{S}_p$ horizontal directions were used, while for $\mathbb{S}'_p$ the main diagonals are considered:

$$(\mathbb{S}'_p v)_{2i+1,2j+1} = \frac{v_{i,j} + v_{i+1,j+1}}{2} - \frac{1}{8}H_p(\Delta_z^2 v_{i-1,j-1}, \Delta_z^2 v_{i,j}),$$

where $\Delta_z^2 v_{i,j} := v_{i,j} - 2v_{i+1,j+1} + v_{i+2,j+2}$. We call $\mathbb{S}'_p$ fully parallel, because we have three independent directions, and thus the entries $(\mathbb{S}'_p v)_{2i+1,2j}, (\mathbb{S}'_p v)_{2i,2j+1}, (\mathbb{S}'_p v)_{2i+1,2j+1}$ can be simultaneously computed. Using first-order divided difference operator Δ, the triangle inequality $|\Delta_z v_{i,j}| \le |(\Delta_x v_{\cdot,j+1})_i| + |(\Delta_y v_{i,\cdot})_j|$ and similar estimations as for $\mathbb{S}_p$ we derive

$$\|\Delta \mathbb{S}'_p v\| \le \frac{7}{8}\|\Delta v\|, \qquad \forall v \in \ell_\infty(\mathbb{Z}^2),\ p \ge 1. \tag{3.3.7}$$

Applied in this form, the operator Δ breaks the symmetry among the directions, since it captures Δ_x and Δ_y, but not Δ_z. Let us consider

$$F(v) := \sup_{i,j\in\mathbb{Z}} \{|\Delta_x v_{i,j}|, |\Delta_y v_{i,j}|, |\Delta_z v_{i,j}|\}, \qquad \forall v \in \ell_\infty(\mathbb{Z}^2)$$

instead. If we denote by $\lambda_0 = [0,1]\times[0,1]$, and take $P = I_0^0$, i.e., the linear projection $P(v|_{\lambda_0}) = v_{0,0}$, then $F(v) = G(v,P)$ and Corollary 3.1.3 implies $F \cong \|\Delta\|$. Now

$$\left|(\Delta_y \mathbb{S}'_p v_{2i+1,\cdot})_{2j}\right| = \left|\frac{(\Delta_y v_{i+1,\cdot})_j}{2} - \frac{1}{8}H_p(\Delta_z^2 v_{i-1,j-1}, \Delta_z^2 v_{i,j}) + \frac{1}{8}H_p((\Delta_x^2 v_{\cdot,j})_{i-1}, (\Delta_x^2 v_{\cdot,j})_i)\right| \le \frac{3}{4}F(v),$$

and due to symmetry we conclude

$$F(\mathbb{S}'_p v) \le \frac{3}{4}F(v), \qquad \forall v \in \ell_\infty(\mathbb{Z}^2),\ p \ge 1. \tag{3.3.8}$$

Therefore, by Theorem 3.1.4, the fully parallel family $\{\mathbb{S}'_p\}_{p\ge1}$ is uniformly convergent. Moreover, (3.3.8) assures smoothness of order $-\log_2(3/4) \approx 0.4150$ for each $\mathbb{S}'_p$, which is better than the $-\log_2(7/8) \approx 0.1926$ smoothness, guaranteed by (3.3.7). Again, we are still far away from proving Hölder regularity of order 1 for $\{\mathbb{S}'_p\}$. Finally, since there is a smooth local mapping that preserves $(0,0)$ and sends $(\pm1,0)$, $(0,\pm1)$, $(1,1)$ and $(-1,-1)$ into the vertices of a regular hexagon around the origin, F establishes a convergence and smoothness result also for $\mathbb{S}'_p$ applied on a regular triangular grid. There F coincides with the norm of the natural divided difference operator Δ for the setting. This last observation is further explored in the Section 3.4.

The stability analysis of $\{\mathbb{S}_p\}$ and $\{\mathbb{S}'_p\}$ is much more computationally involved and requires taking into account several consecutive levels of refinement. Hence, we do not do it. Of course, Theorem 2.3.5 tells us that for $p > 4$ both $\mathbb{S}_p$ and $\mathbb{S}'_p$ are not stable, but for small values of the parameter (even $p = 2$), up to our knowledge, the answer remains unknown. In [6] the Lipschitz stability of a relaxed version $\mathbb{S}_{rel}$ of $\mathbb{S}_2$ is established. The relaxation used there allows for the verification of a one-step contractivity property (3.2.8) for $\mathbb{S}_{rel}$, which in turn implies stability of the associated $\mathbb{S}_{rel}$ multi-scale transform. Even though numerical simulations suggest that the $\mathbb{S}_{rel}$ multi-scale transform inherits the useful practical properties (such as avoiding Gibbs-like phenomena, exhibiting high quality of the reconstructed image, etc.) of the $\mathbb{S}_2$ multi-scale transform (see [4]), it acts quite differently than the $\mathbb{S}_2$ multi-scale transform in presence of singularities, so no theoretical conclusions for the stability of $\mathbb{S}_2$ or its associate multi-scale transform can be drawn from the stability of the modified transform.

3.4 A note on semi-regular subdivision

This section is a step towards extending the regular tensor-grid subdivision analysis from Section 3.1 to subdivision schemes on semi-regular triangulated surfaces. Hence, throughout the section we only work with $s = 2$.

Let the triangulation Γ^0 be a a particular embedding on $\mathbb{R}^2$ of the topological set $\Phi_0 = (V_0, E_0, F_0)$ of vertices, edges, and "triangular" faces, meaning that the boundary of each of the

faces consists of exactly three edges, and each edge is entirely shared by two adjacent triangles. In practice one does not work with the whole plane but with some compact subset K of it. In order to avoid analysis on the boundary of K and for simplicity, it is assumed that our triangles cover a slightly bigger set K', which due to the locality of the subdivision operator leads to analysis equivalent to the one on $\mathbb{R}^2$. For each $j \in \mathbb{N}$ we obtain Γ^j from Γ^{j-1} via regular, dyadic refinement, i.e., by dividing each old triangle into four new ones, using the midpoints of its sides. Obviously, at all levels all the newly-inserted vertices in the refined triangulations are of valence six. Thus, even if the vertices of Γ^0 are of different valence (i.e., are *extraordinary* or *irregular*), their number is finite and after sufficiently many refinement steps they will all be well separated, meaning that for the purpose of analysis it is enough to consider only one extraordinary vertex in Γ^0 from the very beginning. From now on we work within this assumption and, as a consequence, all the grids Γ^j are topologically equivalent, having only one extraordinary vertex. Hence, we can drop the indices and once again define a stationary, local subdivision operator $S : \ell_\infty(\Gamma) \to \ell_\infty(\Gamma)$, such that for every real sequence v^0 on Γ^0 and every $j \in \mathbb{N}$, $v^j = S^j v^0$ is a real sequence on Γ^j. This process is known as semi-regular subdivision, and in this section we will consider only shift and 1-offset invariant operators S. (Here, by shift-invariance we mean, that the action of S depends only on the topology of Γ, but not on the shape of the particular triangles.) For more general theory see [90].

For any vertex $\nu \in V_\Gamma$, we define the set of all adjacent vertices by $\lambda_\nu := \{\mu \in V_\Gamma : (\nu, \mu) \in E_\Gamma\}$ and refer to it as *the topological 1-ring* of ν. Analogously, we can define the *geometrical 1-ring* of ν $\lambda'_\nu \subset \Gamma$, by replacing adjacent vertices with adjacent faces. In order to simplify the notation, we will refer to both of them as the 1-ring of ν, will denote them via λ_ν, and it will be clear from the context which one we consider. Let $\Lambda := \{\lambda_\nu \ : \ \nu \in V_\Gamma\}$. For every $e = (\nu_1, \nu_2) \in E_\Gamma$ we can define first-order divided difference $\Delta v_e := |v_{\nu_1} - v_{\nu_2}|$, and $\|\Delta v\| := \sup_{e \in E_\Gamma} \Delta v_e$. As in Section 3.1, we can obtain $\|\Delta v\|$ via the action of the interpolating operator I^0_ν on $v|_{\lambda_\nu}$, and immediately derive

$$\|\Delta v\| = G(v, I^0) = \sup_{\nu \in V_\Gamma} \|v - v_\nu \mathbf{1}\|_{\lambda_\nu} \le 2\|v\|, \qquad \forall v \in \ell_\infty(V_\Gamma).$$

Constant reproduction does not depend on the geometry of Γ, so we can think of Γ being the three-directional mesh with vertices in $\mathbb{Z}^2$, discussed at the end of the previous section, away from the extraordinary vertex where some adjustments are made. Hence, defining

$$\|\!|v|\!\|_1 := \sup_{\nu \in V_\Gamma} \inf_{c \in \mathbb{R}} \left| v|_{\lambda_\nu} - c\mathbf{1}|_{\lambda_\nu} \right|,$$

and showing that $\|\Delta v\| \cong \|\!|v|\!\|_1$ follows from Section 3.1. Moreover if $\|Sv\| \le C\|v\|$ for all v, we have that (3.1.1) and (3.2.1) are always satisfied with $F = \|\!|\cdot|\!\|_1$, and that there exists C_1, such that $\|\!|Sv|\!\|_1 \le C_1 \|\!|v|\!\|_1$. Let us, for sake of complicity, repeat the argument for the validity of (3.1.1).

$$|f^1 - f^0| = \sup_{\nu \in V_\Gamma} \|Sv - v_\nu \mathbf{1}\|_{\lambda'_\nu} \le C \sup_{\nu \in V_\Gamma} \|v - v_\nu \mathbf{1}\|_{\bar{\lambda}'_\nu} \le C' \|\!|v|\!\|_1.$$

Here, for every $\nu \in V_\Gamma$, λ'_ν is the topological 2-ring of ν', where ν' is the vertex on Γ^1 that corresponds to the vertex ν on Γ^0, e.g., in the regular case $\Gamma = \mathbb{Z}^s$, $\nu' = 2\nu$. The set $\bar{\lambda}'_\nu$ is the minimal one that determines Sv on λ'_ν. Due to the existence of an irregular vertex, we don't always have that $\bar{\lambda}'_\mu$ is topologically equivalent to $\bar{\lambda}'_\nu$, for $\mu \ne \nu \in \Gamma$. However, the latter is true away from the extraordinary point, leaving us with only finitely many topologically different elements $\bar{\lambda}'_{\nu_i}$.

Moreover, since S is local and the extraordinary vertex has finite valence, there exists a constant $L \in \mathbb{N}$, such that for any i, $\bar{\lambda'}_{\nu_i}$ is contained in the corresponding L-ring of ν_i, leading to

$$\sup_{\nu \in V_\Gamma} \|v - v_\nu \mathbf{1}\|_{\bar{\lambda'}_\nu} \leq L \|\!| v |\!\|_1.$$

Now, it is straightforward to extend our previous results to semi-regular triangulations.

Theorem 3.4.1. *Let S be a local, shift and 1-offset invariant subdivision operator on a semi-regular mesh. Assume that there exists a constant $C \in \mathbb{R}$ such that for any $v \in \ell_\infty(V_\Gamma)$, $\|Sv\| \leq C\|v\|$. If there exists $n \in \mathbb{N}$, $\rho \in (0,1)$ and a function $F \cong \|\!| \cdot |\!\|_1$ such that*

$$F(S^n v) \leq \rho F(v), \qquad \forall v \in \ell_\infty(V_\Gamma) \tag{3.4.1}$$

then the associated subdivision scheme S is uniformly convergent.

Moreover, if there exists a constant $C' \in \mathbb{R}$ such that for any $v, \tilde{v} \in \ell_\infty(\Gamma)$, $\|Sv - S\tilde{v}\| \leq C'\|v - \tilde{v}\|$ and if there exist $\tilde{n} \in \mathbb{N}$ and $\tilde{\rho} \in (0,1)$ satisfying

$$F(S^{\tilde{n}} v - S^{\tilde{n}} \tilde{v}) \leq \tilde{\rho} F(v - \tilde{v}), \qquad \forall v, \tilde{v} \in \ell_\infty(\Gamma) \tag{3.4.2}$$

then S is Lipschitz stable.

As discussed in Section 3.1, the verification of (3.4.1) and (3.4.2) can be done through estimating the joint spectral radius of an IFS. Away from the extraordinary point, we have the same picture as before - a set of finitely many functions $\{F_i^P\}$. However, the analysis becomes more technical close to the irregular vertex [86, 78]. For instance, the smoothness analysis heavily depends on the geometry of Γ and we will not consider it here. The interested reader may refer to the work of Weinmann [106, 107, 108].

Lemma 3.1.5 and Lemma 3.2.3 are based on the operator Δ^k, which heavily depends on the regularity of the grids Γ^j. Thus, those results cannot be extended to the semi-regular case and we do not have a proof for Theorem 3.4.1 with $F \cong \|\!| \cdot |\!\|_k$. However, [53] suggests that the problem might be only due to the technique we use for the analysis, while the result may still be true. There, the author is interested in analyzing convergence and smoothness of multivariate subdivision schemes, defined on even irregular meshes. As we already mentioned in the beginning of the chapter, the smoothness analysis in the regular setting is built on the existence of derived schemes $S^{[k]}$ because it approximates the k-th derivatives of the generated via S limit functions. Thus, in general one needs a local operator defined as a linear combination of discrete values which would converge to the k-th order derivative of a multivariate function as the underlying mesh size goes to zero on an arbitrary (irregular) mesh. The latter can be achieved if one replaces the finite divided difference operator with a standard divided difference operator, related to the multivariate Lagrange interpolation. For instance, on any set $\lambda \in \Gamma^0 \subset \mathbb{R}^s$ (called *stencil* in [53]) of cardinality $\dim(\Pi_k(\mathbb{R}^s))$ that admits interpolation, i.e., there exists a unique polynomial $p \in \Pi_k(\mathbb{R}^s)$, such that $p|_\lambda = v|_\lambda$ for all $v \in \ell_\infty(\Gamma^0)$, one can define operator $D^k(\lambda)$ satisfying

$$D^k_\alpha(\lambda) v = \frac{a_\alpha}{\alpha!}, \qquad \forall \alpha \in \mathbb{Z}^s_+ \ : \ |\alpha| = k, \tag{3.4.3}$$

where $p = \sum_{|\beta|\le k} a_\beta x^\beta$. Note, that in the univariate regular case $\Gamma^j = r^{-j}\mathbb{Z}$ all the stencils are of the type $\lambda_i = [i, i+k]$ and $r^{-kj}D^k(\lambda_i)v = \Delta^k v_i$. In general, whenever the grids $\{\Gamma^j\}$ are nested and if for every $j \in \mathbb{N}$ there exists a special set Λ^j that covers Γ^j and is a *normal collection of stencils for a homogeneous multi-level grid* they prove that the straightforward extension of the left-hand-side of the last univariate, regular equality remains equivalent to $\|\!|v|\!\|_k$ with respect to the notation in Section 3.1. More precisely [53, Lemma 22], together with (3.4.3) implies that for any finite set $\lambda^* \subset \Gamma^j$ and for any covering connected collection $\Lambda^* \subset \Lambda^j$ for it

$$A \sup_{\lambda\in\Lambda^*} [diam(\lambda^*)]^k \|D^k(\lambda)v\| \le \inf_{p\in\Pi_k(\mathbb{R}^s))} \|v-p\|_{\lambda^*} \le B \sup_{\lambda\in\Lambda^*} [diam(\lambda^*)]^k \|D^k(\lambda)v\|,$$

holds for any $v \in \ell_\infty(\Gamma^j)$. Furthermore, for k-offset invariant interpolatory (but possibly nonlinear!) S there exist k-th derived scheme $S^{[k]}$ that satisfies a general commutation formula (2.1.3) with respect to D^k, and convergence criteria in the vicinity of Theorem 3.4.1 (see [53, Theorem 24]). The result is considerably weaker than Theorem 3.1.4, but illustrates that the local map approach can be a useful tool for analyzing irregular subdivision, too.

We finish the section with one last remark. Corollary 3.1.3 gives room for further generalizations of $G(v, P)$. E.g., let $\Lambda = \{\lambda_i : i \in \mathbb{Z}^s\}$ covers the whole $\mathbb{R}^s$, and let there exist $N \in \mathbb{N}$, satisfying $T_i\mathcal{T}_k \subseteq \lambda_i \subseteq [i-N, i+N]^s$, $\forall i$. Consider a family $\mathcal{P} = \{P_i : v|_{\lambda_i} \to \Pi_{k-1}(\mathbb{R}^s)|_{\lambda_i}\}$ of linear projectors onto $\Pi_{k-1}(\mathbb{R}^s)$, and assume that there exists $C \in \mathbb{R}$ with $\|P_i\| \le C$ for all $i \in \mathbb{Z}^s$. Then

$$\|\Delta^k v\| \cong G(v, \mathcal{P}) := \sup_i \|v - P_i v\|_{\lambda_i}, \qquad \forall v \in \ell_\infty(\mathbb{Z}^s).$$

So far we considered only the shift-invariant setting $\lambda_i = T_i\lambda_0$ with only one projector involved, i.e., $P_i = P_0 \circ T_i$. A natural question is whether we can benefit from the more degrees of freedom in $G(\cdot, \mathcal{P})$. For example, if we are given a finite set of projectors $\{P^j\}_1^L$, v is fixed, and if for every subset λ_i we cleverly choose an optimal projector (in some sense) P^{j_i} and set $P_i := T_i P^{j_i}$. Then is contracting property of the type (3.1.2) still enough to claim convergence? Since the choice of projectors depends on the data, the question is to some extend equivalent to the following one: if $\Lambda = \{T_i\lambda_0\}$, P_1, P_2 are two projectors acting on λ_0, and

$$G(S^n v, P_1) \le \rho G(v, P_2), \qquad \forall v \in \ell_\infty(\mathbb{Z}^s)$$

holds together with (3.1.1) and (3.1.3), then is S uniformly convergent? The answer is negative. Indeed, take $s = k = 1$, $Sv_{2i} = Sv_{2i+1} = v_i$, $\lambda_0 = [0, 1]$, and let P_1, P_2 correspond to the polynomial of best approximation of order 1 (i.e., $P_1(v) = (v_0+v_1)/2$), respectively the interpolating polynomial at 0 (i.e., $P_2(v) = v_0$). Then, $G(\cdot, P_1) \equiv \|\!|\cdot|\!\|_1$ and $G(\cdot, P_2) \equiv \|\Delta v\|$. For any $v \in \ell_\infty(\mathbb{Z})$, $\|\!|v|\!\|_1 = \|\Delta v\|/2$ and for any $n \in \mathbb{N}$, $\|\!|S^n v|\!\|_1 = \|\!|v|\!\|_1$. Hence $G(S^n v, P_1) = G(v, P_2)/2$, but S does not converge.

4. NORMAL MULTIRESOLUTION

4.1 Introduction, mathematical formulation, and literature review

Normal multi-scale transforms (MTs) for curves and surfaces were firstly introduced in [55]. Since then, they have been used for multi-scale representation and compression of geometric objects [68, 76, 43], for adaptive approximation of level curves [12], in image analysis [66, 1, 65, 98, 99], and recently for interface tracking [92]. They allow efficient computational processing of high dimensional data and support progressive reconstruction, which makes them useful also for streaming applications in networked environments. Roughly speaking, the normal MT works as follows: given a (continuous, smooth) curve $\mathcal{C}$ in $\mathbb{R}^2$, resp. surface $\mathcal{S}$ in $\mathbb{R}^3$, an initial (discrete) sequence of vertices $\mathbf{v}^0 \subset \mathcal{C}$, resp. triangular mesh of vertices $\mathbf{v}^0 \subset \mathcal{S}$ is fixed. Then the coarse-scale data $\mathbf{v}^0$ is refined level by level via first predicting a new, denser data set via a univariate linear subdivision operator S applied componentwise, and then adjusting the finer-scale data so that it lies on the curve, resp. on the surface (see Fig. 4.1 for the 2D case). Analytically, one-level refinement is described by

$$\mathbf{v}^j = S\mathbf{v}^{j-1} + d^j\hat{\mathbf{n}}^j, \qquad \forall j \in \mathbb{N}. \tag{4.1.1}$$

For the "adjustment" (and, thus, for the reconstruction of $\mathbf{v}^j$ from $\mathbf{v}^{j-1}$) a set of unit "normals" $\hat{\mathbf{n}}^j$ (typically unit normal vectors with respect to the edges of the polygonal line associated with $\mathbf{v}^{j-1}$, resp., to the faces of the triangulated surface) are used, and sequences of scalar "details" d^j are stored. In the analysis step, a new point $\mathbf{v}^j = S\mathbf{v}^{j-1} + d^j\hat{\mathbf{n}}^j$ resp. detail coefficient d_i^j requires the determination of intersection points of the "normal lines" $S\mathbf{v}_i^{j-1} + t\hat{\mathbf{n}}_i^j$ with $\mathcal{C}$, resp. $\mathcal{S}$.

In our thesis, we deal only with normal MT for curves, so from now on all the definitions will be with respect to this setting. Let us first explain the general setup and its specifics in more detail. Due to the different nature of data and details, and the fact that the unit normal directions $\hat{\mathbf{n}}^j$ depend in a nonlinear way on the coarse-scale data $\mathbf{v}^{j-1}$, the normal MT

$$\mathcal{C} \quad \longleftrightarrow \quad \{\mathbf{v}^0, d^1, d^2, \ldots\},$$

given by (4.1.1) is a nonlinear transform, and its mathematical analysis is nontrivial. Unlike other MTs, the decomposition (analysis) part of the normal MT, which is the part we deal mostly with, is a coarse-to-fine procedure. We start with a finite number N of distinct points on $\mathcal{C}$: $\mathbf{v}_i^0 = \mathbf{v}(s_i^0)$, $i = 0, \ldots, N-1$, which we assume linearly ordered w.r.t. arc-length, i.e., $s_0^0 < s_1^0 < \ldots < s_{N-1}^0 < s_0^0 + L$. Extending with period N, we get two sequences $\mathbf{v}^0 = (\mathbf{v}_i^0)_{i\in\mathbb{Z}}$ and $s^0 = (s_i^0)_{i\in\mathbb{Z}}$ (i.e., $\mathbf{v}_{i+N}^0 = \mathbf{v}_i$ and $s_{i+N}^0 = s_i^0 + L$ for all $i \in \mathbb{Z}$) which correspond to the coarsest scale $j = 0$ in the normal MT. To find the finer scale representations $\mathbf{v}^j$ and s^j, $j \geq 1$, with the properties $\mathbf{v}_{i+N2^j}^j = \mathbf{v}_i^j = \mathbf{v}(s_i^j)$ and $s_{i+N2^j}^j - L = s_i^j < s_{i+1}^j$, $i \in \mathbb{Z}$, respectively, we use (4.1.1): Given $\mathbf{v}^{j-1}$, we predict "twice as many"

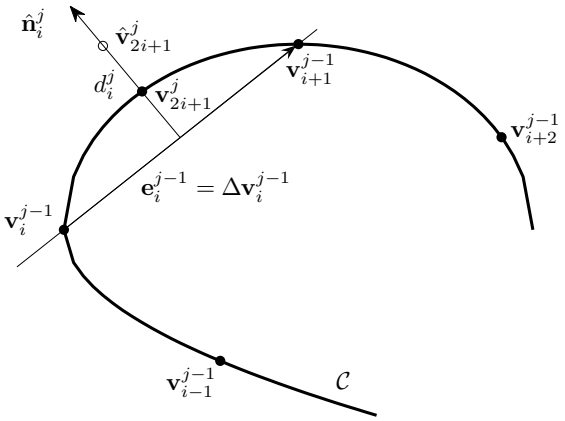

Fig. 4.1: One step of a normal MT

points $\hat{\mathbf{v}}^j = S\mathbf{v}^{j-1}$ using the subdivision operator S, and compute approximate normal directions $\hat{\mathbf{n}}^j$ for each of them. A standard choice is simply taking $\hat{\mathbf{n}}_{2i}^j = \hat{\mathbf{n}}_{2i+1}^j$ as the unit vector in the direction $(\mathbf{v}_{i+1}^{j-1} - \mathbf{v}_i^{j-1})^\perp$. The important thing is that both $\hat{\mathbf{v}}^j$ and $\hat{\mathbf{n}}^j$ are computable from $\mathbf{v}^{j-1}$, and need not be stored. Given these two sequences, we can find the $\mathbf{v}_i^j$ by intersecting $\mathcal{C}$ with the line through $\hat{\mathbf{v}}_i^j$ in the direction $\hat{\mathbf{n}}_i^j$ for all $i \in \mathbb{Z}$. This is the most ambiguous step, as there might be no intersection points, or many intersection points, where taking a wrong candidate may lead to violation of the monotonicity condition $s_{i+1}^j > s_i^j$, ruining the grid connectivity (topology) and leading to a non-nested data structure that cannot be reconstructed from the detail information. In both the cases, i.e., when there is no intersection point or when the monotonicity condition is violated, we say that the normal MT is *ill-posed*. In practice, normal MT is used up to an a priori fixed fine-scale J (e.g., in image processing the cardinality of any sample can not exceed the number of pixels, while in encoding algorithms the limitation is on the number of bits). In theory, however, we study the asymptotical behavior of the method, hence we let $J \to \infty$. The mathematical analysis of normal MTs consists of answering the following questions:

- Under which conditions on $\mathcal{C}$, S, the initial point set $\mathbf{v}^0$, and the assignment rule for approximate normal directions is the reconstruction part of the normal MT well-defined for all $j \geq 1$?
- Let $\mathbf{v}^j(t)$ denote the linear interpolant (polygonal line) for the data vector v^j at the grid $2^{-j}\mathbb{Z}$. Does $\mathbf{v}^j(t)$ converge to a regular parametrization of $\mathcal{C}$, and how smooth is this limit (called normal re-parametrization of $\mathcal{C}$)? This question is equivalent to asking about the convergence of the linear interpolants $s = s^j(t)$ for the data s^j at the grid $2^{-j}\mathbb{Z}$ to a smooth limit $s = s(t)$ satisfying $s'(t) > 0$ since $\mathbf{v}(s(t))$ coincides with the limit of $\{\mathbf{v}^j(t)\}$.
- Which decay rates can be expected for the detail sequences d^j? Besides the fact that the details are scalar, this has immediate consequences for compression applications.

- Under which assumptions on given normal MT data $\{\mathbf{v}^0, d^1, d^2, \ldots\}$ can we say something about the asymptotic properties of the reconstruction part? E.g., do we get a smooth curve? This question can also be viewed as part of the stability problem for normal MT. Indeed, stability of the reconstruction part means to show that, given the normal MT data $\{\mathbf{v}^0, d^1, d^2, \ldots\}$ of a smooth curve $\mathcal{C}$, the reconstruction from slightly perturbed data $\{\tilde{\mathbf{v}}^0, \tilde{d}^1, \tilde{d}^2, \ldots\}$ leads to a close-by limit curve $\tilde{\mathcal{C}}$.

The first theoretical results can be found in [24] where properties like regularity, convergence, and stability of interpolating normal MT for curves are established. The central idea of the authors there is to study normal approximation as a perturbation of a linear subdivision scheme and to use proximity conditions. The latter works only under additional smoothness assumptions on the initial curve $\mathcal{C}$, and thus only $C^{1,\alpha}(\mathbb{R}^2), \alpha > 0$ curves are considered. Here and throughout this chapter, we denote by $C^{k,\alpha}$ the Hölder smoothness class of k-times differentiable functions f with $f^{(k)} \in Lip\ \alpha$. In [24], the authors always assume that $\mathcal{C}$ can be locally parameterized by its x-coordinate with respect to a (properly chosen) local coordinate system, and interpret the normal MT as a nonregular scalar-valued multi-scale transform on the grid x^j. They assume that the new nodes are "well placed", i.e., starting with a monotonic sequence x^0, leads to a monotonic sequence x^j, as well, for all $j > 0$, and that the points of x^j do not cluster. Both these conditions are defined via formulae on x that are not rotationally-invariant, and thus optimal choice of the coordinate system is crucial for the analysis. Under these assumptions the authors prove uniform convergence, regularity of the normal re-parametrization (that depends on the regularity of S and the smoothness of $\mathcal{C}$), exponential detail decay rates, and stability of the normal MT. Moreover, they produce a counterexample that their analysis does not hold for initial curves $\mathcal{C} \in C^{0,\alpha}, \alpha \leq 1$ unless a meaningful rule for the choice of the newly inserted point $\mathbf{v}^j_{2i+1}$ is established in the cases of more than one intersection points between a normal line and the curve. The question about normal surfaces and how normal meshes work for less smooth spaces, particularly spaces that are used to model natural images such as BV, and the Besov space $B_{1,1}$ remains open. The other uninvestigated direction is the use of approximating prediction operators. In [91] the general theory from [24] has been worked out on a concrete example, namely the mid-point interpolating (S_1) normal MT. There explicit local coordinate frames based on the arc-length parametrization of the original curve are used, which helps for the better understanding of the very technical paper [24]. Moreover, the author proves that the S_1 normal MT is globally/unconditionally well-defined, i.e., no matter what the C^1 curve $\mathcal{C}$ and the coarse-scale sample $\mathbf{v}^0$ are, the multi-scale transform converges to a $Lip\ 1$ normal re-parametrization. However, it is shown on an example that the above procedure does not "regularize" the fine-scale data, i.e., the samples $\mathbf{v}^j$ does not tend to a regularly spaced distribution with respect to the arc-length of $\mathcal{C}$, as $j \to \infty$.

The S_1 normal MT has been used in [12] as well, but in a slightly different context. There, the authors aim at the best and sparsest approximation of a continuous planar curve $\mathcal{C}$ by polygonal lines with respect to the Hausdorff metric. Hence, not all coarse-scale intervals have been refined, but only those for which the approximation error surpasses a certain threshold ϵ. This leads to an adaptive algorithm that places lots of points in the regions of low smoothness of $\mathcal{C}$ and very few ones in those of higher smoothness. Another difference from [91] is that here in case of more than one intersection points between the normal line and the curve arc, a specific criteria for choosing the newly inserted point is necessary, namely, one should always take the piercing point that is farthest away from the prediction. Such an algorithm is easy to implement and is currently used in the authors' surface

encoding software. However, from a theoretical point of view, it is convenient to replace the S_1 normal MT with a more geometrical, data-dependent refinement rule that places the new vertex directly on $\mathcal{C}$, e.g., to choose the midpoint of the corresponding curve arc. For both the versions of the proposed method it is proved that $\mathcal{C}$ being of finite length guarantees linear approximation order $\mathrm{O}(n^{-1})$, where n is the number of sample points on the finest level. Furthermore, for a $C^{0,1}$ initial curves $\mathcal{C}$ with curvature $\kappa \in L \log L$ (i.e., some Hardy-Littlewood maximal operator, applied to κ to be in L^1 - see [12] for details) both the algorithms have approximation order $\mathrm{O}(n^{-2})$. While the first result remains true for non-adaptive refinements, too, the second one holds in that setup only for $\mathcal{C} \in C^2$ curves (i.e., one needs uniformly bounded curvature). Hence, [12] can be viewed as an attempt to extend the existing optimal approximation rates to $C^{1,\alpha}$ curves.

Our paper [62] extends the theory from [24] to the approximating setting and to a larger class of admissible normal directions, called "generalized normals". The main observation is that both the detail decay rate and the smoothness of the normal re-parametrization for the S normal MT depend on the exact order of polynomial reproduction P_e of the prediction rule S. For interpolating schemes S this number coincides with the well-known order of polynomial reproduction P, while in case of approximating schemes this number is usually significantly smaller, suggesting that the corresponding normal MT does not perform well in terms of compression and visualization. On the other hand, we prove that the S_2 (corner-cutting or Chaikin) normal MT is globally well-defined and, unlike the S_1 normal MT, it does "regularize" the fine-scale data. Finally, the paper [87] successfully extends the planar curve theory from [62] to the surface setting. More precisely, the author deals with the normal MT based on edge midpoint prediction and on normal directions, obtained via averaging the two corresponding normal vectors with respect to the neighboring coarse-scale triangles the given edge belongs to, and shows that such a transform inherits all the expected properties of the S_1 normal MT for curves. The fundamental difference between 2D and 3D is that, due to the more complicated topology for triangulations, the normal MT for surfaces may fail for coarse distorted meshes, independently of the choice of the prediction rule S. The lack of any hope for global well-posedness restricts the analysis, and hence the derived results, to be of only asymptotic nature, and makes the "regularity" assumptions on the initial sample $\mathbf{v}^0$ and the initial surface $\mathcal{S}$ to play a crucial part in the proofs. In [87] only $C^{1,\alpha}$ surfaces and c-regular triangular meshes with small enough global mesh width $h(\mathbf{v}^0)$ are considered. The questions about the stability of the transform and possible extensions to the image analysis setting (i.e., $\mathcal{S}$ being only $C^{0,1}$) are left open. Another contribution of that paper is the introduction of a combined scheme, based on Loop [80] MT to determine the fine-scale meshes, and of additional post-processing of the details, based on the Butterfly [39] scheme, yielding an improved base point along the same normal line, located at a distance asymptotically much smaller that either scheme alone could achieve. Testing on simple surfaces and $\mathbf{v}^0$ confirms that the Loop/Buterfly normal MT possesses high detail decay rates in the regular parts of the triangular meshes, and at the same time improves mesh regularity around the extraordinary vertices.

Apart from theoretical developments, there are several experimental papers, mainly in the surface case where the efficiency of the "normal idea" is better highlighted. The pioneer paper [55] presents an algorithm to approximate any surface arbitrarily closely with a normal semi-regular mesh. Motivated by the observation that the geometric information of a surface can be contained in only a single dimension (the height over its corresponding tangent plane), the authors propose a hierarchical procedure based on Butterfly subdivision of triangle meshes, so that all the detail

coefficients when expressed in local frames have only a normal component. Their algorithm consists of several steps, namely: mesh simplification, building an initial net of curves, fixing the global vertices and edges, initial parameterization, piercing, and adjusting the parameterization. The need of combining so many different procedures lies in the generally complicated and subtle analysis on surfaces, and the fact that the algorithm is practically oriented. Let us briefly mention the main obstacles. First of all, in the curve case, ordering the initial data $\mathbf{v}^0$ with respect to the arc-length parameterization of the initial curve $\mathcal{C}$ suffices for determining the connectivity (topology) of the mesh, while in the surface case the vertices cannot be linearly ordered, and the corresponding edges and faces of the triangle mesh need to be additionally specified. Hence, even when the vertices have already been chosen, the correct choice of the mesh connectivity is crucial for well-posedness of the normal MT. Second of all, in applications the given initial triangle mesh on the surface is the finest one (the one at level J), it is in general not normal, and the only way to obtain a normal mesh from it is to change the initial triangulation. Therefore, one should first choose a proper base mesh (the coarsest level of the future normal semi-regular mesh) with vertices among those from the input mesh, and connectivity that captures well the surface geometry. This is achieved within the first three steps of the algorithm. Once the base mesh is fixed, the actual Butterfly normal MT takes part. The problem here is that no matter how good the base mesh is, it is still possible that the normal line through a predicted point does not intersect the surface or intersects it in more than one point. In case of no intersection, the algorithm chooses the midpoint of the corresponding coarse-scale edge as the newly inserted point and stores the 3D vector with endpoints the predicted and inserted point, respectively. In case of many intersection points, the algorithm chooses the closest one to the coarse-edge midpoint. The metric is inherited from $\mathbb{R}^2$ via a bijective map between the surface patch and a planar triangulation, with the same connectivity, and edges of the same length as those from the triangle mesh. Finally, the continuous readjustment of surface parameterizations after the insertion of every fine-scale vertex is important for the correct choice of the next-level intersection points. The authors tried the naive piercing procedure without parameterization from the base domain and found that it typically fails on all the models, they consider in [55].

In [68], the above normal "remeshing" technique is applied for irregular highly detailed triangle meshes and is implemented in the progressive geometry compression framework described in [69]. (The term *progressive compression* means that an early coarse approximation is subsequently improved through additional bits.) The algorithm accepts as input an arbitrary connectivity 2-manifold (with boundary) triangulation. Using the normal "remeshing" technique from [55], successive adaptive approximations with semi-regular connectivity are computed and then subsequently wavelet transformed and progressively compressed via zerotrees. The authors use non-lifted Butterfly wavelets [94], because the exact same transform is used to produce normal meshes, as well as Loop wavelets [69], because this is the wavelet transform used in [69] and this allows for fair comparison between the normal remesher and the MAPS remesher [77] used there. As expected, normal meshes using Butterfly wavelets possess best compression rates. Also a better compression rate of normal meshes versus other remeshes is observed when the Loop wavelets are used. On the other hand, for non-normal meshes the Loop wavelet transform avoid Gibbs-type phenomena and typically yields better visual appearance than the Butterfly transform, with comparable error measures. Another possible direction for further generalizations and improvements of the progressive geometry compression is to allow irregular refinements, as well. Such kind of approach is investigated in [54], where each step of a regular refinement is followed by an irregular one. The irregular

operations are limited and they are as many as needed for topology changes, feature alignment, and stretching resolution. The main problem of the regular multi-scale transform is that "spiky" features lead to a stretched map, which may cause bad aspect ratio polygons, poor approximation, and numerical problems. On the other hand, the irregular algorithms are more complex for multiresolution, smoothing, compression, editing, etc. The construction in [54] combines the advantages of both the refinements, and "controls" the disadvantages. All the results in the paper are experimental, which leaves room for research. Moreover, representing high topological complexity models such as isosurfaces from medical imaging or scientific computing, and approximating dynamically changing, topologically complex geometries does not give good results with the novel approach, so further generalizations are expected.

Another interesting application of normal MTs has been recently proposed in [92]. There the propagation of an interface in a time-varying velocity field (i.e., a field that does not depend on the shape of the front, but only on its location) is considered. In many numerical models it is better to track the front, described by a set of marker points with given topology, rather than a set of individual points from it, since the connectivity between paths is then maintained. The latter is incorporated in a new model via the use of S_1 normal MT, leading to a computational cost of only $\mathrm{O}(\log N/\Delta t)$ or even $\mathrm{O}(1/\Delta t)$ for fixed small enough accuracy. (For comparison, the cost of standard front tracking algorithm is $\mathrm{O}(N/\Delta t)$, so basically the cost of the new method is comparable with that of propagating just a single point!) The key observation is that not only the details of the "static" S_1 normal MT decay with order 2, but also their time derivatives in the dynamic setting. This allows to double the time-steps at each finer scale without worsening the overall accuracy of the approximation. Since it is not possible to write a closed ODE system for the $d_k^j(t)$ which maintains the normality of the detail vectors, for the purposes of this application the constraints in the description of the normal MTs have to be relaxed. Hence, only at the beginning ($t = 0$) we have "classical" normal directions, orthogonal to the coarse-scale edges. However, for any $t \in [0, T]$, where $T < \infty$ is fixed a priori, using proximity analysis, one can still obtain exponential decay rates for $\|\Delta \mathbf{v}^j(t)\|$ and $\|d^j(t)\|$ similar to those in [91] for $t = 0$. Although theoretically verified only for S_1, numerical experiments indicate that the above phenomena in the behavior of the details and their time derivatives with respect to the scale j they belong to remain for general normal MTs, based on arbitrary linear, local, shift-invariant, interpolating S. Prediction with higher order subdivision schemes results in substantial improvement in accuracy, while making the method only marginally slower. Further updates of the proposed method are expected, since in this form, the representation of the interface can deteriorate, if the length (or area) of the interface expands quickly and the number of marker points used initially is not enough to resolve it, or if the "dynamic" normal directions rapidly shift away from the corresponding "static" ones.

Normal mesh techniques have been recently used for image approximation and image compression, an application which is totally different from the previously mentioned ones. Indeed, digital images can be considered as height fields and they are not just surfaces, but also functions on the pixels, i.e., 1D piecewise constant functions on a uniform, regular lattice. Hence, even standard linear multiresolutions incorporate scalar details, so there is no bonus to gain in this direction. However, unlike surfaces in computer graphics, images are non-smooth and the edges become information carrying features. In [66] it has been proved that normal triangulated meshes rapidly place more and more vertices directly on the edge contours, enabling a direct representation of the location and the geometry information of edges as well as extracting the information on (the

height of) the singularity itself. Hence, the use of normal meshes gives rise to a sparse, but yet truthful, image decomposition. More precisely, for the Horizon class [29] of images (also known as *cartoons*) consisting of uniformly colored region separated by a smooth contour, the normal mesh representation has an optimal n-term approximation rate $\sigma_{L^2} = \mathrm{O}(n^{-1})$ as the number of terms in the representation grows. This is twice as good as standard wavelet approximation [27], a log factor faster than the one obtained with curvelets [14], and comparable to techniques based on contourlets [28], wedgelets [29] or other nonlinear adaptive schemes such as bandelets [88], or geometric wavelets based on binary partitioning algorithms [25]. On the other hand, in contrast to the other methods, the normal mesh representation relies on the implicit boundary locating property of normal meshes, and, thus, has only linear computational complexity. Compression is not addressed in [66], but since approximation and compression are tightly related, their results indicate that the normal offset method should be considered for the development of efficient rate-distortion image encoders. The latter aspect is further elaborated on in [98, 99, 1]. The major difference between their normal mesh approach for image compression and the previous one proposed in [66] is the choice of normal direction. In [66] the normal line through the midpoint of a coarse-scale triangular edge is collinear with the normal to a surface fitting its four neighbor vertices. Since cartoons are only piecewise continuous, the theoretical results from [87] are not applicable and examples from the curve setting in [24] suggest that no decay rate is to be expected for the fine scale offsets. This leads to piercing points far away from the predicted midpoints, and, thus, the projection on the domain (i.e., the xy-plane) destroys previous existing topologies. Therefore, in this setting one needs to combine normal offsets with standard (vertical) ones giving rise to a nonnested multiresolution model for which additional side information is stored in order to encode the complex dependency relations between consecutive resolution levels. In [98], by restricting the normals to be in a plane, orthogonal to the domain, the author assures that the piercing point projection always lies on the corresponding edge of the coarse-scale domain triangle $\mathcal{T}$ and preserves topology. In case of more than one intersections, the closest point to the prediction is to be considered. Moreover, in order the line singularities of the initial image to be well approximated by polylines formed by the triangle edges on the corresponding multiresolution level, an additional procedure, besides prediction and correction, has been added at each step of the normal offset refinement scheme - interconnection. In other words, the inner edges of the tessellation are chosen in such a way that they minimize the L^2 error metric between the original surface and the approximating mesh. It is an extra topological parameter per triangle, but it pays off at the level of compression when the meshes are truncated, plus it guarantees that the optimal approximation rates from the previous setting [66] remain valid here, too, i.e. $\sigma_{L^1} = \mathrm{O}(n^{-1})$. Note that the last result is slightly weaker than the one in [66] because in general the normal transforms perform best in L^1-norm, where a few big errors are preferred over a lot of little ones! In [99] the authors discuss the underlying datastructures that are essential to make the algorithm from [98] compact and efficient, and explain how both these datastructures and normal offset coefficients are encoded to bit level. The experimental results in the end indicate that for images of geometrical nature the normal offset decomposition is a promising compression technique. The paper [1] is rather practically oriented and the authors focus on small n, where the theoretical asymptotical behavior of the multi-scale transform is not yet visible. The main contribution is the development of a model for the offsets such that they can be encoded efficiently by an entropy coder. Compared with the JPEG2000 encoder, the proposed normal offset encoder does not yet outperform it over the entire image, mainly because of the vertical offsets away from the contour that are stored losslessly, even though they do not contribute much to the image quality.

But once the mesh is fine enough the distortion decays rapidly.

All the proposed normal mesh techniques [66, 98, 99, 1] are based on the mid-point prediction rule S_1 that has only order 2 of polynomial reproduction, and thus the theoretical results in [87] imply that in the smooth regions of the image the detail decay rate is very slow. This was not a problem in case of cartoons, since away from the singularity the function was constant and the details were zero anyway. But if one extends the objects of interest to the space of piecewise smooth images (rather than piecewise constant ones, considered so far) with smooth contours, they immediately see that the JPEG2000 encoder, as based on a more regular prediction rule (i.e., one that is equipped with more vanishing moments), capture the smooth regions much more efficiently that the normal offset encoder. The standard remedy in this case is adaptivity, i.e., to try to combine the nice smoothing properties of the wavelets away from the singularities with the sharp edge detection of the normal mesh techniques into a single data-dependent multi-scale transform. This has been done in [65], the major contribution of which is the design of a new class of wavelet transforms that can be extended to normal offset decomposition. The main observation is that the normal offset decomposition can be embedded into the lifting scheme [96, 97]. However, the combination of normal offsets and a stable lifting scheme is nontrivial and naive implementations of the normal offset decomposition are ill conditioned in L^2 and hence of no use in applications to noise reduction. Although the adaptive method is of practical interest in higher dimensions, the scope of the paper is limited to a 1D discussion. The difference between the standard lifting transform and the one, implemented in [65], is that the first transform computes fine-to-coarse, while, due to the dependence of the normal directions on the coarse-scale edges, we need a coarse-to-fine procedure. This is achieved via interchanging the order of the dual lifting (or Prediction) step with the primal lifting (or Update) one. The approach in the paper includes a genuine linear polynomial prediction, but on "filtered", preconditioned updated values, where the exact prediction procedure follows from the design of the update step. On an equidistant grid, this leads to a transform that is the adjoint to the corresponding predict-first lifting scheme. The proposed decomposition is fully adaptive to the locations of the jumps, with no limitations as imposed by dyadic subdivision schemes. The experimental results at the end of the paper suggest that even for a univariate data the jump localization is so fast that the use of normal offsets may still have a substantial benefit. (Note that, due to the specifics of the normal approach one needs to store both a normal and a local offset around jumps, while the standard lifting schemes stores only a single vertical offset!)

4.2 General analysis on normal multi-scale transforms for curves

This section follows closely our paper [62].

4.2.1 Notation, definitions, and auxiliary results

Throughout this chapter boldfaced letters are used for vector-valued quantities (points in $\mathbb{R}^2$, sequences of such points, or $\mathbb{R}^2$-valued functions). The notation $|\cdot|$ is used both for the absolute value in $\mathbb{R}$ and the Euclidean norm in $\mathbb{R}^2$ which should be clear from the context. The scalar product of two vectors $\mathbf{a}, \mathbf{b}$ in $\mathbb{R}^2$ is simply denoted by $\mathbf{ab}$. If a, b are sequences in $\mathbb{R}$, and $\mathbf{b}$ is a sequence in $\mathbb{R}^2$ then $ab := (a_i b_i)_{i\in\mathbb{Z}}$, $a\mathbf{b} := (a_i \mathbf{b}_i)_{i\in\mathbb{Z}}$ for short.

We consider closed, non-self-intersecting $C^{k,\alpha}$ curves $\mathcal{C}$ in $\mathbb{R}^2$ given by a regular arc-length parametrization $\mathbf{v}(s) \in C^k([\mathbb{R} \to \mathbb{R}^2)$ such that $\mathbf{v}(s+L) = \mathbf{v}(s)$, $\mathbf{v}(s) \neq \mathbf{v}(s')$, $0 < |s-s'| < L$, $\mathbf{v}' \neq \mathbf{0}$, and

$$|\mathbf{v}^{(k)}(s) - \mathbf{v}^{(k)}(s')| \leq C|s-s'|^\alpha, \qquad s, s' \in \mathbb{R}, \tag{4.2.1}$$

where $k \geq 1$ is integer, L is the length of $\mathcal{C}$, and $\alpha \in (0,1]$. (Our results work for self-intersecting curves, as well, provided that the curves can be split into several closed non-self-intersecting parts and that all of them are sufficiently represented in the sample $\mathbf{v}^0$.) The positive parameter C denotes the Lipschitz constant of order α of the k-th derivative of the parametrization. Note that the smoothness characteristics of the parametrization $\mathbf{v}$ of $\mathcal{C}$ (i.e., the Lipschitz constant C, the bounds for $\mathbf{v}^{(m)}(s)$, $m = 1, \ldots, k$ as well as k and α) and L may change if we switch to different representation. The arc-length parametrization generates a local frame given by unit tangent $\mathbf{t}(s) = \mathbf{v}'(s)$ and normal vectors $\mathbf{n}(s) = \mathbf{t}(s)^\perp$ to the curve which is used in the analysis.

Obviously, the analysis depends on the initial curve $\mathcal{C}$, the prediction rule S, the initial sample $\mathbf{v}^0$, and the choice of normal directions. We already explained what our assumptions on $\mathcal{C}$ are, so what is left is to say a couple of words for the remaining three objects.

We consider dyadic, linear, local, shift-invariant subdivision schemes S. Among all the other examples, we are particularly interested in the family $\{S_p\}_{p\in\mathbb{N}}$ that generates B-splines of degree p. Using the Lane-Riesenfeld [75] algorithm, for any $p \in \mathbb{N}$ we define:

$$(S_0 x)_{2i} = (S_0 x)_{2i+1} = x_i, \quad (S_p x)_i = \frac{(S_{p-1}x)_i + (S_{p-1}x)_{i+1}}{2}, \quad i \in \mathbb{Z}. \tag{4.2.2}$$

We say that the *(Hölder) regularity* of S is $s_\infty(S) = m + \beta$ if, as operator $S : \ell_\infty(\mathbb{Z}) \to \ell_\infty(\mathbb{Z})$ it generates $C^{m,\beta}$ limit functions $S^\infty x$, no matter what the initial sequence x is, and $m+\beta$ is the maximal number that satisfies the property. Note that, since S is linear, the regularity of S coincides with the regularity of the limit function for the delta sequence that is one at zero, and zero elsewhere. For example, $s_\infty(S_p) = p - 1 + 1$. (Again, note that this differs from $s_\infty(S_p) = p$, since the latter implies that the limit function is always p times differentiable, while the first one only implies that the $p-1$st derivative of the limit function is Lipschitz continuous.)

We assume that S has polynomial reproduction order $P \geq 2$ which means that for any polynomial $p = p(t)$ of degree $\deg(p) < P$ there is a polynomial $q = q(t)$ with $\deg(q) < \deg(p)$ such that

$$S(p|_\mathbb{Z}) = p|_{2^{-1}\mathbb{Z}} + q|_{2^{-1}\mathbb{Z}}. \tag{4.2.3}$$

Here, $p|_\mathbb{Z}$ denotes the sequence $(p(i))_{i\in\mathbb{Z}}$, and $p|_{2^{-1}\mathbb{Z}}$ the sequence $(p(i/2))_{i\in\mathbb{Z}}$. We say that S has polynomial exactness order P_e if the above identity holds with some shift parameter c_S in the following form:

$$S(p|_\mathbb{Z}) = p|_{2^{-1}\mathbb{Z}+c_S} = (p(i/2 + c_S))_{i\in\mathbb{Z}}. \tag{4.2.4}$$

I.e., S applied to a polynomial sequence of degree $< P$ reproduces the exact values on a possibly shifted grid. Below, P and P_e always denote the maximal values of polynomial reproduction resp. polynomial exactness order. If $P \geq 2$ then also $P_e \geq 2$ for some choice of c_S. Indeed, since $P \geq 2$, according to (4.2.3) constant sequences are reproduced exactly, and for the monomial sequence

$t = \mathbb{Z}$ we have $St = \frac{1}{2}t + c_S$, where c_S is the contribution of the polynomial $q(t)$ of degree 0. By linearity, this implies (4.2.4) for all linear polynomials $p(x) = c_1 x + c_2$:

$$S(p|_{\mathbb{Z}}) = S(c_1 t + c_2) = c_1(t/2 + c_S) + c_2 = p(t/2 + c_S) = p|_{2^{-1}\mathbb{Z}+c_S}.$$

On the other hand, if S has non-negative mask $a \geq 0$ then we are restricted to $P_e \leq 2$. Indeed, suppose that (4.2.4) holds for quadratic polynomials. Choose $i = 0$ or $i = 1$ such that $i/2 + c_S \notin \mathbb{Z}$, and consider $p(x) = (x - i/2 - c_S)^2$. Then evidently $p(i/2 + c_S) = 0$ while $(S(p|_{\mathbb{Z}}))_i > 0$ as a linear combination of only positive numbers $p(i)$ and coefficients from the sequence a (not all of which can vanish because of the exact reproduction of constant sequences by S). Last but not least, for interpolating schemes $P_e = P$ and $c_S = 0$. For S_p we have order of polynomial reproduction $P = p + 1$, order of exact polynomial reproduction $P_e = 2$, and $c_S = 0$ if p is odd and $c_S = 1/4$ if p is even.

Polynomial reproduction of order P implies the existence of derived subdivision operators $S^{[n]}$, $n = 1, \ldots, P$. For S_p we even have the explicit formulae of all the derived subdivision operators for free due to (4.2.2) and subtraction being the inverse operation to addition. Indeed, since

$$(S_1^{[1]}\Delta x)_{2i} = (S^{[1]}\Delta x)_{2i+1} = \frac{\Delta x_i}{2} \quad \Longrightarrow \quad S_1^{[1]} = \frac{1}{2}S_0,$$

assuming that $S_p^{[1]} = S_{p-1}/2$ we get

$$(S_{p+1}^{[1]}\Delta x)_i = (\Delta S_{p+1} x)_i = \frac{(\Delta S_p x)_i + (\Delta S_p x)_{i+1}}{2} = \frac{\frac{1}{2}S_{p-1}\Delta x_i + \frac{1}{2}S_{p-1}\Delta x_{i+1}}{2} = \left(\frac{1}{2}S_p \Delta x\right)_i,$$

and by induction

$$S_p^{[q]} = \frac{1}{2^q} S_{p-q}, \qquad \forall p \geq q \geq 0. \tag{4.2.5}$$

We will directly work with the local subdivision maps related to invariant neighborhoods for S and $S^{[n]}$, $n = 1, \ldots, P$. The most economic choice for such an invariant neighborhood I for S is as follows: Let $I = [N, N']$ be the smallest index interval in $\mathbb{Z}$ such that $[0, P] \subset I$, and all $(Sx)_i$ with indices in $[0, 1] + I = [N, N' + 1]$ should be computable solely from values x_i with indices $i \in I$. For S_p, this invariant neighborhood would be $I = [0, p + 1]$. Note that the invariant neighborhoods $I^{[n]}$ of the derived subdivision operators $S^{[n]}$ are smaller: $I^{[n]} = [N, N' - n]$. Denote by $I_i = i + I$ the invariant neighborhood of index i, similarly for $I_i^{[n]} = i + I^{[n]}$. The local subdivision operators are pairs of linear maps $A_0^{[n]}$, $A_1^{[n]}$ acting on $\mathbb{R}^{N'-N-n+1}$, and mapping the vector $y = (\Delta^n x)|_{I_i^{[n]}}$ to $y' = (\Delta^n Sx)|_{I_{2i}^{[n]}}$ resp. $y'' = (\Delta^n Sx)|_{I_{2i+1}^{[n]}}$. Due to shift-invariance, these maps do not depend on i. The relationship with $S^{[n]}$ is obvious, since $y' = (S^{[n]}y)|_{I_{2i}^{[n]}}$ and $y'' = (S^{[n]}y)|_{I_{2i+1}^{[n]}}$ by the commutator properties. Similarly, we define A_0, A_1 related to S itself (see [15, 37] for details).

The necessary assumptions on $\mathbf{v}_0$ and $\hat{\mathbf{n}}$ are inspired by our proof for well-posedness of normal MT. We work in local frames, so let us first define them. For $C^{k,\alpha}$ curves we write the Taylor formula in the form

$$\mathbf{v}(s) = \sum_{n=0}^{k} \frac{\mathbf{v}^{[n]}(\xi)}{n!}(s - \xi)^n + \mathbf{r}(s, \xi), \qquad \mathbf{r}(s, \xi) := \int_\xi^s \frac{\mathbf{v}^{[k]}(t) - \mathbf{v}^{[k]}(\xi)}{(k-1)!}(s - t)^{k-1}\,\mathrm{d}t, \tag{4.2.6}$$

where

$$|\mathbf{v}^{[k]}(s) - \mathbf{v}^{[k]}(s')| \le C_{\mathcal{C}}|s - s'|^{\alpha}, \qquad |\mathbf{r}(s,\xi)| \le C_{\mathcal{C}}|s-\xi|^{k+\alpha}. \tag{4.2.7}$$

For an arbitrary but fixed ξ, we call $x(s), y(s)$ the local frame coordinates of $\mathcal{C}$, given by

$$\mathbf{v}(s) = \mathbf{v}(\xi) + x(s)\mathbf{t}(\xi) + y(s)\mathbf{n}(\xi), \quad x(s) = \mathbf{t}(\xi)(\mathbf{v}(s) - \mathbf{v}(\xi)), \quad y(s) = \mathbf{n}(\xi)(\mathbf{v}(s) - \mathbf{v}(\xi)). \tag{4.2.8}$$

That $x(s), y(s)$ depend on ξ is not made explicit by the notation but has to be kept in mind.

Lemma 4.2.1. *Let $\mathcal{C}$ be a closed $C^{k,\alpha}$ curve, $k \ge 1$, $\alpha \in (0,1]$. There exists a $\sigma_0 = \sigma_0(\mathcal{C}) > 0$ such that for any choice of ξ, the associated local frame coordinate $x(s)$ satisfies*

$$1 \ge x'(s) \ge 1 - C|s-\xi|^{2\alpha'} \ge \frac{1}{2}, \qquad s \in [\xi - \sigma_0, \xi + \sigma_0],$$

where $\alpha' := \min(1, k + \alpha - 1)$. Thus, $x = x(s)|_{[\xi-\sigma_0,\xi+\sigma_0]}$ is strictly monotone, and possesses an inverse function $s = s(x)$ which belongs to $C^{k,\alpha}$, with bounds on the derivatives $s^{[n]}$, $n = 1, \dots, k$, and the Lipschitz constant of $s^{[k]}$, independently of ξ. As a consequence, the arc of $\mathcal{C}$ corresponding to $s \in [\xi - \sigma_0, \xi + \sigma_0]$ can be viewed as the graph of a $C^{k,\alpha}$ function $y = f(x) := y(s(x))$.

Proof. Since $C^{k,\alpha} \subset C^{1,\alpha'}$ and $x'(s) = \mathbf{v}'(s)\mathbf{t}(\xi) = \cos(\angle(\mathbf{v}'(s), \mathbf{v}'(\xi))) \le 1$, the lower bound for $x'(s)$ follows from the cosine theorem

$$\cos(\angle(\mathbf{v}'(s), \mathbf{v}'(\xi))) = 1 - |\mathbf{v}'(s) - \mathbf{v}'(\xi)|^2/2 \ge 1 - C|s-\xi|^{2\alpha'},$$

where the final C depends on the smoothness characteristics of $\mathcal{C}$, only. Now, set $\sigma_0 = (2C)^{-1/(2\alpha')}$. The rest follows from the implicit function theorem, and from the fact that $C^{k,\alpha}$ is closed under superposition. □

Our assumption on the initial sample $\mathbf{v}^0 = \mathbf{v}(s^0)$ states that, for any positive constant C_0 and $0 < \delta < \min(k - 1 + \alpha, m - 1 + \beta, 1)$, there exists a small enough (but positive!) step-size h, s. t.,

$$\|\Delta s^0\| \le h; \qquad \|\Delta^2 s^0\| \le C_0 \|\Delta s^0\|^{1+\delta},$$

shall hold. The constant h depends on $\mathcal{C}$, S, C_0, δ, and σ. The following lemma gives some insight on this technical condition, written in its equivalent local form.

Lemma 4.2.2. *Let $\mathcal{C}$ be a closed, non-self-intersecting $C^{1,\alpha}$ curve, and let $\mathbf{v}$, s be sequences satisfying $\mathbf{v}_i = \mathbf{v}(s_i)$, and $s_i < s_{i+1}$ for all $i \in \mathbb{Z}$. Denote the local step-size by $h_i = \|\Delta s\|_{I_i}$. Finally, let $\delta \in (0, \alpha]$, and σ_0 as in Lemma 4.2.1. Then the following are equivalent:*
(i) There are positive constants C_0 and $h \le \sigma_0$ such that for $h_i \le h$

$$\|\Delta^2 s\|_{I_i} \le C_0 h_i^{1+\delta}. \tag{4.2.9}$$

(ii) There are positive constants $\hat{C}$, $h \le \sigma_0$ such that for $h_i \le h$ and all $k, l \in I_i$

$$s_k = s_l + (k-l)h_i + r_{k,l}, \qquad |r_{k,l}| \le \hat{C} h_i^{1+\delta}. \tag{4.2.10}$$

(iii) There are positive constants $\tilde{C}$ and $\tilde{h} \le \sigma_0$ such that for $h_i \le \tilde{h}$

$$\mathcal{N}(s|_{I_i}) := \max_{k,l \in I_i^{[1]}} \left| \frac{\Delta s_k}{\Delta s_l} - 1 \right| \le \tilde{C} h_i^{\delta}.$$

(iv) There are positive constants $\bar{C}$ and $\bar{h} \le \sigma_0$, such that for $\bar{h}_i := \|\Delta \mathbf{v}\|_{I_i} \le \bar{h}$

$$\|\Delta^2 \mathbf{v}\|_{I_i} \le \bar{C} \bar{h}_i^{1+\delta}.$$

Proof. The equivalence of (i) and (ii) is easy to show. If (i) holds, we use the identity

$$s_k = s_{i'} + (k-i')\Delta s_{i'} + \sum_{l=1}^{k-i'-1} (k-i'-l)\Delta^2 s_{i'+l-1}, \quad k \ge i',$$

where we choose i' such that $h_i = \Delta s_{i'}$. A similar identity holds for $k < i'$. Thus, $s_k - s_l - (k-l)h_i$ can be bounded by $C\|\Delta^2 s\|_{I_i} \le C C_0 h_i^{1+\delta}$ for any two indices $k, l \in I_i$. This is (ii) with $\hat{C} \le C C_0$. If (ii) holds then $\Delta^2 s_k = r_{k+2,l} - 2r_{k+1,l} + r_{k,l}$ for any $l \in I_i$, which yields (i) with $C_0 \le 4\hat{C}$.

From (4.2.10), it follows that for any $k, l \in I_i^{[1]}$

$$\Delta s_k = \Delta s_l + r_{k+1,l+1} - r_{k,l} \quad \Longrightarrow \quad \left| \frac{\Delta s_k}{\Delta s_l} - 1 \right| \le \frac{2\hat{C} h_i^{1+\delta}}{|\Delta s_l|} \le \frac{2\hat{C} h_i^{1+\delta}}{h_i - |r_{l+1,l}|} \le 4\hat{C} h_i^{\delta},$$

whenever $\hat{C}\tilde{h}^{\delta} \le 1/2$. Hence, (ii) implies (iii). Assuming that (iii) holds and taking $k \in I_i^{[2]}$, $l = k+1$ in it, we derive $|\Delta^2 s_k| \le \tilde{C} h_i^{\delta} |\Delta s_{k+1}| \le \tilde{C} h_i^{1+\delta}$, which yields (i).

In order to work with the points on the curve themselves, we need to mention some well-known facts: The shortest distance between two points in $\mathbb{R}^2$ equals the length of the line segment that connects them, i.e., $|\Delta \mathbf{v}_k| \le |\Delta s_k|$; If $\mathcal{C}$ is rectifiable, closed and non-self-intersecting the inverse function $\mathbf{v}^{-1}(s)$ of its arc-length parameterization is Lipschitz continuous (see (6) in [91]), i.e., there exists $q > 0$ that depends only on $\mathcal{C}$, such that $|\Delta \mathbf{v}_k| \ge q|\Delta s_k|$; Since $\mathcal{C} \in C^{1,\alpha}$, $\|\Delta^2 v\|_{I_i} \le C(\|\Delta s\|_{I_i}^{1+\alpha} + \|\Delta^2 s\|_{I_i})$ (see, for example [62, Lemma 2.4.]), where $C < \infty$ depends on α and $|I_i|$. Now, assuming that (i) holds, we derive

$$\|\Delta^2 \mathbf{v}\|_{I_i} \le C(\|\Delta s\|_{I_i}^{1+\alpha} + \|\Delta^2 s\|_{I_i}) \le C(C_0 + h_i^{\alpha-\delta}) \|\Delta s\|_{I_i}^{1+\delta} \le \frac{C(C_0 + h^{\alpha-\delta})}{q^{1+\delta}} \bar{h}_i^{1+\delta}.$$

For the other direction, let $k \in I_i^{[2]}$ and use (4.2.6) around s_{k+1}. This leads to $\Delta^2 \mathbf{v}_k = \mathbf{t}(s_{k+1})\Delta^2 s_k + \mathbf{r}(s_k, s_{k+1}) + \mathbf{r}(s_{k+2}, s_{k+1})$. Hence,

$$\|\Delta^2 s\|_{I_i} - 2C_{\mathcal{C}} h_i^{1+\alpha} \le \|\Delta^2 \mathbf{v}\|_{I_i} \le \bar{C} \bar{h}_i^{1+\delta} \le \bar{C} h_i^{1+\delta} \quad \Longrightarrow \quad \|\Delta^2 s\|_{I_i} \le (\bar{C} + 2C_{\mathcal{C}} h_i^{\alpha-\delta}) h_i^{1+\delta}.$$

□

Conditions (iii) and (iv) are added only for reference: (iii) allows for the comparison with the assertions on the non-uniformity measure $\mathcal{N}(x)$ used in [24, 91], (iv) works with the point sets $\mathbf{v} \subset \mathcal{C}$ directly, which is of practical importance, since it allows for checking how good the initial

sample is without explicitly knowing the arc-length parameterization of $\mathcal{C}$. As seen from the proof, the restriction $\delta \leq \alpha$ is needed only for the equivalence of (iv) with the remaining statements. For the equivalence of (i), (ii), and (iii), $\delta \in (0, 1]$ is enough.

The proof of Lemma 4.2.2 shows that the equivalence of (i), (ii), and (iv) holds for $h \leq \sigma$ and $\bar{h} \leq qh$. Both σ and q are global constants that depend solely on $\mathcal{C}$ and are known a priori. However, in order for (iii) to kick in, we need to restrict ourselves to smaller scales (e.g., (ii) implies (iii) only if $\hat{C}\tilde{h}^{\delta} < 1$, and (iii) implies (ii) only if $\tilde{h} \leq h$), making the choice for h and $\bar{h}$ to also depend on δ and all the constants $C_0, \hat{C}, \bar{C}$. In other words, our assumption (4.2.9) is asymptotically the same as the non-uniformity measure, introduced in [24], but the two approaches significantly differ on coarse-scale data. To explain this better, we will introduce $\mathcal{N}(\mathbf{v}|_{I_i})$ - the $\mathbb{R}^2$ analogue of $\mathcal{N}(s|_{I_i})$. Since (iv) is the $\mathbb{R}^2$ analogue of (i), whenever (i), (iii), and (iv) are equivalent, so is
(v) There are positive constants $\bar{C}'$, $\bar{h} \leq \sigma$ such that for $\bar{h}_i \leq \bar{h}$

$$\mathcal{N}(\mathbf{v}|_{I_i}) := \max_{k,l \in I_i^{[1]}} \left| \frac{|\Delta \mathbf{v}_k|}{|\Delta \mathbf{v}_l|} - 1 \right| \leq \bar{C}' \bar{h}_i^{\delta}.$$

Note that (v) works solely with $\Delta \mathbf{v}$, while (iv) involves $\Delta^2 \mathbf{v}$, as well, adding extra geometrical meaning. Indeed, the non-uniformity measure is small, whenever the Euclidean distance between every two neighbors remains close to a constant. On the other hand $\Delta^2 \mathbf{v}$ measures not only distance, but also flatness. E.g., even when all the points $\mathbf{v}$ are equally-spaced and $\mathcal{N}(\mathbf{v}|_{I_i}) = 0$, the angle $\theta = \angle(\Delta \mathbf{v}_k, \Delta \mathbf{v}_{k+1})$ for some $k \in I_i^{[2]}$ may still be large, and, thus, $|\Delta^2 \mathbf{v}_k| = 2\bar{h}_i \sin \theta/2 >> 0$.

Finally, for the choice of the normal directions we assume that, with some fixed constant C_1, the sequence of approximate normals $\hat{\mathbf{n}}$ associated with $\hat{\mathbf{v}} = S\mathbf{v}$ satisfies

$$\hat{\mathbf{n}}_K = \mathbf{n}(\xi_K): \qquad |\xi_K - s_k| \leq C_1 h_i, \quad k \in I_i, \quad K \in I_{2i} \cup I_{2i+1}. \tag{4.2.11}$$

with some ξ_K for all $K \in I_{2i} \cup I_{2i+1}$ and all $i \in \mathbb{Z}$. Note that this should hold for all the scales j in the normal MT, even though it is not explicitly mentioned in the formula.

This very mild condition can be seen as a straightforward generalization of the classical approach in [24, 91]. Indeed, if $\hat{\mathbf{n}}_{2i} = \hat{\mathbf{n}}_{2i+1}$ is taken normal to $\Delta \mathbf{v}_i$, (4.2.11) is automatically satisfied, since it gives rise to $s_i < \xi_{2i+1} < s_{i+1}$. The normals $\hat{\mathbf{n}}_{2i}$ are not needed for interpolating S. On the other hand it extends the notion of "normality", allowing directions normal not only to the coarse-scale polyline $\mathbf{v}^j$, but also to the initial curve $\mathcal{C}$ itself. Later we will see that this flexibility leads to improving the smoothness of the normal re-parametrization for the S_p normal MT, even though the detail decay rate remains only 2.

4.2.2 Main theorem

Theorem 4.2.3. *Let $\mathcal{C}$ be a regular $C^{k,\alpha}$ curve with $k \geq 1$, $0 < \alpha \leq 1$, and denote by $\mathbf{v}(s)$ its arc-length parametrization. Assume that S is a linear subdivision operator with finitely supported mask, orders of polynomial reproduction resp. exactness $P \geq P_e \geq 2$, and Hölder smoothness exponent $s_\infty(S) = m + \beta > 1$, where $m \geq 1$ denotes the largest integer $< s_\infty(S)$. Suppose that (4.2.9) holds for $\mathbf{v}^0$ with constants C_0, h, and that throughout the recursion for the approximate normals the condition (4.2.11) is satisfied with constant C_1.*

(i) For small enough h^0 (how small depends on $\mathcal{C}$, S, and the fixed constants appearing in (4.2.11) and (4.2.9)), the normal MT is well-defined for all $j \geq 1$, and produces point sequences $\mathbf{v}^j = (\mathbf{v}(s_i^j))_{i\in\mathbb{Z}} \subset \mathcal{C}$ and scalar detail sequences $d^j = (d_i^j)_{i\in\mathbb{Z}}$ such that

$$\|d^j\|_\infty = \mathrm{O}((h^0 2^{-j})^\mu), \qquad \mu < \min(k+\alpha, m+\beta+1, P_e).$$

The mesh-width sequence $h^j := \|\Delta s^j\|_\infty = \max_i |s_{i+1}^j - s_i^j|$ satisfies $h^j \asymp 2^{-j} h_0$.
(ii) The piecewise linear functions $s = s^j(t)$ interpolating the data s^j at the uniform grid $2^{-j}\mathbb{Z}$, $j \geq 0$, converge to a limit function $s = s(t) \in C^{k',\alpha'}$ if $k' + \alpha' < \min(k+\alpha, m+\beta, P_e)$. Moreover, the normal re-parametrization $\mathbf{v}(s(t))$ of the curve $\mathcal{C}$ is regular, and belongs to $C^{k',\alpha'}$ as well.

The complete proof is very technical and lengthy, and can be found in [62]. Here, we will just briefly sketch the main steps and only try to give the reader an intuition of what goes on. The proof is divided into two parts. For well-posedness and convergence it suffices to consider $k = m = 1$, and, thus, $\delta < \min(\alpha, \beta)$ in (4.2.9), while for computing the detail decay rates and the smoothness of the normal re-parameterization, the exact values of the two parameters do matter. We use the notation, established in Section 4.2.1.

The first part is built on classical perturbation analysis. Since S reproduces constants, applying the Taylor expansion (4.2.7) together with (4.2.11) for small enough h, gives rise to an existence of a unique intersection point $\tilde{\mathbf{v}}_K = \mathbf{v}(\tilde{s}_K)$, $K \in I_{2i} \cup I_{2i+1}$, between the normal line through $(S\mathbf{v})_K$ and the curve arc $\mathcal{C}_i = \mathbf{v}(s|_{I_i})$. Due to the smoothness of $\mathcal{C}$ we derive

$$|d_K| \leq C_3 h_i^{1+\alpha}; \qquad |\tilde{s}_K - (Ss)_K| \leq C_3 h_i^{1+\alpha},$$

with constant C_3 that depends on $\mathcal{C}$, S, and C_1. Combining it with (4.2.10) and $P_e \geq 2$, we get

$$|\Delta\tilde{s}_K - h_i/2| \leq C_4 h_i^{1+\delta},$$

where C_4 depends on C_0 and C_3. Since S is dyadic and generates $C^{1,\beta}$ limit curves,

$$|\Delta^2 S s_K| \asymp C_S 2^{-(1+\beta)} \|\Delta^2 s\|_{I_i} \leq 2^{-(1+\beta)} C_S C_0 h_i^{1+\delta} \leq 2^{\delta-\beta} C_S C_0 \left(\frac{h_i}{2}\right)^{1+\delta}.$$

Working with $\delta < \beta' < \beta$, instead of β will guarantee that $C_S \to 0$, as $h_i \to 0$, so we can freely set $C_S = 1$ and disregard it from the future estimates. Putting all together, we derive

$$\begin{aligned} |\Delta^2\tilde{s}_K| &\leq |\Delta^2 S s_K| + |\Delta^2(\tilde{s} - Ss)_K| \leq 2^{\delta-\beta} C_0 \left(\frac{h_i}{2}\right)^{1+\delta} + 2^{3+\delta} h_i^{\alpha-\delta} C_3 \left(\frac{h_i}{2}\right)^{1+\delta} \\ &\leq C_0 \left(\frac{h_i}{2}\right)^{1+\delta} \left(2^{\delta-\beta} + h_i^{\alpha-\delta} \frac{2^{3+\delta} C_3}{C_0}\right) \leq C_0 \left(|\Delta\tilde{s}_K| + C_4 h_i^{1+\delta}\right)^{1+\delta} \left(2^{\delta-\beta} + h_i^{\alpha-\delta} \frac{2^{3+\delta} C_3}{C_0}\right). \end{aligned}$$

Now, we fix C_0 and $0 < \delta < \min(\alpha, \beta)$, compute the intermediate constants C_3 and C_4, and then, take a sufficiently small step-size h, that guarantees

$$\left(X + C_4 h^{1+\delta}\right)^{1+\delta} \left(2^{\delta-\beta} + h^{\alpha-\delta} \frac{2^{3+\delta} C_3}{C_0}\right) \leq X^{1+\delta}, \qquad X \geq h/4. \tag{4.2.12}$$

This is enough to conclude, that for the above choice of h, (4.2.9) remains true after one level of the normal MT. Now, by induction we get well-posedness of the transform on all the levels $j \in \mathbb{N}$, plus $\|\Delta s^j\| \asymp 2^{-j}\|\Delta s^0\|$, implying that S normal MT converges.

The second part of the proof is based on analysis by proximity (see [50] for a survey of proximity conditions and their use in the analysis of manifold-valued subdivision), combined with bootstrapping arguments. It can be shown that

$$|d_K| \le C|(S\mathbf{v})_K - \mathbf{v}(Ss_K)| \le C' \left(\sum_{\nu \in E_M} \prod_{m=1}^{M} \|\Delta^m s\|_{I_i}^{\nu_m} + \|\Delta s\|_{I_i}^{M+\rho} \right),$$

where both C and C' depend only on $\mathcal{C}$ and S, $M + \rho = \min(k + \alpha, P_e)$ and

$$E_M := \{\nu \in \mathbb{Z}_+^M : \quad \sum_{m=1}^{M} m\nu_m = M + 1, \quad 2 \le \sum_{m=1}^{M} \nu_m \le M\}.$$

In the first part of the proof we have already verified that

$$\|\Delta s^j\| = \mathrm{O}(2^{-j}\|\Delta s^0\|), \qquad \|d^j\| = \mathrm{O}((2^{-j}\|\Delta s^0\|)^{1+\alpha}),$$

holds for $C^{1,\alpha}$ curves. In addition, we need

$$\|\Delta^2 s^j\| = \mathrm{O}(2^{-(1+\alpha')j}), \qquad 0 < \alpha' < \min(1, \alpha, m + \beta - 1).$$

To achieve the latter, we have to switch to local frames and we will skip it here. In the next section we will show for the S_2 normal MT how exactly it is done. Once all these estimates have been established, we use the following technique to improve the order:

- If for some $2 \le n < \min(P, k + 1)$ the estimates

  $$\|d^j\| = \mathrm{O}(2^{-j\mu}), \quad 0 < \mu < n; \quad \text{and} \quad \|\Delta^r s^j\| = \mathrm{O}(2^{-j\beta'}), \quad 0 < \beta' < r, \quad r = 1, \dots, n.$$

  are satisfied then

  $$\|\Delta^{n+1} s^j\|_\infty = \mathrm{O}(2^{-j\gamma}), \qquad 0 < \gamma < \min(n + 1, m + \beta, k + \alpha).$$

- If for some $2 \le n < \min(P_e, k + 1)$ and some $\gamma \in (n - 1, n]$ we have

  $$\|\Delta^r s^j\|_\infty = \begin{cases} \mathrm{O}(2^{-j\beta'}), & 0 < \beta' < r, \quad r = 2, \dots, n - 1, \\ \mathrm{O}(2^{-j\beta'}), & 0 < \beta' < \gamma, \quad r = n, \end{cases}$$

  then

  $$\|d^j\|_\infty = \mathrm{O}(2^{-j\mu}), \qquad j \ge 0, \quad 0 < \mu < \min(\gamma + 1, k + \alpha).$$

This concludes the proof of Theorem 4.2.3.

The first part of the proof differs from the approach in [24]. Indeed, the analysis there is performed with $\delta = 0$. But in this setting, (4.2.12) cannot be established, since the term $C_4 h^{1+\delta}$ is

no longer a high-order perturbation of X and may be even bigger than X. In order to control C_4, and, thus the whole term, an additional restriction on S has been introduced, namely S is taken to be weakly contractive. Our approach verifies that this restriction on S is not necessary for the statements in the theorem to be true. As discussed in Section 4.2.1, the more general statement of Theorem 4.2.3 comes at the price of working with the more complicated and restricting assumption on the initial sample (4.2.9). Another consequence of our choice $\delta > 0$ is the inability to treat S normal MTs, when $P = 1$ or $s_\infty(S) = 1$. The analysis of such transforms is covered in [24]. For example, (4.2.9) does not hold for the mid-point-interpolating scheme S_1 with any $\delta > 0$, even though S_1 normal MT is always well-defined and convergent [91]. To see this we use (4.2.5) and conclude that for any $j \in \mathbb{N}$, $\|\Delta S_1^j s\| = 2^{-j}\|\Delta s\|$, and $\|\Delta^2 S_1^j s\| = 2^{-j}\|\Delta^2 s\|$. Fix any $\delta > 0$ and initial data s, such that $A_0 = \|\Delta^2 s\|/\|\Delta s\|^{1+\delta} > 0$. Hence

$$\|\Delta^2 S_1^j s\| = 2^{-j}\|\Delta^2 s\| = 2^{-j} A_0 \|\Delta s\|^{1+\delta} = 2^{j\delta} A_0 \|\Delta S_1^j s\|^{1+\delta} = A_j \|\Delta S_1^j s\|^{1+\delta},$$

and no matter how small A_0 and δ are, $A_j \to \infty$ as $j \to \infty$.

For the second part of the proof, the new observation compared to [24] is the role of the order of exact polynomial reproduction P_e which bounds the order of proximity for $|\mathbf{v} \cdot S - S \cdot \mathbf{v}|$. In [24] all the statements are in terms of the order of polynomial reproduction P. Since they consider only interpolating S, $P_e = P$ and $c_S = 0$. This indicates that in general it is tricky to extend theory from the interpolating to the approximating setting, since there are two different candidates for P there. E.g., S possesses derived schemes up to order P and its regularity $m + \beta$ depends on P, too, but the S normal MT has detail decay rate not faster than P_e. Later, we will see that these oddities, unlike the interpolating case, allow us to separate the analysis on the details from the one on the smoothness of the normal re-parameterization and to change one of the two characteristics of the transform without affecting the other.

4.3 Chaikin normal multi-scale transform

In this section we study the S_2 normal MT for closed $C^{1,\alpha}$ curves $\mathcal{C}$, and the text repeats our papers [62, Section 4.1] and [60, Section 2]. The constants C_i used in the exposition are different from those in Section 4.2. Recall that the Chaikin scheme

$$(S_2\mathbf{v})_{2i} = \frac{3\mathbf{v}_i + \mathbf{v}_{i+1}}{4}, \qquad (S_2\mathbf{v})_{2i+1} = \frac{\mathbf{v}_i + 3\mathbf{v}_{i+1}}{4}, \qquad i \in \mathbb{Z}, \tag{4.3.1}$$

is approximating with $P = 3$, $P_e = 2$, and $c_S = 1/4$ and generates $C^{1,1}$ limit functions. Although its analysis is covered by Theorem 4.2.3, we will give an independent treatment, and obtain an unconditional global convergence result. I.e., for the natural choice of normal directions

$$\mathbf{n}_{2i}^j = \mathbf{n}_{2i+1}^j \perp \Delta\mathbf{v}_i^{j-1}, \qquad i \in \mathbb{Z}, \quad j \geq 1, \tag{4.3.2}$$

we prove the following

Theorem 4.3.1. *Let $\mathcal{C}$ be a closed, non-self-intersecting $C^{1,\alpha}$ curve, $0 < \alpha \leq 1$. For any (ordered) initial point sequence $\mathbf{v}^0 \subset \mathcal{C}$ the S_2 normal MT that satisfies (4.3.2) is well-defined. It produces point sequences $\mathbf{v}^j \subset \mathcal{C}$ and scalar detail sequences $d^j = (d_i^j)_{i\in\mathbb{Z}}$ such that*

$$\|\Delta\mathbf{v}^j\| \leq C_0\|\Delta\mathbf{v}^0\|2^{-j}, \quad \|\Delta^2\mathbf{v}^j\| \leq C_1\|\Delta\mathbf{v}^0\|2^{-j(1+\alpha')}, \quad j \geq 1, \tag{4.3.3}$$

$0 < \alpha' < \alpha$, *and*

$$\|d^j\| \le C_2 \|\Delta \mathbf{v}^{j-1}\|^{1+\alpha} \le C_3 (\|\Delta \mathbf{v}^0\| 2^{-j})^{(1+\alpha)}, \qquad j \ge 1, \tag{4.3.4}$$

hold. The finite constants C_0, C_1, C_2, C_3 depend solely on the curve $\mathcal{C}$.

Moreover, if $\{\mathbf{w}^0, \tilde{d}^1, \tilde{d}^2, \dots, \tilde{d}^J\}$ with arbitrary $J \in \mathbb{N}$ is a perturbed representation of the actual multi-scale data, i.e.,

$$\|\mathbf{v}^0 - \mathbf{w}^0\| \le \epsilon_0, \qquad \|d^j - \tilde{d}^j\| \le \epsilon_d 2^{-j\nu}, \quad 1 \le j \le J,\ \nu > 0$$

then there exists a constant C_4, depending on $\mathcal{C}, \mathbf{v}^0, \epsilon_0$ and ϵ_d, but not on J, s.t.,

$$\|\mathbf{v}^j - \mathbf{w}^j\| \le C_4(\epsilon_0 + \epsilon_d), \qquad \forall j \le J. \tag{4.3.5}$$

Proof. Step 1. We first argue that the S_2 normal MT is always well-defined. Let $\mathcal{C}$ be given by its arc-length parametrization $\mathbf{v}(s)$. Fix an arbitrary level $j \in \mathbb{N}$ and an arbitrary position $i \in \mathbb{Z}$. Since $\mathcal{C}$ is continuous and the points $\mathbf{v}(s_i^{j-1})$ and $\mathbf{v}(s_{i+1}^{j-1})$ belong to different hyper-planes with respect to the parallel normal lines $L_{i,\ell}(t) = (S_2 \mathbf{v}^{j-1})_{2i+\ell} + t\hat{\mathbf{n}}^j_{2i+\ell}$, $\ell = 0, 1$, these two lines will intersect at least once the open arc $\mathbf{v}(s)|_{s_i^{j-1} < s < s_{i+1}^{j-1}}$ connecting $\mathbf{v}_i^{j-1}$ and $\mathbf{v}_{i+1}^{j-1}$. Now, if we choose $\mathbf{v}_{2i}^j = \inf_{s > s_i^{j-1}} \{\mathbf{v}(s) \ : \ \mathbf{v}(s) \in L_{i,0}\}$, resp. $\mathbf{v}_{2i+1}^j = \sup_{s < s_{i+1}^{j-1}} \{\mathbf{v}(s) \ : \ \mathbf{v}(s) \in L_{i,1}\}$ as the left-most (for $\ell = 0$) resp. the right-most (for $\ell = 1$) intersection point of $L_{i,\ell}(t)$ with this arc, then automatically $s_i^{j-1} < s_{2i}^j < s_{2i+1}^j < s_{i+1}^{j-1}$. This guarantees the well-posedness.

Step 2. Next we establish that $h^j = \|\Delta s^j\| \to 0$ for any initial set of correctly ordered points $\mathbf{v}^0$ on $\mathcal{C}$. Denote by L the length of $\mathcal{C}$. A small modification of equation (6) in [91] gives that for any $L_1 < L$ there exists a constant $q > 0$ (depending only on $\mathcal{C}$ and $L - L_1$) such that

$$|\mathbf{v}(s') - \mathbf{v}(s)| \ge q|s' - s|, \qquad |s' - s| \le L_1 \tag{4.3.6}$$

holds. Now, given any $\mathbf{v}^0 = \{\mathbf{v}(s_i^0)\}_{i \in \mathbb{Z}}$ containing $N \ge 2$ different points on $\mathcal{C}$, denote $h_i^0 := (\Delta s^0)_i$, $h^0 := \sup_i h_i^0$, and set $H_i^0 := h_{i-1}^0 + h_i^0$, $H^0 := \sup_i H_i^0$. Apply (4.3.6) with appropriately fixed L_1, and derive

$$\begin{aligned}
H_{2i-1}^1 &= s_{2i}^1 - s_{2i-2}^1 = H_i^0 - \big((s_{2i-2}^1 - s_{i-1}^0) + (s_{i+1}^0 - s_{2i}^1)\big) \\
&\le H_i^0 - |\mathbf{v}(s_{2i-2}^1) - \mathbf{v}(s_{i-1}^0)| - |\mathbf{v}(s_{i+1}^0) - \mathbf{v}(s_{2i}^1)| \\
&\le H_i^0 - \frac{1}{4}|\mathbf{v}(s_i^0) - \mathbf{v}(s_{i-1}^0)| - \frac{3}{4}|\mathbf{v}(s_{i+1}^0) - \mathbf{v}(s_i^0)| \\
&\le H_i^0 - \frac{q}{4} h_{i-1}^0 - \frac{3q}{4} h_i^0 < (1 - q/4) H_i^0 = r H_i^0,
\end{aligned}$$

where $r < 1$ depends only on $\mathcal{C}$ and $\mathbf{v}^0$. Analogously

$$H_{2i}^1 \le H_i^0 - \frac{3q}{4} h_{i-1}^0 - \frac{q}{4} h_i^0 < r H_i^0.$$

Hence $H^1 < rH^0$, and repeating the same argument for every subdivision step, we conclude that $h^j < H^j < r^j H^0$ and thus $h^j \to 0$ as $j \to 0$ at some geometric decay rate. Note that $h^j \to 0$ implies $\bar{h}^j \to 0$, where, as in Lemma 4.2.2, $\bar{h}^j = \|\Delta \mathbf{v}^j\|_\infty = \sup_{i \in \mathbb{Z}} \bar{h}_i^j$, where $\bar{h}_i^j = |\Delta \mathbf{v}_i^j|$.

Step 3. Now we turn to the first asymptotic estimate in (4.3.3). According to Lemma 4.2.1, we can work with local parameterizations $(x, f(x))$, $x \in [-\rho, \rho]$, of the $C^{1,\alpha}$ curve $\mathcal{C}$, where $x = x(s+\xi) - x(\xi)$ and $y = f(x) \equiv y(s+\xi) - y(\xi)$ are the coordinates with respect to the frame $(\mathbf{v}(\xi), \mathbf{t}(\xi), \mathbf{n}(\xi))$ with arbitrarily fixed ξ. Note that both $0 < \rho \leq 1$ and the Lipschitz constant C_f in

$$|f'(x_1) - f'(x_2)| \leq C_f |x_1 - x_2|^\alpha, \qquad x_1, x_2 \in [-\rho, \rho], \tag{4.3.7}$$

can be assumed to be independent of ξ. Also note that $f(0) = 0$ and $f'(0) = 0$ in the local frame coordinates, and that $x = x(s)$ is a monotonically increasing function of s. The following simple inequality for $f(x)$ will be used frequently,

$$|f(x)| = |f(x) - f(0)| = |f'(\eta)||x| = |f'(\eta) - f'(0)||x| \leq C_f |\eta|^\alpha |x| \leq C_f |x|^{1+\alpha}, \quad x \in [-\rho, \rho]. \tag{4.3.8}$$

It is sufficient to prove (4.3.3) under the assumption that the initial step-size $\bar{h}^0$ is already small enough. More precisely, without loss of generality, we can assume that

$$C_f (\bar{h}^0)^\alpha < 1/2; \qquad \bar{h}^0 \leq \rho \leq 1. \tag{4.3.9}$$

Indeed, since $\bar{h}^j \to 0$, for some finite j_0 the corresponding step-size $\bar{h}^{j_0}$ will satisfy these two inequalities, and we can then apply the result to $\mathbf{v}^{j_0}$ as new initial point set to get the asymptotic result in (4.3.3).

We first investigate a single step of the S_2 normal MT. To simplify the notation, the sequence $\mathbf{v} = (\mathbf{v}_i)_{i \in \mathbb{Z}}$, where $\mathbf{v}_i = \mathbf{v}(s_i)$, will denote the current point set $\mathbf{v}^{j-1}$ on $\mathcal{C}$, and $\tilde{\mathbf{v}} = (\tilde{\mathbf{v}}_i)_{i \in \mathbb{Z}}$ will denote the sequence $\mathbf{v}^j$ generated on the next level. Fix an arbitrary i, put $\xi = s_i$, and consider the local frame coordinates attached to the point $\mathbf{v}_i$. If $\bar{h} := \|\Delta \mathbf{v}\| \leq \rho$ we can write $\mathbf{v}_{i-1} = (-x', f(-x'))$, $\mathbf{v}_{i+1} = (x, f(x))$, with some $x', x \in (0, \rho]$. This notation is also depicted in Figure 4.2. We would like to compare $\bar{h}$ with $\bar{\tilde{h}} := \|\Delta \tilde{\mathbf{v}}\|$. We only need to investigate two subcases, namely to compare $\bar{\tilde{h}}_{2i} := |\tilde{\mathbf{e}}_{2i}|$ to $\bar{h}_i := |\mathbf{e}_i|$, and the similarly defined $\bar{\tilde{h}}_{2i-1}$ to $\bar{h}_{i-1}$ and $\bar{h}_i$, where $\tilde{\mathbf{e}} := \Delta \tilde{\mathbf{v}}$ and $\mathbf{e} = \Delta \mathbf{v}$.

In the first case, we have $\hat{\mathbf{v}}_{2i} := (S_2 \mathbf{v})_{2i} = (\frac{1}{4}x, \frac{1}{4}f(x))$. Let ϵ_x be such that $\tilde{\mathbf{v}}_{2i} = (\frac{1}{4}x + \epsilon_x, f(\frac{1}{4}x + \epsilon_x))$ (since S_2 normal MT is well-defined such an ϵ_x exists, and satisfies $0 < x/4 + \epsilon_x < x$). By (4.3.2), we have $\tilde{\mathbf{v}}_{2i} - \hat{\mathbf{v}}_{2i} \perp \mathbf{e}_i$, and substituting the coordinate representations of these vectors, we find

$$-\epsilon_x x + f(x) \left(\frac{1}{4} f(x) - f(\frac{1}{4}x + \epsilon_x) \right) = 0. \tag{4.3.10}$$

Straightforward calculations lead to

$$\frac{1}{4} f(x) - f(\frac{1}{4}x + \epsilon_x) = \frac{1}{4} f'(t_1) x - (\frac{1}{4}x + \epsilon_x) f'(t_2) = \frac{1}{4} x (f'(t_1) - f'(t_2)) - \epsilon_x f'(t_2), \tag{4.3.11}$$

where $t_1 \in (0, x)$, $t_2 \in (0, \frac{1}{4}x + \epsilon_x)$. Substituting (4.3.11) into (4.3.10), we obtain

$$\epsilon_x (f'(t_2) f(x) + x) = \frac{1}{4} x f(x) (f'(t_1) - f'(t_2)).$$

Hence, using (4.3.9), (4.3.8) and the Lipschitz condition for f' appropriately, we arrive at

$$|\epsilon_x| \leq \frac{|f(x)||f'(t_1) - f'(t_2)|}{4(1 - |f'(t_2) f(x)|/x)} \leq \frac{C_f^2}{4(1 - C_f^2 x^{2\alpha})} x^{1+2\alpha} \leq \frac{C_f^2}{3} x^{1+2\alpha}.$$

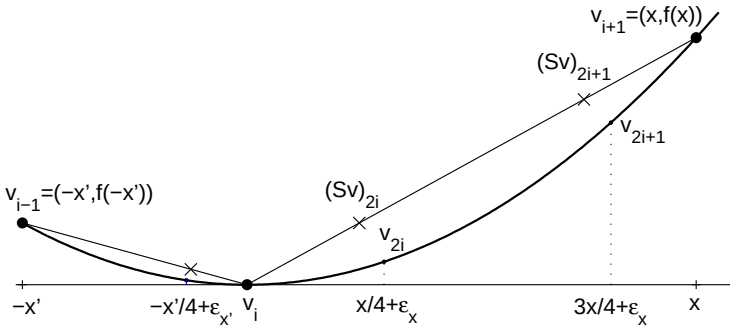

Fig. 4.2: One step of S_2 normal MT

Similarly, for the points $\hat{\mathbf{v}}_{2i+1}$ and $\tilde{\mathbf{v}}_{2i+1} = (\frac{3}{4}x + \hat{\epsilon}_x, f(\frac{3}{4}x + \hat{\epsilon}_x))$, we obtain

$$|\hat{\epsilon}_x| \le \frac{3C_f^2}{4(1 - C_f^2 x^{2\alpha})} x^{1+2\alpha} \le C_f^2 x^{1+2\alpha}.$$

Therefore, we can write

$$\begin{aligned} \tilde{\bar{h}}_{2i} &= |\tilde{\mathbf{e}}_{2i}| = [(\frac{3}{4}x + \hat{\epsilon}_x - \frac{1}{4}x - \epsilon_x)^2 + (f(\frac{3}{4}x + \hat{\epsilon}_x) - f(\frac{1}{4}x + \epsilon_x))^2]^{1/2} \\ &= (\frac{1}{2}x + \hat{\epsilon}_x - \epsilon_x)\sqrt{1 + f'(t_3)^2} =: \frac{1}{2}x + \tilde{\delta}_x, \end{aligned}$$

where $0 < t_3 < x$. Using the standard estimate $\sqrt{1+a} \le 1 + a/2$ for $a \ge 0$, and $|f'(t_3)|^2 < C_f^2 x^{2\alpha} < 1/4$, see (4.3.9), we estimate the term $\tilde{\delta}_x$ by

$$\begin{aligned} |\tilde{\delta}_x| &\le (|\hat{\epsilon}_x| + |\epsilon_x|)\sqrt{1 + f'(t_3)^2} + \frac{x}{2}(\sqrt{1 + f'(t_3)^2} - 1) \\ &\le \frac{4}{3}C_f^2 x^{1+2\alpha}(1 + \frac{C_f^2 x^{2\alpha}}{2}) + \frac{1}{4}C_f^2 x^{1+2\alpha} < \frac{7}{4}C_f^2 x^{1+2\alpha}. \end{aligned}$$

Since $x \le \bar{h}_i$, for the first case we thus obtain

$$\tilde{\bar{h}}_{2i} \le \frac{1}{2}\bar{h}_i + \frac{7}{4}C_f^2(\bar{h}_i)^{1+2\alpha}. \tag{4.3.12}$$

For the second case, we also need estimates for $\tilde{\mathbf{v}}_{2i-1} = (-\frac{1}{4}x' + \epsilon_{x'}, f(-\frac{1}{4}x' + \epsilon_{x'}))$. By repeating the above calculations for $\tilde{\mathbf{v}}_{2i}$ with x replaced by $-x'$, we arrive at

$$|\epsilon_{x'}| \leq \frac{C_f^2}{4(1 - C_f^2(x')^{2\alpha})}(x')^{1+2\alpha} \leq \frac{C_f^2}{3}(x')^{1+2\alpha},$$

and can write

$$\tilde{\bar{h}}_{2i-1} \quad = |\tilde{\mathbf{v}}_{2i-1}| = \left(\tfrac{1}{4}(x + x') + \epsilon_x - \epsilon_{x'}\right)\sqrt{1 + f'(t_4)^2} \equiv \tfrac{1}{4}(x + x') + \tilde{\delta}_{x'},$$

where $-x' < -x'/4 + \epsilon_{x'} < t_4 < x/4 + \epsilon_x < x$, and

$$\begin{aligned}
|\tilde{\delta}_{x'}| &\leq (|\epsilon_x| + |\epsilon_{x'}|)\sqrt{1 + f'(t_4)^2} + \frac{(x + x')}{4}(\sqrt{1 + f'(t_4)^2} - 1) \\
&\leq \frac{C_f^2}{3}(x^{1+2\alpha} + (x')^{1+2\alpha})\sqrt{1 + f'(t_4)^2} + \frac{(x + x')}{8}C_f^2 \max(x, x')^{2\alpha} \\
&\leq \frac{2C_f^2}{3}\max(x, x')^{1+2\alpha}(1 + \frac{C_f^2 \max(x, x')^{2\alpha}}{2}) + \frac{C_f^2}{4}\max(x, x')^{1+2\alpha} \leq C_f^2 \max(x, x')^{1+2\alpha},
\end{aligned}$$

since $1 + C_f^2 \max(x, x')^{2\alpha}/2 < 9/8$. Taking into account $x' \leq \bar{h}_{i-1}$ and $x \leq \bar{h}_i$, we deduce

$$\tilde{\bar{h}}_{2i-1} \leq \frac{1}{2}\max(\bar{h}_{i-1}, \bar{h}_i) + C_f^2 \max(\bar{h}_{i-1}, \bar{h}_i)^{1+2\alpha}. \tag{4.3.13}$$

Now, using (4.3.12), (4.3.13), and passing to the maximum with respect to i, we conclude that

$$\tilde{\bar{h}} \leq \frac{1}{2}\bar{h}(1 + \frac{7}{2}C_f^2 \bar{h}^{1+2\alpha}) \tag{4.3.14}$$

holds, whenever $\bar{h}$ satisfies (4.3.9). Applying (4.3.9) one more time, we get $\tilde{\bar{h}} \leq r\bar{h}$ with $r := 15/16 < 1$, so $\tilde{\bar{h}}$ satisfies (4.3.9) as well. Iterating, we get $\bar{h}^j \leq r^j \bar{h}^0$ but also the stronger result

$$\bar{h}^j \leq 2^{-j}\bar{h}^0 \prod_{l=0}^{j-1}(1 + \frac{7}{2}C_f^2(r^l \bar{h}^0)^{2\alpha}) \leq 2^{-j}\bar{h}^0 \prod_{l=0}^{\infty}(1 + \frac{7}{8}r^{2\alpha l}) \leq C_0 2^{-j}\bar{h}^0,$$

with a constant C_0 depending on α only. This finishes the proof of the first part of (4.3.3).

Step 4. Regarding the detail decay, observe that

$$|d_{2i}| = |\tilde{\mathbf{v}}_{2i} - \hat{\mathbf{v}}_{2i}| \leq |\epsilon_x| + \left|f(\frac{1}{4}x + \epsilon_x) - \frac{1}{4}f(x)\right| \leq \frac{C_f^2}{3}x^{1+2\alpha} + \frac{5}{4}C_f x^{1+\alpha} \leq \frac{17}{12}C_f \bar{h}^{1+\alpha} \tag{4.3.15}$$

where we have again used (4.3.9). The same estimate can be obtained for d_{2i-1}, and for all other indices by shifting to the corresponding local coordinate system. Thus,

$$\|d^j\|_\infty \leq C_2(\bar{h}^{j-1})^{1+\alpha} \leq C_2(C2^{-(j-1)}\bar{h}^0)^{1+\alpha} \leq C_3(\bar{h}^0 2^{-j})^{1+\alpha}, \tag{4.3.16}$$

with C_2, C_3 depending on α. By [62, Lemma 2.2], (4.3.16) also assures $C^{1,\alpha'}$ smoothness of the normal re-parametrization.

Step 5. To verify the asymptotic decay of $\|\Delta^2\mathbf{v}^j\|$ claimed in (4.3.3) we use Step 3. For $\tilde{\mathbf{v}} = \mathbf{v}^j$ we have

$$\begin{aligned}|\Delta^2\tilde{\mathbf{v}}_{2i-1}| &\le \left|\frac{x-x'}{4} + \hat{\epsilon}_x - 2\epsilon_x + \epsilon_{x'}\right| + \left|f(\frac{3}{4}x + \hat{\epsilon}_x) - 2f(\frac{1}{4}x + \epsilon_x) + f(-\frac{1}{4}x' + \epsilon_{x'})\right| \\ &\le \frac{1}{4}\frac{|x-x'|}{4} + |\hat{\epsilon}_x| + 2|\epsilon_x| + |\epsilon_{x'}| + 2\bar{h}\sup_{\eta\in[-\rho,\rho]}|f'(\eta)| \le \frac{1}{4}|\Delta^2\mathbf{v}_{i-1}| + 3C_f\bar{h}^{1+\alpha}.\end{aligned}$$

The same estimation holds for $|\Delta^2\tilde{\mathbf{v}}_{2i-2}|$. Now pick any $\alpha' \le \alpha$ with $\alpha' < 1$. Taking the supremum over all i and iterating over all the levels j gives rise to

$$\begin{aligned}\|\Delta^2\mathbf{v}^j\|_\infty &\le \frac{1}{4}\|\Delta^2\mathbf{v}^{j-1}\|_\infty + 3C_f(\bar{h}^{j-1})^{1+\alpha'} \le \frac{1}{4}\|\Delta^2\mathbf{v}^{j-1}\|_\infty + 3C_f(C2^{-(j-1)}\bar{h}^0)^{1+\alpha'} \\ &\le 4^{-j}\|\Delta^2\mathbf{v}^0\|_\infty + CC_f(2^{-j}\bar{h}^0)^{1+\alpha'}\sum_{l=0}^{j-1}2^{-(1-\alpha')l} \le C_1(\|\Delta\mathbf{v}^0\|_\infty 2^{-j})^{1+\alpha'}.\end{aligned}$$

Step 6. The last step is to prove stability. For any $j \in \mathbb{N}$, any $i \in \mathbb{Z}$ and $l \in \{0,1\}$

$$\begin{aligned}|\mathbf{v}^j_{2i+l} - \mathbf{w}^j_{2i+l}| &\le |S(\mathbf{v}^{j-1} - \mathbf{w}^{j-1})_{2i+l}| + |d^j_{2i+l}\mathbf{n}^j_{2i+l} - \tilde{d}^j_{2i+l}\tilde{\mathbf{n}}^j_{2i+l}| \\ &\le \|\mathbf{v}^{j-1} - \mathbf{w}^{j-1}\| + \|d^j - \tilde{d}^j\| + |d^j_{2i+l}||\mathbf{n}^j_{2i+l} - \tilde{\mathbf{n}}^j_{2i+l}|.\end{aligned}$$

The main trick is to estimate the last summand in a way that the perturbed data plays as less a role as possible, namely to verify

$$|\mathbf{n}^j_{2i+l} - \tilde{\mathbf{n}}^j_{2i+l}| \le \frac{4\|\mathbf{v}^{j-1} - \mathbf{w}^{j-1}\|}{|\Delta\mathbf{v}^{j-1}_i|}. \tag{4.3.17}$$

Indeed, (4.3.2) gives rise to $\mathbf{n}^j_{2i} = \mathbf{n}^j_{2i+1} = (\Delta\mathbf{v}^{j-1}_i)^\perp/|\Delta\mathbf{v}^{j-1}_i|$, and $\tilde{\mathbf{n}}^j_{2i} = \tilde{\mathbf{n}}^j_{2i+1} = (\Delta\mathbf{w}^{j-1}_i)^\perp/|\Delta\mathbf{w}^{j-1}_i|$, respectively. First, assume that $|\Delta\mathbf{w}^{j-1}_i| > 0$ and the $\mathbb{R}^2$ scalar product $\langle\Delta\mathbf{v}^{j-1}_i, \Delta\mathbf{w}^{j-1}_i\rangle \ge 0$. Then the trivial estimation (see Fig. 4.3)

$$|\mathbf{n}^j_{2i+l} - \tilde{\mathbf{n}}^j_{2i+l}| = 2\sin\frac{\alpha}{2} = \frac{\sin\alpha}{\cos\alpha/2} \le \frac{2\|\mathbf{v}^{j-1} - \mathbf{w}^{j-1}\|}{\cos(\alpha/2)|\Delta\mathbf{v}^{j-1}_i|} \le \frac{2\sqrt{2}\|\mathbf{v}^{j-1} - \mathbf{w}^{j-1}\|}{|\Delta\mathbf{v}^{j-1}_i|}, \qquad l = 0,1,$$

holds, where $\alpha = \angle(\Delta\mathbf{v}^{j-1}_i, \Delta\mathbf{w}^{j-1}_i) \in (0, \pi/2)$. For the case $\langle\Delta\mathbf{v}^{j-1}_i, \Delta\mathbf{w}^{j-1}_i\rangle < 0$, we derive $2\|\mathbf{v}^{j-1} - \mathbf{w}^{j-1}\| > |\Delta\mathbf{v}^{j-1}_i|$ and (4.3.17) is again fulfilled. Finally, unless some additional restrictions on $\epsilon_{\mathcal{C}}, \epsilon_d$ and ν are imposed, $|\Delta\mathbf{w}^{j-1}_i|$ can be zero and, thus, $\tilde{\mathbf{n}}^j_{2i+l}$ may not be defined. In this case take arbitrary unit vectors $\tilde{\mathbf{n}}^j_{2i}, \tilde{\mathbf{n}}^j_{2i+1}$ and let $\mathbf{w}^j_{2i+l} = \mathbf{w}^{j-1}_i + \tilde{d}^j_{2i+l}\tilde{\mathbf{n}}^j_{2i+l}$, $l = 0,1$. From triangle inequality we have $2\|\mathbf{v}^{j-1} - \mathbf{w}^{j-1}\| \ge |\Delta\mathbf{v}^{j-1}_i|$, so (4.3.17) remains true.

Once (4.3.17) is established, we use (4.3.15) together with the first part of (4.3.3) to conclude

$$\|\mathbf{v}^j - \mathbf{w}^j\| \le (1 + \underbrace{2^{2-\alpha}C_2C_0^\alpha\|\Delta\mathbf{v}^0\|^\alpha}_{C}2^{-j\alpha})\|\mathbf{v}^{j-1} - \mathbf{w}^{j-1}\| + \epsilon_d 2^{-j\nu}.$$

The latter gives rise to (4.3.5) (see [91, Theorem 4] for more details). Hence, the proof of Theorem 4.3.1 is complete. □

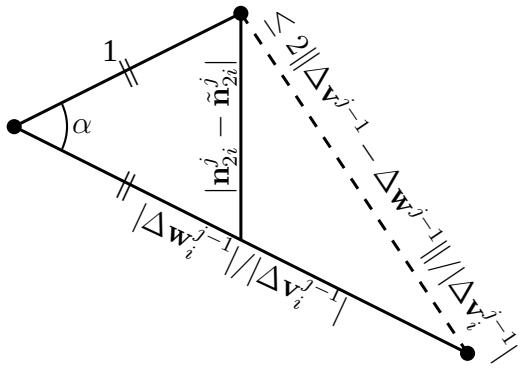

Fig. 4.3: The estimations for (4.3.17) in the case $\langle \Delta \mathbf{v}_i^{j-1}, \Delta \mathbf{w}_i^{j-1} \rangle \geq 0$.

Some remarks are in order: Note that for $\alpha = 1$, the above computations yield a detail decay rate of $\|d^j\| = \mathrm{O}(2^{-2j})$ but only $\|\Delta^2 \mathbf{v}^j\| \leq Cj\|\Delta \mathbf{v}^0\| 2^{-2j}$ which falls short of establishing the second estimate in (4.3.3), and the $C^{1,\alpha'}$ property with $\alpha' = \alpha = 1$ in this case. The latter is verified in Theorem 5.1.3, where a slightly different technique is used. Even though (4.3.5) measures the L_∞ distance between the actual curve $\mathcal{C}$ and the perturbed limit $\tilde{\mathcal{C}}$, both given analytically by their normal re-parameterizations, the same bound is valid for the Hausdorff distance $dist_{\mathcal{H}}(\mathcal{C}, \tilde{\mathcal{C}})$ between the geometric curves. Indeed, at each level $j \in \mathbb{N}$ the Hausdorff distance between the piecewise linear interpolants of $\mathbf{v}^j$ and $\mathbf{w}^j$ does not exceed $\|\mathbf{v}^j - \mathbf{w}^j\|_\infty$, since the Hausdorff distance between two line segments is less or equal to the maximum of the distances between the corresponding end points of the segments. Under the assumptions of Theorem 4.3.1, (4.3.5) uniformly bounds the point-wise distance between the original data and the perturbed one (confirming that compression is a numerically stable procedure [91, Remark 1]) but none of the nice properties of $\mathcal{C}$ and $\mathbf{v}^j$ are automatically inherited by $\tilde{\mathcal{C}}$ and $\mathbf{w}^j$. Indeed, $\mathbf{w}^j$ may not be even well-defined (e.g., two neighboring vertices may coincide) or when it is well-defined, inequalities such as (4.3.3) do not necessarily hold. Furthermore, $\tilde{\mathcal{C}}$ may have an arbitrary number of self-intersecting-points and is only continuous in general. However, it seems that small/controlled perturbations may still preserve the additional structure of the data, but to prove this, different approaches than the one presented in this section should be used.

4.4 Globally convergent normal MTs based on adaptivity

A significant drawback in terms of applications of the normal multi-scale technique is the nonexistence of a globally/unconditionally well-posed and convergent transform, that at the same time has high compression rates. To show this we prove the following result.

Proposition 4.4.1. *Let S be linear, local, shift-invariant subdivision scheme that reproduces constants. A necessary condition for the S normal MT to be well-posed for any initial curve $\mathcal{C}$ and any (admissible) initial data $\mathbf{v}^0$ is that the coordinate-wise definition of S takes the form*

$$(Sx)_{2i} = \alpha x_i + (1-\alpha) x_{i+1}; \qquad (Sx)_{2i+1} = \beta x_i + (1-\beta) x_{i+1}; \qquad 0 \leq \beta < \alpha \leq 1.$$

Proof. Fix $k \in \mathbb{Z}$. The proof elaborates the simple idea, that whenever at least one of the predictions $(S\mathbf{v})_{2k}$ or $(S\mathbf{v})_{2k+1}$ (w.l.o.g. let it be $(S\mathbf{v})_{2k}$) is not restricted to lie directly on the coarse-scale edge $\mathbf{v}_k\mathbf{v}_{k+1}$, one can construct a set $\mathbf{v}^0$ such that the normal line through $(S\mathbf{v}^0)_{2k}$ does not intersect the edge at all. Finally, one can construct a curve $\mathcal{C}$, interpolating $\mathbf{v}^0$, such that one step of the S normal MT distorts the topology on $\mathbf{v}^1$, i.e., the arc-length parameter s^1_{2k}, associated to $\mathbf{v}^1_{2k}$ is smaller than the corresponding s^1_{2k-1}. This is exactly one of the cases, when the normal MT is considered to be ill-posed. The actual computations follow this paragraph.

Let S be such that the S normal MT is globally well-defined. Denote by I_k the invariant neighborhood of S around k. First, consider $\mathcal{C}$ to be the line segment $\{y = 0, 0 \le x \le 1\}$ in $\mathbb{R}^2$. This leads to the degenerate case $d^j_i = 0$ and $\mathbf{v}^j_i = (s^j_i, 0)$ for all $j \in \mathbb{N}$, $i \in \mathbb{Z}$. Then the S normal MT is well-defined on $\mathcal{C}$ if for each scale j, s^j is a monotonically increasing sequence, which is the same as S being a monotonicity preserving scheme. The latter is true if and only if the first derived scheme $S^{[1]}$ has a positive mask $a^{(1)}$ (see for example [114]). But in the first chapter we have already shown that the symbols of $S^{[1]}$ and S are linked with the formula

$$a^{(1)}(z) = \frac{za(z)}{z+1},$$

meaning that $a_i = a^{(1)}_i + a^{(1)}_{i+1}$, $i \in \mathbb{Z}$. Hence, S has positive mask, itself. The next step is to show that S has the smallest possible support, i.e., that $(S\mathbf{v})_{2k}$ and $(S\mathbf{v})_{2k+1}$ depend solely on $\mathbf{v}_k$ and $\mathbf{v}_{k+1}$. This is equivalent to proving that $a_i = 0$ for $i \notin A := \{-2, -1, 0, 1\}$. If S is interpolatory, then $a_{2i} = 0$ for all $i \neq 0$. But

$$0 = a_{2i} = a^{(1)}_{2i} + a^{(1)}_{2i+1} \quad \& \quad a^{(1)}_{2i}, a^{(1)}_{2i-1} \ge 0 \qquad \Longrightarrow \qquad a^{(1)}_{2i} = a^{(1)}_{2i+1} = 0,$$

leading to $a_i = 0$, $|i| \ge 2$. Now, assume that S is an approximating scheme with support of its mask bigger than A. We will construct a point set $\mathbf{v}^0$ and a curve $\mathcal{C}$ through it, such that for the data $\mathbf{v}^1 = S\mathbf{v}^0 + d^1\mathbf{n}^1$ the corresponding arc-length sequence s^1 can not be monotonically increasing, and, thus, the process is ill-defined. We work with normals, given via (4.3.2), but it is clear how to do it in general. By $\mathbf{v}^0$ being admissible we mean that s^0 is monotonically increasing. Let

$$1 < \max\{i \in \mathbb{Z} \ : \ a_i \neq 0\} = 2\ell, \qquad \ell > 0.$$

The cases when ℓ is odd, or when $\min\{i \in \mathbb{Z} \ : \ a_i \neq 0\} < -2$ are analogous. Then

$$(Sx)_{2k} = a_{2\ell}x_{k-\ell} + \sum_{i>k-\ell} a_{2(k-i)}x_i,$$

which, together with the fact that S reproduces constants gives rise to

$$(Sx)_{2k} - x_k = -a_{2\ell}\Delta x_{k-\ell} + \sum_{i>k-\ell} b_{k-i}\Delta x_i. \tag{4.4.1}$$

The sequence b can be computed from a and has smaller support. Note that from the very beginning we have silently assumed that $(Sx)_{2k}$ and $(Sx)_{2k+1}$ are centered with respect to x_k and x_{k+1}. More precisely, when Δx is constant $x_k \le (Sx)_{2k} < (Sx)_{2k+1} \le x_{k+1}$. This, together with (4.4.1) and $a_{2\ell} > 0$, implies that there exists such an $x^0 \in \ell_\infty(\mathbb{Z})$ that

$$x^0_{k-1} < (Sx^0)_{2k-2} < (Sx^0)_{2k-1} < (Sx^0)_{2k} < x^0_k.$$

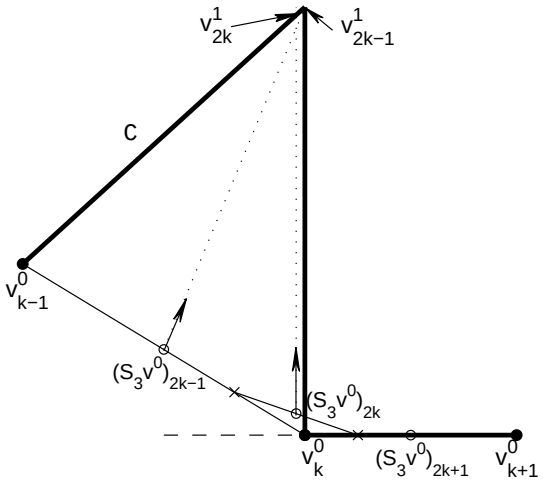

Fig. 4.4: An example that the "standard" normal S_3 MT is not necessarily well-posed in general.

The rest is easy. Take a set of points $\{\mathbf{v}^0 : \mathbf{v}^0_i = (x^0_i, y^0_i),\ i \in I_{k-1} \cup I_k\}$ in $\mathbb{R}^2$, where $y^0_i = \epsilon x^0_i,\ i < k$, $y^0_i = 0,\ i \geq k$. The constant ϵ is an arbitrary positive constant and its role is simply to assure that $\mathbf{n}^1_{2k-1}$ is not parallel to $\mathbf{n}^1_{2k}$. Let $L_{k-1}(t) \cap L_k(t) = P$, where, as always, $L_{k-1}(t)$ and $L_k(t)$ are the corresponding normal lines. Choose $\mathcal{C}$ to be a continuous planar curve that interpolates $\mathbf{v}^0$ but does not intersect the angle-shaped region between $\overrightarrow{P\mathbf{v}^0_{k-1}}$ and $\overrightarrow{P\mathbf{v}^0_k}$ (see Fig. 4.4). Then with respect to the arc-length parameterization $\mathbf{v}(s)$ of $\mathcal{C}$, and the notation $\mathbf{v}^1 = \mathbf{v}(s^1)$ we have $s^1_{2k-1} > s^1_{2k}$. Hence, the S normal MT for $\mathcal{C}$ with initial sample $\mathbf{v}^0$ is ill-defined. A contradiction. □

Corollary 4.4.2. *Let S be linear, local, symmetric, shift-invariant subdivision scheme with order of polynomial reproduction $P \geq 2$. Then the S normal MT is globally well-posed if and only if S is the mid-point-interpolating scheme S_1 or the Chaikin scheme S_2. In both the cases*

$$d^j = \mathrm{O}(2^{-2j}), \qquad j \in \mathbb{N}.$$

Proposition 4.4.1 implies that such an S reproduces linear functions only if $(\Delta S x)_{2k} = \Delta x_k/2$, leading to $\alpha - \beta = 1/2$. In order S to be symmetric and, thus, independent of the way the data is processed (i.e., from left to right, or from right to left), we should either take $\beta = 0$ which is S_1, or $\beta = 1/4$, which is S_2. Note that in this setting β plays the role of the shift parameter c_S introduced earlier in the definition of P_e.

Due to Corollary 4.4.2, the only geometrically meaningful choices for S are S_1 and S_2. The S_1 normal MT is studied in detail in [91], and there it is confirmed that the transform is well-defined, convergent and satisfies (4.3.4), while the analysis on S_2 normal MT was the subject of our previous section. To summarize, given a concrete curve $\mathcal{C}$ that needs to be efficiently stored, we seem to have two options, provided we want to use normal multi-scale transforms: Start with an arbitrary sample $\mathbf{v}^0 \in \mathcal{C}$, perform S_1 or S_2 normal MT, store relatively big details, and, when the details are finally below some a priori given threshold and we may not store them anymore, end up with at

most $C^{1,1}$ approximation of $\mathcal{C}$, no matter how smooth the initial curve is. Or use a normal MT based on high-regular S for which, compute the arc-length parameterization of $\mathcal{C}$ (usually the curve is given to us only as a geometrical set of points in $\mathbb{R}^2$), the exact constants in (4.2.9), and the size of h, find an admissible initial sample $\mathbf{v}^0$, and realize $\|\Delta\mathbf{v}^0\|$ is already so small that there is no point of further refining the data. A natural way to compromise between those two is to introduce adaptivity. In what follows we repeat our paper [60, Sections 3 and 4].

4.4.1 Theoretical approach

The aim of this section is to show that S_2 normal MT has the property to "uniformize" the fine-scale data $\mathbf{v}^j$. Hence, it is suitable for adaptive procedures together with any high-regular subdivision scheme S. In other words, using S_2 for prediction on finitely many coarse levels (the exact number depends on the initial data $\mathbf{v}^0$, the initial curve $\mathcal{C}$, and the choice of S) guarantees that if we switch to S afterwards, the normal MT will be well-defined and the detail decay rate will be as high as the smoothness of $\mathcal{C}$ and the regularity of S allow. Thus, storing more data in the beginning (based on approximating prediction operator, S_2 normal MT produces twice as many details as the S_1 normal MT) may potentially lead to a better compression later. This does not hold for S_1 normal MT. For example, let $\mathcal{C}$ be just a line segment and

$$|\Delta\mathbf{v}^0_{-1}| = 9|\Delta\mathbf{v}^0_0| = 9|\Delta\mathbf{v}^0_1|.$$

Let T be the 4-point (also known as Dubuc-Deslauriers) subdivision scheme

$$(T\mathbf{v})_{2i} = \mathbf{v}_i, \qquad (T\mathbf{v})_{2i+1} = \frac{-\mathbf{v}_{i-1} + 9\mathbf{v}_i + 9\mathbf{v}_{i+1} - \mathbf{v}_{i+2}}{16}, \qquad i \in \mathbb{Z}. \tag{4.4.2}$$

Note that this is the same scheme as (1.1.3), defined in the introduction, but we changed the notation from S_c to T in order to better distinguish the scheme from the family S_p! Then T is not well-defined on $\mathbf{v}^0$ since $(T\mathbf{v}^0)_1 = \mathbf{v}^0_1 = (T\mathbf{v}^0)_2$. Moreover, for each $j \geq 1$

$$|(\Delta S_1^j\mathbf{v}^0)_{-1}| = 9|(\Delta S_1^j\mathbf{v}^0)_0| = 9|(\Delta S_1^j\mathbf{v}^0)_1|,$$

so one can never switch to T around $\mathbf{v}^0_0$. To show that S_2 always works in adaptive algorithms, we need the following result.

Proposition 4.4.3. *Let $\mathcal{C}$ be a closed non-self-intersecting $C^{k,\alpha}$ curve. Then, for any $\delta \in (0, \alpha)$ and any initial set $\mathbf{v}^0 \subset \mathcal{C}$*

$$\frac{\|\Delta^2\mathbf{v}^j\|}{\|\Delta\mathbf{v}^j\|^{1+\delta}} \to 0, \qquad j \to \infty, \tag{4.4.3}$$

where $\mathbf{v}^j$ is the multi-scale data at level j, obtained from $\mathbf{v}^0$ via S_2 normal MT.

Proof. From (4.3.1) it follows that for any given sequence $\mathbf{v}^{j-1} \subset \mathcal{C}$,

$$(\Delta^2 S_2\mathbf{v}^{j-1})_{2i} = (\Delta^2 S_2\mathbf{v}^{j-1})_{2i+1} = \frac{\Delta^2\mathbf{v}^{j-1}_i}{4}, \qquad \forall i \in \mathbb{Z}.$$

Therefore, $\|\Delta^2 S_2 \mathbf{v}^{j-1}\| = \|\Delta^2 \mathbf{v}^{j-1}\|/4$. (4.3.2) implies that $\mathbf{v}^j_{2i}$ and $\mathbf{v}^j_{2i+1}$ lie on parallel lines, orthogonal to $\Delta\mathbf{v}_i$. Hence, $|\Delta\mathbf{v}^j_{2i}|$ cannot be smaller than the distance $|(\Delta S_2\mathbf{v}^{j-1})_{2i}| = |\Delta\mathbf{v}^{j-1}_i|/2$ between the lines. This gives rise to

$$\|\Delta\mathbf{v}^j\| \geq \frac{\|\Delta\mathbf{v}^{j-1}\|}{2}.$$

Now, denote by $r_j := \|\Delta^2\mathbf{v}^j\|/\|\Delta\mathbf{v}^j\|^{1+\delta}$. Using (4.3.3), (4.3.4), and the above we derive

$$r_j \leq \frac{\|\Delta^2\mathbf{v}^{j-1}\|/4 + 4\|d^j\|}{(\|\Delta\mathbf{v}^{j-1}\|/2)^{1+\delta}} \leq 2^{\delta-1} r_{j-1} + C2^{-(j-1)(\alpha-\delta)} \leq q r_{j-1} + Cq^{j-1},$$

where the constant C depends on C_0, C_2, and $\|\Delta\mathbf{v}^0\|$, while $q := 2^{(\delta-\alpha)} < 1$. Thus,

$$r_j \leq q^j r_0 + Cjq^{j-1} \to 0, \qquad j \to \infty.$$

□

Indeed, Proposition 4.4.3, together with (4.2.9), implies that, for any given closed non-self-intersecting $C^{k,\alpha}$ curve $\mathcal{C}$ with $k + \alpha > 1$, any choice of a linear subdivision scheme S, and any choice of (at least two) initial points $\mathbf{v}^0 \subset \mathcal{C}$, there exists $j \in \mathbb{N}$ (that depends on all $\mathcal{C}$, S and $\mathbf{v}^0$), such that the S normal MT for $\mathcal{C}$ with initial data $\mathbf{v}^j$, obtained from $\mathbf{v}^0$ after j refinement steps based on the S_2 normal MT, is well-defined, converges and possesses the detail decay rate and the smoothness of the normal re-parameterization as predicted in Theorem 4.2.3.

4.4.2 Adaptive algorithm

The direct implementation of the adaptive normal MT, introduced in Section 4.4.1 is wasteful, as we do not take into account the locality of the prediction operators. E.g., if we want to store a curve $\mathcal{C}$ that is the graph $(x, f(x)) \in \mathbb{R}^2$ of a smooth function (mollifier) f, with $f(x) = 0$, $|x| > \epsilon$ and $f(0) = 1/\epsilon$, where $\epsilon > 0$ is a priori fixed, we need to perform pure S_2 normal MT on a huge number of scales, provided $\epsilon << 1$, before the mesh-size h^j becomes small enough so that the corresponding (4.2.9) for the four-point scheme is globally satisfied and we switch to it. Since f is a straight line away from $|x| \leq \epsilon$ this does not seam to be a problem (all the details there are zero, so we do not have to store anything), but if our data is noisy or due to machine errors we get some very small (but nonzero! details) we end up spending twice as much memory as for the S_1 normal MT on regions where the output from two transforms is practically the same. Hence, a reduction of the number of segments, where S_2 is used is desirable for faster detail decay and less data storage. The adaptive algorithm we propose here allows different prediction operators to be used for different neighborhoods within the same scale. From now on, unless something else is specified, T will denote the Dubuc-Deslauriers operator (4.4.2). Suppose a closed curve $\mathcal{C}$ with initial $\mathbf{v}^0 \subset \mathcal{C}$ is given, a constant $RB > 0$ has been (manually) chosen, and the normal MT $\mathbf{v}^1, \mathbf{v}^2, \ldots, \mathbf{v}^{j-1}$ up to level $j-1$ has been carried over. Any vertex $\mathbf{v}^{j-1}_i$ is marked by an extra bit, which is zero if it is an S *vertex*, i.e., predicted by S_2 or S_1, and one if it is a T *vertex*, i.e., predicted by T. Initially, in $\mathbf{v}^0$ all vertices are declared S vertices. Note that we work only with finite initial data $\mathbf{v}^0$, so $\mathbf{v}^{j-1}$ is finite, as well. Let its cardinality be N. The algorithm consists of the following steps

- Enlarge $\mathbf{v}^{j-1}$ in a cyclic way by adding two elements $\mathbf{v}_{-1}^{j-1} = \mathbf{v}_{N-1}^{j-1}, \mathbf{v}_0^{j-1} = \mathbf{v}_N^{j-1}$ to the left and three elements $\mathbf{v}_{N+1}^{j-1} = \mathbf{v}_1^{j-1}, \mathbf{v}_{N+2}^{j-1} = \mathbf{v}_2^{j-1}, \mathbf{v}_{N+3}^{j-1} = \mathbf{v}_3^{j-1}$ to the right.
- Create an empty set V^j and whenever a vertex is marked, add it to V^j.
- For each $i \in [1, N]$:
  - If one of the vertices $\mathbf{v}_i^{j-1}$ and $\mathbf{v}_{i+1}^{j-1}$ is an S vertex, while the other is a T vertex, use S_1 to predict a new node between $\mathbf{v}_i^{j-1}$ and $\mathbf{v}_{i+1}^{j-1}$. Compute the new vertex $\hat{\mathbf{v}}_i$. In case of multiple intersection points, take an arbitrary one among them. Store the corresponding detail, and mark $\hat{\mathbf{v}}_i$ as an S vertex. Do not mark $\mathbf{v}_i^{j-1}$ or $\mathbf{v}_{i+1}^{j-1}$.
  - Else, i.e., when $\mathbf{v}_i^{j-1}$ and $\mathbf{v}_{i+1}^{j-1}$ are both either S or T vertices, determine the local neighborhood $\bar{\mathbf{v}} = \{\bar{\mathbf{v}}_{i-1}, \bar{\mathbf{v}}_i, \bar{\mathbf{v}}_{i+1}, \bar{\mathbf{v}}_{i+2}\}$. $\bar{\mathbf{v}}$ may differ from $\mathbf{v}^{j-1}\big|_{[i-1,i+2]}$ and its exact derivation will be explained later. If

$$|\Delta^2 \bar{\mathbf{v}}_{i-1}| \le RB \min\{|\Delta \bar{\mathbf{v}}_{i-1}|, |\Delta \bar{\mathbf{v}}_i|\},\ |\Delta^2 \bar{\mathbf{v}}_i| \le RB \min\{|\Delta \bar{\mathbf{v}}_i|, |\Delta \bar{\mathbf{v}}_{i+1}|\}, \tag{4.4.4}$$

    holds and the normal line through $T\bar{\mathbf{v}}$ intersects the corresponding arc $\widehat{\mathbf{v}_i^{j-1}\mathbf{v}_{i+1}^{j-1}} = \{\mathbf{v}(s) : s_i^{j-1} < s < s_{i+1}^{j-1}\}$ at least once, use T as prediction operator. Store the detail for the new vertex $\hat{\mathbf{v}}_i$ (in case of multiple intersection points, take an arbitrary one among them) and mark all $\{\mathbf{v}_i^{j-1}, \hat{\mathbf{v}}_i, \mathbf{v}_{i+1}^{j-1}\}$ as T vertices. Else, use S_2 as prediction operator, compute two new vertices, mark them as S vertices and store the details. Do not mark $\mathbf{v}_i^{j-1}$ or $\mathbf{v}_{i+1}^{j-1}$.
- Go one more time through V^j, store a single copy for each of the vertices in it (those from $\mathbf{v}^{j-1}$ may have two copies at the beginning) and delete all the S vertices, surrounded by both T neighbors. What remains is $\mathbf{v}^j$.

Let us explain first how to construct $\bar{\mathbf{v}}$. T is a primal scheme, i.e., node-oriented (averages the values in the nodes of the grid), while S_2 is a dual one, i.e., interval-oriented (averages the mean values of the function between adjacent nodes of the grid). Hence, taking $\bar{\mathbf{v}} = \mathbf{v}_{i+1}^{j-1}$ is not always appropriate, because the transition from one to the other leads to highly irregular data on the next level. We create $\bar{\mathbf{v}}$ of a pure S or pure T type via $\bar{\mathbf{v}}_i = \mathbf{v}_i^{j-1}$, $\bar{\mathbf{v}}_{i+1} = \mathbf{v}_{i+1}^{j-1}$,

$$\bar{\mathbf{v}}_{i-1} = \begin{cases} \mathbf{v}_{i-1}^{j-1}, & \text{if } \mathbf{v}_{i-1}^{j-1} \text{ and } \mathbf{v}_{i-2}^{j-1} \text{ are of the same type} \\ \frac{\mathbf{v}_{i-2}^{j-1} + \mathbf{v}_{i-1}^{j-1}}{2}, & \text{otherwise} \end{cases},$$

and analogously for $\bar{\mathbf{v}}_{i+2}$. Note that our algorithm guarantees that $\mathbf{v}_{i-1}^{j-1}$ and $\mathbf{v}_{i-2}^{j-1}$ are of the same type whenever $\mathbf{v}_{i-1}^{j-1}$ and $\mathbf{v}_i^{j-1}$ are not, so we never average vertices of different nature! Taking equally spaced points on a line and applying the above procedure, randomly choosing for each i whether T or S_2 normal MT should be used, gives rise to neighborhoods $\bar{\mathbf{v}}$ that consist of equidistant points, again. On the other hand, the experimental results indicate that our algorithm quickly improves the regularity of an initially irregular data set.

Let us now explain the rationale behind (4.4.4) in more detail. In order to use as few S_2 and S_1 steps as possible, we need a very local criteria, such as (4.4.4), for the choice of the prediction operator. Note that (4.4.4) implies (4.2.9) with $\delta = 0$. There are several reasons why we chose to

work with $\delta = 0$. First of all, the size of δ does not play any role for the detail decay rate, which can be seen from the proofs in [24, 62]. Secondly, by relaxing the restriction (4.2.9) we favor the T normal MT, and, thus, avoid the S_2 normal MT as much as possible (of course, we do not have theoretical guarantee that the T normal MT is well-defined and we need to check it every time we want to use it). Finally, (4.4.4) allows us to relate our work to [24], since the quantity we bound is asymptotically the same as their non-uniformity measure

$$\mathcal{N}(s) := \sup_i \mathcal{N}(s_i) = \sup_i \max\{\Delta s_{i+1}/\Delta s_i, \Delta s_i/\Delta s_{i+1}\}. \tag{4.4.5}$$

Indeed, since $\mathbf{v}(s) \in C^{1,\alpha}$, there exists a constant $C < \infty$ such that

$$|\mathbf{v}'(s) - \mathbf{v}'(s')| \le C|s - s'|^\alpha, \qquad \forall s, s' \in [0, L).$$

Hence, by Taylor formula

$$\left| \frac{|\Delta^2 \mathbf{v}^j_{i-1}|}{|\Delta \mathbf{v}^j_i|} - \frac{|\Delta^2 s^j_{i-1}|}{\Delta s^j_i} \right| \le \frac{\left|\Delta s^j_i |\Delta \mathbf{v}^j_i - \Delta \mathbf{v}^j_{i-1}| - |\Delta \mathbf{v}^j_i||\Delta s^j_i - \Delta s^j_{i-1}|\right|}{(\Delta s^j_i)^2 - C(\Delta s^j_i)^{2+\alpha}}.$$

For the expression $|A|$ in the numerator we derive

$$\begin{aligned} A &\le C(\Delta s^j_i)^{2+\alpha}\left(1 + \left(\frac{\Delta s^j_{i-1}}{\Delta s^j_i}\right)^{1+\alpha} + \left|\frac{\Delta s^j_{i-1}}{\Delta s^j_i} - 1\right|\right); \\ -A &\le \Delta s^j_i \underbrace{\left(|\Delta s^j_i - \Delta s^j_{i-1}| - |\Delta \mathbf{v}^j_i - \Delta \mathbf{v}^j_{i-1}|\right)}_{B}. \end{aligned}$$

To continue the estimations in the second line, we need to consider two cases.

$$\begin{aligned} 1)\quad |\Delta s^j_i - \Delta s^j_{i-1}| &\ge C((\Delta s^j_{i-1})^{1+\alpha} + (\Delta s^j_i)^{1+\alpha}) \implies \\ |\Delta \mathbf{v}^j_i - \Delta \mathbf{v}^j_{i-1}| &\ge |\Delta s^j_i - \Delta s^j_{i-1}| - C((\Delta s^j_{i-1})^{1+\alpha} + (\Delta s^j_i)^{1+\alpha}) \implies \\ B &\le C(\Delta s^j_i)^{1+\alpha}\left(1 + \left(\frac{\Delta s^j_{i-1}}{\Delta s^j_i}\right)^{1+\alpha}\right); \\ 2)\quad |\Delta s^j_i - \Delta s^j_{i-1}| &\le C((\Delta s^j_{i-1})^{1+\alpha} + (\Delta s^j_i)^{1+\alpha}) \implies \\ B &\le |\Delta s^j_i - \Delta s^j_{i-1}| \le C(\Delta s^j_i)^{1+\alpha}\left(1 + \left(\frac{\Delta s^j_{i-1}}{\Delta s^j_i}\right)^{1+\alpha}\right). \end{aligned}$$

Combining the above inequalities with the analogous ones for $\Delta \mathbf{v}^j_{i-1}$ resp. Δs^j_{i-1}, instead of $\Delta \mathbf{v}^j_i$ resp. Δs^j_i, and using $|x - 1| \le |x|^{1+\alpha} + 1$ we get

$$\left| \frac{|\Delta^2 \mathbf{v}^j_{i-1}|}{\min\{|\Delta \mathbf{v}^j_{i-1}|, |\Delta \mathbf{v}^j_i|\}} - \frac{|\Delta^2 s^j_{i-1}|}{\min\{\Delta s^j_{i-1}, \Delta s^j_i\}} \right| \le \frac{2C \max\{\Delta s^j_{i-1}, \Delta s^j_i\}^\alpha (1 + \mathcal{N}(s^j_{i-1})^{1+\alpha})}{1 - C \max\{\Delta s^j_{i-1}, \Delta s^j_i\}^\alpha}.$$

But $|\Delta^2 s^j_{i-1}| / \min\{\Delta s^j_{i-1}, \Delta s^j_i\} = \mathcal{N}(s^j_{i-1}) - 1$, so

$$\sup_i \left| \frac{|\Delta^2 \mathbf{v}^j_{i-1}|}{\min\{|\Delta \mathbf{v}^j_{i-1}|, |\Delta \mathbf{v}^j_i|\}} - (\mathcal{N}(s^j_{i-1}) - 1) \right| \le \frac{2C\|\Delta s^j\|^\alpha (1 + \mathcal{N}(s^j)^{1+\alpha})}{1 - C\|\Delta s^j\|^\alpha}. \tag{4.4.6}$$

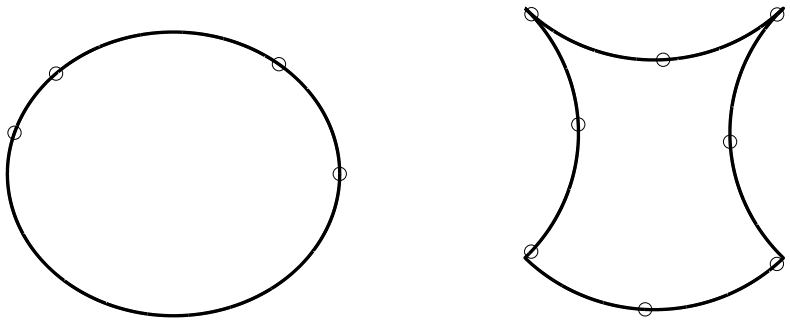

Fig. 4.5: Our test data

What we see from (4.4.6) is that, whenever $\|\Delta s^j\| \to 0$ and $\mathcal{N}(s^j) \to 1$, we have

$$\sup_i \frac{|\Delta^2 \mathbf{v}_{i-1}^j|}{\min\{|\Delta \mathbf{v}_{i-1}^j|, |\Delta \mathbf{v}_i^j|\}} \to 0, \qquad j \to \infty. \tag{4.4.7}$$

Vice versa, due to (4.3.6), we have $\forall j \in \mathbb{N}$

$$\sup_i \left| \frac{|\Delta^2 \mathbf{v}_{i-1}^j|}{\min\{|\Delta \mathbf{v}_{i-1}^j|, |\Delta \mathbf{v}_i^j|\}} - (\mathcal{N}(s_{i-1}^j) - 1) \right| \leq \frac{2Cq^\alpha \|\Delta \mathbf{v}^j\|^\alpha (1 + q^{1+\alpha} \mathcal{N}(\mathbf{v}^j)^{1+\alpha})}{1 - Cq^\alpha \|\Delta \mathbf{v}^j\|^\alpha},$$

and, thus, $\|\Delta \mathbf{v}^j\| \to 0$ together with (4.4.7) implies $\mathcal{N}(s^j) \to 1$, when $j \to \infty$.

Some remarks are in order. According to the Appendix A in [24], T is weakly contractive with bound $R = 3+2\sqrt{2}$, i.e., for any strictly increasing $u \in \ell_\infty(\mathbb{Z})$ such that $\mathcal{N}(u) \leq 3+2\sqrt{2}$, Tu is also strictly increasing and $\mathcal{N}(Tu) \leq \mathcal{N}(u)$. The bound is sharp and, together with (4.4.6), suggests the restriction $RB < 2+2\sqrt{2}$, because otherwise we allow applications of T normal MT even when $\mathcal{N}(s^j) > R$ which could even worsen the regularity of our data! Secondly, our algorithm can be generalized for smoother both interpolating schemes T and approximating schemes S. However, the transition between S and T vertices should always be smooth, i.e., only S_2 and the 4-point scheme can be applied to neighboring intervals. Then in each of the directions one can upgrade the prediction operator with a smoother one of the same type. For example, in order to work with the central interpolating scheme of degree 9, we intermediately have to use the central interpolating schemes of degree 3, 5 and 7, as well.

For the two data sets illustrated in Fig. 4.5, we compare the behavior of the normal MTs based on S_1, S_2, T, S_1/T, and S_2/T (we use the notation S_2/T normal MT for the adaptive algorithm, presented in the previous section, and S_1/T normal MT for its exact counterpart, when S_2 predictions are replaced by S_1 predictions). In the first example, we consider a small, irregularly spaced initial vertex set $\mathbf{v}^0$ (indicated by circles) on a C^∞ curve, namely the unit circle. In the second example we consider well-spaced initial points $\mathbf{v}^0$ on a curve with four isolated singularities, which we will refer to as twisted circle, since it is obtained by dividing the unit circle into four arcs of equal length, and flipping three of them around their corresponding edges. Although close, none

of the points in $\mathbf{v}^0$ coincides with any of the singularity points of the twisted circle. The twisted circle is only $C^{0,1}$. Hence the crucial inequality (4.3.6), needed for the well-posedness of the S_2 normal MT does not automatically hold. However, direct computations show that if P, Q lie on neighboring arcs of the twisted circle, then $|PQ| \geq |\widehat{PQ}|/(\pi\sqrt{2})$, which for the given choice of $\mathbf{v}^0$ is enough. As we will see, for both examples the T normal MT fails at some level.

4.4.3 Experimental results

In Fig. 4.6 we show experimental data for the first example. The non-uniformity measures $\mathcal{N}(\mathbf{v}^j)$ is computed in the same fashion as (4.4.5) by just replacing Δs_i by $|\Delta \mathbf{v}_i|$. We prefer to work with this measure, because at each level j it can be directly computed from $\mathbf{v}^{j-1}$, while for $\mathcal{N}(s^{j-1})$ one needs to take into account the underlying curve $\mathcal{C}$. In the second and third columns, by setting $RB = 0$, we simply apply pure S_2 resp. S_1 normal MT. The second row compares the detail decay, combining the details from all levels $j \leq 5$, while the last one compares the details only from the finest scale.

T normal MT fails after 6 iteration steps, and this can be observed by the rapidly increasing values of its non-uniformity measure. Since S_2, resp. S_1, normal MT is always well-defined, the adaptive transforms never fail and this is confirmed by the graphs of the associated non-uniformity measures. From these plots, we see the potential problem of working with large RB-values. Indeed, when we set $RB = 5$ (which is slightly larger than the theoretical bound $2+2\sqrt{2}$ for T, as discussed in Section 4.4.2), we allow T normal MT steps, that even increase the irregularity of the initial data. While the S_2/T normal MT is able to "recover" and after five more iterations decreases the non-uniformity measure to the level of the pure S_2 normal MT, this is not the case with the S_1/T normal MT. Indeed, applied on the circle, mid-point prediction never improves $\mathcal{N}(\mathbf{v})$, since if $(\Delta \mathbf{v}^0)_{-1}$, resp. $(\Delta \mathbf{v}^0)_0$ cut arcs of length 2α, resp. 2β from the unit circle, where $\pi > \alpha > \beta > 0$, then for any $j \in \mathbb{N} \cup \{0\}$, $a_j := (\Delta \mathbf{v}^j)_{-1}/(\Delta \mathbf{v}^j)_0 = \sin(\alpha/2^j)/\sin(\beta/2^j)$ and $\{a_j\}$ is monotonically increasing sequence with $\lim_{j\to\infty} a_j = \alpha/\beta$. (However, for all intermediate i's, e.g., $i \in \{0, 1, \ldots, 2^j - 2\}$, $(\Delta \mathbf{v}^j)_i/(\Delta \mathbf{v}^j)_{i+1} = 1$ which is illustrated in the bottom right graph of Fig. 4.6, where the details, obtained via S_1 normal MT possess only four different values, corresponding to the different arcs in the original partition.) When $RB = 1$, the adaptive S_2/T, resp S_1/T normal MT applies S_2, resp. S_1, in all regions of highly non-uniform spacing. This explains the almost identical plots for S_2/T and S_2, resp. S_1/T and S_1, normal MTs for small j. As discussed before, $RB = 1$ corresponds to $\mathcal{N}(\mathbf{v}) \approx 2$ and, thus, the corresponding plots for S_2 and S_2/T normal MTs start to slightly differ only when the data is already close to regular. Moreover, once $\mathcal{N}(\mathbf{v}^j) < 2$ is achieved, the S_2/T normal MT with $RB = 1$ turns into pure T normal MT. This is confirmed by the $\log_2 |d^5|$ plots which contain half as many data points for S_2/T as compared with S_2 normal MT. On the other hand, because of the inability of S_1 to improve the non-uniformity measure, for every level $j \in \mathbb{N}$ in the S_1/T normal MT there will be points (in our particular case it is one point when $RB = 5$ and two points when $RB = 1$), predicted via mid-point interpolation, which leads to the same ℓ_∞ norm for the details as in the case of pure S_1 normal MT. Hence the worst-case detail decay rate of the S_1/T adaptive scheme will be only 2, instead of 3.

Another observation is that, since the circle has constant curvature, looking at the details at some fixed level (in our example - level 6) gives us an idea about the the global regularity of $\mathbf{v}^j$, when pure S_2 or S_1 normal MT are used. In our particular example, we see that in case of S_2 normal

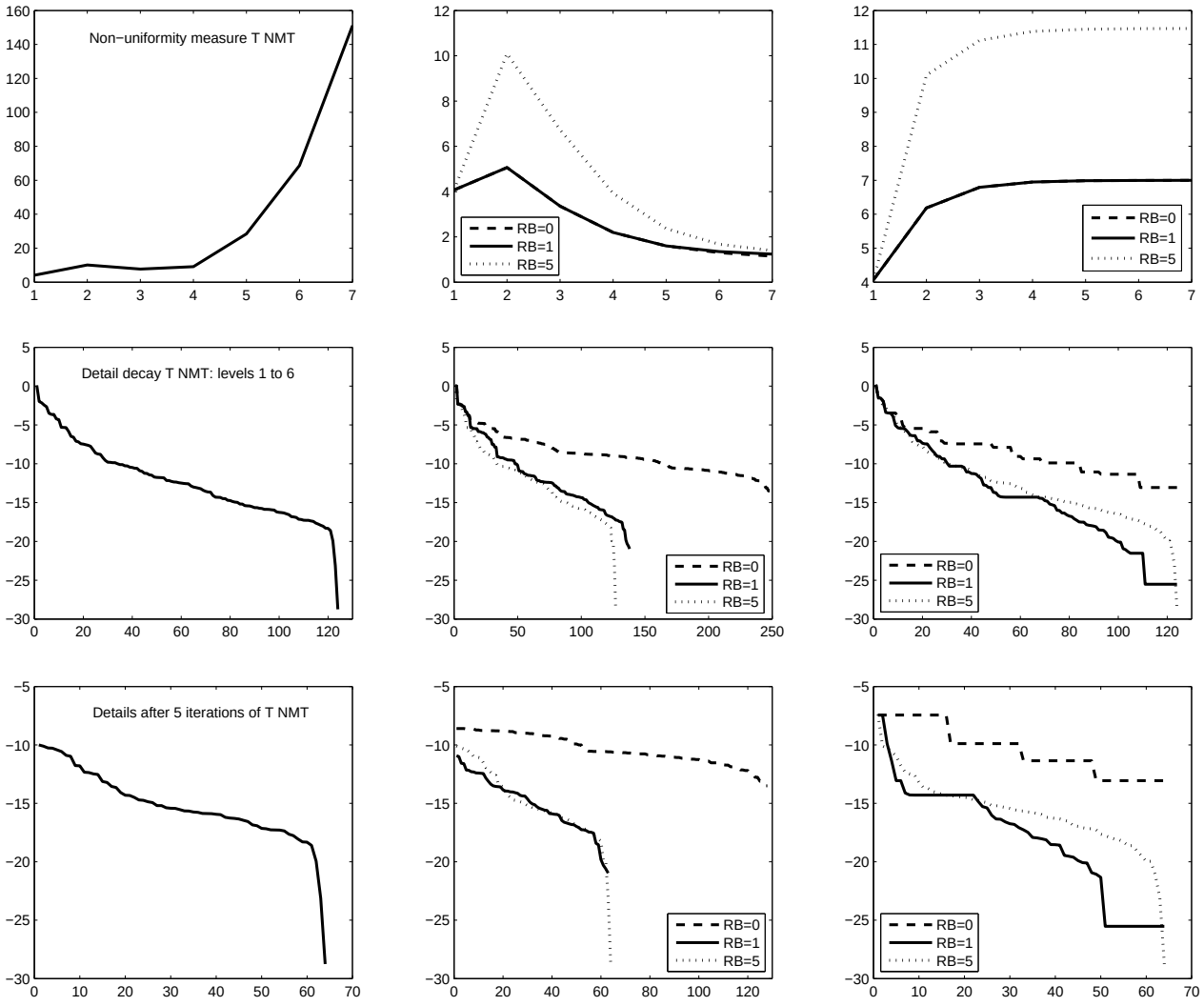

Fig. 4.6: Comparison among T normal MT (left), S_2/T normal MT (middle) and S_1/T normal MT (right), when performed on the circle setup from Fig 4.5. The upper row plots $\mathcal{N}(\mathbf{v}^{j-1})$ for $j = 1, 2, \ldots, 7$. The middle row plots the corresponding $\log_2$-values of $|d^j|$ for levels $j \leq 5$ in descending order. The lower row plots $\log_2(|d^5|)$.

MT all the details are within a narrow range, and, thus, our data is close to regular even globally, while S_1 normal MT leads to four regular pieces, that correspond to the four initial arcs, which we already knew. Finally, the graphs for the details after five iterations are in line with Theorem 4.2.3 regarding the expected detail decay rate. Indeed, the average values of the logarithm of the details, obtained by T normal MT, as well as by S_2/T and S_1/T normal MT with $RB > 0$ are all close to -15, while the corresponding averages for the S_2 and the S_1 normal MT are close to -10, which means that $\|d^5\|_1 \approx 2^{-5\cdot 3}$, resp., $\|d^5\|_1 \approx 2^{-5\cdot 2}$.

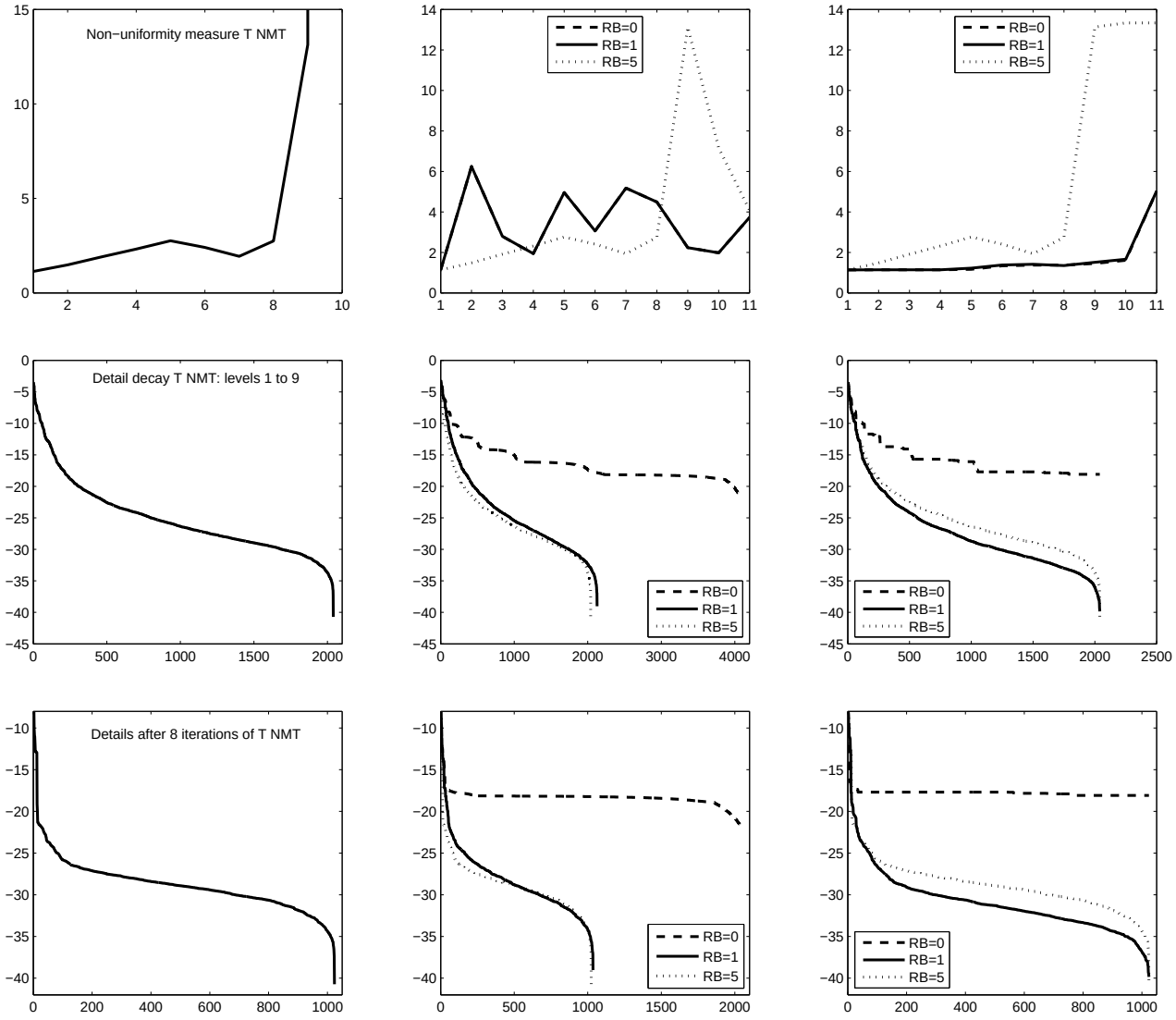

Fig. 4.7: Numerical results for twisted circle. Plots position is analogous to Fig. 4.6.

In the second example (twisted circle), we performed the same experiments. However, since the T normal MT brakes down after 9 iterations, we take into account more steps and compare the details after 8 iterations, instead of 5. The results are summarized in Fig. 4.7. Since the twisted circle is composed of circle arcs, some of the phenomena observed on the first example appear here, too, but due to the low smoothness of $\mathcal{C}$, there are also additional effects. First of all, as we start

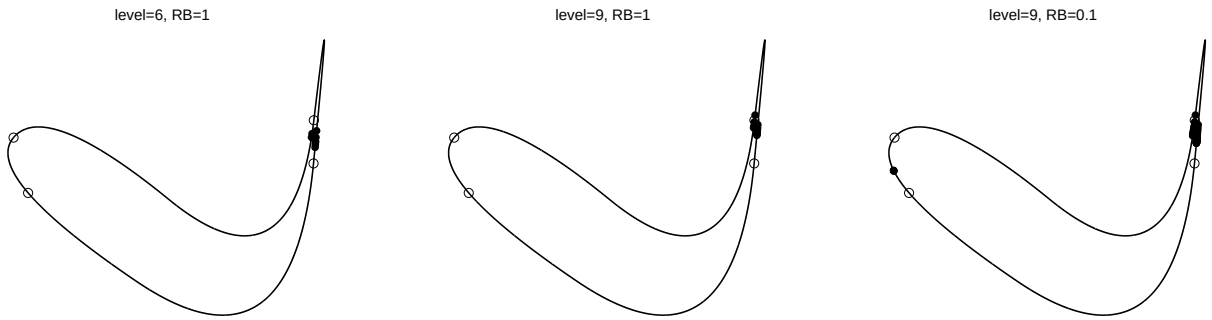

Fig. 4.8: The adaptive schemes detect singularities.

with almost equally spaced points $\mathbf{v}^0$, the non-uniformity measure for T and S_1 normal MT stays low for small j, until the singularities of the initial curve are "detected". This happens only at level $j = 8$ because the initial points were chosen very close to the singularities. Then the non-uniformity measure $\mathcal{N}(\mathbf{v}^j)$ corresponding to the T normal MT jumps from 3 to 13, and the transform fails at the next level. Therefore, as can be seen from the graphs, for levels $j \leq 9$ both S_2/T and S_1/T normal MT with $RB = 5$ coincide with the pure T normal MT. After that S_2/T manages to improve the non-uniformity measure, while S_1/T just keeps it as it is.

On the other hand, as shown on Fig. 4.8, the S_2 normal MT detects the presence of singularities from the very beginning, although it cannot localize them as well as an interpolating normal MT would do. Indeed, once an interpolating scheme hits a point it keeps it throughout all the following iterations, while, even on a straight line and uniformly spaced data, once a point is hit by S_2, it never appears again on any of the finer scales. To stress this effect we set the following example. On a smooth curve with a single singularity point, we start with a $\mathbf{v}^0$ consisting of 4 irregularly spaced points, and show the locations where S_2/T normal MT still uses S_2, i.e., where the local non-uniformity measure exceeds RB. On the left plot, we see that at level $j = 5$ the irregularity of the initial data is essentially removed, and the only places, where S_2 prediction is used, is near the singularity. In the middle plot, we show how the localization of the singularity by the S_2/T normal MT improves after three more iterations. On the right plot, we see that even for very small values of RB (in the particular case $RB = 0.1$) this still works, even though only after slightly more iterations. The isolated S_2 interval away from the singularity disappears for $j = 10$. This cannot be achieved with the S_1/T normal MT, since it can never fully recover from the irregularity of the initial data and will use S_1 predictions near vertices in $\mathbf{v}^0$ for any j.

We conclude our experiments with a comparison between our S_2/T normal MT and the T_ω normal MT proposed in [24]. To the best of our knowledge, the latter is the only other normal MT that is well-defined, converges and (in case of smooth initial curve) after finitely many iterations turns into a pure T normal MT. The family T_ω is defined via

$$T_\omega = (1 - \omega)S_1 + \omega T, \qquad 0 < \omega \leq 1,$$

and T_ω is proven to be weakly contractive (see [24] for details) with bound

$$R(\omega) = \frac{4}{\omega}\left(1 + \sqrt{1 - \frac{\omega}{2}} - 1\right) \tag{4.4.8}$$

for each specific $0 \leq \omega \leq 1$. Combined with [24, Theorem 5.7], this implies the existence of an increasing sequence $0 < \omega_1 < \omega_2 < \ldots < \omega_J < 1 = \omega_{J+1} = \ldots$ such that (4.1.1) with S replaced by T_{ω_j} leads to a well-defined transform called T_ω normal MT (the ω_j as well as the level J after which the T_ω normal MT coincides with the T normal MT, depend on $\mathcal{C}$ and $\mathbf{v}^0$). All one has to do is to choose ω_j such that $\mathcal{N}(\mathbf{v}^{j-1}) \leq R(\omega_j)$ (concrete rules for picking the ω_j resp. a locally adaptive version of the T_ω normal MT have not been elaborated on in [24]).

Fig. 4.9 displays the decay of the non-uniformity measure $\mathcal{N}(\mathbf{v}^j)$ for $j \leq 8$ associated with S_2, T_ω, and $T_{3\omega/4}$ normal MT. Since the decay of the non-uniformity measure for smooth $\mathcal{C}$ is basically a property of the underlying subdivision operator, for this test we let $\mathcal{C}$ be a straight line, and $\mathbf{v}^0$ consist of randomly chosen points on it with large $\mathcal{N}(\mathbf{v}^0)$ value. For the T_ω normal MT, we always work with the largest possible value $\omega_j = 8\mathcal{N}(\mathbf{v}^{j-1})/(\mathcal{N}(\mathbf{v}^{j-1})+1)^2$ satisfying (4.4.8), while for the $T_{3\omega/4}$ normal MT we use $T_{3\omega_j/4}$ as prediction operator. In Fig. 4.9 we have plotted two examples. We observe that S_2 improves the non-uniformity measure faster (actually, for S_2 it can be straightforwardly verified that on a straight line $\mathcal{N}(\mathbf{v}^j) < (\mathcal{N}(\mathbf{v}^{j-1})+1)/2$, $j \in \mathbb{N}$), and allows us to switch to T at an earlier level. In the first example we can do this after three iterations, while we need four iterations if using $T_{3\omega/4}$ or seven iterations if using T_ω, and in the second example we can do this after five iterations, while we need six iterations if using $T_{3\omega/4}$ or more than eight if using T_ω). The other observation is that for both examples $T_{3\omega/4}$ normal MT performs better than T_ω normal MT, which indicates that, in order to minimize the fine-scale non-uniformity measure, the ω_j should be chosen carefully.

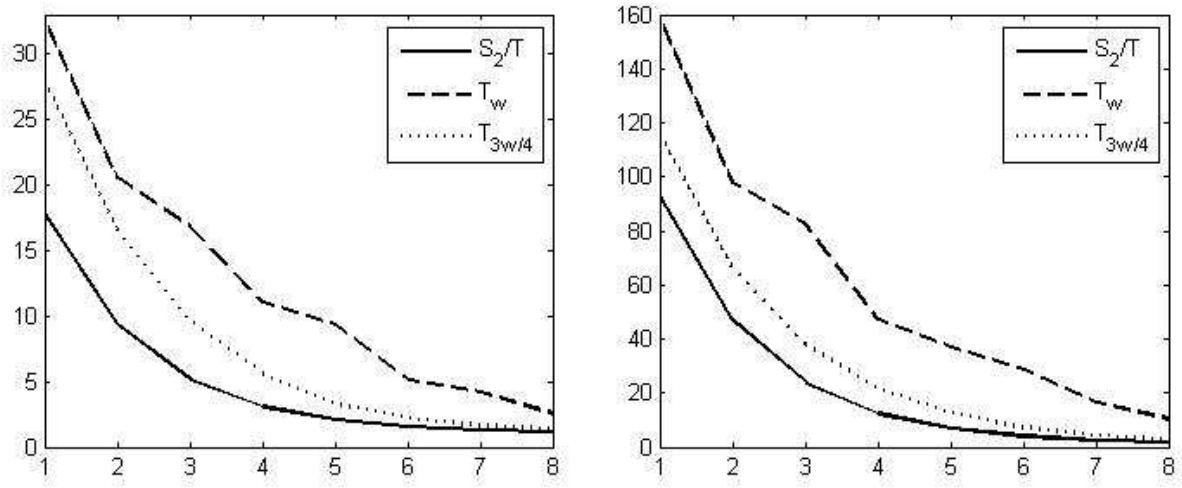

Fig. 4.9: Comparison between our adaptive scheme and the family T_ω proposed in [24].

5. IMPROVED NORMAL MTS. CASE STUDIES

The restrictive role of the exact order of polynomial reproduction P_e of the approximating subdivision operator S in the analysis of the S normal MT, established in Theorem 4.2.3, significantly disfavors the practical use of these transforms whenever $P_e << P$. Moreover, numerical experiments confirm that the detail decay rate of the S normal MT is indeed related to P_e, and not to P. On the other hand, bigger details lead to bigger displacements of the newly inserted points, when different normal directions for the S normal MT are considered (see Fig. 5.1). Hence, the choice of ξ_K in (4.2.11) has big impact on the regularity of the generated data. Another observation is that the two limitations on the detail decay rate $\mu < \min(s_\infty(S)+1, P_e)$ have completely different nature, can be "decoupled", and treated independently.

In this chapter, both the above ideas are further elaborated and improved normal MTs in terms of smoothness of their normal re-parameterization and detail decay rates are presented. The following lemma from [62] is repeatedly used for our arguments, so we highlight it here. Its proof is given in the appendix.

Lemma 5.0.4. *For given S with $P_e \geq 2$, let $1 \leq M < P_e$, and assume that $F : [a,b] \to \mathbb{R}$ is $C^{M,\rho}$ for some $0 < \rho \leq 1$. Then for any finite sequence $(s_l)_{l\in I} \subset [a,b]$ and any index K such that $Ss_K \in [a,b]$ is well-defined we have*

$$|F(Ss_K) - SF(s)_K| \leq C\Big(\sum_{\nu\in E_M}\prod_{m=1}^{M}\|\Delta^m s\|_I^{\nu_m} + \|\Delta s\|_I^{M+\rho}\Big), \qquad K \in I \cup I_1,$$

where the constant C is independent of the sequence s and K, and

$$E_M := \{\nu \in \mathbb{Z}_+^M : \quad \sum_{m=1}^{M} m\nu_m = M+1, \quad 2 \leq \sum_{m=1}^{M}\nu_m \leq M\}.$$

Our main computational tool for the forthcoming analysis is the use of local frames. Let $\mathcal{C}$ be a closed, non-self-intersecting, planar curve, with smooth enough arc-length parameterization $\mathbf{v}(s)$, and let $\mathbf{v}_0 = \mathbf{v}(s_0) \in \mathcal{C}$ be a point on it. The local frame $(\mathcal{T},\mathcal{N})$, centered at $\mathbf{v}_0$, is defined via $\mathbf{v}'(s_0) = \mathcal{T}$, and $\mathbf{v}''(s_0) = \mathrm{k}(s_0)\mathcal{N}$. The scalar function $\mathrm{k}(s)$ is the curvature of $\mathcal{C}$ at a given point $\mathbf{v}(s)$ and is continuously differentiable, whenever $\mathbf{v}(s) \in C^3$. Due to the Taylor expansion, for C^5 curves $\mathcal{C}$ we have

$$\mathbf{v}(s) = \mathbf{v}_0 + \mathbf{v}'(s_0)(s-s_0) + \frac{\mathbf{v}''(s_0)}{2!}(s-s_0)^2 + \frac{\mathbf{v}'''(s_0)}{3!}(s-s_0)^3 + \frac{\mathbf{v}^{(iv)}(s_0)}{4!}(s-s_0)^4 + \mathrm{O}((s-s_0)^5).$$

Combining it with the Frenet-Serret formulae

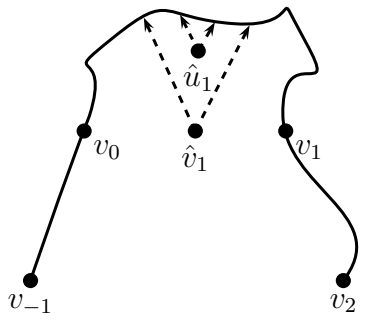

Fig. 5.1: Comparison of the arc-length difference between the two fine-scale-point candidates that correspond to two admissible choices of normal directions and predicted via S_3 ($\hat{v}_1$) and T ($\hat{u}_1$), resp.

$$\mathcal{T}' = \alpha\mathcal{N}, \qquad \mathcal{N}' = -\alpha\mathcal{T},$$

we derive

$$\begin{aligned}\mathbf{v}(s) = \mathbf{v}_0 &+ \left((s-s_0) - \frac{\mathrm{k}(s_0)^2}{6}(s-s_0)^3 - \frac{\mathrm{k}(s_0)\mathrm{k}'(s_0)}{8}(s-s_0)^4 + \mathrm{O}((s-s_0)^5)\right)\mathcal{T} \\ &+ \left(\frac{\mathrm{k}(s_0)}{2}(s-s_0)^2 + \frac{\mathrm{k}'(s_0)}{6}(s-s_0)^3 + \mathrm{O}((s-s_0)^4)\right)\mathcal{N} =: x(s)\mathcal{T} + y(s)\mathcal{N}.\end{aligned} \tag{5.0.1}$$

For analyzing different transforms in the chapter we truncate the Taylor expansion differently, but we never work with terms that are of higher order than 5, so from this point of view formula (5.0.1) is given in its most general form. Finally, we are interested only in the asymptotical behavior of the considered quantities (detail decay rates and regularity of $\mathbf{v}(s^j(t))$). Moreover, due to locality, we restrict ourselves to the invariant neighborhood $s \in I_0$ of s_0. Therefore, without loss of generality we can consider I_0 dense enough so that Lemma 4.2.1 holds. Without further mentioning, this will always be the setup for our estimations below.

5.1 Improving the regularity of the fine-scale data via suitable choice of generalized normals

Section 5.1 exploits the additional degree of freedom that the choice of generalized normals gives, and uses it for improving the regularity of the B-spline normal multi-scale transforms. To get started, we need to reformulate (4.2.11) in order to meet the specifics of the process. Note first that the formula $\hat{\mathbf{n}}_K^j = \mathbf{n}(\xi_K)$ emphasizes the role of the curve $\mathcal{C}$ and is to some extend misleading because the main property of the normals, which basically makes the whole approach appealing from a practical point of view, is that they depend solely on the coarse-scale data $\mathbf{v}^{j-1}$ (since $\mathbf{v}^{j-1} \in \mathcal{C}$, this encodes curve information, as well but in a discrete way). In this section we will define generalized normals for the normal MT based on a given S with the help of another linear subdivision operator N via the following formula

$$\hat{\mathbf{n}}_K^j = \frac{(N\Delta\mathbf{v}^{j-1})_K^\perp}{|(N\Delta\mathbf{v}^{j-1})_K|}, \qquad K \in I_{2i} \cup I_{2i+1}. \tag{5.1.1}$$

For N we assume that it reproduces constants, has positive mask and support, not bigger than the one of the first derived scheme $S^{[1]}$ of S.

It is not hard to see that (5.1.1) implies (4.2.11). Indeed, the assumptions on N give rise to $(N\Delta\mathbf{v}^{j-1})_K$ being a convex combination of $\{\Delta\mathbf{v}_k^{j-1} : k \in I_i\}$. Hence, there exists a $\xi_k \in s|_{I_i}$ such that its tangent vector $\mathbf{t}(\xi_k)$ to $\mathcal{C}$ is collinear with $(N\Delta\mathbf{v}^{j-1})_K$, making $\hat{\mathbf{n}}_K^j = \mathbf{n}(\xi_K)$. Finally, due to the locality of S, $|\xi_K - s_k| \leq |supp(S)|h_i$.

Due to (5.1.1) we can talk about (S, N) *normal MT*, meaning that the prediction points on the fine-scales are computed by S, while the normal directions are generated by N. The above generalization of the method is of no practical interest when S is interpolatory, since this will not lead to improvements of either the detail decay rate or the smoothness of the normal re-parameterization. The detail decay observation follows from classical approximation theory. S produces $C^{m,\beta}$ limit functions where $m + \beta + 1 \leq P = P_e$, the prediction $S\mathbf{v}^{j-1}$ can be interpreted as an approximation to $\mathcal{C}$ within the class of $C^{m,\beta}$ curves, leading to best approximation error of order $m + \beta + 1$. For the smoothness, consider once again $\mathcal{C}$ to be a line interval, and $\mathbf{v}^0$ be a non-uniform sample of it. For this setup the smoothness of the normal re-parameterization coincides with the Hölder regularity of the prediction operator. Now compare both the results with Theorem 4.2.3 and see that the transform performs in an optimal way even with the standard normals (4.3.2). When S is approximating, however, this is no longer the case, because P_e may differ from P. More precisely, $P_e < m + \beta + 1 \leq P$ may hold, suggesting that there might still be room for improvement of the above two quantities.

5.1.1 (S_p, S_q) normal MT

From now on we concentrate our attention on the family of B-spline operators $\{S_p\}$ (4.2.2). Note that the recursive definition for S_p shifts the refined data to the right, e.g., $(S_3x)_{2i} = (x_i + x_{i+1})/2 = (S_1x)_{2i+1}$, and the larger the p the bigger the effect. In order to keep the schemes centered we silently shift the indexes back as much as necessary, e.g., we actually deal with the operator S_3' such that $(S_3'x)_i = (S_3x)_{i-1}$, but for simplicity we denote this modified versions of S_p by S_p, as well. There are several reasons for our choice to work with the B-spline family. First of all, our previous results are too pessimistic if applied to S_p normal MTs: Theorem 4.2.3 implies detail decay rate and smoothness of the normal re-parametrization up to order two no matter how big p is, and Proposition 4.4.1 states that those transforms are not globally well-posed, either. At the same time, the S_p operators are still among the most favorable schemes used in practice, because of their nice geometric and analytic properties, and are one of the main reasons why people are interested in normal MTs based on approximating prediction rules. Hence, the S_p normal MTs are good as test case since improvements should be possible. Last, but not least, they seem the best candidate to test our (S, N) framework: Intuitively, if one wants the (S, N) normal MT to perform well, the two schemes S and N should be closely related. From this point of view, the Lane-Riesenfeld algorithm and the positiveness of the mask of S_p which makes S_p admissible for an N-operator, look very promising and so does the observation that the standard S normal MTs exploited so far fit nicely into the new paradigm as (S, S_0) normal MTs.

Remark 5.1.1. *For any $p \in \mathbb{N}$ and any admissible choice for N, the detail decay rate of the (S_p, N) normal MT does not exceed two.*

Normal MT on a circle			Number of initial points (always placed equidistantly)						
S_p	$\hat{\mathbf{n}}_i^j$	levels used	4	5	6	7	8	9	10
S_2	standard	3 – 12	2.0011	2.0008	2.0005	2.0004	2.0003	2.0002	2.0002
S_2	radial	3 – 12	1.9952	1.9974	1.9984	1.9989	1.9992	1.9993	1.9995
S_3	radial	3 – 12	1.9997	1.9998	1.9999	1.9999	1.9999	1.9999	2.0000
S_4	radial	3 – 12	1.9993	1.9995	1.9996	1.9997	1.9998	1.9998	1.9998
S_2	standard	6 – 12	2.0000	2.0000	2.0000	2.0000	2.0000	2.0000	2.0000
S_2	radial	6 – 12	1.9952	1.9974	1.9984	1.9989	1.9992	1.9993	1.9995
S_3	radial	6 – 12	2.0000	2.0000	2.0000	2.0000	2.0000	2.0000	2.0000
S_4	radial	6 – 12	2.0000	2.0000	2.0000	2.0000	2.0000	2.0000	2.0000

Tab. 5.1: Decay of the detail coefficients for (S_p, N) normal MT

To show this, we set $\mathcal{C}$ to be a circle of radius $R > 0$. Let us first consider $p = 1$ and take any $\mathbf{v}_i, \mathbf{v}_{i+1} \in \mathcal{C}$. In this setting the standard normal directions are *radial*, i.e., the normal line through $(S_1\mathbf{v})_{2i+1}$ contains the center of $\mathcal{C}$, the detail d_{2i+1} with respect to the S_1 normal MT equals the Hausdorff distance from $(S_1\mathbf{v})_{2i+1}$ to $\mathcal{C}$, and, thus, is the smallest possible among all the (S_1, N) normal MTs. But we can directly compute

$$d_{2i+1} = \left(1 - \sqrt{1 - \frac{\bar{h}_i^2}{4R^2}}\right) R = \frac{\bar{h}_i^2}{8R^2} + \mathrm{o}(\bar{h}_i^2), \qquad \bar{h}_i = |\Delta \mathbf{v}_i|.$$

Since S_1 is dyadic, it is clear that for any initial sample $\mathbf{v}^0$ and any $j \geq 1$, $\bar{h}^j = \|\Delta \mathbf{v}^j\| = \mathrm{O}(\bar{h}^0 2^{-j})$, implying $|d^j| \geq C\bar{h}^0 2^{-2j}$, where $C > 0$ is some constant. Hence, detail decay rate higher than two cannot be expected from an (S_1, N) normal MT. The case (S_2, N) is absolutely analogous, while for $p \geq 3$ we have $(S_p\mathbf{v})_K$, $K \in I_{2i} \cup I_{2i+1}$, to be a convex combination of $\{\mathbf{v}_k : k \in I_i\}$, meaning that $(S_p\mathbf{v})_K$ and the circle lie in different regions with respect to the polyline, interpolating $\mathbf{v}$. In other words, the Hausdorff distance from $(S_p\mathbf{v})_K$ to $\mathcal{C}$ is bigger than the corresponding one from $(S_1\mathbf{v})_K$, if p is odd, $(S_2\mathbf{v})_K$, if p is even, respectively, making it impossible for the detail decay order to be higher than two. Finally, since $\bar{h}^j \to 0$ when æ $\to \infty$, for any given curve $\mathcal{C} \in C^2$ there exists a sufficiently large j, such that for all $j > 0$ the invariant neighborhood I_i of S_p is concentrated within a $\mathcal{C}$ region of almost constant curvature, i.e., the asymptotical behavior of the details in an (S_p, N) normal MT for an arbitrary C^2 curve $\mathcal{C}$ is the same as for the circle case. These heuristic arguments are backed-up by the experimental data in Table 5.1. There we have tested S_2, S_3, and S_4 on a set of equally-distant points on the unit circle. We assume that the detail decay behaves like $\|d^j\| \approx C2^{-j\alpha}$. Therefore, to estimate the order exponent α, we use a least-squares fit on $-\log_2(\|d^j\|) \approx \alpha j - \log C$.

Remark 5.1.1 confirms that the order of exact polynomial reproduction P_e is responsible for the detail decay rate of the B-spline transforms. At first glance the result seems negative and disfavors the use of S_p normal MTs for applications. But, as we will see throughout this section, big details significantly increase the role of the choice of N for the regularity of the (S_p, N) normal MT, and lead to improvements in the smoothness of the normal re-parameterization when the right N is considered. The above observation illustrates one of the main reasons why the analysis of normal

MTs, based on approximating S is richer and more subtle than the one based on interpolating S! Indeed, let S be interpolatory, with smoothness $s_\infty(S) = m + \beta$, and order of polynomial reproduction P. Then $m + \beta + 1 \leq P = P_e$, and the (S, N) normal MT has detail decay order $m + \beta + 1$ for all admissible N. Hence, no matter what N we choose, the size of the displacement with respect to the arc-length parameter between a newly inserted point by the (S, N) normal MT and a newly inserted point by the S normal MT is, by triangle inequality, at most twice the details size, and thus at least of order $m+\beta+1$. The latter quantity is negligible for the smoothness analysis of the normal re-parameterization, explaining why the whole idea of generalized normal directions does not lead to anything in the interpolating setting. On the other hand, in the approximating case, and for B-spline normal MTs in particular where $m + \beta >> P_e$, such displacements affect the smoothness analysis, and if properly adjusted, improve the regularity of the fine-scale data. Before supporting the above claim with mathematical arguments, we would like to mention a useful fact regarding the well-posedness of the (S_p, S_q) normal MT, that is related to the argument used for the proof of Remark 5.1.1.

Proposition 5.1.2. *Let $\mathcal{C}$ be a closed, non-self-intersecting C^2 curve that has non-negative, resp. non-positive, curvature at every point. Then, for any choice $\mathbf{v}^0$ of initial data, the (S_p, S_q) normal MT, with $p > q \geq 0$, is globally well-defined.*

Proof. Fix $p \in \mathbb{N}$. Note that, in order to apply S_p, we need the cardinality of $\mathbf{v}^0$ to be at least $|I_0|$, where I_0 is the minimal invariant neighborhood around zero for S_p, defined in Section 4.2.1. As always, we assume that $\mathcal{C}$ is given via its arc-length parameterization $\mathbf{v}(s)$ and that, together with $\mathbf{v}^0$ we have access to $\{s^0 : \mathbf{v}_i^0 = \mathbf{v}(s_i^0)\ \forall i \in \mathbb{Z}\}$. Since S_p has a positive mask and the sign of the curvature of $\mathcal{C}$ is constant, for any sample $\mathbf{v}^0$, any $i \in \mathbb{Z}$, and any $K \in I_{2i} \cup I_{2i+1}$, the predicted point $(S_p\mathbf{v}^0)_K$ and the curve $\mathcal{C}$ lie in the two different regions of the plane, separated by the polyline through $\mathbf{v}^0$. The point at infinity belongs to the same planar region as $\mathcal{C}$ and taking into account the continuity and the closeness of $\mathcal{C}$, as well as the formula (5.1.1), we conclude that for any admissible normal-generating operator N there will be a unique intersection point between the line through $(S_p\mathbf{v}^0)_K$, collinear with $(N\Delta\mathbf{v}^0)_K^\perp$, and the curve arc $\{v(s|_{I_i})\}$. What remains to be checked is the proper connectivity of the derived finer sample $\mathbf{v}^1$, i.e., that its points are ordered in an ascending way with respect to the arc-length parameterization of $\mathcal{C}$. For this part, we take advantage of the properties of the B-spline schemes, and thus restrict ourselves to $N = S_q$. Take $q = 0$, i.e., use the standard normals (4.3.2). The above "separation argument" for the set of predicted points and the curve, implies that the details d^1 are all non-negative, or all non-positive, depending on the sign of the curvature of $\mathcal{C}$. The oriented angles $\angle(\Delta\mathbf{v}_k^0, \Delta\mathbf{v}_{k+1}^0)$, $k \in I_i^{[1]}$ are also non-negative, resp. non-positive, and, thus the normals $\mathbf{n}_K^1$ are sorted in a descent, resp. ascent order according to the size of the oriented angles $\angle(\mathbf{n}_K^1, \overrightarrow{Ox})$ between them and the x-axis of a suitable local frame. A simple geometric argument implies that $s_K^1 < s_{K+1}^1$ for all K, establishing the well-posedness of the (S_p, S_0) normal MT. The rest is induction. For $p = 1$, we have the only possibility $q = 0$ and this has already been covered. Assume we have proved the proposition for all $p < P$. Take $p = P$ and $q < P$. If $q = 0$ we are done. If $q > 0$, we already know that the (S_{P-1}, S_{q-1}) normal MT is well-posed. But, from (4.2.2) we have that $(S_P\mathbf{v}^0)_K$ is the midpoint of the edge $(S_P\mathbf{v}^0)_K(S_P\mathbf{v}^0)_{K+1}$, while $\mathbf{n}_K^1$ is the average of the normals $\hat{\mathbf{n}}_K^1$ and $\hat{\mathbf{n}}_{K+1}^1$, generated by S_{q-1}. Thus, $\hat{s}_K^1 < s_K^1 < \hat{s}_{K+1}^1$, where s^1 is the arc-length sequence generated by the (S_P, S_q) normal MT, while $\hat{s}^1$ is the arc-length

sequence generated by the (S_{P-1}, S_{q-1}) normal MT. Since $\hat{s}^1$ monotonically increases, so does s^1, and the (S_P, S_q) normal MT is well-posed. □

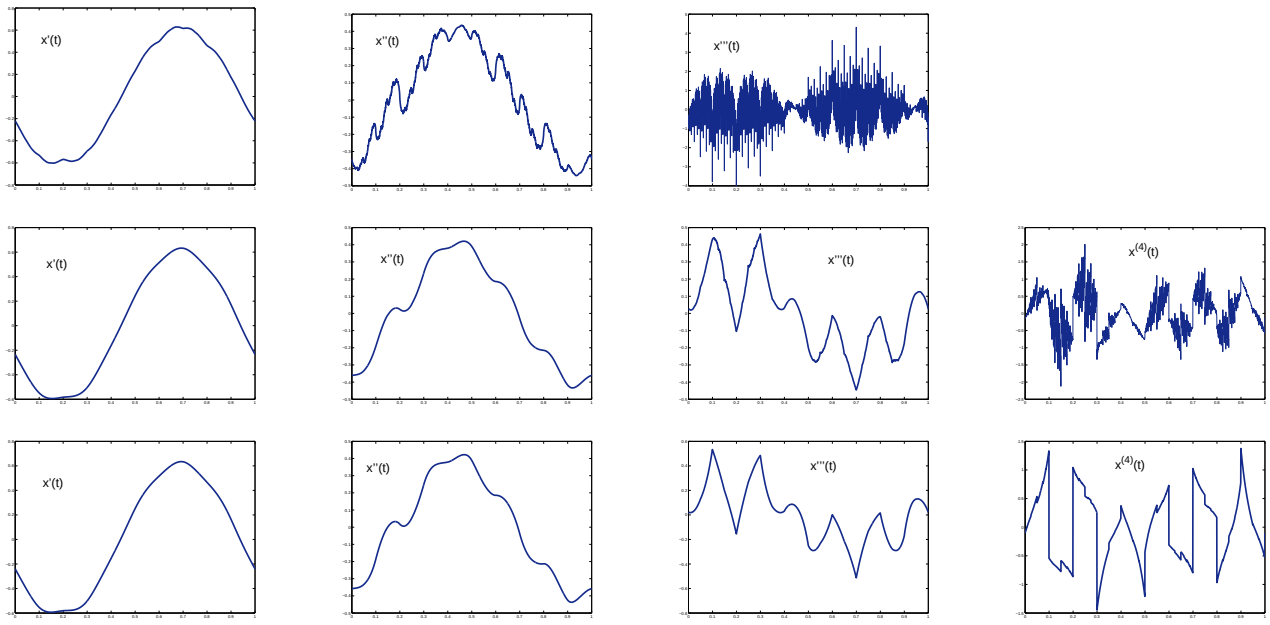

Fig. 5.2: Regularity of the normal re-parametrization for normal MT with S_4.

Proposition 5.1.2 gives a very easy criteria regarding when the (S_p, S_q) normal MT can be safely applied. Moreover, unless $\mathcal{C}$ is very complicated, starting with an arbitrary initial point set $\mathbf{v}^0$, and performing S_2 or S_1 normal MT the curve will split into locally convex/concave arcs after very few refinements. Hence, we can quickly switch from S_2 to higher S_p prediction operators in the extended version of our adaptive algorithm, mentioned at the very end of Section 4.4.2. Whether this is of any practical value or not, depends on how much faster the normal MT based on S_p "regularizes" the data than the S_2 normal MT does. And an indicator for the latter is exactly the smoothness of the normal re-parametrization, which further motivates our interest in the (S_p, S_q) normal MTs.

For smooth curves $\mathcal{C}$ such as the circle and graphs of simple polynomials, we have monitored the smoothness behavior of the global x-coordinate function of the normal re-parameterization $\mathbf{v}(t)$ by plotting the graphs of the first component of $2^{jm}(\Delta^m \mathbf{v}^j)(t)$ for $j = 8$ for various $m \geq 1$ (we can assume that this function is close to $x^{(m)}(t)$ if the re-parametrization is in $C^{k,\alpha}$ for some $k \geq m$). The curve was the unit circle, with fixed initial set $\mathbf{v}^0$ of 10 non-uniformly distributed points at start. The series of plots in Fig. 5.2 is for the (S_4, S_q) normal MT with $q = 0, 1, 2$ (from top to bottom), and show graphs with $m = 1, 2, 3, 4$ (from left to right). The plots confirm the theoretical result from Theorem 4.2.3 regarding the $\mathrm{O}(2^{-(1+\alpha')j})$ decay with any $\alpha' < 1$ for the monitored quantities, but also suggest that for smooth $\mathcal{C}$, the larger the q the smoother the $\mathbf{v}(t)$. Moreover, since $s_\infty(S_4) = 4$, for $q = 2$ we already observe optimal smoothness $C^{3,\alpha'}$ for the re-parameterization. The following theorem concurs that those observations are true at least for small p.

Theorem 5.1.3. *Fix $p \in \{2, 3, 4\}$. Let $\mathcal{C}$ be closed, non-self-intersecting, regular C^{p+1} curve, given by its arc-length parameterization $\mathbf{v}(s)$. Let $\mathbf{v}^0 \in \mathcal{C}$ be such that the (S_p, S_{p-2}) normal MT is globally*

well-posed and convergent. Then the normal re-parameterization of $\mathcal{C}$ *is* $C^{p-1,1}$ *for* $p = 2, 3$, *and* $C^{3,\alpha}$, $\alpha < 1$ *for* $p = 4$. *Finally,*

$$\|\Delta^n s^j\| = \mathrm{O}(2^{-nj}) = \mathrm{O}(\|\Delta s^j\|^n), \qquad 1 \le n \le p; \quad j \to \infty.$$

Proof. Fix $p \in \{2, 3, 4\}$. Following our notation from Section 4.2, it suffices to show that the limit scalar function $s(t)$ of the corresponding arc-length sequences $\{s^j : s_i^j = s(t_i^j) = s(i2^{-j}),\ i \in [0, 2^j L]\}$, $j \in \mathbb{Z}$, is $C^{p-1,1}$. But, re-writing it in the form $s^j = S_p s^{j-1} + \omega^j$, leads us to a standard linear univariate multiresolution where the perturbation argument from [24, Theorem 4.4] is applicable. In our setting, it simplifies to the following

Lemma 5.1.4. *Let* $s^j = S_p s^{j-1} + \omega^j$, *where the data* s^j *is associated to the uniform grid* $2^{-j}\mathbb{Z}$. *Then, if*

$$\|\omega^j\| = \|s^j - S_p s^{j-1}\| = \mathrm{O}(2^{-\nu(j-1)}), \qquad \nu > p,$$

the piece-wise linear interpolants $s^j(t)$ *converge uniformly to a* $C^{p-1,1}$ *limit* $s(t)$, *while if*

$$\|\omega^j\| = \|s^j - S_p s^{j-1}\| = \mathrm{O}(2^{-p(j-1)}),$$

the piece-wise linear interpolants $s^j(t)$ *converge uniformly to a* C^{p-1} *limit* $s(t)$, *s.t.,*

$$|s^{p-1}(t + \Delta t) - s^{p-1}(t)| \le C|\Delta t|(1 + |\log|\Delta t||), \qquad \forall t, t + \Delta t \in [0, 1].$$

Note that this is just a logarithmic factor worse than a $C^{p-1,1}$ *smoothness.*

Here we estimate the quantity $\|\omega^j\|$ for $p = 2, 3, 4$ and derive that

$$\|\omega^j\| = \mathrm{O}(2^{-(p+1)(j-1)}), \quad p = 2, 3; \qquad \|\omega^j\| = \mathrm{O}(2^{-p(j-1)}), \quad p = 4, \tag{5.1.2}$$

which, together with Lemma 5.1.4 completes the proof of the first part of the theorem. The second part follows from (4.2.5) and (5.1.2) via

$$\begin{aligned} \Delta^n s^j = 2^{-n} S_{p-n} \Delta^n s^{j-1} + \Delta^n \omega^j \quad &\Longrightarrow \quad \|\Delta^n s^j\| \le 2^{-n} \|\Delta^n s^{j-1}\| + \mathrm{O}(2^{-\nu j}) \\ &\Longrightarrow \quad \|\Delta^n s^j\| = \mathrm{O}(2^{-nj} \|\Delta^n s^0\|) = \mathrm{O}(\|\Delta s^j\|^n), \end{aligned}$$

for $1 \le n \le p$, apart from $n = p = 4$ when we get the slightly weaker $\|\Delta^4 s^j\| = \mathrm{O}(j\|\Delta s^j\|^4)$. Note that Theorem 4.2.3 implies $\|\omega^j\| \le C 2^{-2(j-1)}$, with a constant $C < \infty$, independent of j and, thus $\|\Delta s^j\| \asymp 2^{-j}$.

To verify (5.1.2) it is enough to work with only one step of the normal MT, so instead of the notation $\mathbf{v}^{j-1}$, $\mathbf{v}^j$ we use $\mathbf{v}$ for the coarse-scale data and $\bar{\mathbf{v}}$ for its refinement. Throughout the computations we use the geometrical interpretation of the (S_p, S_{p-2}) normal MT based on the Lane-Riesenfeld algorithm, namely for any $K \in \mathbb{Z}$, $(S_p \mathbf{v})_K$ halves the edge $\Delta(S_{p-1}\mathbf{v})_K$ while the generalized normal $(S_{p-2}\Delta\mathbf{v})_K^{\perp}$ is orthogonal to the same edge. Due to the locality of S_p for $p \le 4$, we need to work only with the triplet $(\mathbf{v}_{-1}, \mathbf{v}_0, \mathbf{v}_1) = \big(\mathbf{v}(s_{-1}), \mathbf{v}(s_0), \mathbf{v}(s_1)\big)$. We choose the local frame $(\mathcal{T}, \mathcal{N})$, centered at $\mathbf{v}_0$ (see Fig. 5.3), and to simplify the notation, we set $s_0 = 0$, $\mathbf{v}(s_0) = 0$, $\alpha = \mathrm{k}(s_0)$, and $\beta = \mathrm{k}'(s_0)$. Furthermore, note, that whenever $\mathbf{v} \in C^3$ the curvature is uniformly bounded, i.e., there exists a constant $C_{\mathcal{C}} < \infty$ that depends solely on $\mathcal{C}$ such that $\alpha < C_{\mathcal{C}}$. If $\mathbf{v} \in C^4$

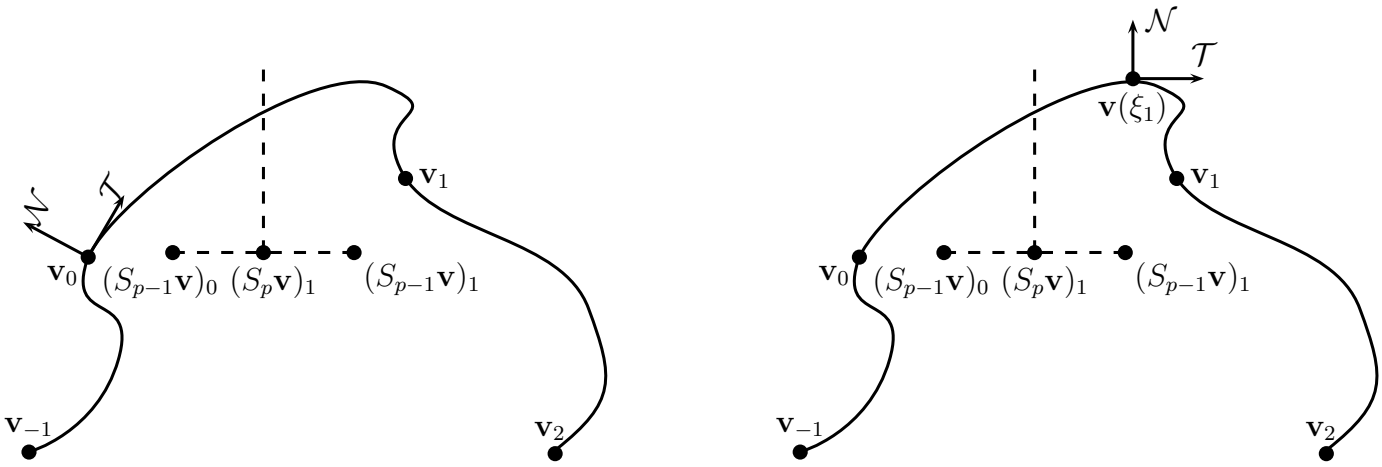

Fig. 5.3: Local (S_p, S_{p-2}) normal MT analysis with two different choices of coordinate frames: left - the one centered at $\mathbf{v}_0$; right - the one, coinciding with the generated normal direction.

then $\mathrm{k}'(s)$ is also uniformly bounded, and there exists another constant $C_{\mathcal{C}}$ (possibly larger than the previous one, but still finite) satisfying $\alpha, \beta < C_{\mathcal{C}}$.

p=2: Let $\bar{s}$ be the argument sequence for $\bar{\mathbf{v}}$. For the Chaikin operator, due to symmetry, it suffices to provide estimations for $\omega_0 = \bar{s}_0 - s_1/4$. From the orthogonality relation between $\Delta\mathbf{v}_0$ and $\bar{\mathbf{v}}_0 - (S_2\mathbf{v})_0$, and the Taylor expansion (5.0.1) we derive

$$\begin{aligned}\tfrac{1}{4}s_1^2 - \tfrac{\alpha^2}{48}s_1^4 + \mathrm{o}(s_1^4) = \tfrac{x^2(s_1)+y^2(s_1)}{4} = x(\bar{s}_0)x(s_1) + y(\bar{s}_0)y(s_1) = \\ = \left(\bar{s}_0 - \tfrac{\alpha^2}{6}\bar{s}_0^3 + \mathrm{o}(\bar{s}_0^3)\right)\left(s_1 - \tfrac{\alpha^2}{6}s_1^3 + \mathrm{o}(s_1^3)\right) + \left(\tfrac{\alpha}{2}\bar{s}_0^2 + \tfrac{\beta}{6}\bar{s}_0^3 + \mathrm{o}(\bar{s}_0^3)\right)\left(\tfrac{\alpha}{2}s_1^2 + \tfrac{\beta}{6}s_1^3 + \mathrm{o}(s_1^3)\right).\end{aligned}$$

Comparing the coefficients in front of the corresponding powers of s_1, we immediately see that if $\bar{s}_0 = a_0 + a_1 s_1 + a_2 s_1^2 + a_3 s_1^3 + \mathrm{o}(s_1^3)$ then

$$\left|\begin{array}{l} a_0 = 0 \\ a_1 = 1/4 \\ a_2 = 0 \\ a_3 = \alpha^2\left(\frac{1}{24} + \frac{1}{384} - \frac{1}{64} - \frac{1}{48}\right) = \frac{\alpha^2}{128}\end{array}\right. ,$$

or

$$\omega_0 = \bar{s}_0 - \frac{1}{4}s_1 = \frac{\alpha^2}{128}s_1^3 + \mathrm{o}(s_1^3) = \mathrm{O}\big((\Delta s_0)^3\big), \tag{5.1.3}$$

whenever $\mathbf{v} \in C^3$.

p=3: We need to consider separately $\bar{s}_0$ and $\bar{s}_1$. For the second case, the generalized normal coincides with the standard one and the computations are absolutely analogous to the (S_2, S_0)

normal MT, so without further explanation we derive

$$x(\bar{s}_1)x(s_1)+y(\bar{s}_1)y(s_1)=\tfrac{x^2(s_1)+y^2(s_1)}{2}=\tfrac{1}{2}s_1^2-\tfrac{\alpha^2}{24}s_1^4-\tfrac{\alpha\beta}{24}s_1^5+\mathrm{o}(s_1^5)$$
$$\Longrightarrow\quad x(\bar{s}_1)\left(1-\tfrac{\alpha^2}{6}s_1^2-\tfrac{\alpha\beta}{8}s_1^3+\mathrm{o}(s_1^3)\right)+y(\bar{s}_1)\left(\tfrac{\alpha}{2}s_1+\tfrac{\beta}{6}s_1^2+\mathrm{o}(s_1^2)\right)=\tfrac{1}{2}s_1-\tfrac{\alpha^2}{24}s_1^3-\tfrac{\alpha\beta}{24}s_1^4+\mathrm{o}(s_1^4)$$
$$\Longrightarrow\quad \left|\begin{array}{l} a_0=0\\ a_1=1/2\\ a_2=0\\ a_3=\alpha^2\left(\frac{1}{12}+\frac{1}{48}-\frac{1}{16}-\frac{1}{24}\right)=0\\ a_4=\alpha\beta\left(\frac{1}{16}+\frac{1}{128}-\frac{1}{48}-\frac{1}{96}-\frac{1}{24}\right)=-\frac{\alpha\beta}{384}\end{array}\right. ,$$

or

$$\omega_1=\bar{s}_1-\frac{1}{2}s_1=\frac{\alpha\beta}{384}s_1^4+\mathrm{o}(s_1^4)=\frac{\alpha\beta}{384}(\Delta s_0)^4+\mathrm{o}(\|\Delta s\|^4). \tag{5.1.4}$$

For $\bar{s}_0$ the computations are a little bit more complicated. First of all, using the Lane-Riesenfeld algorithm, we can conclude that our prediction point is the midpoint of the neighboring Chaikin points, more precisely, it is $\big((x(s_1)+x(s_{-1}))/8,(y(s_1)+y(s_{-1}))/8\big)$, while the normal direction is orthogonal to the Chaikin edge $\big((x(s_1)-x(s_{-1}))/4,(y(s_1)-y(s_{-1}))/4\big)$. Secondly, by Theorem 4.2.3(ii) we already know that the limit $s(t)\in C^1$, and, thus, for all $j\in\mathbb{N}$ $(\Delta s^j)_{-1}\asymp(\Delta s^j)_0$. Hence, in our notation we can let $s_{-1}=-(\Delta s)_{-1}=r(\Delta s)_0=rs_1$, with $r=\mathrm{O}(1)$. Now, we have the following equation

$$\left(x(\bar{s}_0)-\tfrac{x(s_1)+x(s_{-1})}{8}\right)(x(s_1)-x(s_{-1}))+\left(y(\bar{s}_0)-\tfrac{y(s_1)+y(s_{-1})}{8}\right)(y(s_1)-y(s_{-1}))=0\quad\Longrightarrow$$
$$x(\bar{s}_0)\left((1-r)s_1-\tfrac{\alpha^2(1-r^3)}{6}s_1^3-\tfrac{\alpha\beta(1-r^4)}{8}s_1^4+\mathrm{o}(s_1^4)\right)+y(\bar{s}_0)\left(\tfrac{\alpha(1-r^2)}{2}s_1^2+\tfrac{\beta(1-r^3)}{6}s_1^3+\mathrm{o}(s_1^3)\right)=$$
$$=\tfrac{1-r^2}{8}s_1^2-\tfrac{\alpha^2(1-r^4)}{96}s_1^4-\tfrac{\alpha\beta(1-r^5)}{96}s_1^5+\mathrm{o}(s_1^5)\quad\Longrightarrow\quad\left|\begin{array}{l}a_0=0\\ a_1=(1+r)/8\\ a_2=0\end{array}\right. .$$

Hence, $\bar{s}_0=(s_1+s_{-1})/8+a_3s_1^3+a_4s_1^4+\mathrm{o}(s_1^4)$. Direct computations for a_3 and a_4 give rise to

$$a_3=\tfrac{\alpha^2(21r^2+39r+21)(1+r)}{3\cdot2^{10}};$$
$$a_4=\tfrac{\alpha\beta}{32}\left(\tfrac{(1+r)^2(1+r^2)}{2}+\tfrac{(1+r)^4}{2^{10}}-\tfrac{(1+r^2)(1+r+r^2)}{24}-\tfrac{(1+r)^4}{192}-\tfrac{1+r+r^2+r^3+r^4}{3}\right).$$

Now we need a bootstrapping argument. Since $r\in\mathrm{O}(1)$, it is bounded, and thus, so is a_3. Therefore $\|\omega^j\|=\mathrm{O}(2^{-3j})=\mathrm{o}(2^{-2j})$ and, since $s_\infty(S_3)=3>2$, $s(t)\in C^2$ due to Lemma 5.1.4. This implies $\|\Delta^2 s^j\|=\mathrm{O}(2^{-2j})$, i.e., $|(\Delta s^j)_0-(\Delta s^j)_{-1}|=\mathrm{O}((\Delta s^j)_0^2)$. But the latter is equivalent to $r=-1+\mathrm{O}(s_1)$, so $a_3=\mathrm{O}(s_1)$ and

$$\omega_0=\bar{s}_0-\frac{s_1+s_{-1}}{8}=\mathrm{O}(s_1^4)=\mathrm{O}(\|\Delta s\|^4). \tag{5.1.5}$$

Equations (5.1.4) and (5.1.5) lead to $s^j=S_3s^{j-1}+\omega^j$ with $\|\omega^j\|=\mathrm{O}(2^{-4j})$, so we conclude that $s(t)\in C^{2,1}$. This result is optimal, since there is no way to obtain a more regular normal re-parametrization than the smoothness of the prediction operator!

p=4: As with the Chaikin operator ($p = 2$), due to symmetry, we need to consider only one case. From the equation

$$\left(x(\bar{s}_0) - \frac{5x(s_1) + x(s_{-1})}{16}\right)(3x(s_1) - x(s_{-1})) + \left(y(\bar{s}_0) - \frac{5y(s_1) + y(s_{-1})}{16}\right)(3y(s_1) - y(s_{-1})) = 0,$$

we deduce

$$\begin{gathered} x(\bar{s}_0)(3x(s_1) - x(s_{-1})) + y(\bar{s}_0)(3y(s_1) - y(s_{-1})) = \\ = \tfrac{1}{16}\Big(15(x^2(s_1) + y^2(s_1)) - 2(x(s_1)x(s_{-1}) + y(s_1)y(s_{-1})) - (x^2(s_{-1}) + y^2(s_{-1}))\Big); \\ x(\bar{s}_0)\left((3-r)s_1 - \tfrac{\alpha^2(3-r^3)}{6}s_1^3 - \tfrac{\alpha\beta(3-r^4)}{8}s_1^4 + \mathrm{o}(s_1^4)\right) + y(\bar{s}_0)\left(\tfrac{\alpha(3-r^2)}{2}s_1^2 + \tfrac{\beta(3-r^3)}{6}s_1^3 + \mathrm{o}(s_1^3)\right) = \\ = \tfrac{15-2r-r^2}{16}s_1^2 + \tfrac{\alpha^2(r^4+4r^3-6r^2+4r-15)}{12\cdot 16}s_1^4 + \tfrac{\alpha\beta(r^5+3r^4-2r^3-2r^2+3r-15)}{12\cdot 16}s_1^5 + \mathrm{o}(s_1^5). \end{gathered}$$

Again, it is trivial to show that $\bar{s}_0 = \frac{5+r}{16}s_1 + a_3 s_1^3 + a_4 s_1^4 + \mathrm{o}(s_1^4)$ and direct computations (which we prefer to skip) give rise to

$$a_3 = \frac{\alpha^2(105r^2 + 330r - 495)}{3 \cdot 2^{13}(r-3)}(1+r)^2.$$

Analogously to $p = 3$, we have $r = -1 + \mathrm{O}(s_1)$, and thus, $a_3 = \mathrm{O}(s_1^2)$. For a_4 we obtain

$$a_4 = \frac{\alpha\beta(3555r^5 + 31315r^4 + 1550r^3 + 15510r^2 - 41505r - 16665)}{3 \cdot 2^{19}(r-3)},$$

which doesn't have -1 for a root, and thus, is $\mathrm{O}(1)$, making $\|\omega_0\| = \mathrm{O}(\|\Delta s\|^4)$. This is enough only for assuring $C^{3,\alpha}$, $\alpha < 1$ smoothness for the normal re-parametrization. □

Note that the assumption $\mathcal{C} \in C^{p+1}$ is too restrictive and is needed only to argue that $\|\omega^j\|$ decays with order, higher than p. Thus, any smoothness greater than C^p would do, but to keep the statement as transparent as possible, we choose not to go into this. Unfortunately the technique above cannot be performed further for $p > 4$, since computer simulations indicate that in this case $\|\omega^j\| = \mathrm{O}(2^{-\nu j})$ with $\nu < p$, and, thus, Lemma 5.1.4 does not apply. The latter, however, is just a sufficient, but not a necessary condition for producing $C^{p-1,1}$ limits. Indeed, take arbitrary s^0 and let $\omega_i^j = 2^{-j}\|\Delta s^0\|$ be a constant sequence at any level j. Then the limit $s(t)$ of the $s^j = S_p s^{j-1} + \omega^j$ equals the B-spline of order $p+1$, generated by $s^j = S_p^j s^0$, shifted upwards by $\|\Delta s^0\|$. Hence, its smoothness is the same as for the B-spline (i.e., $s(t) \in C^{p-1,1}$), but $\|\omega^j\| = \mathrm{O}(2^{-j})$. This implies that a more close-to-necessary criterium should replace the lemma, e.g., the following straightforward generalization of it

Lemma 5.1.5. *Let $s^j = S_p s^{j-1} + \omega^j$, where the data s^j is associated to the uniform grid $2^{-j}\mathbb{Z}$, and $p \geq 1$. If there exists $\epsilon \in (0, 1]$, $q \in \{0, \ldots, p\}$, and $C < \infty$, such that*

$$\|\Delta^n \omega^j\| \leq C 2^{-(n+\epsilon)j}, \qquad \forall j \in \mathbb{N}, \quad \forall n \ : \ 0 \leq n \leq q, \tag{5.1.6}$$

then the piece-wise linear interpolants $s^j(t)$ converge uniformly to a $C^{k,\alpha}$ limit $s(t)$ with

$$k + \alpha = \begin{cases} q + \epsilon, & q < p, \epsilon < 1; \\ q + 1^-, & q < p, \epsilon = 1; \\ (p-1) + 1, & q = p. \end{cases} .$$

We have used the short notation 1^- *to denote that the result holds for all* $0 < \delta < 1$ *but may fail for* 1.

On the other hand, if there exists $\epsilon \in (0, 1]$, $c > 0$, *and* $q < p$, *such that*

$$\|\Delta^q \omega^j\| \geq c 2^{-(q-\epsilon)j}, \qquad \forall j \in \mathbb{N}$$

then the limit $s(t)$ *(if it exists!) is at most* $C^{q-1,1-\epsilon}$.

Proof. Once again, the proof is by induction on q using the Lane-Riesenfeld algorithm (4.2.2). Let $q = 0$ and assume $\|\omega^j\| \leq C 2^{-\epsilon j}$ for all levels $j \in \mathbb{N}$. We have to show that $s^j(t) \to s(t)$ as $j \to \infty$ and $s(t) \in C^{0,\epsilon}$, if $\epsilon < 1$ and $s(t) \in C^{0,1^-}$, otherwise. In order to do so, we need to estimate the difference in $L_\infty(\mathbb{R})$ between two consecutive interpolants $s^j(t)$.

$$\|s^j(\cdot) - s^{j-1}(\cdot)\| = \|s^j - S_1 s^{j-1}\| \leq \|(S_p - S_1)s^{j-1}\| + \|\omega^j\| \leq C(\|\Delta s^{j-1}\| + 2^{-\epsilon j}).$$

We used the well-known fact in linear subdivision that, since $p \geq 1$ $(S_p - S_1)\mathbf{1} = \mathbf{0}$, there exists another linear, local subdivision scheme T, such that $(S_p - S_1)x = T\Delta x$, for all $x \in \ell_\infty(\mathbb{Z})$, and thus $\|(S_p - S_1)x\| \leq \|T\|\|\Delta x\|$. The constant C is the maximum of the a priori given C and $\|T\|$ that we denote again by C in order to simplify the equations. The only important thing is that this constant is bounded and independent on the level j. Now, using (4.2.5), $\|S_{p-1}\| = 1$, and the trivial $\|\Delta\omega^j\| \leq 2\|\omega^j\|$ we derive

$$\|\Delta s^j\| \leq \frac{1}{2}\|\Delta s^{j-1}\| + 2C\|\omega^j\| \leq \cdots \leq 2^{-j}\|\Delta s^0\| + \underbrace{\sum_{l=0}^{j-1} 2^{-l}(2C2^{-\epsilon(j-l)})}_{f(\epsilon,j)}.$$

The sum $f(\epsilon, j)$ is monotonically decreasing as function of its first argument, and monotonically increasing as function of its second argument. Furthermore, for $0 < \epsilon < 1$ we have

$$f(\epsilon, j) = 2C2^{-\epsilon j}\sum_{l=0}^{j-1} 2^{(\epsilon-1)l} \leq f(\epsilon, \infty) = \frac{2C}{1 - 2^{\epsilon-1}}2^{-\epsilon j}$$

$$\Longrightarrow \quad \|\Delta s^j\| \leq 2^{-\epsilon j}\left(2^{\epsilon-1}\|\Delta s^0\| + \frac{2C}{1 - 2^{\epsilon-1}}\right) \leq C2^{-\epsilon j},$$

while for $\epsilon = 1$ we have

$$f(1, j) = 2Cj2^{-j} \quad \Longrightarrow \quad \|\Delta s^j\| \leq C2^{-\delta j}, \qquad \forall \delta \in (0, 1).$$

This leads to

$$\|s^j(\cdot) - s^{j-1}(\cdot)\| \leq C \begin{cases} 2^{-\epsilon j}, & \epsilon \in (0, 1); \\ 2^{-\delta j}, & \epsilon = 1, \forall \delta < 1. \end{cases}.$$

Hence $\{s^j(t)\}$ is a Cauchy sequence in $L_\infty(\mathbb{R})$ and converges to a continuous limit $s(t)$. The Hölder smoothness of $s(t)$ follows from the boundedness of $2^{\epsilon j}\|\Delta s^j\|$, resp., $2^{\delta j}\|\Delta s^j\|$.

Now, let (5.1.6) be satisfied for some pair (q, p) with $0 < q \leq p$. The computations above guarantee that $s^j(t)$ uniformly converges to a continuous limit $s(t)$. Moreover, since

$$s^j_{[1]} := 2^j \Delta s^j = S_{p-1}2^{j-1}\Delta s^{j-1} + 2^j \Delta\omega^j = S_{p-1}s^{j-1}_{[1]} + \omega^j_{[1]},$$

by induction we know that $s^j_{[1]}(t)$ converges uniformly to $s_{[1]}(t)$ that is as smooth as Lemma 5.1.5 states for the pair $(q-1, p-1)$. Finally, since $s^j(t)$ and $s^j_{[1]}(t)$ are both converging sequences, classical results in [31, 15] assure that $s(t)$ is differentiable with derivative $s_{[1]}(t)$.

On the other hand, having $\|\Delta^q \omega^j\| \geq c2^{-(q-\epsilon)j}$ implies that the corresponding sequence $s^j_{[q]}(t)$ does not converge in $L_\infty(\mathbb{R})$, and thus, $s(t) \notin C^q$. This finishes the proof. □

Some comments are in order. Since for any given $p \in \mathbb{N}$ we have $\|\Delta^n \omega^j\| \leq 2^n \|\omega^j\| \leq 2^p \|\omega^j\|$, $\forall n \leq p$, and the constant $C = 2^p$ is bounded and independent on j, Lemma 5.1.4 is a corollary of Lemma 5.1.5, apart from the boundary case, which we did not treat. Our proof follows basically the same steps as the proof in [24] and the only difference is that in the interpolating case one always has optimal detail decay rates, which guarantee that the more restricted conditions of Lemma 5.1.4 are sufficient for the smoothness analysis of the normal MTs, while for our problem we know that the detail decay rate remains two. Moreover, computer simulations indicate that for large p the regularity of the (S_p, S_{p-2}) normal re-parameterization is below $(p-1, 1)$, implying that we have to deal with negative statements, as well. But, unlike Lemma 5.1.5, Lemma 5.1.4 is not a necessary condition and we cannot use it to disprove things.

Remark 5.1.6. *For any S_p and any admissible N, the offsets ω^j in the associated to (S_p, N) normal MT linear multi-scale transform $s^j = S_p s^{j-1} + \omega^j$ satisfy $\|\omega^j\| = \mathrm{O}(2^{-3j})$, provided $\mathcal{C} \in C^3$.*

In particular, Remark 5.1.6 implies that the normal re-parameterization of the (S_p, N) normal MT is $C^{2,1^-}$ for all $p \geq 3$ and smooth initial curves $\mathcal{C}$, which is stronger than the $C^{1,1^-}$ smoothness, guaranteed by Theorem 4.2.3. To show that, let $\mathbf{v}_k$, resp. s_k, $k \in I_i$ be the coarse-scale data and $\bar{\mathbf{v}}_K$ be its refinement via one step of the (S_p, N) normal MT. Furthermore, let ξ_K be as in (4.2.11), and $(x(s), y(x(s)))$ be the local coordinates with respect to the frame $(\mathcal{T} = \mathbf{t}(\xi_K), \mathcal{N} = \mathbf{n}(\xi_K))$ centered at $\mathbf{v}(\xi_K)$ (see Fig. 5.3). We have that $\xi_K \in s|_{I_i}$ and (5.0.1) gives rise to

$$x(s) = (s - \xi_K) - \frac{\alpha^2}{6}(s - \xi_K)^3 + \mathrm{O}(|s - \xi_K|^4), \qquad \forall s \in s|_{I_i}, \tag{5.1.7}$$

where, as before, $\alpha = \mathrm{k}(\xi_K)$. The benefit of using this local frame is that the detail d_K has no horizontal component and the useful equality

$$x(\bar{s}_K) = (S_p x)_K$$

holds. Now we can restrict the problem to proximity analysis via subtracting $x((S_p s)_K)$ from both the sides, and using (4.2.11) we deduce:

$$x(\bar{s}_K) - x((S_p s)_K) = (S_p x)_K - x((S_p s)_K) \quad \Longrightarrow \quad \omega_K + \mathrm{O}(\|\Delta s\|^3) = (S_p x)_K - x((S_p s)_K). \tag{5.1.8}$$

For the decay order of $(S_p x)_K - x((S_p s)_K)$ we can apply Lemma 5.0.4 and Lemma 4.2.2, and derive that, whenever $\mathcal{C} \in C^3$, $|\omega_K| = \mathrm{O}(\|\Delta s\|^2)$. What we did so far is just to confirm the detail decay result from Theorem 4.2.3 for the (S_p, N) normal MT. However, we can benefit from the fact that

$x(s)$ is a third-order perturbation of s and improve the result. Indeed

$$\begin{aligned}(S_p x)_K - x((S_p s)_K) &= \Big(S_p\Big((s-\xi_k) - \frac{\alpha^2}{6}(s-\xi_K)^3 + \mathrm{O}(|s-\xi_K|^4)\Big)\Big)_K \\ &\quad -((S_p s)_K - \xi_K) + \frac{\alpha^2}{6}((S_p s)_K - \xi_K)^3 + \mathrm{O}(|(S_p s)_K - \xi_K|^4) \\ &= \frac{\alpha^2}{6}\big((S_p(s-\xi_K)_K)^3 - (S_p(s-\xi_K)^3)_K\big) + \mathrm{O}(\|\Delta s\|^4); \\ \Longrightarrow \quad |(S_p x)_K - x((S_p s)_K)| &\le \frac{\alpha^2}{6}\Big(|(S_p s)_K - \xi_K|^3 + \|(s-\xi_K)^3\|_{I_i}\Big) + \mathrm{O}(\|\Delta s\|^4) \le \mathrm{O}(\|\Delta s\|^3).\end{aligned}$$

For the estimations we also used that S_p has exact order of polynomial reproduction 2.

For $N = S_q$, the Lane-Riesenfeld algorithm gives rise to the additional relation

$$\Delta(S_{q+1} y)_K = 0 \qquad \Longrightarrow \qquad (S_q \Delta y)_K = 0,$$

which, as seen in Theorem 5.1.3, improves the decay order for ω^j, if q is chosen appropriately. On the other hand, this improvement cannot be arbitrary big as $p \to \infty$, because of the already mentioned third-order perturbation between the coordinate systems that correspond to discrete and continuous data, respectively. Indeed, the local frame $(\mathcal{T}, \mathcal{N})$ depends solely on coarse-scale data, so it should be intuitively clear that all our actions can smoothen up just the sequence $x^j = x(s^j)$ we have control of, but not the sequence s^j that also depends on the curve information between the points from the sample $\mathbf{v}^j$ (an information that the (S_p, N) prediction operator has no chance to capture). For instance, if we obtain $\|\Delta^4 x^j\| = \mathrm{O}(\|\Delta x^j\|^4) = \mathrm{O}(2^{-4j})$ for some (S_p, S_q) normal MT, it does not automatically imply $\|\Delta^4 s^j\| = \mathrm{O}(2^{-4j})$, because $s^j = x^j + \mathrm{O}((x^3)^j)$. Actually, we have already observed the problem in the proof of Theorem 5.1.3, where we derived the suboptimal $\|\Delta^4 s^j\| = \mathrm{O}(j\|\Delta s^j\|^4)$ for the (S_4, S_2) normal MT. Finding the exact limit of the (S_p, S_q) normal MT ability for improving data regularity seems a very technical problem, and we do not pursue it. Another reason for not digging deeper there is the result from the forthcoming Section 5.2.1, where it is observed that smoothness of the normal re-parameterization higher than C^3 does not affect the detail decay order of the combined normal MT. For the sake of the smoothness analysis, however, one may relax the restrictions on the normal-generating operator N and allow it to be geometric, thus nonlinear. For example, the curvature preserving subdivision rules [10] or the normal-interpolating schemes [115, 116] are promising candidates for N. The prediction operator S_p can be generalized, as well, by replacing the linear Lane-Riesenfeld algorithm (4.2.2) used for its construction with a nonlinear one [34]. We postpone our research in this direction to the future.

5.2 Improving the detail decay rate via additional pre-processing. Combined normal MTs

Having dealt with the regularity of the normal re-parameterization in Section 5.1, here we concentrate on the detail decay rate of the normal MTs. Of course, there is no chance to achieve $\|d^j\| = \mathrm{O}(2^{-\mu j})$, $\mu > k + \alpha$, limitation for detail decay under $\mathcal{C} \in C^{k,\alpha}$, so throughout this section we always assume that $\mathcal{C}$ is smooth enough (e.g., one can think of $\mathcal{C} \in C^\infty$). According to

Theorem 4.2.3 and its proof, there are two different restrictions on the speed of the detail decay for a normal MT: the regularity of the data, and the polynomial exactness order of the prediction operator. Both the properties depend on the chosen prediction operator S, and for any S there is a tradeoff between the two characteristics. Indeed, high order exact polynomial reproduction P_e implies existence of negative coefficients in the mask of S, and thus Hölder regularity $s_\infty(S)$ significantly lower than P_e, as well as ill-posedness of the S normal MT, in general. Vice versa, high Hölder regularity of S leads to mask of S with only few and small in absolute value negative coefficients, hence small P_e. In any case, the detail decay rates of the S normal MT remain considerably smaller than the order of polynomial reproduction P of S, that serves as an upper bound for both P_e and $s_\infty(S)+1$. Our main goal is to construct normal multi-scale transforms that allow detail decay rates $\mu = P$ for larger P. A closer look into the proof of Theorem 4.2.3 explains that the two restrictions $\mu \le m+\beta+1$ and $\mu \le P_e$ are used in a different way and can be decoupled. More precisely, the first one assures the regularity of the refined data, and thus, of the normal re-parameterization, while the second comes from classical approximation theory and estimates the error between a smooth curve and its approximation with P-order polynomials that interpolate $\mathcal{C}$ on such a regular set of points. In simpler words, the first restriction deals with the data distribution in the tangential direction of the local coordinates, while the second one deals with the corresponding distribution in the normal direction. Or, as it was said in [69]: *"while geometry and parameter information are globally intertwined, they disconnect locally: infinitesimally, we may think of parameter information as being described by displacements in the tangent plane"*.

Our idea is to combine two different rules S and $\tilde{S}$ for predicting the new point, and use them for computing the tangential and the normal component of the point, respectively. We propose the following procedure: given $\mathbf{v}^{j-1}$ and $K \in \mathbb{Z}$, compute $(S\mathbf{v}^{j-1})_K$ and $(\tilde{S}\mathbf{v}^{j-1})_K$. Compute $\hat{\mathbf{n}}^j_K$ via (5.1.1), where the scheme N is a priori fixed. Then, the predicted point $\hat{\mathbf{v}}^j_K$ is the orthogonal projection of $(\tilde{S}\mathbf{v}^{j-1})_K$ onto the normal line $L_K(t) = (S\mathbf{v}^j)_K + t\hat{\mathbf{n}}^j_K$. In the local frame $(\mathcal{T}, \mathcal{N} = \hat{\mathbf{n}}^j_K)$, the following formula:

$$\mathbf{v}^j_K = \hat{\mathbf{v}}^j_K + d^j_K \hat{\mathbf{n}}^j_K; \qquad \hat{x}^j_K = (Sx^{j-1})_K, \quad \hat{y}^j_K = (\tilde{S}y^{j-1})_K, \tag{5.2.1}$$

describes the process, which we will refer to as the $(S, N, \tilde{S})$ *normal MT* (see Fig. 5.4 for the (S_3, S_1, T) normal MT). In comparison to the (S, N) normal MT, (5.2.1) involves only an additional pre-processing of the data via $\tilde{S}$ that takes place solely in the normal direction $\hat{\mathbf{n}}^j_K$, and, thus, the refined data $\mathbf{v}^j$ is the same. Hence, the analysis of well-posedness, convergence, and regularity of the normal re-parameterization depends on S but not on $\tilde{S}$.

5.2.1 (S_p, S_{p-2}, T_p) normal MT

In this subsection, we illustrate the concept of combined normal MTs on the family of (S_p, S_{p-2}, T_p) normal MTs, where S_p is, as before, the B-spline subdivision operator of degree p. The family $\{T_p\}$ is the union of the $2p$-point interpolatory schemes T_{2p-1} of Deslauriers and Dubuc [26], and the odd counterpart T_{2p} of the dual $2p$-point schemes of Dyn et al. [33], that locally fits a Lagrange interpolation polynomial of degree $2p$ to the $2p+1$ points that are closest to the interval to be refined with $c_S = 1/4$. For example, $T_1 = S_1$, $T_3 = T$, and

$$(T_2x)_{2i} = \frac{1}{32}(-3x_{i-1} + 30x_i + 5x_{i+1}), \qquad (T_2x)_{2i+1} = \frac{1}{32}(5x_i + 30x_{i+1} - 3x_{i+2}), \qquad i \in \mathbb{Z}.$$

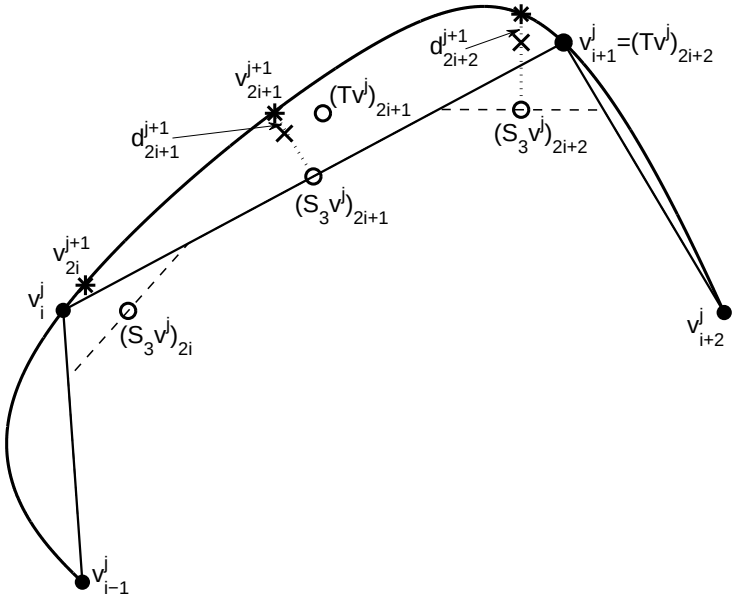

Fig. 5.4: One step of the (S_3, S_1, T) normal MT.

Further motivation for the choice of $\{T_p\}$ are the results in [35, Section 6]. The odd-indexed members of the family are interpolating schemes with $P_e(T_{2p-1}) = P(T_{2p-1}) = 2p$, while the even-indexed ones are approximating with $P_e(T_{2p}) = 2p + 1$. Therefore for the detail decay analysis, the family of (S_p, S_{p-2}, T_p) normal MTs seems the most appropriate, since with resect to the support size of their masks, S_p is the smoothest scheme, while T_p possesses the highest order of exact polynomial reproduction. On the other hand, this family can be viewed as an extension of the (S_1, S_0, T_1) normal MT, which is nothing else but the classical S_1 normal MT, and is the only example of a normal MT, where the detail decay rate $\mu = 2$ reaches the order of polynomial reproduction P (see [91] for proof). As in Section 5.1.1, our construction performs excellent for small values of p.

Theorem 5.2.1. *Let $\mathcal{C}$ be closed, non-self-intersecting, regular C^{p+1} curve, given by its arc-length parameterization $\mathbf{v}(s)$. Fix $p \in \{2, 3\}$. Let $\mathbf{v}^0 \in \mathcal{C}$ be such that the (S_p, S_{p-2}, T_p) normal MT is globally well-posed and convergent. Then*

$$\|d^j\| = \mathrm{O}(\|\Delta s^j\|^{p+1}) = \mathrm{O}(2^{-(p+1)j}) \quad j \to \infty.$$

Proof. Let, as before, $\mathbf{v}_k$, resp. s_k, $k \in I_i(T_p)$ be the coarse-scale data and $\bar{\mathbf{v}}_K$ be its refinement via one step of the (S_p, S_{p-2}, T_p) normal MT. Furthermore, let ξ_K be as in (4.2.11), and $(x(s), y(x(s)))$ be the local coordinates according to the frame $(\mathcal{T} = \mathbf{t}(\xi_K), \mathcal{N} = \mathbf{n}(\xi_K))$. From Theorem 5.1.3 we already have that

$$\|\Delta^n x^j\|_{I_i} = \|\Delta^n s^j\|_{I_i} = \mathrm{O}(\|\Delta s^j\|^n_{I_i}) = \mathrm{O}(2^{-nj}), \qquad 1 \le n \le p; \quad j \to \infty. \tag{5.2.2}$$

Applying Lemma 5.0.4 for the C^{p+1} function $y(x)$ and the scheme T_p, and using (5.2.2) we derive

$$|y((T_p x)_K) - (T_p y)_k| = C \left(\sum_{\nu \in E_p} \prod_{m=1}^{p} \|\Delta^m x\|_{I_i}^{\nu_m} + \|\Delta x\|_{I_i}^{p+1} \right) = \mathrm{O}(2^{-j(p+1)}), \tag{5.2.3}$$

where C depends only on $\mathcal{C}$ and T_p. Now, Lemma 4.2.2 implies

$$x_k = x_l + (k-l)\|\Delta x\|_{I_i} + r_{k,l}, \qquad |r_{k,l}| = \mathrm{O}(\|\Delta s\|_{I_i}^2), \qquad \forall k, l \in I_i,$$

which, since both S_p and T_p exactly reproduce linear polynomials, gives rise to

$$|(S_p x - T_p x)_K| = \mathrm{O}(\|\Delta s\|_{I_i}^2). \tag{5.2.4}$$

Following the same computational technique as in the proof of Theorem 5.1.3, it is not difficult to check that for both $p = 2, 3$, $|\bar{s}_K - \xi_K| = \mathrm{O}(\|\Delta s\|_{I_i}^2)$. The explicit estimation can be found in the appendix. Taylor expansion (5.0.1) implies

$$\begin{aligned} y((S_p x(s))_K) &= y(\bar{s}_K) = \frac{\alpha}{2}(\bar{s}_K - \xi_K)^2 + \cdots = \mathrm{O}(\|\Delta s\|_{I_i}^4); \\ y((T_p x(s))_K) &= y(\bar{s}_K + \mathrm{O}(\|\Delta s\|_{I_i}^2)) = \mathrm{O}(\|\Delta s\|_{I_i}^4), \end{aligned}$$

with $\alpha = \mathrm{k}'(\xi_K)$. Now, combining the last result with (5.2.3), we conclude

$$|d_K| = |y((S_p x)_K) - (T_p y)_k| \le |y((T_p x)_K) - (T_p y)_k| + |y((S_p x)_K) - y((T_p x)_K)| \le \mathrm{O}(\|\Delta s\|_{I_i}^{\min(p+1,4)}).$$

Since $\min(p+1, 4) = p+1$ for $p = 2, 3$, the proof is completed. More detailed and explicit computations as in the proof of Theorem 5.1.3 can be found in the appendix. □

A remarkable corollary of Theorem 5.1.3 and Theorem 5.2.1 is the case $p = 3$, which we will highlight in a separate theorem. Note that the (S_3, S_1, T) normal MT can be viewed as a particular generalization of the 4-point scheme T, a direction that has been actively explored for many years now. Moreover, this generalized 4-point normal MT performs in an optimal way with respect to both smoothness of the normal re-parameterization and high detail decay rates.

Theorem 5.2.2 (Optimal 4-point normal MT)**.** *Let $\mathcal{C}$ be closed, non-self-intersecting, regular C^4 curve, given by its arc-length parameterization $\mathbf{v}(s)$. Let $\mathbf{v}^0 \in \mathcal{C}$ be such that the (S_3, S_1) normal MT is globally well-posed and convergent. Let T be the four-point scheme (4.4.2). Then for the (S_3, S_1, T) normal MT the detail decay rate is 4, i.e.,*

$$\|d^j\| = \mathrm{O}(\|\Delta s^j\|^4) = \mathrm{O}(2^{-4j}), \qquad j \to \infty,$$

and the normal re-parameterization is $C^{2,1}$.

Some comments are in order. Since S_3 exactly reproduces only linear polynomials, we know from before that the (S_3, S_1) normal MT has detail decay rate two, i.e., $\|d^j\| = \mathrm{O}(2^{-2j})$, while, since T generates $C^{1,1}$ limits, the T normal MT has detail decay rate three up to a logarithmic factor, i.e., $\|d^j\| = \mathrm{O}(j2^{-3j})$ [24, Section 7.1.2]. Thus, their combined action improves by a whole

factor the order of the better one between them, if applied alone. Secondly, as already discussed in Section 4.4, finding and justifying an admissible sample $\mathbf{v}^0$ for the T normal MT is a complicated task on its own, while Proposition 5.1.2 implies that for the (S_3, S_1, T) normal MT we only need $\mathbf{v}^0$ to divide $\mathcal{C}$ into locally convex/concave regions - a criteria that is very easy to check in practice. The only drawback of the combined transform is that it remains approximating, and thus, twice as many details as for the T normal MT are stored. However, taking into account all the positive features of the (S_3, S_1, T) normal MT, the latter does not seem to be much of a problem. Last, but not least, there is strong numerical evidence that the above phenomena holds in 3D, as well. Indeed, in [87, Section 4] the (S_3, S_1, T) normal MT analogue for triangulated surfaces has been considered, where S_3 has been replaced by the Loop subdivision scheme, while T has been replaced by the Butterfly subdivision scheme. Performed on irregular data sample of the unit sphere, the combined Loop/Butterfly normal MT leads to detail decay rate of order four away from extraordinary vertices. The theoretical understanding of this empirical observation is still ahead.

Remark 5.2.3. *For $p > 3$, the detail decay rate of the (S_p, S_{p-2}, T_p) normal MT cannot be improved and remains 4.*

The claim follows from the proof of Theorem 5.2.1. Indeed, all the estimations there are asymptotical in their nature and provide not only sufficient but also necessary conditions for rapid detail decay. First of all, it is clear the summand $|y((S_p x)_K) - y((T_p x)_K)|$ in the $|d_K|$ estimation cannot be neglected and its order bounds the detail decay rate. Now, let us see whether we can make it smaller than $\mathrm{O}(\|\Delta s\|^4_{I_i})$. Equation (5.0.1) assures that, whenever the curvature $\alpha = \mathrm{k}(\xi_K) \neq 0$ we have

$$|y((S_p x)_K) - y((T_p x)_K)| = \mathrm{O}(|(S_p x - T_p x)_K|^2).$$

The order in the inequality

$$\|(S_p - T_p)u\| \leq C\|\Delta^2 u\|, \qquad u \in \ell_\infty(\mathbb{Z}),$$

cannot be improved, where for the latter we used that by construction $(S_p - T_p)q|_{\mathbb{Z}} = \mathbf{0}$ for all polynomials q of degree one, and the well known fact that in this case there exists another bounded linear operator D, such that $(S_p - T_p)u = D\Delta^2 u$ for all $u \in \ell_\infty(\mathbb{Z})$. Indeed, due to symmetry and since S_p reproduces quadratic polynomials whenever $p \geq 2$, it follows that for $q(x) = x^2$, $S_p(q|_{\mathbb{Z}}) = (q + a_p\mathbf{1})|_{2^{-1}\mathbb{Z}+c_S}$, where $a_p \neq 0$ depends only on p, while since T_p exactly reproduces quadratic polynomials, $T_p(q|_{\mathbb{Z}}) = q|_{2^{-1}\mathbb{Z}+c_S}$. Therefore

$$\|(S_p - T_p)q|_{\mathbb{Z}}\| = a_p \neq 0,$$

while all the higher order divided differences $\Delta^n q|_{\mathbb{Z}}$, $n > 2$ are zero. We ended up with (4.2.10), being the only place which potentially allows room for improvement. But from Remark 5.1.6 it follows that for every $p \geq 2$

$$\Delta^2 s^j = \Delta^2 S_p s^{j-1} + \Delta^2 \omega^j \quad \Longrightarrow \quad \|\Delta^2 s^j\| = 2^{-2}\|\Delta^2 s^{j-1}\| + \mathrm{O}(2^{-3j}) = \mathrm{O}(2^{-2j}\|\Delta^2 s^0\|),$$

so, unless form the very beginning we have $\|\Delta^2 s^0\| = 0$, the order in (4.2.10) cannot be improved.

The above heuristic arguments are confirmed experimentally by the results in Table 5.2. On the unit circle we consider two different irregular initial data samples $\mathbf{v}^0$ and $\hat{\mathbf{v}}^0$, such that the

Estimation of the detail decay order via computing $-\log_2(\|d^j\|)/j$ for each level j										
Normal MT	$j=1$	$j=2$	$j=3$	$j=4$	$j=5$	$j=6$	$j=7$	$j=8$	$j=9$	$j=10$
(S_3, S_1, T_3)	5.4040	4.7841	4.5647	4.4079	4.3217	4.2681	4.2313	4.2041	4.1831	4.1649
	2.0019	2.4977	2.8437	3.0704	3.2251	3.3354	3.4184	3.4830	3.5347	3.5770
(S_5, S_3, T_5)	5.2305	5.1804	4.9641	4.7860	4.6559	4.5629	4.4926	4.4379	4.3938	4.3502
	1.9547	3.0385	3.3760	3.5156	3.5967	3.6549	3.6982	3.7318	3.7586	3.7805
(S_7, S_5, T_7)	5.0745	5.1475	4.9214	4.7465	4.6244	4.5357	4.4689	4.4168	4.3747	4.3304
	1.8226	3.0567	3.3541	3.4896	3.5766	3.6375	3.6829	3.7182	3.7464	3.7694

Tab. 5.2: Numerical verification that the detail decay rate of a combined scheme cannot exceed 4. The unit circle has been considered and two sets of initial data - uniform samples of $\pi(x+x^2)$ with step size 0.01 (upper results) and 0.1 (lower results).

corresponding s^0 and $\hat{s}^0$ are just the projection of the quadratic polynomial $\pi(x+x^2)$ on the regular grids $10^{-2}\mathbb{Z}$ and $10^{-1}\mathbb{Z}$, respectively. Due to periodicity, $\mathbf{v}^0_{i+100} = \mathbf{v}^0_i$, and $\hat{\mathbf{v}}^0_{i+10} = \hat{\mathbf{v}}^0_i$, so we have 100 distinct points in $\mathbf{v}^0$ and 10 distinct points in $\hat{\mathbf{v}}^0$. The idea of sampling a quadratic polynomial is inspired by the theoretical arguments in Remark 5.2.3. For both the initial samples we perform 10 steps of the (S_p, S_{p-2}, T_p) normal MTs with $p = 3, 5, 7$, while for each step we store the quantity $-\log_2(\|d^j\|)/j$ that corresponds to the detail decay order μ. We consider only odd members of the family, because for them the schemes T_p are well known and we do not have to compute their masks. For each of the three transforms we observe the same phenomena. Applied on the denser sample $\mathbf{v}^0$, the values of the logarithm monotonically decrease, while applied on the coarser sample $\hat{\mathbf{v}}^0$, the values of the logarithm monotonically increase with each refinement. Both the sequences tend to 4, which for the (S_3, S_1, T_3) normal MT remains in line with Theorem 5.2.1.

5.3 Normal MT based on prediction via circle arcs

The only drawback of the (S_3, S_1, T) normal MT is that it is approximating and we have to store twice as many details. In this section we deal with interpolating transforms of the type (S_1, S_0, S_{NL}) and investigate if for a suitable choice of S_{NL} the detail decay rate can exceed two - the rate, obtained via the standard S_1 normal MT. Our main motivation to consider such transforms is the fact that, since

$$(S_1 x)_{2k+1} = (S_3 x)_{2k+1}, \qquad k \in \mathbb{Z},\ x \in \ell_\infty(\mathbb{Z}),$$

the action of S_1 coincides with the action of the smoother (but approximating) subdivision scheme S_3 at the odd entries. Hence, (5.1.4) holds for S_1, as well, meaning that the arc-length analogue $s^j = S_1 s^{j-1} + \omega^j$ of the S_1 normal MT satisfies

$$\|\omega^j\| = \mathrm{O}(\|\Delta s^{j-1}\|^4) = \mathrm{O}(2^{-4j}), \qquad j \to \infty,$$

whenever the initial curve $\mathcal{C} \in C^5$. Now, Lemma 5.1.4 suggests that the only obstacle for achieving smoother normal re-parameterizations for the S_1 normal MT is the low Hölder regularity of the prediction operator. As we will see from the following paragraphs, we can overcome the problem by using non-linear prediction operators S_{NL} for dealing with the normal components of the data in the

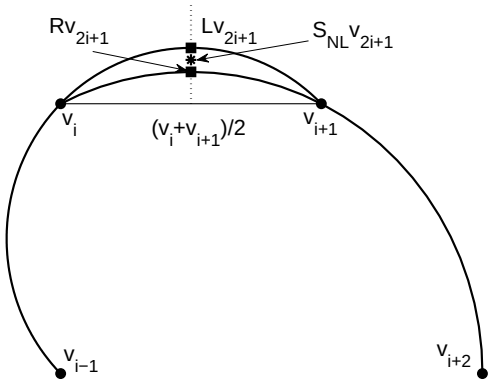

Fig. 5.5: Prediction via circle arcs, using the left circle L, the right circle R, and their average S_{NL}.

combined normal MT framework. Indeed, Section 5.2.1 implies that neither linear nor univariate S_{NL} can improve the detail decay rates of the (S_1, S_0, S_{NL}) normal MT, because in order to do so the predicted points should depend on the geometry of the coarse-scale data. Therefore, the restrictions on S_{NL} need to be relaxed. However, many of the known non-linear bivariate rules favor certain directions in $\mathbb{R}^2$, which makes them dependent on the underlying coordinate system, and thus bad candidates for prediction operators. Dyn *et. al.* proposed several geometrical subdivision schemes [37, 33, 81, 38] that are of interest for our setting. Here we choose to deal with circle preservation, and thus consider S_{NL} to be based on circle arcs.

Let a closed, non-self-intersecting, smooth planar curve $\mathcal{C}$ in $\mathbb{R}^2$ be given via its arc-length parametrization $\mathbf{v}(s) \in C^5$. We consider a normal MT based on the following procedure: for a given sample $\mathbf{v}^0 \in \mathcal{C}$, $j \in \mathbb{N}$, and $k \in \mathbb{Z}$, the normal vector $\hat{\mathbf{n}}^j_{2k+1}$ is orthogonal to the coarse edge $\Delta\mathbf{v}^{j-1}_k$, while the prediction point $(S_{NL}\mathbf{v})^{j-1}_{2k+1}$ is the intersection point of the circle, passing through $\mathbf{v}^{j-1}_{k-1}, \mathbf{v}^{j-1}_k, \mathbf{v}^{j-1}_{k+1}$ and the bisector of $\Delta\mathbf{v}^{j-1}_k$ (see Fig. 5.5). Obviously this is a (S_1, S_0, S_{NL}) normal MT. Note that, since by construction $(S_{NL}\mathbf{v}^{j-1})_{2k+1}$ lies on the normal line $L_{2k+1}(t) = (S_1\mathbf{v}^{j-1})_{2k+1} + t\hat{\mathbf{n}}^j_{2k+1}$ the transform coincides with the (S_{NL}, S_0) normal MT. However, writing it in the redundant form (S_1, S_0, S_{NL}) helps us to relate our analysis to Section 5.2.1, plus emphasizes on the fact that the questions regarding well-posedness, convergence and smoothness of the normal re-parameterization have already been answered in [91], when dealing with the S_1 normal MT. Working in local frames as in the previous sections, we will show that the detail decay rate of the above introduced combined scheme is already of order three.

From Theorem 4.2.3 we already know that $\Delta s^j = \mathrm{O}(2^{-j})$, and thus it suffices to consider only one step of the transform. Moreover, due to the locality of the procedure, we need to work only with the triplet $(\mathbf{v}_{-1}, \mathbf{v}_0, \mathbf{v}_1) = \big(\mathbf{v}(s_{-1}), \mathbf{v}(s_0), \mathbf{v}(s_1)\big)$. We consider the local frame $(\mathcal{T}, \mathcal{N})$, centered at $\mathbf{v}_0$, where $\mathbf{v}'(s_0) = \mathcal{T}$, and $\mathbf{v}''(s_0) = \mathrm{k}(s_0)\mathcal{N}$. To simplify the notation, we set $s_0 = 0$, $\alpha = \mathrm{k}(s_0)$, and $\beta = \mathrm{k}'(s_0)$, and, as before, derive (5.0.1).

Now, let the circle through $(\mathbf{v}_{-1}, \mathbf{v}_0, \mathbf{v}_1)$ be also given by its arc-length parametrization $\Gamma(t)$,

and analogously, $t_0 = 0$, and $\mu = \hat{\mathrm{k}}(t_0)$. (Note that, since it is a circle, $\hat{\mathrm{k}}(t) \equiv \mu$, and $\hat{\mathrm{k}}'(t) \equiv 0$!). For the circle case, the Taylor expansion (5.0.1) simplifies to

$$\Gamma(t) = \mathbf{v}_0 + \left(t - \frac{\mu^2}{6}t^3 + \mathrm{O}(t^5)\right)\hat{\mathcal{T}} + \left(\frac{\mu}{2}t^2 + \mathrm{O}(t^4)\right)\hat{\mathcal{N}} = \hat{x}(t)\hat{\mathcal{T}} + \hat{y}(t)\hat{\mathcal{N}}, \qquad \forall t << 1, \quad (5.3.1)$$

where $\Gamma'(0) = \hat{T}$ and $\Gamma''(0) = \mu\hat{N}$.

Hence, we can express the length of $\Delta\mathbf{v}_0$ in terms of both $\Delta s_0 = s_1$ and $\Delta t_0 = t_1$, and compare the corresponding summands in the two formulae:

$$\sqrt{\left(s_1 - \tfrac{\alpha^2}{6}s_1^3 - \tfrac{\alpha\beta}{8}s_1^4 + \mathrm{O}(s_1^5)\right)^2 + \left(\tfrac{\alpha}{2}s_1^2 + \tfrac{\beta}{6}s_1^3 + \mathrm{O}(s_1^4)\right)^2} = \sqrt{\left(t_1 - \tfrac{\mu^2}{6}t_1^3 + \mathrm{O}(t_1^5)\right)^2 + \left(\tfrac{\mu}{2}t_1^2 + \mathrm{O}(t_1^4)\right)^2}$$

$$\Leftrightarrow\ s_1^2 - \tfrac{\alpha^2}{12}s_1^4 - \tfrac{\alpha\beta}{12}s_1^5 + \mathrm{O}(s_1^6) = t_1^2 - \tfrac{\mu^2}{12}t_1^4 + \mathrm{O}(t_1^6)\ \Leftrightarrow\ \tfrac{\mu^2}{12}t_1^4 - t_1^2 + s_1^2 - \tfrac{\alpha^2}{12}s_1^4 - \tfrac{\alpha\beta}{12}s_1^5 + \mathrm{O}(s_1^6) = 0.$$

Note that for the last expression we used $\mathrm{O}(s_1) = \mathrm{O}(t_1)$ which follows from the Taylor expansions:

$$|\Delta\mathbf{v}_0| = s_1 + \mathrm{O}(s_1^2) = t_1 + \mathrm{O}(t_1^2).$$

Now, we have a biquadratic equation with respect to t_1, which we can solve. Again, since $t_1 \asymp s_1$, t_1^2 is the smaller root of the equation, i.e.

$$t_1^2 = \frac{6}{\mu^2}\left(1 - \sqrt{1 - \frac{\mu^2 s_1^2}{3}\left(1 - \frac{\alpha^2}{12}s_1^2 - \frac{\alpha\beta}{12}s_1^3 + \mathrm{O}(s_1^4)\right)}\right).$$

Since $\sqrt{1-x} = 1 - x/2 - x^2/8 + \mathrm{O}(x^3)$, we deduce

$$t_1^2 = \frac{6}{\mu^2}\left(\frac{\mu^2 s_1^2}{6}\left(1 - \frac{\alpha^2}{12}s_1^2 - \frac{\alpha\beta}{12}s_1^3\right) + \frac{\mu^4}{72}s_1^4 + \mathrm{O}(s_1^6)\right) = s_1^2\left(1 - \frac{\alpha^2 - \mu^2}{12}s_1^2 - \frac{\alpha\beta}{12}s_1^3 + \mathrm{O}(s_1^4)\right).$$

This leads to

$$t_1 = s_1\sqrt{1 - \frac{\alpha^2 - \mu^2}{12}s_1^2 - \frac{\alpha\beta}{12}s_1^3 + \mathrm{O}(s_1^4)} = s_1 - \frac{\alpha^2 - \mu^2}{24}s_1^3 - \frac{\alpha\beta}{24}s_1^4 + \mathrm{O}(s_1^5). \quad (5.3.2)$$

Note that, since we needed to divide by μ, we silently assumed that $\mu \neq 0$. However in (5.3.2) $\mu = 0$ is not a problem anymore, and by continuity we can extend the argument to all μ. By directly computing the case $\mu = 0$ one can easily check that the formula is indeed true. From (5.3.2) we see that t_1 is at least a third order perturbation of s_1. The next step is to show that it is actually a fourth order perturbation, since $\alpha - \mu = \mathrm{O}(s_1)$ itself. Denote by (κ_1, κ_2) the coordinates of the center of the circle $\Gamma(t)$ with respect to our local frame $(\mathcal{T}, \mathcal{N})$. Since $\mathbf{v}_0 = (0,0) \in \Gamma$, the circle is given by the formula

$$(x - \kappa_1)^2 + (y - \kappa_2)^2 = \mu^{-2}.$$

Thus,

$$\left|\begin{array}{l} x(s_1)\kappa_1 + y(s_1)\kappa_2 = (x^2(s_1) + y^2(s_1))/2 \\ x(s_{-1})\kappa_1 + y(s_{-1})\kappa_2 = (x^2(s_{-1}) + y^2(s_{-1}))/2 \end{array}\right. \quad \Longrightarrow \quad \left|\begin{array}{l} \kappa_1 = \frac{(x^2(s_1)+y^2(s_1))y(s_{-1}) - (x^2(s_{-1})+y^2(s_{-1}))y(s_1)}{2(x(s_1)y(s_{-1}) - x(s_{-1})y(s_1))} \\ \kappa_2 = \frac{(x^2(s_{-1})+y^2(s_{-1}))x(s_1) - (x^2(s_1)+y^2(s_1))x(s_{-1})}{2(x(s_1)y(s_{-1}) - x(s_{-1})y(s_1))} \end{array}\right. .$$

Let us start with the denominator. From Theorem 4.2.3 we already know that $s_1 = \Delta s_0 \asymp \Delta s_{-1} = -s_{-1}$ so

$$\begin{aligned} x(s_1)y(s_{-1}) - x(s_{-1})y(s_1) &= s_1 s_{-1}\left(\left(1-\frac{\alpha^2}{6}s_1^2\right)\left(\frac{\alpha}{2}s_{-1}+\frac{\beta}{6}s_{-1}^2\right) - \left(1-\frac{\alpha^2}{6}s_{-1}^2\right)\left(\frac{\alpha}{2}s_1+\frac{\beta}{6}s_1^2\right) + \mathrm{O}(s_1^3)\right) \\ &= s_1 s_{-1}(s_{-1}-s_1)\left(\frac{\alpha}{2}+\frac{\beta}{6}(s_1+s_{-1})+\mathrm{O}(s_1^2)\right). \end{aligned}$$

Note that $\mu = 0$ (i.e., the circle is a straight line) if and only if the denominator equals to zero. Since the S_1 normal MT is well-defined, $s_1 s_{-1}(s_{-1}-s_1) \neq 0$, and, thus in this case $\alpha = -\beta(s_1+s_{-1})/3 + \mathrm{O}(s_1^2)$, or in other words the difference $\mu - \alpha = \beta(s_1+s_{-1})/3 + \mathrm{O}(s_1^2)$ is indeed of order one.

From now on we assume that $\mu, \alpha \neq 0$, so the denominator is non-zero and all the algebraic operations are well-defined. Let us work out the corresponding numerators for κ_1 and κ_2.

$$\begin{aligned} &(x^2(s_1)+y^2(s_1))y(s_{-1}) - (x^2(s_{-1})+y^2(s_{-1}))y(s_1) \\ &= s_1^2 s_{-1}^2\Bigg(\left(\left(1-\tfrac{\alpha^2}{6}s_1^2\right)^2 + \left(\tfrac{\alpha}{2}s_1+\tfrac{\beta}{6}s_1^2\right)^2\right)\left(\tfrac{\alpha}{2}+\tfrac{\beta}{6}s_{-1}\right) \\ &\quad -\left(\left(1-\tfrac{\alpha^2}{6}s_{-1}^2\right)^2 + \left(\tfrac{\alpha}{2}s_{-1}+\tfrac{\beta}{6}s_{-1}^2\right)^2\right)\left(\tfrac{\alpha}{2}+\tfrac{\beta}{6}s_1\right) + \mathrm{O}(s_1^2)\Bigg) \\ &= s_1^2 s_{-1}^2(s_{-1}-s_1)\left(\tfrac{\beta}{6}+\mathrm{O}(s_1)\right); \end{aligned}$$

$$\begin{aligned} &(x^2(s_{-1})+y^2(s_{-1}))x(s_1) - (x^2(s_1)+y^2(s_1))x(s_{-1}) \\ &= \left(s_{-1}^2 - \tfrac{\alpha^2}{12}s_{-1}^4 + \mathrm{O}(s_{-1}^5)\right)\left(s_1 - \tfrac{\alpha}{6}s_1^3 + \mathrm{O}(s_1^4)\right) - \left(s_1^2 - \tfrac{\alpha^2}{12}s_1^4 + \mathrm{O}(s_1^5)\right)\left(s_{-1} - \tfrac{\alpha}{6}s_{-1}^3 + \mathrm{O}(s_{-1}^4)\right) \\ &= \left(s_1 s_{-1}^2 - \tfrac{\alpha^2}{12}s_1 s_{-1}^4 - \tfrac{\alpha^2}{6}s_1^3 s_{-1}^2 + \mathrm{O}(s_1^6)\right) - \left(s_1^2 s_{-1} - \tfrac{\alpha^2}{12}s_1^4 s_{-1} - \tfrac{\alpha^2}{6}s_1^2 s_{-1}^3 + \mathrm{O}(s_1^6)\right) \\ &= s_1 s_{-1}(s_{-1}-s_1)\left(1 - \tfrac{\alpha^2}{12}(s_1^2 - s_1 s_{-1} + s_{-1}^2) + \mathrm{O}(s_1^3)\right). \end{aligned}$$

Hence,

$$\begin{aligned} \kappa_1 &= \frac{s_1^2 s_{-1}^2(s_{-1}-s_1)\left(\frac{\beta}{6}+\mathrm{O}(s_1)\right)}{2s_1 s_{-1}(s_{-1}-s_1)\left(\frac{\alpha}{2}+\frac{\beta}{6}(s_1+s_{-1})+\mathrm{O}(s_1^2)\right)} = \frac{\beta}{6\alpha}s_1 s_{-1} + \mathrm{O}(s_1^3); \\ \kappa_2 &= \frac{s_1 s_{-1}(s_{-1}-s_1)\left(1-\frac{\alpha^2}{12}(s_1^2 - s_1 s_{-1} + s_{-1}^2) + \mathrm{O}(s_1^3)\right)}{2s_1 s_{-1}(s_{-1}-s_1)\left(\frac{\alpha}{2}+\frac{\beta}{6}(s_1+s_{-1})+\mathrm{O}(s_1^2)\right)} = \frac{1}{\alpha} - \frac{\beta}{3\alpha^2}(s_1+s_{-1}) + \mathrm{O}(s_1^2). \end{aligned}$$

Using again that $(0,0) \in \Gamma$ we estimate μ by the following

$$\kappa_1^2 + \kappa_2^2 = \frac{1}{\alpha^2} - \frac{2\beta}{3\alpha^3}(s_1+s_{-1}) + \mathrm{O}(s_1^2) \quad \Longrightarrow \quad \mu = \frac{1}{\sqrt{\kappa_1^2+\kappa_2^2}} = \alpha - \frac{\beta}{3}(s_1+s_{-1}) + \mathrm{O}(s_1^2).$$

Therefore

$$\mu - \alpha = \frac{\beta}{3}(s_1+s_{-1}) + \mathrm{O}(s_1^2). \tag{5.3.3}$$

Again, due to continuity (5.3.3) remains valid for $\alpha = 0$, as well. Our prediction point is exactly $\Gamma(t_1/2)$ and the newly inserted point is $\mathbf{v}(\bar{s}_1)$, so the detail is

$$d = |\mathbf{v}(\bar{s}_1) - \Gamma(t_1/2)| \leq |\mathbf{v}(\bar{s}_1) - \mathbf{v}(s_1/2)| + |\mathbf{v}(s_1/2) - \Gamma(t_1/2)|.$$

From (5.1.4) we already know that $|\bar{s_1} - s_1/2| = \mathrm{O}(s_1^4)$, so we further estimate only the second term.

$$\begin{aligned} |\mathbf{v}(s_1/2) - \Gamma(t_1/2)| &= |x(s_1/2)\mathcal{T} + y(s_1/2)\mathcal{N} - \hat{x}(t_1/2)\hat{\mathcal{T}} - \hat{y}(t_1/2)\hat{\mathcal{N}}| \\ \leq \sqrt{(x(s_1/2) - \hat{x}(t_1/2))^2 + (y(s_1/2) - \hat{y}(t_1/2))^2} &+ |\hat{x}(t_1/2)||\mathcal{T} - \hat{\mathcal{T}}| + |\hat{y}(t_1/2)||\mathcal{N} - \hat{\mathcal{N}}| \\ = \sqrt{(x(s_1/2) - \hat{x}(t_1/2))^2 + (y(s_1/2) - \hat{y}(t_1/2))^2} &+ \big(|\hat{x}(t_1/2)| + |\hat{y}(t_1/2)|\big)|\mathcal{T} - \hat{\mathcal{T}}|. \end{aligned}$$

We used that $\mathcal{T}$ and $\mathcal{N}$, resp. $\hat{\mathcal{T}}$ and $\hat{\mathcal{N}}$, are orthogonal unit vectors. Let us first estimate $|\mathcal{T} - \hat{\mathcal{T}}|$. Equations (5.3.2) and (5.3.3) give rise to

$$\begin{aligned} \hat{x}(t_1) &= t_1 - \frac{\mu^2}{6}t_1^3 + \mathrm{O}(t_1^5) = s_1 - \frac{\mu^2}{6}s_1^3 + \mathrm{O}(s_1^4) = s_1 - \frac{\alpha^2}{6}s_1^3 + \mathrm{O}(s_1^4) = x(s_1) + \mathrm{O}(s_1^4); \\ \hat{y}(t_1) &= \frac{\mu}{2}t_1^2 + \mathrm{O}(t_1^4) = \frac{\mu}{2}s_1^2 + \mathrm{O}(s_1^4) = \frac{\alpha}{2}s_1^2 + \mathrm{O}(s_1^3) = y(s_1) + \mathrm{O}(s_1^3). \end{aligned}$$

Hence

$$\begin{aligned} x(s_1)\mathcal{T} + y(s_1)\mathcal{N} = \hat{x}(t_1)\hat{\mathcal{T}} + \hat{y}(t_1)\hat{\mathcal{N}} \quad &\Longrightarrow \quad x(s_1)(\mathcal{T} - \hat{\mathcal{T}}) + y(s_1)(\mathcal{N} - \hat{\mathcal{N}}) = \mathrm{O}(s_1^3) \\ &\Longrightarrow \quad \left| \begin{array}{l} s_1\varepsilon_1 - (\alpha/2)s_1^2\varepsilon_2 = \mathrm{O}(s_1^3) \\ s_1\varepsilon_2 + (\alpha/2)s_1^2\varepsilon_1 = \mathrm{O}(s_1^3) \end{array} \right. , \end{aligned}$$

where $\mathcal{T} - \hat{\mathcal{T}} = (\varepsilon_1, \varepsilon_2)^T$, and, thus $\mathcal{N} - \hat{\mathcal{N}} = (-\varepsilon_2, \varepsilon_1)^T$. From the second equation we see that $\varepsilon_2 = \mathrm{O}(s_1)$ and plugging this into the first one, we conclude that $\varepsilon_1 = \mathrm{O}(s_1^2)$. Now, using the latter in the second equation, we derive that $\varepsilon_2 = \mathrm{O}(s_1^2)$, too. Therefore, $|\mathcal{T} - \hat{\mathcal{T}}| = \mathrm{O}(s_1^2)$.

For the other term in the expression we have the following:

$$\begin{aligned} x(s_1/2) &= \frac{1}{2}s_1 - \frac{\alpha^2}{48}s_1^3 + \mathrm{O}(s_1^4); \qquad\qquad y(s_1/2) = \frac{\alpha}{8}s_1^2 + \frac{\beta}{48}s_1^3 + \mathrm{O}(s_1^4); \\ \hat{x}(t_1/2) &= \frac{1}{2}t_1 - \frac{\mu^2}{48}t_1^3 + \mathrm{O}(t_1^5) = \frac{1}{2}s_1 - \frac{\alpha^2}{48}s_1^3 + \mathrm{O}(s_1^4); \quad \hat{y}(t_1/2) = \frac{\mu}{8}t_1^2 + \mathrm{O}(t_1^4) = \frac{\mu}{8}s_1^2 + \mathrm{O}(s_1^4). \\ &\Rightarrow \quad \sqrt{(x(s_1/2) - \hat{x}(t_1/2))^2 + (y(s_1/2) - \hat{y}(t_1/2))^2} = \left|\frac{\beta}{48}s_1^3 - \frac{\beta}{24}s_1^2(s_1 + s_{-1})\right| + \mathrm{O}(s_1^4) = \mathrm{O}(s_1^3). \end{aligned}$$

Thus, $|\mathbf{v}(s_1/2) - \Gamma(t_1/2)| = \mathrm{O}(s_1^3)$, and the third order detail decay rate has been established.

In order to derive the leading term of the last expression, a little more detailed computations are needed. Let $\Delta^2 s_{-1} = s_1 + s_{-1} = r s_1 = r\Delta s_0$. Since $s_{-1} < 0$, we have that $r < 1$. Moreover, (5.1.4) tells us that in most of the cases $r = \mathrm{O}(s_1^4)$. Now, (5.3.3) gives rise to

$$\hat{x}(t_1) = x(s_1) + \mathrm{O}(s_1^4); \qquad \hat{y}(t_1) = \frac{\alpha}{2}s_1^2 + \frac{\beta}{6}r s_1^3 + \mathrm{O}(s_1^4);$$

Let us denote $\hat{\mathcal{T}} = (e_1, e_2)^T$. Then $\hat{\mathcal{N}} = (-e_2, e_1)^T$ and

$$x(s_1)\mathcal{T} + y(s_1)\mathcal{N} = \hat{x}(t_1)\hat{\mathcal{T}} + \hat{y}(t_1)\hat{\mathcal{N}} \quad \Longrightarrow \quad \left| \begin{array}{l} x(s_1) = \hat{x}(t_1)e_1 - \hat{y}(t_1)e_2 \\ y(s_1) = \hat{x}(t_1)e_2 + \hat{y}(t_1)e_1 \end{array} \right.$$

$$\Longrightarrow \quad \left| \begin{array}{l} s_1 - \frac{\alpha^2}{6}s_1^3 + \mathrm{O}(s_1^4) = \left(s_1 - \frac{\alpha^2}{6}s_1^3 + \mathrm{O}(s_1^4)\right) e_1 - \left(\frac{\alpha}{2}s_1^2 + \frac{\beta}{6}rs_1^3 + \mathrm{O}(s_1^4)\right) e_2 \\ \frac{\alpha}{2}s_1^2 + \frac{\beta}{6}s_1^3 + \mathrm{O}(s_1^4) = \left(s_1 - \frac{\alpha^2}{6}s_1^3 + \mathrm{O}(s_1^4)\right) e_2 + \left(\frac{\alpha}{2}s_1^2 + \frac{\beta}{6}rs_1^3 + \mathrm{O}(s_1^4)\right) e_1 \end{array} \right.$$

$$\Longrightarrow \quad \left| \begin{array}{l} e_1 = 1 + \mathrm{O}(s_1^3) \\ e_2 = \frac{\beta}{6}(1-r)s_1^2 + \mathrm{O}(s_1^3) \end{array} \right. ,$$

where for the last result we compared the corresponding coefficients in front of the same powers of s_1. Hence, in the local frame $(\mathcal{T}, \mathcal{N})$

$$\mathbf{v}(s_1/2) - \Gamma(t_1/2) = \Big(x(s_1/2) - \hat{x}(t_1/2)e_1 + \hat{y}(t_1/2)e_2 \ , \ y(s_1/2) - \hat{x}(t_1/2)e_2 - \hat{y}(t_1/2)e_1\Big)^T.$$

From the above computations we immediately see that the $\mathcal{T}$ component of the vector is $\mathrm{O}(s_1^4)$, while the $\mathcal{N}$ component is $\mathrm{O}(s_1^3)$, and thus

$$\begin{aligned} |\mathbf{v}(s_1/2) - \Gamma(t_1/2)| &= |y(s_1/2) - \hat{x}(t_1/2)e_2 - \hat{y}(t_1/2)e_1| + \mathrm{O}(s_1^4) \\ &= \left| \tfrac{\alpha}{8}s_1^2 + \tfrac{\beta}{48}s_1^3 - \left(\tfrac{1}{2}s_1 - \tfrac{\alpha^2}{48}s_1^3\right)\left(\tfrac{\beta}{6}(1-r)s_1^2 + \mathrm{O}(s_1^3)\right) - \left(\tfrac{\alpha}{8}s_1^2 + \tfrac{\beta}{24}rs_1^3\right)(1 + \mathrm{O}(s_1^3))\right| + \mathrm{O}(s_1^4) \\ &= \tfrac{|(2r-3)\beta|}{48}s_1^3 + \mathrm{O}(s_1^4). \end{aligned}$$

To summarize, so far we proved that for any initial curve $\mathcal{C}$ given by its arc-length parametrization $\mathbf{v}(s) \in C^5$ and any three points $\mathbf{v}_{-1} = \mathbf{v}(s_{-1})$, $\mathbf{v}_0 = \mathbf{v}(s_0)$, and $\mathbf{v}_1 = \mathbf{v}(s_1)$ on it, such that

$$c\Delta s_0 \le \Delta s_{-1} \le C\Delta s_0; \qquad \text{and} \qquad \Delta s_0 << 1$$

holds with uniform constants $0 < c \le C < \infty$, independent of $\|\Delta s\|$, the detail vector between the circle midpoint prediction $(S_{NL}\mathbf{v})_1$ and the actual inserted point $\bar{\mathbf{v}}_1 = \mathbf{v}(\bar{s}_1)$ for the (S_1, S_0, S_{NL}) normal MT is of the form

$$d_1 = \bar{\mathbf{v}}_1 - (S_{NL}\mathbf{v})_1 = \left(\ \mathrm{O}((\Delta s_0)^4), \ \ \tfrac{(-1-2\Delta s_{-1}/\Delta s_0)\mathrm{k}'(s_0)}{48}(\Delta s_0)^3 + \mathrm{O}((\Delta s_0)^4) \ \right) \begin{pmatrix} \mathcal{T} \\ \mathcal{N} \end{pmatrix},$$

where $\mathcal{T}, \mathcal{N}$ is the unit tangent, unit normal vector, respectively, to the initial curve $\mathcal{C}$ at $\mathbf{v}_0$. The result shows that in general, if we use any "admissible" circle interpolation as prediction operator, the detail d_1 should be of order $\mathrm{O}(\|\Delta s\|^3)$, or in particular $\|d^j\| = \mathrm{O}(2^{-3j})$ at any level $j \in \mathbb{N}$.

Further, we want to see if we can gain an extra order of detail decay when using a linear combination of two circles as prediction operator instead of only a single one. In particular, we will investigate the rule, proposed by Dyn in [41], namely the average of $\mathcal{L}\mathbf{v}$ and $\mathcal{R}\mathbf{v}$, where in the first case we interpolate via the "left" circle through $\mathbf{v}_{-1}, \mathbf{v}_0, \mathbf{v}_1$, while in the second case we interpolate via the "right" circle through $\mathbf{v}_0, \mathbf{v}_1, \mathbf{v}_2$ (see Fig. 5.5). Note that the corresponding formulae for $\mathcal{R}\mathbf{v}$

can be obtained from the already derived ones for the $\mathcal{L}\mathbf{v}$ via simply replacing s_{-1} with $-(\Delta s_0+\Delta s_1)$ whenever it appears. Direct computation gives rise to

$$\begin{aligned}\bar{\mathbf{v}}_1-\frac{(\mathcal{L}\mathbf{v})_1+(\mathcal{R}\mathbf{v})_1}{2} &= \left(\begin{array}{cc}\mathrm{O}((\Delta s_0)^4), & \frac{(\Delta s_1-\Delta s_{-1})\mathrm{k}'(s_0)}{48}(\Delta s_0)^2+\mathrm{O}((\Delta s_0)^4)\end{array}\right)\begin{pmatrix}\mathcal{T}\\ \mathcal{N}\end{pmatrix}\\ \Longrightarrow \quad |d_1| &= \frac{|\mathrm{k}'(s_0)|}{48}(\Delta s_0)^2|\Delta s_1-\Delta s_{-1}|+\mathrm{O}((\Delta s_0)^4).\end{aligned}$$

Some comments are in order: First of all, the last formula is fully in line with the observation that if the curve is symmetric with respect to the midpoint $\mathbf{v}(s_0+\Delta s_0/2)$ then all the considered functions are even in the local frame centered at that point, and thus the detail decay order should be even, as well. Indeed, in this case we have $\Delta s_{-1}=\Delta s_1$ and the cubic term in the detail decay estimation vanishes. Second of all, (5.1.4) indicates that for big enough J, $(\Delta^2 s^J)_{2i}=\mathrm{O}((\Delta s^J)^4)$. This leads to $|\Delta s^j_{i+1}-\Delta s^j_{i-1}|=\mathrm{O}((\Delta s^j)^4)$ for $j>J$ and almost all $i\in\mathbb{Z}$, and, thus, for most of the details the decay rate is indeed 4. However, the prediction operator is interpolatory, so around coarse-scale vertices the above estimation fail (unless we start with close-to-uniform and dense enough initial data) guaranteeing only $|\Delta s^j_{i+1}-\Delta s^j_{i-1}|=\mathrm{O}((\Delta s^j)^1)$ in general. Therefore, $|d^j|_\infty=\mathrm{O}(2^{-3j})$, even though for other ℓ_p norms the decay might be faster.

Our computations show that in order to assure a forth order detail decay for the same choice of the normals, a data-dependent adaptive prediction rule is needed. Direct calculation gives rise to the following "adjustment" that will work:

$$\begin{aligned}(S_{NL}\mathbf{v})_{2i+1} &= x(\mathcal{L}\mathbf{v})_{2i+1}+(1-x)(\mathcal{R}\mathbf{v})_{2i+1}\\ &= \left(x(-1-2\tfrac{\Delta s_{i-1}}{\Delta s_i})+(1-x)(1+2\tfrac{\Delta s_{i+1}}{\Delta s_i})\right)\tfrac{\mathrm{k}'(s_i)(\Delta s_i)^3}{48}\mathcal{N}+\mathrm{O}((\Delta s)^4);\\ x(-1-2\tfrac{\Delta s_{i-1}}{\Delta s_i})+(1-x)(1+2\tfrac{\Delta s_{i+1}}{\Delta s_i})=\mathrm{O}(\Delta s) \quad &\Leftrightarrow \quad x=\tfrac{1}{2}+\tfrac{\Delta s_{i+1}-\Delta s_{i-1}}{2(s_{i+2}-s_{i-1})}+\mathrm{O}(\Delta s).\end{aligned}$$

Knowing only the discrete data $\mathbf{v}^j$ doesn't allow us to build prediction rules based on the arc-length parameter s of the planar curve, but since (for small enough s) we already showed that $|\Delta\mathbf{v}|=\Delta s+\mathrm{O}((\Delta s)^2)$ we can use it and switch from arc-length to edge-length quantities that are directly computable from the data. For example,

$$\Delta s_{i+1}-\Delta s_{i-1}=s_{i+2}-s_{i+1}-s_i+s_{i-1}=\left(s_{i+2}-\frac{s_{i+1}+s_i}{2}\right)-\left(\frac{s_{i+1}+s_i}{2}-s_{i-1}\right),$$

and, thus the S_{NL} normal MT given by

$$\begin{aligned}(S_{NL}\mathbf{v})_{2i+1}=&\left(\frac{1}{2}+\frac{|\mathbf{v}_{i+2}-(\mathbf{v}_{i+1}+\mathbf{v}_i)/2|-|(\mathbf{v}_{i+1}+\mathbf{v}_i)/2-\mathbf{v}_{i-1}|}{2|\mathbf{v}_{i+2}-\mathbf{v}_{i-1}|}\right)(\mathcal{L}\mathbf{v})_{2i+1}+\\ &+\left(\frac{1}{2}-\frac{|\mathbf{v}_{i+2}-(\mathbf{v}_{i+1}+\mathbf{v}_i)/2|-|(\mathbf{v}_{i+1}+\mathbf{v}_i)/2-\mathbf{v}_{i-1}|}{2|\mathbf{v}_{i+2}-\mathbf{v}_{i-1}|}\right)(\mathcal{R}\mathbf{v})_{2i+1}\end{aligned}$$

has already detail decay of order 4. Note that, since S_1 normal MT has detail decay of order two, we know that any point q on the bisector of $\Delta\mathbf{v}^j_i$, between its midpoint and the inserted point $\mathbf{v}^{j+1}_{2i+1}$

has the property $|(\mathbf{v}_{i+1}+\mathbf{v}_i)/2-q| = \mathrm{O}((\Delta s^j)^2)$, so we can use the more general prediction operator

$$(S_{NL}\mathbf{v})_{2i+1} = \left(\frac{1}{2} + \frac{|\mathbf{v}_{i+2}-q| - |q-\mathbf{v}_{i-1}|}{2|\mathbf{v}_{i+2}-\mathbf{v}_{i-1}|}\right)(\mathcal{L}\mathbf{v})_{2i+1} + \left(\frac{1}{2} - \frac{|\mathbf{v}_{i+2}-q| - |q-\mathbf{v}_{i-1}|}{2|\mathbf{v}_{i+2}-\mathbf{v}_{i-1}|}\right)(\mathcal{R}\mathbf{v})_{2i+1}. \tag{5.3.4}$$

So far we considered S_{NL} to be a convex combination of the two prediction candidates $\mathcal{L}$ and $\mathcal{R}$, so that our rule reproduces constants. However, if we forget about that we can simplify the above formula and derive an analog of the famous Neville's algorithm. More precisely, since

$$(2\Delta s_{i+1} + \Delta s_i)\left(-1 - 2\frac{\Delta s_{i-1}}{\Delta s_i}\right) + (2\Delta s_{i-1} + \Delta s_i)\left(1 + 2\frac{\Delta s_{i+1}}{\Delta s_i}\right) = 0,$$

following the above strategy we have that the normal MT based on S_{NL}

$$(S_{NL}\mathbf{v})_{2i+1} = \frac{|\mathbf{v}_{i+2}-q|}{|\mathbf{v}_{i+2}-\mathbf{v}_{i-1}|}(\mathcal{L}\mathbf{v})_{2i+1} + \frac{|q-\mathbf{v}_{i-1}|}{|\mathbf{v}_{i+2}-\mathbf{v}_{i-1}|}(\mathcal{R}\mathbf{v})_{2i+1} \tag{5.3.5}$$

has detail decay rate four. The most natural choice for q is the midpoint of the coarse-scale edge $\Delta\mathbf{v}_i$, but for certain applications other candidates may be preferred, so we decide to leave (5.3.5) written in its general form. To summarize, we proved the following

Theorem 5.3.1. *Let $\mathcal{C}$ be a closed, non-self-intersecting, regular C^5 curve, and $\mathbf{v}^0 \in \mathcal{C}$ consists of at least four different points. For any scheme S_{NL} that is an affine linear combination of circle-preserving prediction rules, the (S_1, S_0, S_{NL}) normal MT has detail decay rate three. Furthermore, if S_{NL} is given via (5.3.4) or (5.3.5), the (S_1, S_0, S_{NL}) normal MT has detail decay rate four.*

There are other interesting options for the S_{NL} operator that might be worth investigating. Numerical experiments with the centripetal and chordal subdivision schemes [33] indicate that the detail decay rate there may again be three.

6. CONCLUSIONS AND FUTURE WORK

In conclusion, through the lines of this thesis we developed a general stability analysis of both univariate schemes and their associated multi-scale transforms in the nonlinear functional setting. We showed that, unlike the linear setting, convergence and stability analysis were no longer equivalent, and we derived efficient numerical criteria for the verification of each of them. We extended the univariate convergence and stability results to the multivariate regular setting via local approximation techniques.

We established a general theory for normal multi-scale transforms for curves, based on approximating prediction operators. We proposed a globally-convergent normal MT, and built an adaptive algorithm based on it that defined a well-posed transform with smooth limits and high detail decay rates. We investigated several extensions of the classical setup for normal MTs, namely we used another subdivision operator to generate the normal directions, the combined action of two different subdivision operators for the prediction step, and nonlinear geometry-based predictors, respectively, and showed that the properties of the normal MTs improved when such extensions were considered.

Apart from the many answers, our work gave rise to plenty of questions, as well. Some of them, such as completion of the univariate Power-p stability analysis, extension of our general stability theory to the normal MT case, determination of the exact limitations of the smoothness improvements of the (S_p, S_{p-2}) normal MT as $p \to \infty$, and investigation of other geometric predictors that lead to normal MTs with high detail decay rates, are very concrete and need mostly computational efforts. Others, such as how to extend the regular multivariate analysis via local maps in order to cover the high-order smoothness analysis on semi-regular grids, how to further optimize the properties of the normal MT if possible, how to extend the normal MT analysis from the curve setting to the surface one, and how to adapt the normal MTs framework so that it covers a broader range of applications, e.g., fast interface tracking, are more abstract and need development of new tools and introduction of fresh ideas.

BIBLIOGRAPHY

[1] W. Van Aerschot, M. Jansen, and A. Bultheel. Normal mesh based geometrical image compression. *Image and Vision Computing*, 27(4):459–468, 2009.

[2] S. Amat, F. Aràndiga, A. Cohen, and R. Donat. Tensor product multiresolution analysis with error control for compact image representation. *Signal Processing*, 82:587–608, 2002.

[3] S. Amat, F. Arandiga, A. Cohen, R. Donat, G. Garcia, and M. von Oehsen. Data compression with ENO schemes: A case study. *Appl. Comput. Harmon. Anal.*, 11(16):273–288, 2001.

[4] S. Amat, K. Dadourian, and J. Liandrat. Analysis of a class of nonlinear subdivision schemes and associated multiresolution transforms. *Adv. Comput. Math.*, 34(3):253–277, 2010.

[5] S. Amat, K. Dadourian, and J. Liandrat. On a nonlinear subdivision scheme avoiding Gibbs oscillations and converging towards C^s functions with $s > 1$. *Mathematics of Computation*, 80:959–971, 2011.

[6] S. Amat, K. Dadourian, J. Liandrat, J. Ruiz, and J. C. Trillo. A family of stable nonlinear nonseparable multiresolution schemes in 2D. *J. Comput. Appl. Math.*, 234:1277–1290, 2010.

[7] S. Amat, R. Donat, J. Liandrat, and J. C. Trillo. Analysis of a new nonlinear subdivision scheme. Applications in image processing. *Found. Comput. Math.*, 6:193–225, 2006.

[8] S. Amat and J. Liandrat. On the stability of the PPH nonlinear multiresolution. *Appl. Comput. Harmon. Anal.*, 18:198–206, 2005.

[9] N. Aspert, T. Ebrahimi, and P. Vandergheynst. Non-linear subdivision using local spherical coordinates. *Comput. Aided Geom. Des.*, 20(3):165–187, 2003.

[10] U. H. Augsdörfer, N. A. Dodgson, and M. A. Sabin. Variations on the four-point subdivision scheme. *Comput. Aided Geom. Design*, 27:78–95, 2010.

[11] C. Beccari, G. Casciola, and L. Romani. A non-stationary uniform tension controlled interpolating 4-point scheme reproducing conics. *Comp. Aided Geom. Design*, 24(1):1–9, 2007.

[12] P. Binev, W. Dahmen, R.A. DeVore, and N. Dyn. Adaptive approximation of curves. In *Approximation Theory*, pages 43–57. Acad. Publ. House, Sofia, 2004.

[13] C. Cabrelli, C. Heil, and U. Molter. *Self-similarity and multiwavelets in higher dimensions*, volume 170. Mem. Amer. Math. Soc., 2004.

[14] E. J. Candes and D. L. Donoho. New tight frames of curvelets and optimal representations of objects with piecewise C^2 singularities. *Comm. Pure Appl. Math.*, 57(2):219–266, 2002.

[15] A. S. Cavaretta, W. Dahmen, and C. A. Micchelli. *Stationary Subdivision*, volume 93. Mem. Amer. Math. Soc., 1991.

[16] G.M. Chaikin. An algorithm for high speed curve generation. *Computer Graphics and Image Processing*, 3:346–349, 1974.

[17] M. Charina. Vector multivariate subdivision schemes: Comparison of spectral methods for their regularity analysis. *Appl. Comput. Harmon. Anal.*, 2011.

[18] M. Charina, C. Conti, and T. Sauer. L_p-convergence of subdivision schemes: joint spectral radius versus restricted spectral radius. In C.K. Chui, M. Neamtu, and L. Schumaker, editors, *Approximation Theory XI: Gatlinburg 2004*, pages 101–122. Nashboro Press, Brentwood, TN, 2005.

[19] R. Claypoole, G. Davis, W. Sweldens, and R. Baraniuk. Nonlinear wavelet transform for image coding. In *Proceedings of the 31st Asilomar Conference on Signals, Systems, and Computers, Volume 1*, pages 662–667, 1997.

[20] R. Claypoole, R. Davis, W. Sweldens, and R. Baraniuk. Nonlinear wavelet transforms for image coding via lifting. *IEEE Transactions on Image Processing*, 12:1449–1459, 2003.

[21] A. Cohen, N. Dyn, and B. Matei. Quasilinear subdivision schemes with applications to ENO interpolation. *Appl. Comput. Harmon. Anal.*, 15:89–116, 2003.

[22] K. Dadourian and J. Liandrat. Analysis of some bivariate non-linear interpolatory subdivision schemes. *Numer. Algorithms*, 48(1-3):261–278, 2008.

[23] I. Daubechies, I. Guskov, and W. Sweldens. Regularity of irregular subdivision. *Constr. Approx.*, 15(3):381–426, 1999.

[24] I. Daubechies, O. Runborg, and W. Sweldens. Normal multiresolution approximation of curves. *Constr. Approx.*, 20:399–463, 2004.

[25] S. Dekel and D. Leviatan. Adaptive multivariate approximation using binary space partitions and geometric wavelets. *SIAM J. Numer. Anal.*, 43(2):707–732, 2005.

[26] G. Deslauriers and S. Dubuc. Symmetric iterative interpolation processes. *Constr. Approx.*, 5(1):1–46, 1989.

[27] R. A. DeVore. Nonlinear approximation. *Acta Numer.*, 7:51–150, 1998.

[28] M. N. Do and M. Vetterli. The contourlet transform: An efficient directional multiresolution image representation. *IEEE Transaction on Image Processing*, 14(12):2091–2106, 2005.

[29] D. L. Donoho. Wedgelets: nearly-minimax estimation of edges. *Ann. Statist*, 27(3):859–897, 1999.

[30] D. L. Donoho and T.P.-Y. Yu. Nonlinear pyramid transforms based on median-interpolation. *SIAM J. Math. Anal.*, 31(5):1030–1061, 2000.

[31] N. Dyn. Subdivision schemes in CAGD. In W. A. Light, editor, *Adv. Numer. Anal.*, volume II, pages 36–104. Oxford University Press, 1992.

[32] N. Dyn, M. Floater, and K. Hormann. Four-point curve subdivision based on iterated chordal and centripetal parameterizations. *Comput. Aided Geom. Des.*, 26:279–286, 2009.

[33] N. Dyn, M. S. Floater, and K. Hormann. A C^2 four-point subdivision scheme with fourth order accuracy and its extensions. In M. Dæhlen, K. Mørken, and L. L. Schumaker, editors, *Mathematical Methods for Curves and Surfaces: Tromsø 2004*, pages 145–156. Nashboro Press, Brentwood, TN, 2005.

[34] N. Dyn and R. Goldman. Convergence and smoothness of nonlinear Lane-Riesenfeld algorithms in the functional setting. *Found. Comput. Math.*, 11(1):79–94, 2011.

[35] N. Dyn, K. Hormann, M. A. Sabin, and Z. Shen. Polynomial reproduction by symmetric subdivision schemes. *J. Approx. Theory*, 155(1):28–42, 2008.

[36] N. Dyn and D. Levin. Analysis of asymptotically equivalent binary subdivision schemes. *J. Math. Anal. Appl.*, 193:594–621, 1995.

[37] N. Dyn and D. Levin. Subdivision schemes in geometric modelling. *Acta Numer.*, 11:73–7144, 2002.

[38] N. Dyn, D. Levin, and J. A. Gregory. A four-point interpolatory subdivision scheme for curve design. *Comput. Aided Geom. Design*, 4:257–268, 1987.

[39] N. Dyn, D. Levin, and J.A. Gregory. A butterfly subdivision scheme for surface interpolation with tension control. *ACM Trans. Graph.*, 9(2):160–169, 1990.

[40] N. Dyn, D. Levin, and D. Liu. Interpolatory convexity-preserving subdivision schemes for curves and surfaces. *Comput. Aided Design*, 24(4):211–216, 1992.

[41] N. Dyn and P. Oswald. Univariate subdivision and multiscale transforms: The nonlinear case. In R. A. DeVore and A. Kunoth, editors, *Multiscale, Nonlinear, and Adaptive Approximation*, pages 203–247. Springer, 2009.

[42] M.S. Floater and C.A. Micchelli. Nonlinear stationary subdivision. In N. K. Govil, R. N. Mohapatra, Z. Nashed, A. Sharma, and J. Szabados, editors, *Approximation Theory: in Memory of A. K. Varma*, pages 209–224. Marcel Dekker, New York, 1998.

[43] I. Friedel, A. Khodakovsky, and P. Schröder. Variational normal meshes. *ACM Trans. Graph.*, 23(4):1061–1073, 2004.

[44] C. Gérot, B. Matei, and S. Meignen. A new formalism for nonlinear and non-separable multiscale representation.

[45] J. Goutsias and H.J.A.M. Heijmans. Nonlinear multiresolution signal decomposition schemes - Part I: Morphological pyramids. *IEEE*, 9(11):1862–1876, 2000.

[46] J. Goutsias and H.J.A.M. Heijmans. Nonlinear multiresolution signal decomposition schemes - Part II: Morphological wavelets. *IEEE*, 9(11):1897–1913, 2000.

[47] P. Grohs. Smoothness analysis of subdivision schemes on regular grids by proximity. *SIAM J. Numer. Anal.*, (46):2169–2182, 2008.

[48] P. Grohs. Smoothness equivalence properties of univariate subdivision schemes and their projection analogues. *Numer. Math.*, 113(2):163–180, 2009.

[49] P. Grohs. Approximation order from stability for nonlinear subdivision schemes. *J. Approx. Theory*, 162(5):1085–1094, 2010.

[50] P. Grohs. A general proximity analysis of nonlinear subdivision schemes. *SIAM J. Math. Anal.*, 42(2):729–750, 2010.

[51] P. Grohs. Stability of manifold-valued subdivision schemes and multi-scale transformations. *Constr. Approx.*, 32(3):569–596, 2010.

[52] P. Grohs and J. Wallner. Log-exponential analogues of univariate subdivision schemes in Lie groups and their smoothness properties. In M. Neamtu and L.L. Schumaker, editors, *Approximation Theory XII: San Antonio 2007*, pages 181–190. Nashboro Press, 2008.

[53] I. Guskov. Multivariate subdivision schemes and divided differences. Technical report, Program for Applied and Computational Mathematics, Princeton University NJ 08544, 1998.

[54] I. Guskov, A. Khodakovsky, P. Schröder, and W. Sweldens. Hybrid meshes: Multiresolution using regular and irregular refinement. In *Proceedings of the Eighteenth Annual Symposium on Computational Geometry*, pages 264–272, 2002.

[55] I. Guskov, K. Vidimce, W. Sweldens, and P. Schröder. Normal meshes. In K. Akeley, editor, *Computer Graphics (SIGGRAPH '00: Proceedings)*, pages 95–102. ACM Press, 2000.

[56] B. Han. Vector cascade algorithms and refinable function vectors in Sobolev spaces. *J. Approx. Theory*, 124:44–88, 2003.

[57] B. Han and R.Q. Jia. Multivariate refinement equations and convergence of subdivision schemes. *SIAM J. Math. Anal.*, 29:1177–1199, 1998.

[58] S. Harizanov. Stability of nonlinear subdivision schemes and multiresolutions. Master's thesis, Jacobs University Bremen, 2007.

[59] S. Harizanov. Stability of nonlinear multiresolution analysis. *PAMM*, 8(1):10933–10934, 2008.

[60] S. Harizanov. Globally convergent adaptive normal multi-scale transforms. In *Curves and Surfaces*, 2011. accepted.

[61] S. Harizanov and P. Oswald. Stability of nonlinear subdivision and multiscale transforms. *Constr. Approx.*, 31:359–393, 2010.

[62] S. Harizanov, P. Oswald, and T. Shingel. Normal multi-scale transforms for curves. *Found. Comput. Math.*, 2011. accepted.

[63] A. Harten. Multiresolution representation of data: a general framework. *SIAM J. Numer. Anal.*, 33(3):1205–1256, 1996.

[64] A. Harten, B. Engquist, S. Osher, and S. Chakravarthy. Uniformly high order essentially non-oscillatory schemes. *J. Comput.Physics*, 71:231–303, 1987.

[65] M. Jansen. Stable edge-adaptive multiscale decompositions using updated normal offsets. *IEEE Transactions on Signal Processing*, 56(7-1):2718–2727, 2008.

[66] M. Janssen, R. Baraniuk, and S. Lavu. Multiscale approximation of piecewise smooth two-dimensional functions using normal triangulated meshes. *Appl. Comput. Harm. Anal.*, 19:92–130, 2005.

[67] R.Q. Jia. Subdivision schemes in L_p spaces. *Adv. Comput. Math.*, 3(4):309–341, 1995.

[68] A. Khodakovsky and I. Guskov. Compression of normal meshes. In *Geometric Modeling for Scientific Visualization*, pages 189–207. Springer-Verlag, 2003.

[69] A. Khodakovsky, P. Schröder, and W. Sweldens. Progressive geometry compression. In K. Akeley, editor, *Computer Graphics (SIGGRAPH '00: Proceedings)*, pages 271–278. ACM Press, 2000.

[70] L. Kobbelt. A variational approach to subdivision. *Comp. Aided Geom. Design*, 13(8):743–761, 1996.

[71] F. Kuijt and R. van Damme. Smooth interpolation by a convexity preserving non-linear subdivision algorithm. In A. Le Méhauté, C. Rabut, and L. L. Schumaker, editors, *Surface Fitting and Multiresolution Methods*, pages 219–224. Vanderbilt University Press, Nashville, TN, 1997.

[72] F. Kuijt and R. van Damme. Convexity preserving interpolatory subdivision schemes. *Constr. Approx.*, 14:609–630, 1998.

[73] F. Kuijt and R. van Damme. Monotonicity preserving interpolatory subdivision schemes. *J. Comput. Appl. Math.*, 101(1-2):203–229, 1999.

[74] F. Kuijt and R.M.J. van Damme. Stability of subdivision schemes. *TW memorandum 1469, Faculty of Applied Mathematics, University of Twente, the Netherlands*, 1998.

[75] J. M. Lane and R. F. Riesenfeld. A theoretical development for the computer generation and display of piecewise polynomial surfaces. *IEEE Trans. Pattern. Anal. Mach. Intell.*, 2(1):35–46, 1980.

[76] S. Lavu, H. Choi, and R. Baraniuk. Geometry compression of normal meshes using rate-distortion algorithms. In *Proceedings of the Eurographics/ACM SIGGRAPH Symposium on Geometry Processing*, pages 52–61, RWTH Aachen, 2003.

[77] A. W. F. Lee, W. Sweldens, P. Schröder, L. Cowsar, and D. Dobkin. MAPS: multiresolution adaptive parameterization of surfaces. In *Annual Conference on Computer Graphics*, pages 95–104, 1998.

[78] A. Levin and D. Levin. Analysis of quasi-uniform subdivision. *Appl. Comput. Harmon. Anal.*, 15(1):18–32, 2003.

[79] X.-D. Liu, S. Osher, and T. Chan. Weighted essentially non-oscillatory schemes. *J. Comput. Physics*, 115:200–212, 1994.

[80] C. Loop. Smooth subdivision surfaces based on triangles. Master's thesis, University of Utah, Department of Mathematics, 1987.

[81] M. Marinov, N. Dyn, and D. Levin. Geometrically controlled 4-point interpolatory schemes. In N. Dogson et al., editor, *Advances in Multiresolution for Geometric Modelling*, pages 301–317. Springer, 2004.

[82] B. Matei. Smoothness characterization and stability in nonlinear multiscale framework: theoretical results. *Asympt. Analysis*, 41(3-4):277–309, 2005.

[83] Y. Ohtake, A. Belyaev, and H.P. Seidel. Interpolatory subdivision curves via diffusion of normals. In *Computer Graphics International (CGI 2003)*, pages 22–27, Tokyo Institute of Technology, Tokyo, July 2003. IEEE.

[84] P. Oswald. Smoothness of nonlinear subdivision schemes. In *Curve and Surface Fitting: Saint-Malo*, pages 323–332. Nashboro Press, 2002.

[85] P. Oswald. Smoothness of nonlinear median-interpolation subdivision. *Adv. Comput. Math.*, 20:401–423, 2004.

[86] P. Oswald. Optimality of multilevel preconditioning for nonconforming P1 finite elements. *Numer. Mathematik*, 111:267–291, 2008.

[87] P. Oswald. Normal multi-scale transforms for surfaces. In *Curves and Surfaces*, 2010. accepted.

[88] E. Le Pennec and S. Mallat. Bandelet image approximation and compression. *SIAM J. Multiscale Model. Simul.*, 4:992–1039, 2005.

[89] I. Ur Rahman, I. Drori, V. C. Stodden, D. L. Donoho, and P. Schröder. Multiscale representations for manifold-valued data. *Mulitiscale Model. Simul.*, 4(4):1201–1232, 2005.

[90] U. Reif. A unified approach to subdivision algorithms near extraordinary verices. *Comput. Aided Geom. Des.*, 12(2):153–174, 1995.

[91] O. Runborg. Introduction to normal multiresolution analysis. In B. Engquist, P. Lötstedt, and O. Runborg, editors, *Multiscale Methods in Science and Engineering*, volume 44 of *Lecture Notes in Computational Science and Engineering*, pages 205–224. Springer, Heidelberg, 2005.

[92] O. Runborg. Fast interface tracking via a multiresolution representation of curves and surfaces. *Commun. Math. Sci.*, 7(2):365–389, 2009.

[93] M. Sabin and N. Dodgson. A circle-preserving variant of the four-point subdivision scheme. In *Mathematical Methods for Curves and Surfaces: Tromsø 2004, Modern Methods in Mathematics*, pages 275–286. Nashboro Press, 2005.

[94] P. Schröder and W. Sweldens. Spherical wavelets: efficiently representing functions on the sphere. In *Annual Conference on Computer Graphics*, pages 161–172, 1995.

[95] S. Serna and A. Marquina. Power ENO methods: a fifth-order accurate Weighted Power ENO method. *J. Comput. Physics*, 194:632–658, 2004.

[96] W. Sweldens. The lifting scheme: A new philosophy in biorthogonal wavelet constructions. In *Wavelet Applications in Signal and Image Processing III*, pages 68–79, 1995.

[97] W. Sweldens. The lifting scheme: A construction of second generation wavelets. *SIAM J. Math. Anal.*, 29:511–546, 1998.

[98] W. Van Aerschot, M. Jansen, and A. Bultheel. Normal offsets for digital image compression. In F. Truchetet and O. Laligant, editors, *Optics East, Wavelet Applications in Industrial Processing III*, volume 6001, pages 148–159. SPIE, Boston, MA, 2005.

[99] W. Van Aerschot, M. Jansen, E. Vanraes, and A. Bultheel. Image compression using normal mesh techniques. In A. Cohen, J.-L. Merrien, and L.L. Schumaker, editors, *Curves and Surface Fitting, Avignon 2006*, pages 266–275, Brentwood, 2007. Nashboro Press.

[100] R. van Damme. Bivariate Hermite subdivision. *Comput. Aided Geom. Design*, 14:847–875, 1997.

[101] J. Wallner. Smoothness analysis of subdivision schemes by proximity. *Constr. Approx.*, 24(3):289–318, 2006.

[102] J. Wallner and N. Dyn. Convergence and C^1 analysis of subdivision schemes on manifolds by proximity. *Comput. Aided Geom. Design*, 22(7):593–622, 2005.

[103] J. Wallner, E. Nava Yazdani, and P. Grohs. Smoothness properties of Lie group subdivision schemes. *Multiscale Model. Simul.*, 6:493–505, 2007.

[104] J. Wallner, E. Nava Yazdani, and A. Weinmann. Convergence and smoothness analysis of subdivision rules in Riemannian and symmetric spaces. *Adv. Comput. Math.*, 34(2):201–218, 2011.

[105] J. Wallner and H. Pottmann. Intrinsic subdivision with smooth limits for graphics and animation. *ACM Trans. Graphics*, 25(2):356–374, 2006.

[106] A. Weinmann. Smoothness of nonlinear subdivision schemes for arbitrary dilation matrices. Geometry preprint 2009/01, TU Graz, April 2009.

[107] A. Weinmann. Interpolatory multiscale representation for functions between manifolds. Geometry preprint 2010/05, TU Graz, April 2010.

[108] A. Weinmann. Nonlinear subdivision schemes on irregular meshes. *Constr. Approx.*, 31(3):395–415, 2010.

[109] G. Xie and T. P.-Y. Yu. Smoothness analysis of nonlinear subdivision schemes of homogeneous and affine invariant type. *Constr. Approx.*, 22(2):219–254, 2005.

[110] G. Xie and T. P.-Y. Yu. Smoothness equivalence properties of manifold-valued data subdivision schemes based on the projection approach. *SIAM J. Numer. Anal.*, 45:1200–1225, 2007.

[111] G. Xie and T. P.-Y. Yu. Smoothness equivalence properties of general manifold-valued data subdivision schemes. *Multiscale Model. Simul.*, 7:1073–1100, 2008.

[112] G. Xie and T. P.-Y. Yu. Smoothness equivalence properties of interpolatory Lie group subdivision schemes. *IMA J. Numer. Anal.*, 30:731–750, 2010.

[113] G. Xie and T. P.-Y. Yu. Approximation order equivalence properties of manifold-valued data subdivision schemes. *IMA J. Numer. Anal.*, pages 1–14, 2011.

[114] I. Yad-Shalom. Monotonicity preserving subdivision schemes. *J. Approx. Theory*, 74:41–58, 1993.

[115] X. Yang. Normal based subdivision scheme for curve design. *Comput. Aided Geom. Des.*, 23:243–260, 2006.

[116] H. Zhao, X. Qiu, L. Liang, C. Sun, and B. Zou. Curvature normal vector driven interpolatory subdivision. In *Shape Modeling International*, pages 119–125, 2009.

APPENDIX

.1 Power-p schemes

.1.1 Explicit construction for the instability argument for $\mathcal{S}_p$, $p > 4$

By the definition of operator norm, (2.3.20) means that there is a $\tilde{u}^0 = \{\tilde{u}^0_{-1}, \tilde{u}^0_0, \tilde{u}^0_1\}$ with unit norm $\|\tilde{u}^0\| = 1$ such that

$$\|\tilde{u}^J\| > \rho^n, \qquad \tilde{u}^n := (D\mathcal{S}_p^{[2]})_{\tilde{w}^{n-1}} \dots (D\mathcal{S}_p^{[2]})_{\tilde{w}^0} \tilde{u}^0.$$

Using the continuity of all $(D\mathcal{S}_p^{[2]})_{\tilde{w}}$ in I, it is clear that we have a similar inequality $\|\tilde{u}^n\| > \frac{1}{2}\rho^n$ for all $\tilde{w}$ in a small open neighborhood $\mathcal{W} \subset I$ of the initial $\tilde{w}^0$. Take

$$v := \Big\{ \dots, 0, 0, 0, \underbrace{\tilde{w}^0_{-1}}_{v_1}, \underbrace{2\tilde{w}^0_{-1} + \tilde{w}^0_0}_{v_2}, \underbrace{3\tilde{w}^0_{-1} + \tilde{w}^0_0 + \tilde{w}^0_1}_{v_3}, \underbrace{4\tilde{w}^0_{-1} + \tilde{w}^0_0 + 2\tilde{w}^0_1}_{v_4}, \underbrace{5\tilde{w}^0_{-1} + \tilde{w}^0_0 + 3\tilde{w}^0_1}_{v_5},$$
$$\underbrace{6\tilde{w}^0_{-1} + \tilde{w}^0_0 + 4\tilde{w}^0_1}_{v_6}, \underbrace{6\tilde{w}^0_{-1} + \tilde{w}^0_0 + 4\tilde{w}^0_1}_{v_7}, \underbrace{6\tilde{w}^0_{-1} + \tilde{w}^0_0 + 4\tilde{w}^0_1}_{v_8}, \dots \Big\},$$

$$z := \Big\{ \dots, 0, 0, 0, \underbrace{\tilde{u}^0_{-1}}_{z_1}, \underbrace{2\tilde{u}^0_{-1} + \tilde{u}^0_0}_{z_2}, \underbrace{3\tilde{u}^0_{-1} + \tilde{u}^0_0 + \tilde{u}^0_1}_{z_3}, \underbrace{4\tilde{u}^0_{-1} + \tilde{u}^0_0 + 2\tilde{u}^0_1}_{z_4}, \underbrace{5\tilde{u}^0_{-1} + \tilde{u}^0_0 + 3\tilde{u}^0_1}_{z_5},$$
$$\underbrace{6\tilde{u}^0_{-1} + \tilde{u}^0_0 + 4\tilde{u}^0_1}_{z_6}, \underbrace{6\tilde{u}^0_{-1} + \tilde{u}^0_0 + 4\tilde{u}^0_1}_{z_7}, \underbrace{6\tilde{u}^0_{-1} + \tilde{u}^0_0 + 4\tilde{u}^0_1}_{z_8}, \dots \Big\}.$$

This gives rise to

$$\Delta^2 v = \Big\{ \dots, 0, 0, \underbrace{\tilde{w}^0_{-1}}_{\Delta^2 v_{-1}}, \underbrace{\tilde{w}^0_0}_{\Delta^2 v_0}, \underbrace{\tilde{w}^0_1}_{\Delta^2 v_1}, 0, 0, 0, \underbrace{-\tilde{w}^0_{-1} - \tilde{w}^0_1}_{\Delta^2 v_5}, 0, 0 \dots \Big\},$$
$$\Delta^2 z = \Big\{ \dots, 0, 0, \underbrace{\tilde{u}^0_{-1}}_{\Delta^2 z_{-1}}, \underbrace{\tilde{u}^0_0}_{\Delta^2 z_0}, \underbrace{\tilde{u}^0_1}_{\Delta^2 z_1}, 0, 0, 0, \underbrace{-\tilde{u}^0_{-1} - \tilde{u}^0_1}_{\Delta^2 z_5}, 0, 0 \dots \Big\}.$$

Note that $\Delta^2 v$ and $\Delta^2 z$ coincide with w^0, respectively u^0 everywhere except the fifth entry, but this is not a problem due to the locality of $\mathcal{S}_p$. Furthermore, $\|z\| \le 11\|\tilde{u}^0\| = 11$.

Set $\tilde{v} := v + \lambda z$, and consider $v(t) := v + t(\tilde{v} - v) = v + t\lambda z$. Fix $\lambda > 0$ small enough so that $w(t) := \Delta^2 v(t) = w^0 + t\lambda u^0$ is completely in $\mathcal{W}$. Define $v^j(t) = S^j v(t)$, $v^j = v^j(0)$, $\tilde{v}^j = v^j(1)$, and $w^j(t) = \Delta^2 v^j(t) = (S^{[2]})^j w(t)$, $j \ge 0$. Then

$$\begin{aligned}
\|v^n - \tilde{v}^n\| &\ge 2^{-2}\|\Delta^2 v^n(1) - \Delta^2 v^n(0)\| = 2^{-2}\| \int_0^1 \frac{\mathrm{d}w^J(t)}{\mathrm{d}t} \mathrm{d}t\| \\
&\ge \lambda 2^{-2} \left| \int_0^1 (DS^{[2]})_{w^{n-1}(t)} \dots (DS^{[2]})_{w^0(t)} \tilde{u}^0 \, \mathrm{d}t \right| \\
&\ge \lambda 2^{-3} \rho^n \ge 11^{-1} 2^{-3} \rho^n \lambda \|z\| \ge (1/88)\rho^n \|v - \tilde{v}\|.
\end{aligned}$$

Letting $n \to \infty$ implies that $\mathcal{S}_p$ cannot be stable.

.1.2 Some useful facts for the power-p schemes

Lemma .1.1. *For $p \leq 4$, $\mathcal{T}$ is well defined, and thus C^∞, over its whole domain $[-1,1) \times (-1,1]$. Moreover, for the componentwise partial derivatives we have:*

$$\begin{aligned}
\frac{\partial T}{\partial t}(t,\bar{t}) &= \frac{4(1+\bar{t})(|\bar{t}|^p + 4\bar{t} + 3)[1 + (p-1)|t|^p - pt|t|^{p-2}]}{[4(1-t)(1+\bar{t}) + (1-|t|^p)(1+\bar{t}) - (1-|\bar{t}|^p)(1-t)]^2} = \frac{8(1+\bar{t})(|\bar{t}|^p + 4\bar{t} + 3)\phi(-t)}{\Phi(t,\bar{t})^2},\\
\frac{\partial T}{\partial \bar{t}}(t,\bar{t}) &= \frac{4(1-|t|^p)(t-1)[1 + (p-1)|\bar{t}|^p + p\bar{t}|\bar{t}|^{p-2}]}{[4(1-t)(1+\bar{t}) + (1-|t|^p)(1+\bar{t}) - (1-|\bar{t}|^p)(1-t)]^2} = -\frac{8(1-|t|^p)(1-t)\phi(\bar{t})}{\Phi(t,\bar{t})^2},\\
\frac{\partial \bar{T}}{\partial t}(t,\bar{t}) &= \frac{-4(1-|\bar{t}|^p)(1+\bar{t})[1 + (p-1)|t|^p - pt|t|^{p-2}]}{[4(1-t)(1+\bar{t}) - (1-|t|^p)(1+\bar{t}) + (1-|\bar{t}|^p)(1-t)]^2} = -\frac{8(1-|\bar{t}|^p)(1+\bar{t})\phi(-t)}{\Phi(-\bar{t},-t)^2},\\
\frac{\partial \bar{T}}{\partial \bar{t}}(t,\bar{t}) &= \frac{4(1-t)(|t|^p - 4t + 3)[1 + (p-1)|\bar{t}|^p + p\bar{t}|\bar{t}|^{p-2}]}{[4(1-t)(1+\bar{t}) - (1-|t|^p)(1+\bar{t}) + (1-|\bar{t}|^p)(1-t)]^2} = \frac{8(1-t)(|t|^p - 4t + 3)\phi(\bar{t})}{\Phi(-\bar{t},-t)^2}.
\end{aligned} \tag{.1.1}$$

Proof. Denote by $\Phi(t,\bar{t})$ the denominator of T, i.e.,

$$\Phi(t,\bar{t}) := 4(1-t)(1+\bar{t}) + (1-|t|^p)(1+\bar{t}) - (1-|\bar{t}|^p)(1-t).$$

Using that $|t|^p$ is monotonically increasing as a function of p, whenever $|t| \leq 1$, we derive

$$\Phi(t,\bar{t}) \geq 4(1-t)(1+\bar{t}) - (1-\bar{t}^4)(1-t) = (1+\bar{t})^2(1-t)((\bar{t}-1)^2 + 2) > 0,$$

for all $(t,\bar{t}) \in [-1,1) \times (-1,1]$. Since the denominator of $\bar{T}$ is $\Phi(-\bar{t},-t)$ the well-definedness of $\mathcal{T}$ is established. Verifying (.1.1) is a direct computation. The efforts are considerably decreased, if one uses the following representations for T and $\bar{T}$:

$$T = -1 + \frac{4(1-|t|^p)(1+\bar{t})}{\Phi(t,\bar{t})}, \qquad \bar{T} = 1 - \frac{4(1-|\bar{t}|^p)(1-t)}{\Phi(-\bar{t},-t)}, \tag{.1.2}$$

as well as the symmetries discussed in Section 2.3.3. □

The equations (.1.1) imply that in our region of interest $[-1,1) \times (-1,1]$ both $\partial T/\partial \bar{t}$ and $\partial \bar{T}/\partial t$ are nonpositive, while $\partial T/\partial t$ and $\partial \bar{T}/\partial \bar{t}$ are nonnegative.

Lemma .1.2. *For any $p > 1$, $p \neq 2$, $\mathcal{T}$ has only $(0,0)$ and $(-1,1)$ as fixed points.*

Proof. Since $T(-1,\bar{t}) = -1$ and $\bar{T}(t,1) = 1$, it is straightforward to show that there are no more fixed points on the boundary of the region. Thus, from now on we will work only within interior, i.e., $(-1,1) \times (-1,1)$. Let $(t,\bar{t})$ be a fixed point for $\mathcal{T}$. Then (.1.2) gives rise to

$$t = -1 + \frac{4(1-|t|^p)(1+\bar{t})}{\Phi(t,\bar{t})}, \qquad \bar{t} = 1 - \frac{4(1-|\bar{t}|^p)(1-t)}{\Phi(-\bar{t},-t)},$$

which is equivalent to

$$\frac{1-t^2}{(3-t)(1-|t|^p)} = \frac{1+\bar{t}}{|\bar{t}|^p + 4\bar{t} + 3}, \qquad \frac{1-\bar{t}^2}{(3+\bar{t})(1-|\bar{t}|^p)} = \frac{1-t}{|t|^p - 4t + 3}. \tag{.1.3}$$

Denote by $f_1(t) := (1-t^2)/((3-t)(1-|t|^p))$ and by $f_2(t) := (1-t)/(|t|^p - 4t + 3)$. Then, (.1.3) implies

$$f_1(t) = f_2(-\bar{t}), \qquad f_1(-\bar{t}) = f_2(t). \tag{.1.4}$$

Note that f_1 is positive in $(-1,1)$ and f_2 is positive in $(-1,s_p)$ and negative in $(s_p,1)$, where $s_p = 1$ for $p \leq 4$, otherwise is the root of $t^p - 4t + 3$ in $[0,1]$. The function $s : (4,+\infty) \to \mathbb{R}$ defined via $s(p) = s_p$ is monotonically decreasing with a limit $\lim_{p\to\infty} s(p) = 3/4$. From (.1.4) it follows that $(t,\bar{t}) \in (-1,s_p) \times (-s_p,1)$. Moreover, for the function $\mathbf{f}(t) := f_1(t) - f_2(t)$ in the interval $(-1,s_p)$ we have

$$\begin{aligned} \mathbf{f}(t) = \frac{1-t^2}{(3-t)(1-|t|^p)} - \frac{1-t}{|t|^p - 4t + 3} &= (1-t)\frac{(1+t)(|t|^p - 4t + 3) - (3-t)(1-|t|^p)}{(3-t)(1-|t|^p)(|t|^p - 4t + 3)} \\ &= \frac{4t^2(1-t)(|t|^{p-2} - 1)}{(3-t)(1-|t|^p)(|t|^p - 4t + 3)} \leq 0. \end{aligned} \tag{.1.5}$$

Equation (.1.4) is equivalent to $\mathbf{f}(t) = -\mathbf{f}(-\bar{t})$, which, due to (.1.5), suggests $\mathbf{f}(t) = \mathbf{f}(-\bar{t}) = 0$. Since only $\mathbf{f}(0) = 0$ in $(-1,s_p)$ the proof is completed. □

Lemma .1.2 can be interpreted in the following way: the only invariant functions under the action of $\mathcal{S}_p$ are the polynomials of degree 0,1 and 2. Indeed, $\mathcal{T}(-1,1) = (-1,1)$ implies that a straight line (and thus either a constant function or a linear polynomial) data sample generates the very same straight line as limit, while $\mathcal{T}(0,0) = (0,0)$ implies that a (regular) data sample from a quadratic polynomial generates the same quadratic polynomial as limit, for any $\mathcal{S}_p$, $p \neq 2$. Thus, the order of polynomial reproduction for the family $\mathcal{S}_p$ is 3.

In the remaining part of the section, we will concentrate on the stability analysis of $\mathcal{S}_p$, $p \leq 4$.

Lemma .1.3. *Denote by I_i, $i = 1,\ldots,4$ the four quadrants of the square $[-1,1) \times (-1,1]$, e.g., $I_2 = [0,1) \times (-1,0]$. Then for any $\mathcal{S}_p \leq 4$*

$$\mathcal{T} : I_1 \to I_1 \cup I_2 \cup I_4; \quad \mathcal{T} : I_2 \to I_2 \cup \{(-1,1)\}; \quad \mathcal{T} : I_3 \to I_3 \cup I_2 \cup I_4; \quad \mathcal{T} : I_2 \to I_2.$$

Proof. Due to symmetries it is enough to prove only the last two statements. Let $(t,\bar{t}) \in I_3$, i.e., $t,\bar{t} \leq 0$ and assume that $\mathcal{T}(t,\bar{t}) \in I_1$, i.e., $T,\bar{T} > 0$. The first part of Lemma .1.1 gives rise to

$$\left| \begin{array}{l} -4(1-t)(1+\bar{t}) + 3(1-|t|^p)(1+\bar{t}) + (1-|\bar{t}|^p)(1-t) > 0 \\ 4(1-t)(1+\bar{t}) - (1-|t|^p)(1+\bar{t}) - 3(1-|\bar{t}|^p)(1-t) > 0 \end{array} \right. .$$

Summing up the two inequalities we derive

$$(1-|t|^p)(1+\bar{t}) > (1-|\bar{t}|^p)(1-t),$$

which is a contradiction, since $1-|t|^p < 1 < 1-t$ and $1+\bar{t} = 1-|\bar{t}| < 1-|\bar{t}|^p$. Note that we proved a stronger result than the one stated in the lemma, namely if $t,\bar{t} \leq 0$ then $T + \bar{T} \leq 0$!

Showing that I_4 is invariant under the action of $\mathcal{T}$ is done in a similar fashion. Here, we use that if $t \le 0$ and $\bar{t} \ge 0$, then

$$\begin{aligned} -4(1-t)(1+\bar{t}) + 3(1-|t|^p)(1+\bar{t}) + (1-|\bar{t}|^p)(1-t) \le \\ -4(1-t)(1+\bar{t}) + 3(1-t)(1+\bar{t}) + (1-t)(1+\bar{t}) \quad \Rightarrow T \le 0; \\ 4(1-t)(1+\bar{t}) - (1-|t|^p)(1+\bar{t}) - 3(1-|\bar{t}|^p)(1-t) \ge \\ 4(1-t)(1+\bar{t}) - (1-t)(1+\bar{t}) - 3(1-t)(1+\bar{t}) \quad \Rightarrow \bar{T} \ge 0. \end{aligned}$$

The proof is completed □

Another useful result is the following lemma that narrows the "bad" sectors, which may lead to instability.

Lemma .1.4. *For all $p \in [1,4]$ and any $w \in \ell_\infty(\mathbb{Z})$,*

$$\| \left(D\mathcal{S}_p^{[2]}\right)_w \big|_{\{2i,2i+1,2i+2\}\times\{i-1,i,i+1\}} \| \ge 1 \quad \Leftrightarrow \quad (-t)^{p-1} + \bar{t}^{p-1} \ge \frac{4}{p}.$$

In particular, $(t,\bar{t}) \in I_4$.

Proof. Again, the proof consists only of computations. It is easy to check, that

$$\phi'(t) = \frac{1}{2}p(p-1)(t+1)|t|^{p-2} \ge 0,$$

meaning that $\phi(t)$ monotonically increases with $\phi(-1) = 0$, $\phi(0) = 1$, and $\phi(1) = p$. For the even and the odd parts of the function we have

$$F_1(t) := \phi(t) + \phi(-t) = 1 + (p-1)|t|^p \in [1,p]; \quad F_2(t) := \phi(t) - \phi(-t) = pt|t|^{p-2} \in [-p,p].$$

Now $\|((D\mathcal{S}_p^{[2]})_w)_{2i,\cdot}\| = F_1(t)/4 < p/4 \le 1$ and analogously for the $2i+2$-nd row. For the $2i+1$-st row we have two cases to consider:

$$\begin{aligned} &Case \quad 1: \ ((D\mathcal{S}_p^{[2]})_w)_{2i+1,i} < 0 \quad \Rightarrow \quad \|((D\mathcal{S}_p^{[2]})_w)_{2i+1,\cdot}\| = \frac{F_1(t)+F_1(\bar{t})}{8} - \frac{1}{2} \le \frac{p}{4} - \frac{1}{2} \le \frac{1}{2}; \\ &Case \quad 2: \ ((D\mathcal{S}_p^{[2]})_w)_{2i+1,i} \ge 0 \quad \Rightarrow \quad \|((D\mathcal{S}_p^{[2]})_w)_{2i+1,\cdot}\| = \frac{F_2(-t)+F_2(\bar{t})}{8} + \frac{1}{2}, \end{aligned}$$

and the letter exceeds 1 if and only if $F_2(-t) + F_2(\bar{t}) \ge 1/2$, which up to simplifications is exactly what we wanted to prove. □

Combining all the four lemmas, we conclude that no matter what initial $\tilde{w}^0 = \{w_{-1}^0, w_0^0, w_1^0\}$ we chose, after finitely many subdivision levels n (the number n depends on $\tilde{w}^0$) we end up with a submatrix $(D\mathcal{S}_p^{[2]})_{\tilde{w}^n}$ which operator norm is less than 1, and so is the norm of any submatrix $(D\mathcal{S}_p^{[2]})_{\tilde{w}^m}$, where $m \ge n$. Of course, as shown in the proof of Theorem **??**, this may happen arbitrarily slow (i.e., $n \to \infty$), but this is not enough to claim instability, since the joint spectral

radius of the limit matrix A in (2.3.19) is not bigger than 1. In fact, we believe that it is possible to prove that there exists global n, and $\rho \in (0,1)$, such that no matter what $\tilde{w}^0$ we take,

$$\|(D\mathcal{S}_p^{[2]})_{\tilde{w}^{n-1}}(D\mathcal{S}_p^{[2]})_{\tilde{w}^{n-2}} \dots (D\mathcal{S}_p^{[2]})_{\tilde{w}^0}\| \leq \rho^n.$$

However this will not be enough to claim stability. Indeed, the invariant neighborhood of $\mathcal{S}_p$ consists of six points (all these subdivision schemes can be viewed as generalized four point schemes), meaning that four second divided differences, resp., three ts should be considered for the stability analysis. This makes the IFS richer and more difficult to analyze. For example, even if we know that both (t_0, t_1) and (t_1, t_2) are far away from the "bad" region, defined in Lemma .1.4, then we just know (or can try to prove) that $(T_0, T_1) = \mathcal{T}(t_0, t_1)$ and $(T_2, T_3) = \mathcal{T}(t_1, t_2)$ are not in the region, as well. However, (T_2, T_3) might be there, and computer simulations show that for $p > 8/3$ this does actually happen from time to time. Nevertheless, we conjecture that for $p \leq 4$, $\mathcal{S}_p$ is Lipschitz stable and hope to be able to prove it in the near future. On the other hand, note that, the higher the p, the higher the n for which $\|A^n\| < 1$, implying that even theoretically stable, the process may need so many steps to stabilize that can be considered instable from a practical point of view.

.2 Normal multi-scale transforms

.2.1 Proof of Lemma 5.0.4

Proof. The proof is taken from our paper [62]. Let $Q_0(x) = 1$, and $Q_m(x) := (m!)^{-1}x(x-1)\dots(x-m+1)$, $m \geq 1$. We have $Q_m(0) = 0$ if $m \geq 1$. Note that for arbitrary $l \in \mathbb{Z}$

$$(\Delta(Q_m|_{\mathbb{Z}}))_l = (m!)^{-1}((l+1)\dots(l-m+2) - l\dots(l-m+1)) = (Q_{m-1}|_{\mathbb{Z}})_l,$$

and by induction $\Delta^n Q_m|_{\mathbb{Z}} = Q_{m-n}|_{\mathbb{Z}}$, $n = 0, \dots, m$. Moreover, $\Delta^n Q|_{\mathbb{Z}} = 0$ for any polynomial Q of degree $m < n$. These properties will be used without further mentioning.

In the following, $K \in I \cup I_1$ is considered fixed and dropped from the notation whenever this cannot lead to confusion. Introduce $r = (r_l)_{l \in I}$ by setting

$$s_l = \sum_{m=0}^{M-1} (\Delta^m Ss)_K Q_m(2l - K - 2c_S) + r_l, \qquad l \in I. \tag{.2.1}$$

Evidently, $\Delta^M s_l = \Delta^M r_l$ for all $l \in I^{[M]}$. Applying S to the above identity, and using (**??**), we have

$$Ss_k = \sum_{m=0}^{M-1} (\Delta^m Ss)_K Q_m(k - K) + Sr_k, \qquad k \in I_0 \cup I_1,$$

and consequently

$$(\Delta^n Ss)_K = \sum_{m=n}^{M-1} (\Delta^m Ss)_K Q_{m-n}(0) + (\Delta^n Sr)_K = (\Delta^n Ss)_K + (\Delta^n Sr)_K, \qquad n = 0, 1, \dots, M-1,$$

i.e., $(\Delta^n Sr)_K = 0$, $n = 0, 1, \ldots, M-1$. Together with the above equality $\Delta^M r_l = \Delta^M s_l$ for the M-th order difference, this implies

$$|r_l| \le C\|\Delta^M r\|_I = C\|\Delta^M s\|_I, \qquad l \in I, \tag{.2.2}$$

similar to the derivation of [24, (4.27)]. Throughout the proof of Lemma 5.0.4, C denotes a generic constant which does not depend on s and K but may change its value from line to line. Moreover, we frequently use the estimates

$$|(\Delta^M s)_K| \le 2^{M-m}\|\Delta^m s\|_I, \qquad m = 1, \ldots, M-1, \tag{.2.3}$$

and

$$|(\Delta^m Ss)_K| \le C\|\Delta^m s\|_I, \qquad m = 1, \ldots, P, \tag{.2.4}$$

where $P \ge P_e$ is the polynomial reproduction order of S. The first one is obvious by the definition of the difference operators Δ^m while the second is a consequence of the existence of derived $S^{[m]}$ for all $0 \le m \le P$.

To estimate the quantity $|SF(s)_K - F(Ss_K)|$, we evaluate $F(s_l)$ using Taylor expansion (4.2.6) of order M for $F(s)$ with respect to Ss_K, then apply S to it, together with the formula

$$s_l - Ss_K = \underbrace{\sum_{m=1}^{M-1} (\Delta^m Ss)_K Q_m(2l - K - 2c_S)}_{=:d_l} + r_l, \qquad l \in I, \tag{.2.5}$$

which follows from (.2.1). This gives

$$\begin{aligned} |SF(s)_K - F(Ss_K)| &= \left| \sum_{n=0}^{M} \frac{F^{(n)}(Ss_K)}{n!} (S(s - Ss_K)^n)_K + SR_K - F(Ss)_K \right| \\ &\le C \left| \sum_{n=2}^{M} (S(d+r)^n)_K \right| + |SR_K|, \end{aligned}$$

where $d = (d_l)_{l \in I}$ and R stands for the sequence of remainder terms $R_l = \mathrm{O}(|s_l - Ss_K|^{M+\rho})$ in the Taylor formula. The terms for $n = 0$ and $n = 1$ have canceled since S reproduces constants, and $(S(s - (Ss)_K))_K = (Ss)_K - (Ss)_K = 0$. The remainder term SR_K satisfies

$$|SR_K| \le C \max_{l \in I} |s_l - Ss_K|^{M+\rho} \le C\|\Delta s\|_I^{M+\rho}.$$

For $M = 1$ this finishes the proof (in this case $E_M = \emptyset$).

For $M \ge 2$, we split any of the remaining terms as follows:

$$(S(d+r)^n)_K = (Sd^n)_K + \sum_{i=1}^{n} \binom{n}{i} (S(r^i d^{n-i}))_K.$$

For the terms in the double sum, we use rough estimates involving (.2.2), (.2.3), and (.2.4). By definition of d in (.2.5), we have

$$\|d\|_I \le C \sum_{m=1}^{M-1} |(\Delta^m Ss)_K| \le C \sum_{m=1}^{M-1} \|\Delta^m s\|_I \le C\|\Delta s\|_I$$

and consequently

$$|S(r^i d^{n-i})_K| \le C\|r\|_I^i \|d\|_I^{n-i} \le C\|\Delta^M s\|_I^i \|\Delta S s\|_I^{n-i} \le C\|\Delta^M s\|_I \|\Delta s\|_I^{n-1}, \qquad i = 1, \dots, n.$$

This yields

$$\begin{aligned}\left|\sum_{n=2}^{M}\sum_{i=1}^{n}\binom{n}{i} S(r^i d^{n-i})_K\right| &\le C\sum_{n=2}^{M}\|\Delta^M s\|_I \|\Delta s\|_I^{n-1} \le C(\|\Delta^M s\|_I \|\Delta s\|_I + \|\Delta s\|_I^{M-1}) \\ &\le C(\|\Delta^M s\|_I \|\Delta s\|_I + \|\Delta^2 s\|_I \|\Delta s\|_I^{M-1}) \le C\sum_{\nu\in E_M}\prod_{m=1}^{M-1}\|\Delta^m s\|_I^{\nu_m},\end{aligned}$$

see the definition of E_M.

According to (.2.5), the remaining terms $(Sd^n)_K$, $n = 2, \dots, M$, can be written as

$$(Sd^n)_K = \sum_{\sum_{m=1}^{M-1}\nu_m = n} \frac{n!}{\nu!} S\left(\prod_{m=1}^{M-1}(\Delta^m Ss)_K^{\nu_m} Q_m(2\cdot - k - 2c_S)^{\nu_m}\right)_K.$$

We now explore the exact polynomial reproduction of order $P_e > M \ge 2$: If $\sum_{m=1}^{M-1} m\nu_m \le M$ then, since $S(p|_{2\mathbb{Z}}) = p|_{\mathbb{Z}+2c_S}$

$$\begin{aligned}S\left(\prod_{m=1}^{M-1}(\Delta^m Ss)_K^{\nu_m} Q_m(2\cdot - K - 2c_S)^{\nu_m}\right)_K &= \left(\prod_{m=1}^{M-1}(\Delta^m Ss)_K^{\nu_m} Q_m(\cdot - K)^{\nu_m}\right)_K \\ &= \prod_{m=1}^{M-1}(\Delta^m Ss)_K^{\nu_m} Q_m(0)^{\nu_m} = 0.\end{aligned}$$

Thus, we obtain

$$\sum_{n=2}^{M}|(Sd^n)_K| \le C \sum_{2\le\sum_{m=1}^{M-1}\nu_m\le M,\ \sum_{m=1}^{M-1} m\nu_m > M} \prod_{m=1}^{M-1}|\Delta^m Ss_K|^{\nu_m} \le C\sum_{\nu\in E_M}\prod_{m=1}^{M-1}\|\Delta^m s\|_I^{\nu_m}.$$

In the last estimation step, we have used (.2.4) and the fact that any term $\prod_{m=1}^{M-1}\|\Delta^m s\|_I^{\nu_m}$ with ν such that $\sum_{m=1}^{M-1} m\nu_m > M+1$ and $\sum_{m=1}^{M-1}\nu_m \le M$ can always be majorized via (.2.3) by a constant multiple of a similar term with $\nu \in E_M$. Together with the already obtained estimates for the other terms involved in the upper bound for $|F(Ss_K) - SF(s)_K|$, this concludes the proof of Lemma 5.0.4. □

.2.2 Alternative proof of Theorem 5.2.1 via explicit computations

Proof. In order to perform the computational technique from the proof of Theorem 5.1.3, and to have control on the leading terms in the estimations we need to assume $\mathcal{C} \in C^{p+2}$, instead of $\mathcal{C} \in C^{p+1}$.

p=3: We use the same technique as in Theorem 5.1.3, so we also keep the same notation. We need to consider separately d_0 and d_1. Let us start with the second case. Since $\hat{\mathbf{n}}_1 \perp \Delta\mathbf{v}_0$ there exists a $\xi_1 \in (s_0, s_1)$, such that $\hat{\mathbf{n}}_1 = \mathbf{n}(\xi_1)$. Let

$$\xi_1 = s_0 + r\Delta s_0 = rs_1, \qquad r \in (0,1).$$

With respect to the local frame $(\mathbf{t}(\xi_1), \mathbf{n}(\xi_1))$, centered at $\mathbf{v}(\xi_1)$ we have $y_0 = y(-rs_1) = y_1 = y\big((1-r)s_1\big)$. Using (5.0.1) with higher order

$$y(s) = \frac{\alpha}{2}s^2 + \frac{\beta}{6}s^3 + \frac{\alpha^3+\gamma}{24}s^4 + \mathrm{O}(s^5), \qquad s << 1, \quad \alpha = \mathrm{k}(\xi_1),\ \beta = \mathrm{k}'(\xi_1),\ \gamma = \mathrm{k}''(\xi_1),$$

writing r in the form $r = a_0 + a_1 s_1 + a_2 s_1^2 + \mathrm{O}(s_1^3)$, and comparing the coefficients in front of the corresponding powers, we derive

$$\begin{gathered}
\tfrac{\alpha}{2}(-rs_1)^2 + \tfrac{\beta}{6}(-rs_1)^3 + \tfrac{\alpha^3+\gamma}{24}(-rs_1)^4 + \mathrm{O}(s_1^5) = \\
= \tfrac{\alpha}{2}((1-r)s_1)^2 + \tfrac{\beta}{6}((1-r)s_1)^3 + \tfrac{\alpha^3+\gamma}{24}((1-r)s_1)^4 + \mathrm{O}(s_1^5) \\
\Longrightarrow \quad \left| \begin{array}{l} (2a_0-1)\alpha/2 = 0 \\ \alpha a_1 - (a_0^3 + (1-a_0)^3)\beta/6 = 0 \ = 0 \\ \alpha a_2 - (6a_0a_1 - 3a_1)\beta/6 \end{array} \right. \qquad \Longrightarrow \qquad r = \tfrac{1}{2} + \tfrac{\beta}{24\alpha}s_1 + \mathrm{O}(s_1^3).
\end{gathered}$$

For the forth-order term we used the simplification, that since $(-rs_1)^2 - ((1-r)s_1)^2 = \mathrm{O}(s_1^3)$, then $(-rs_1)^4 - ((1-r)s_1)^4 = \mathrm{O}(s_1^5)$ and those summands do not contribute. As, in Theorem 5.1.3, $\mathcal{C}$ being of finite length and C^5 assures us that there exists a global constant $C_{\mathcal{C}} < \infty$, that depends only on the initial curve, such that $\alpha, \beta, \gamma < C_{\mathcal{C}} < \infty$. The above computation, together with (5.1.4), give rise to

$$s_0 - \xi_1 = -\xi_1 = -\frac{s_1}{2} - \frac{\beta}{24\alpha}s_1^2 + \mathrm{O}(s_1^4);\ s_1 - \xi_1 = \frac{s_1}{2} - \frac{\beta}{24\alpha}s_1^2 + \mathrm{O}(s_1^4);\ \bar{s}_1 - \xi_1 = -\frac{\beta}{24\alpha}s_1^2 + \mathrm{O}(s_1^4).$$

Hence,

$$\begin{aligned}
y_{-1} &= y(s_{-1} - \xi_1) = \frac{\alpha}{2}\left(s_{-1}^2 + \frac{s_1^2}{4} - s_1 s_{-1}\right) + \frac{\beta}{6}\left(-s_{-1}^3 + \frac{3s_1 s_{-1}^2}{2} - \frac{s_1^2 s_{-1}}{2}\right) + \mathrm{O}(s_1^4); \\
y_0 &= y_1 = \frac{\alpha}{8}s_1^2 + \mathrm{O}(s_1^4); \qquad\qquad \bar{y}_1 = \mathrm{O}(s_1^4); \\
y_2 &= \frac{\alpha}{2}\left((\Delta s_1)^2 + \frac{s_1^2}{4} + s_1\Delta s_1\right) + \frac{\beta}{6}\left((\Delta s_1)^3 + \frac{3s_1(\Delta s_1)^2}{2} + \frac{s_1^2\Delta s_1}{2}\right) + \mathrm{O}(s_1^4).
\end{aligned}$$

We used that $\mathrm{O}(\Delta s_{-1} = -s_{-1}) = \mathrm{O}(\Delta s_0 = s_1) = \mathrm{O}(\Delta s_1)$, which is equivalent to the normal re-parameterization of the (S_3, S_1) normal MT to be $C^{0,1}$, and it follows from Theorem 4.2.3. Now

$$|d_1| = |(Ty)_1 - \bar{y}_1| = \Big| \underbrace{\tfrac{\alpha}{32}\Big(4(\Delta s_0)^2 - (\Delta s_{-1})^2 - (\Delta s_1)^2 - \Delta s_{-1}\Delta s_0 - \Delta s_0\Delta s_1\Big)}_{A} +$$

$$+ \underbrace{\tfrac{\beta}{192}\Big(2(\Delta s_{-1})^3 + 3\Delta s_0(\Delta s_{-1})^2 + (\Delta s_0)^2\Delta s_{-1} - 2(\Delta s_1)^3 - 3\Delta s_0(\Delta s_1)^2 - (\Delta s_0)^2\Delta s_1\Big)}_{B} + \mathrm{O}(\|\Delta s\|^4)\Big|.$$

According to Theorem 5.1.3 $\|\Delta^2 s\| = \mathrm{O}(\|\Delta s\|^2)$ and $\|\Delta^3 s\| = \mathrm{O}(\|\Delta s\|^3)$. Thus

$$\Delta s_{-1} = \Delta s_0 + \mathrm{O}((\Delta s)^2); \qquad \Delta s_1 = \Delta s_0 + \mathrm{O}((\Delta s)^2); \qquad \Delta s_{-1} + \Delta s_1 = 2\Delta s_0 + \mathrm{O}((\Delta s)^3).$$

The first two equalities are enough to conclude that $B = \mathrm{O}(\|\Delta s\|^4)$, while for A we have

$$\begin{aligned} A &= 2(\Delta s_0)^2 + (\Delta s_0 - \Delta s_{-1})(\Delta s_0 + \Delta s_{-1}) + (\Delta s_0 - \Delta s_1)(\Delta s_0 + \Delta s_1) - \Delta s_0(\Delta s_{-1} + \Delta s_1) \\ &= (\Delta s_0 - \Delta s_{-1})(\Delta s_0 + \Delta s_{-1}) - (\Delta s_0 - \Delta s_{-1} + \mathrm{O}(\|\Delta s\|^3))(\Delta s_0 + \Delta s_1) + \mathrm{O}(\|\Delta s\|^4) \\ &= (\Delta s_0 - \Delta s_{-1})(\Delta s_{-1} - \Delta s_1) + \mathrm{O}(\|\Delta s\|^4) = \mathrm{O}(\|\Delta s\|^4). \end{aligned}$$

Thus,

$$|d_1| = \mathrm{O}(\|\Delta s\|^4).$$

Note that at any moment of our estimations we have had full control over the constants in the $\mathrm{O}(\|\Delta s\|^4)$ terms, which guarantees us that $|d^1| \le C\|\Delta s\|^4$ with a global constant $C < \infty$ depending on $\mathcal{C}$ and Δs^0. Also, even though in the formula for r we have α in the denominator, it cancels out in the estimations for d^1 and, thus, by continuity we can extend our result to the case $\alpha = 0$, as well.

The computations for $|d_0|$ are much easier. First, since $\hat{\mathbf{n}}_0 \perp \mathbf{v}_{-1}\mathbf{v}_1$ there exists a $\xi_0 \in (s_{-1}, s_1)$, such that $\hat{\mathbf{n}}_0 = \mathbf{n}(\xi_0)$. Moreover, we already now that

$$s_{-1} - \xi_0 = -\frac{s_1 - s_{-1}}{2} - \frac{\beta}{24\alpha}(s_1 - s_{-1})^2 + \mathrm{O}(s_1^4) \implies s_0 - \xi_0 = -\frac{s_1 + s_{-1}}{2} - \frac{\beta}{24\alpha}(s_1 - s_{-1})^2 + \mathrm{O}(s_1^4) = \mathrm{O}(s_1^2).$$

On the other hand, (5.1.5) implies $\bar{s}_0 = \mathrm{O}(s_1^2)$, as well. Therefore, since $y(s) = \mathrm{O}(s^2)$, and $(T\mathbf{v})_0 = \mathbf{v}_0$, we conclude that

$$|d_0| = |y_0 - \bar{y}_0| = \mathrm{O}(\|\Delta s\|^4).$$

The proof is completed.

p=2: Due to symmetry, it suffices to check only d_0. From Theorem 4.3.1 we know that the S_2 normal MT is globally well-posed and the restriction on the cardinality of $\mathbf{v}^0$ is only to assure that we always use different points for the computation of $T\mathbf{v}^0$. Since $\hat{\mathbf{n}}_0 \perp \Delta\mathbf{v}_0$, we work with the same local frame, centered at ξ_1, as in the first part of the proof for $p = 3$. Hence y_{-1}, y_0, and y_1 are the same as before, but estimated one order less, i.e.,

$$y_{-1} = \frac{\alpha}{2}\left(s_{-1}^2 + \frac{s_1^2}{4} - s_1 s_{-1}\right) + \mathrm{O}(s_1^3); \qquad y_0 = y_1 = \frac{\alpha}{8}s_1^2 + \mathrm{O}(s_1^3),$$

while for $\bar{y}_0$, due to (5.1.3), we have

$$\bar{s}_0 - \xi_1 = -\frac{s_1}{4} - \frac{\beta}{24\alpha}s_1^2 + \mathrm{O}(s_1^3) \quad \Longrightarrow \quad \bar{y}_0 = \frac{\alpha}{32}s_1^2 + \mathrm{O}(s_1^3).$$

Therefore

$$\begin{aligned} |d_0| &= \big|(T_2 y)_0 - \bar{y}_0\big| = \frac{3\alpha}{32}\big|s_1^2 - \frac{s_{-1}^2 - s_1 s_{-1}}{2}\big| + \mathrm{O}(s_1^3) \\ &= \frac{3\alpha}{64}\big|2(\Delta s_0)^2 - (\Delta s_{-1})^2 - \Delta s_0 \Delta s_{-1}\big| + \mathrm{O}(\|\Delta s\|^3) \\ &= \frac{3\alpha}{64}\big|(2\Delta s_0 + \Delta s_{-1})\Delta^2 s_{-1}\big| + \mathrm{O}(\|\Delta s\|^3) = \mathrm{O}(\|\Delta s\|^3), \end{aligned}$$

where, we used that the $C^{1,1}$-normal re-parameterization of the S_2 normal MT gives rise to $\Delta s_{-1} \asymp \Delta s_0 \asymp \|\Delta s\|$ and $|\Delta^2 s_{-1}| = \mathrm{O}((\Delta s_{-1})^2)$ follows from Theorem 5.1.3. □